The temperature-dependent electrical resistivities of the alkali metals

Jack Bass

*Max-Planck-Institut für Festkorperforschung Hochfeld Magnetlabor—Service National
des Champs Intenses Centre National de la Recherche Scientifique, 38042 Grenoble, France
and Department of Physics and Astronomy, Michigan State University, East Lansing, Michigan 48824*

William P. Pratt, Jr.

Department of Physics and Astronomy, Michigan State University, East Lansing, Michigan 48824

Peter A. Schroeder

Department of Physics and Astronomy, Michigan State University, East Lansing, Michigan 48824

This review contains a comprehensive examination of all modern measurements and calculations of the temperature-dependent electrical resistivity $\rho(T)$ for the alkali metals—and especially potassium (K)—from their melting points down to below 0.1 K. The simplicity of the electronic structures of these metals makes them unique for testing our fundamental understanding of $\rho(T)$. At all temperatures down to a few K, $\rho(T)$ is dominated by its electron-phonon scattering component, $\rho_{ep}(T)$. Current quantitative understanding of $\rho_{ep}(T)$ in the alkali metals is examined in detail, including effects of phonon drag at temperatures below $\simeq 10$ K. In the vicinity of 1 K, $\rho(T)$ in pure, unperturbed, bulk alkali metals is predicted to be dominated by electron-electron scattering. $\rho_{ee}(T) = A_{ee}T^2$. In disagreement with previous reviews, the authors argue that A_{ee} is nearly constant for each alkali metal and—at least for K—also in quantitative agreement with calculation. Below 1 K, alloys based on K and lithium display both previously predicted and completely unexpected effects. Perturbations such as deformation and thinning of K wires induce unusual and interesting behaviors. An unexpected Kondo-like effect appears when K contacts polyethylene. Charge-density-wave-based predictions of contributions to $\rho(T)$ in the alkali metals are also considered. Three appendices examine (a) what is involved in a realistic calculation of $\rho(T)$; (b) the experimental problems encountered in high-precision measurements of $\rho(T)$ at low temperatures and how they are solved; and (c) the most recent experimental data concerning charge-density waves in the alkali metals.

It must be admitted, in the end, that although the whole theory of the ideal resistivity of metals, dating back in its essentials to the work of Bloch some 35 years ago, can give fair agreement with experiment, it has not been fully tested quantitatively in even its first term.

J. M. Ziman (1969)

CONTENTS

I. INTRODUCTION AND OVERVIEW

A. The importance of $\rho(T)$ for the alkali metals

"Call me Ishmael." These words introduce the narra-
tor of *Moby Dick*, Herman Melville's (1851) great novel
of the struggle of man to conquer the forces of nature—
personified by the Great White Whale, Moby Dick. Like
Ishmael, physicists are wanderers and observers in
nature's domain. Like Ahab's, their task is to "conquer"
nature. But theirs is not a fight to the death with a na-
ture that has wounded them. Rather, they strive to wrest
from nature her secrets, to understand the behavior of
parts of the physical world, to bring order out of chaos.
To do this, experimentalists normally choose to study
small facets of nature which they anticipate will display
especially simple behaviors, and work to characterize and

understand them as carefully and completely as possible.

The small facet of nature covered in this review is the temperature-dependent electrical resistivity $\rho(T)$ of the alkali metals. The reasons for interest in this topic are the following:

Metals are one of the handful of different classes of solids (see, for example, Kittel, 1976). Their defining characteristic is their electronic transport properties, especially their high electrical and thermal conductivities.

Of the three electronic transport coefficients—the electrical resistivity ρ, the thermal conductivity κ, and the thermopower S—ρ can be measured with the highest precision and also generally calculated most accurately, primarily because a variational procedure permits the calculation of a rigorous upper bound on ρ. (Appendix A gives a brief overview of what a realistic calculation of ρ involves.) At low temperatures, ρ has the additional advantages that (1) it does not manifest the many-body (Opsal, Thaler, and Bass, 1976; Thaler, Fletcher, and Bass, 1978) and higher-order "Nielsen-Taylor" effects (see, for example, Blatt et al., 1976), which greatly complicate any attempt to describe S quantitatively, and (2) because of the Wiedemann-Franz law, it contains all of the information present in κ. For these reasons, we focus upon ρ, discussing S and κ only in cases where they provide important complementary information. We limit ourselves to zero magnetic field, since application of a magnetic field both complicates the experimental situation and introduces an entirely new set of theoretical issues.

The calculation of ρ involves complex integrations over the Fermi surface of the metal. Such calculations are generally tractable only for a metal with a nearly spherical Fermi surface entirely contained within the first Brillouin zone and not contacting its boundaries. De Haas–van Alphen measurements (Cracknell, 1969; O'Shea and Springford, 1981) tell us that only the alkali metals in their bcc forms have such Fermi surfaces. In addition to their particularly simple electronic structures, the alkali metals have two other advantages that make them unique for studies of $\rho(T)$ down to ultralow temperatures. (1) They do not superconduct to any temperatures yet reached—a fundamental problem below a few K in such other nearly-free-electron (NFE) metals as aluminum (Al) and indium (In). (2) In pure form they do not display the large Kondo effects due to very small concentrations of magnetic impurities that complicate low-temperature studies of $\rho(T)$ in the noble metals. The alkali metals thus provide the best hope for testing our fundamental understanding of $\rho(T)$ by means of quantitative comparisons between measurements and realistic calculations. The importance of such tests is indicated by the quote from Ziman in 1969 which begins this review.

Among the alkali metals, most high-precision measurements at very low temperatures have been made on potassium (K), because (a) K and sodium (Na) have the most nearly spherical Fermi surfaces; (b) both Na and lithium (Li) undergo martensitic crystallographic phase

transitions upon cooling through $\simeq 50$ K and $\simeq 75$ K, respectively; and (c) in addition to having less spherical Fermi surfaces than K, rubidium (Rb) and cesium (Cs) cannot be obtained in as high purity.

B. The reasons for this review

In 1984–1985, three reviews of different aspects of the transport properties of metals (Wiser, 1984; Kaveh and Wiser, 1984; van Vucht et al., 1985) included discussions of $\rho(T)$ in the alkali metals. Occupying a central place in the analyses of the low-temperature behavior of $\rho(T)$ in K in those reviews was a model of electron-electron scattering in the presence of anisotropic scatterers that had been developed by Kaveh and Wiser (1980, 1982) to explain a variety of unexpected behaviors found when high-precision measurements on K and other simple metals were first extended down to 1 K.

Since 1984–1985, improvements in experimental capabilities have permitted a substantial amount of new data to be taken at temperatures extending down to below 0.1 K. These data have convinced the authors of the present review that the Kaveh and Wiser (KW) model is not relevant to the alkali metals at low temperatures. Rather, we believe that the explanation of the unexpected behaviors in K and the other alkali metals in the vicinity of 1 K lies in the unanticipated effects of certain very specific perturbations to which early samples were inadvertently subjected. When these perturbations are eliminated, the behavior of $\rho(T)$ in pure K becomes simple and in quantitative accord with theory from its melting point down to well below 1 K.

This review was written (a) to communicate our present understanding of $\rho(T)$ in both pristine and perturbed alkali metals over the entire temperature range from their melting points down to well below 1 K, and (b) to explain what additional work is required to clarify what we still do not understand.

Because of some significant disagreements with the previous reviews, primarily at low temperatures, we felt it incumbent upon us to first carefully and completely reexamine the data and models covered in those reviews before going on to new results, so as to permit the reader to see (a) the manner in which data gradually accumulated; (b) why the models presented in the previous reviews were developed and how successful they were; (c) who should be given credit for specific discoveries and advances; and (d) why additional measurements on a wider variety of samples and extending to temperatures well below 1 K were needed to test the proposed models. We shall then describe how new data, taken since those reviews were published, have led us to reject these models.

We have attempted to make this review complete and self-contained, by collecting together all of the important data on $\rho(T)$ in K and the other alkali metals. We have done this both to minimize the need for the reader to consult the original literature and to give the reader

enough information to be able independently to assess the validity of the conclusions we reach. The story we have to tell is like a detective story, in which the meaning of a large number of confusing and sometimes apparently contradictory clues has to be unraveled. And we still do not have complete explanations for all of the puzzles. We shall see that inspired guesses by theorists sometimes played a more important role in driving the field than did definitive proofs.

C. Organization of the review

The review is organized as follows.

Section I.D describes the variety of different components of the total resistivity ρ_t that must be considered in attempting to understand the behavior of the alkali metals, both in their pristine state and after they have been subjected to various perturbations applied either deliberately or unwittingly. Section I.E contains a brief overview of the components of our proposed picture of $\rho(T)$ in the alkali metals. These sections are intended to provide context for the remainder of the review.

Section II contains additional background material. It begins with a brief discussion of the experimental problems involved in handling the alkali metals, and follows with a table giving a large amount of information about measuring parameters and sample characteristics for all of the experiments that are reviewed. This table is intended to provide a convenient central reference where the reader can quickly see the important differences in sample characteristics and experimental techniques between different studies, as well as the progress that has been made in experimental capabilities over the past 20 years. Section II concludes with explanations of the different types of graphs that are used for presenting data and of the advantages and disadvantages of each.

Section III contains a detailed examination of all of the experimental data and theoretical analyses for K and the other alkali metals published prior to 1984–1985, when the three previous reviews were written.

Section IV covers data from 1984–1985 onward, mostly in the vicinity of 1 K and below, along with brief outlines of the models that have been developed to try to explain the variety of new phenomena that were found. Each discussion begins with a short rationale for the measurements and a summary of the most important results obtained.

Section V compares competing models with both the old and the new experimental data that are presented in this review.

Section VI contains a summary, conclusions, and suggestions for further work.

This review also has three appendices. Appendix A describes what is required for a realistic calculation of $\rho(T)$. Appendix B describes the experimental problems encountered in high-precision measurements of $\rho(T)$ and how these problems have been solved. Appendix C re-

views the most recent experimental data bearing upon the NFE versus CDW debate.

D. Components of the total resistivity ρ_t that must be considered

According to Bloch's theorem (see, for example, Ashcroft and Mermin, 1976), the eigenstates—called Bloch states—of a one-electron Hamiltonian with a potential that has the perfect periodicity of a Bravais lattice can be written in the form of a plane wave times a function that has the periodicity of the lattice. The wave vector $\mathbf{k}$ of the plane wave characterizes the state of the electron. $\mathbf{k}$ can be assumed to extend either over all of reciprocal space, or else over only the first Brillouin zone—in the latter case, a zone index must be used to specify the appropriate Brillouin zone.

In the absence of scattering of electrons by other electrons, the fact that the Bloch states are eigenstates of the periodic Hamiltonian means that a perfectly periodic lattice has zero electrical resistance; resistance arises from the scattering of the electrons by deviations of the system from perfect periodicity. Table I lists the variety of different components of $\rho(T)$ that are relevant to the analysis of experimental data on the alkali metals, along with their expected forms. In this section, we examine each of these components.

1. The dominant components: $\rho_{\mathrm{Nep}}(T), \rho_{\mathrm{Uep}}(T),$ $\rho_0(c)$, and DMR(c,T)

The two most important scatterers of electrons in pure metals and alloys are phonons and impurities: the electron-phonon component $\rho_{\mathrm{ep}}(T)$ dominates ρ_t at high temperatures; the elastic electron-impurity component $\rho_0(c)$ dominates at sufficiently low temperatures. The other scattering processes that are examined in this review usually constitute only small perturbations on the contribution to ρ_t from one or the other of these two dominant scatterers.

a. Electron-phonon resistivity $\rho_{\mathrm{ep}}(T)$

At high temperatures in a high-purity metal, by far the most important deviation from perfect periodicity is due to vibrations of the metallic ions. The electrons are said to be scattered by phonons (quantized lattice vibrations), leading to a resistivity component which we designate as $\rho_{\mathrm{ep}}(T)$. At all but the lowest temperatures, measurements of $\rho_{\mathrm{ep}}(T)$ in different laboratories generally agree with each other to within a few percent (Bass, 1982), so that the experimental data to be explained are well defined. For metals with relatively simple electronic structures, $\rho_{\mathrm{ep}}(T)$ is found to vary at high temperatures approximately linearly with T and gradually to go over at very low temperatures to a higher power of T.

It is convenient to divide $\rho_{\mathrm{ep}}(T)$ into two components.

$\rho_{\mathrm{Nep}}(T)$—called the normal component—involves scattering of electrons by phonons without the participation of a reciprocal lattice vector [Fig. 1(a)]. $\rho_{\mathrm{Uep}}(T)$—called the umklapp component—involves electron-phonon scattering in which a reciprocal lattice vector does participate [Fig. 1(b)]. The results of realistic calculations of $\rho_{\mathrm{ep}}(T)$ from the melting points of the alkali metals down to a few K will be described in Sec. III.B.

b. $\rho_{\mathrm{Nep}}(T)$

The simplest analytical expression for $\rho_{\mathrm{Nep}}(T)$ is given by the Bloch-Gruneisen model (Bloch, 1930; Gruneisen, 1933):

$$\rho_{\mathrm{Nep}}(T) = K(T/\Theta_D)^5 \int_0^{\Theta_D/T} (z^5 dz)/(e^z - 1)(1 - e^{-z}) , \tag{1}$$

where K is a different constant for each metal (Ziman, 1972). This expression is obtained under the assumptions that the metal of interest has a spherical Fermi surface completely contained within the first Brillouin zone and that it has a Debye phonon spectrum described by the Debye temperature Θ_D, which ranges in value from about 50 K to a few hundred K for different metals. The phonons are also assumed to remain in thermal equilibri-
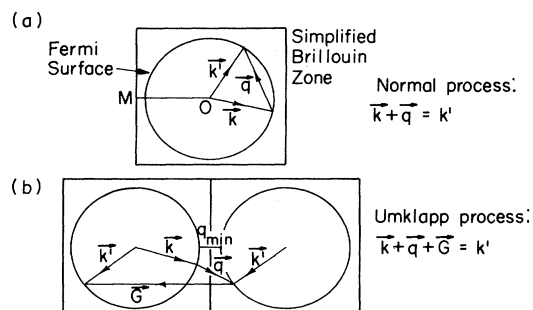
FIG. 1. Schematic illustrations of (a) normal and (b) umklapp electron-phonon scattering for a metal with a spherical Fermi surface completely contained within the first Brillouin zone. **k** and **k'** are electron wave vectors, **q** is a phonon wave vector, and **G** is a reciprocal-lattice vector.

um during the transport process. Equation (1) predicts a linear variation of $\rho_{\mathrm{Nep}}(T)$ with T, from the melting point T_m down to below the Debye temperature, and an ultimate T^5 variation for $T \leq \Theta_D/50$.

Aside from some transition metals, where interband s-d electron-electron scattering produces a low-temperature T^2 variation in $\rho(T)$ (see, for example, Seitz, 1940), the Bloch-Gruneisen model provides a satisfactory

TABLE I. Components of ρ_t that must be considered. Details of these components are given in Sec. I.D.

	Low T	High T	Comments
	Pure metals		
$\rho_{\mathrm{Nep}}(T)$	$+T^5$	$+T$	
$\rho_{\mathrm{Uep}}(T)$	$+T^n e^{-T/\Theta}$ $(n \approx 1)$	$+T$	
Phonon-drag			Reduces $\rho_{\mathrm{Nep}}(T)$ and, to a lesser extent, $\rho_{\mathrm{Uep}}(T)$
$\rho_{ee}(T)$	$+A_{ee}T^2$	Same	
	Alloys		
Dilute			Residual resistivity
$\rho_0(c)$			
$\rho_{iei}(T)$	$+A_I \rho_o T^2$		
Concentrated			
$\rho_{\mathrm{anomalous}}(T)$	$-C\rho_0 T$		
Very concentrated			
$\rho_{\mathrm{localization}}(T)$	$-\rho_0^2 T$		Assumes $\rho(T)$
$\rho_{e\text{-}e\ \mathrm{interaction}}(T)$	$-\rho_0^{5/2} T^{1/2}$		dominated by ρ_{iei} for each
	Perturbations		
Size effects	$\sim +T^n (n \approx 1\text{--}2)$		Generally positive and increasing with increasing T
Dislocations $\rho_{ed}(T)$			
vibrating	$+e^{-T/T_0}$	T	
localized electron states	$+e^{-T/T_0'}$	T^{-n} $(n \geq 1)$	
Kondo effect	$-\ln T$	T^0	

qualitative description of most experimental data on $\rho(T)$ (Seitz, 1940; White and Woods, 1958; Meaden, 1965; Bass, 1982)—especially for the simple metals—if one does not look very closely. For example, if values for $\Theta_D(T)$ are derived from the experimental data for $\rho(T)$, they often display only a modest temperature dependence, and their magnitudes are roughly comparable to those derived from other properties such as heat capacity, thermal expansion, etc. In 1969, before the data described in the present review were taken, most of the data even appeared to be compatible with the predicted T^5 variation at very low temperatures, although the uncertainties in the data were too large to permit reliable determinations of precise powers of T. We shall see in this review that the T^5 behavior of the Bloch-Gruneisen model never actually dominates $\rho(T)$ in any alkali metal (Kaveh and Wiser, 1971).

c. $\rho_{Uep}(T)$

It was known in 1969 that in addition to $\rho_{Nep}(T)$, $\rho_{ep}(T)$ also had to contain an umklapp component $\rho_{Uep}(T)$. But the relative importance of $\rho_{Uep}(T)$ had not been qualitatively established. We shall see in Sec. III.B.2 that $\rho_{Uep}(T)$ dominates $\rho(T)$ in high-purity K from about 1.4 K to well above 4.2 K.

As does $\rho_{Nep}(T)$, $\rho_{Uep}(T)$ should vary approximately linearly with T at high temperatures and go over to a higher power of T with decreasing temperature. But now the higher power of T is not necessarily T^5. For a metal with the spherical Fermi surface illustrated in Fig. 1, Ziman (1954) and Bailyn (1958, 1960) predicted that at still lower temperatures $\rho_{Uep}(T)$ would change from this higher power of T to an exponential form, due to the need for a minimum phonon wave vector to conserve crystal momentum [see Fig. 1(b)]. The temperature at which this transition occurs should generally be lower the larger the distortion of the Fermi surface from a perfect sphere. By 1969, an exponential component had been observed in the low-temperature thermopower, S, of K (Guenault and MacDonald, 1961), but not in $\rho(T)$ in any metal. Its first observation in $\rho(T)$ in K is described in Sec. III.B.2.

d. Residual resistivity—elastic electron-impurity scattering $\rho_0(c)$

The second dominant scatterer of electrons is impurities—either residual impurities in high-purity metals or deliberately added impurities in alloys. We shall specify the impurity concentration c in either atomic percent or atomic parts-per-million (ppm).

The most important characteristic of impurities (as well as of other static defects such as dislocations, grain boundaries, the sample surface, etc.) is simply that they destroy the periodicity of the lattice, thereby producing a temperature-independent term $\rho_0(c)$, called the residual resistivity. For a dilute impurity concentration, $\rho_0(c)$ is proportional to c. At low temperatures, $\rho_0(c)$ represents a large constant background against which the quantity of interest $\rho(T)$ must be measured. This background can be eliminated by taking the temperature derivative of ρ_t.

The presence of impurities with masses and force constants that differ from those of the host metal produces changes in the average Θ_D, which causes the magnitude of $\rho(T)$ to change. For dilute impurity concentrations, these changes are small and difficult to isolate.

e. Matthiessen's rule

In 1864, Matthiessen and Vogt showed experimentally that ρ_t for a variety of alloys could be approximated as simply the sum of $\rho_0(c)$ for the impurities and $\rho_{ep}(T)$ for the pure host metal,

$$\rho_t = \rho_0(c) + \rho_{ep}(T) \ . \tag{2}$$

This simple additivity is called Matthiessen's rule. For strict validity, it requires five conditions to be satisfied: (a) that the impurities not change the properties of the host metal; (b) that there be no interference between the scattering processes due to impurities and to phonons; (c) that scattering due to impurities be temperature independent; (d) that the distribution function of electrons in k space, Φ_k (see Appendix A), be the same for both impurity and pure-metal scattering alone; and (e) that the contributions from all other scatterers—electrons; the sample surface; other point, line, two-dimensional, or three-dimensional defects, etc.—be either negligible or completely temperature independent.

Although condition (a) is always violated, its effects are usually small, as noted just above.

Condition (b), in contrast, seems to be generally valid. A possible exception at high temperatures in concentrated alloys (see, for example, Bass, 1972) will not be of interest in the present review.

Condition (c) can be violated due to higher-order scattering processes, but the resulting contributions to ρ_t are also small. We shall see below that the dominant temperature-dependent term in dilute alloys due to higher-order scattering processes was isolated for the first time in the alkali metals. We shall also examine two additional contributions in more concentrated alloys, one of which is not yet well understood.

Condition (d) is normally the most important limitation on Matthiessen's rule. Large violations of this condition are now known to occur in most metals (see Appendix A, Bass, 1972, and Cimberle et al., 1974). They are included in generalizing Eq. (2) to

$$\rho_t(c,T) = \rho_0(c) + \rho(c,T) \ , \tag{3a}$$

$$\rho_t(c,T) = \rho_0(c) + \rho_{ep}(T) + DMR(c,T) \ , \tag{3b}$$

as shown schematically in Fig. 2. Here $DMR(c,T)$—the deviation from Matthiessen's rule—is the difference be-
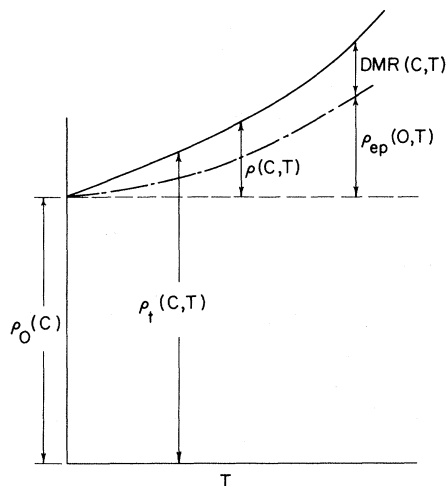
FIG. 2. Schematic drawing of the various resistivities defined in Sec. I.D.1 for a sample containing an impurity concentration c: $\rho_t(c, T)$, its total resistivity; $\rho_0(c)$, its residual resistivity; $\rho(c, T)$, its temperature-dependent resistivity; and DMR(c, T), its deviation from Matthiessen's rule. DMR(c, T) is defined using the temperature-dependent electron-phonon resistivity of an ideally pure metal $\rho_{\mathrm{ep}}(0, T)$.

tween $\rho(c, T)$ and $\rho_{\mathrm{ep}}(T)$ and takes into account all deviations from simple additivity of $\rho_0(c)$ and $\rho_{\mathrm{ep}}(T)$. For simplicity, we usually drop the variable "c" from $\rho(c, T)$, and merely refer to the temperature-dependent component of ρ_t as $\rho(T)$.

Although there are numerous small sources of DMR (such as the changes in Θ_D already noted; Bass, 1972; Cimberle *et al.*, 1974), the primary source of large changes in most metals is generally accepted to be the difference in the angular dependence of $\Phi_{\mathbf{k}}$ for electron-phonon and electron-impurity scattering at low temperatures. At temperatures well below Θ_D, electron-phonon scattering usually produces a strongly angle-dependent (or "anisotropic") $\Phi_{\mathbf{k}}$, primarily because of the angular variation of umklapp scattering. In contrast, electron-impurity scattering normally produces a nearly angle-independent (or "isotropic") $\Phi_{\mathbf{k}}$. The form of $\Phi_{\mathbf{k}}$ can thus change dramatically as the dominant scatterer changes from phonons to impurities. Appendix A describes how changes in $\Phi_{\mathbf{k}}$ give rise to DMR.

Because of their nearly spherical Fermi surfaces, the $\Phi_{\mathbf{k}}$'s of the alkali metals K and Na turn out to be nearly isotropic, both at temperatures where electron-phonon scattering predominates and at temperatures where electron-impurity scattering predominates. We shall see explicitly in Sec. III.B.3 that K manifests only relatively small DMR.

Finally, we turn to item (e)—scattering from entities other than impurities and phonons. Small temperature-dependent resistivities at very low temperatures due to such entities are of great interest, but cannot be examined

in most metals, either because they are swamped by much larger contributions due to electron-phonon scattering and Kondo effects, or because the metals become superconducting. The alkali metals, however, are free from all three of these problems. Moreover, since $\rho_0(c)$ is dominant at low temperatures, $\Phi_{\mathbf{k}}$ should remain isotropic even when these additional resistivity components are present. The metal is then said to be in its "dirty limit," which has the advantage that Matthiessen's rule can be generalized to the statement that the contributions to $\rho(c, T)$ from any different scattering processes are simply additive.

The alkali metals clearly provide a unique opportunity for studying small components of $\rho(T)$ at very low temperatures, provided that sufficient measuring sensitivity is available to resolve these components against the large constant background of $\rho_0(c)$. Appendix B describes how measuring techniques now permit resistances to be measured with precisions of parts in 10^8 and sensitivities of 10^{-15} V (limited only by Johnson noise) to temperatures down to millidegrees Kelvin (mK). In the rest of this section, we describe the small components of $\rho(T)$ in the alkali metals that these techniques have permitted to be isolated at very low temperatures.

2. Additional components of $\rho(T)$ in pure bulk metals

a. Phonon drag

Long before 1969, Peierls (1930) had predicted that $\rho_{\mathrm{Nep}}(T)$ might be greatly reduced at very low temperatures by the dragging of the phonons out of thermal equilibrium by the flowing electrons. Such phonon drag is ubiquitous and important in the thermopower S (see, for example, Blatt *et al.*, 1976), but had not been seen in $\rho(T)$ for any metal by 1969. ρ_{Uep} should also be reduced by phonon drag (see, for example, Leavens and Laubitz, 1975), but not by nearly as much as ρ_{Nep}. In Secs. III.B.3, III.D.3, and III.D.7 we shall examine both the appearance of phonon drag in K (and perhaps also Na) and how it is "quenched" (i.e., greatly reduced) in K by scatterers which return the phonon system to thermal equilibrium. Wiser (1984) has argued that phonon drag in $\rho_{\mathrm{ep}}(T)$ should occur only in the alkali metals, because the Fermi surfaces of other metals permit complex scattering events to relax the phonons back to equilibrium.

b. Electron-electron scattering, $\rho_{\mathrm{ee}}(T)$

The traditional picture was developed by Landau and Pomeranchuk (1936, 1937) and Baber (1937), who showed that electron-electron scattering should contribute to $\rho(T)$ a term of the form

$$\rho_{\mathrm{ee}}(T) = A_{\mathrm{ee}} T^2 , \qquad (4)$$

with the coefficient A_{ee} being constant for a given metal [but see Lawrence and Wilkins (1973), for a comment concerning possible minor deviations from a T^2 form]. A_{ee} contains both normal (A_{Nee}) and umklapp (A_{Uee}) components. Although the actual scattering of electrons by other electrons is predominantly normal scattering, such scattering is so ineffective in contributing to $\rho(T)$ in an alkali metal that A_{Uee} is predicted to dominate A_{Nee}.

A_{ee} has been estimated for the alkali metals by three groups. The initial, pioneering calculation was made by Lawrence and Wilkins (1973), who assumed that the only interaction between electrons was the repulsive Coulomb interaction. They obtained the values of A_{ee} for K and Na listed in the fifth column of Table II. We discuss their calculation in Sec. III.C.

The Lawrence-Wilkins calculation stood unchallenged for nearly a decade, until MacDonald et al. (1981) recalculated A_{ee} using a more sophisticated procedure, a more realistic Fermi surface, and—most importantly—a higher-order phonon-mediated interaction between electrons that MacDonald (1980) had newly shown to be important (Sec. III.D.9). This phonon-mediated interaction increases A_{Uee}, but leaves A_{Nee} nearly unchanged. In K, MacDonald et al.'s more realistic Fermi surface caused the A_{Uee} due to Coulomb scattering alone to decrease by more than an order of magnitude from the value estimated by Lawrence and Wilkins. The phonon-mediated interaction then restored A_{Uee} precisely to the value that Lawrence and Wilkins had calculated. For Na, in contrast, MacDonald et al. found A_{ee} to be an order of magnitude larger than had Lawrence and Wilkins. We view the MacDonald et al. values of A_{ee} for the alkali metals—listed in the fourth column of Table II—as the best available estimates for these metals. Given the difficulty of these calculations, and their sensitivity both to the detailed shape of the Fermi surface and to phonon-mediated scattering, even these best values are probably uncertain by a factor of 2.

Similar values to those of MacDonald et al. were obtained soon afterward by Awasthi and Sathish (1981), using a much less sophisticated procedure based upon equations given by Ziman (1972), which Ziman indicated

should overestimate A_{ee}. This calculation included only Coulomb electron-electron scattering, and treated the fractional umklapp contribution via overlap integrals of the plane-wave conduction electron states with core states. Its values are listed in the sixth column of Table II.

The three calculations just described all assumed that the electron distribution function Φ_k is isotropic at low temperatures because $\rho_0(c)$ is dominated by impurity scattering. These calculations thus all yielded $A_{Uee} \gg A_{Nee}$. Kaveh and Wiser (1980, 1982) have argued that A_{Nee} can become $\gg A_{Uee}$ if a scatterer that produces an anisotropic Φ_k (e.g., dislocations) becomes dominant in $\rho_0(c)$. Since the KW model formed the basis of much of the analysis in the previous reviews, we shall describe it in detail in Sec. III.D.6. One of the important conclusions of the present review is that this model is not important in the alkali metals.

c. Electron-phason scattering

Overhauser (1968, 1973, 1978, 1985a) has ably and vigorously defended for more than two decades the proposition that the ground state of the alkali metals is not the nearly-free-electron (NFE) state which we have so far assumed, but rather a charge-density-wave (CDW) state— a state in which the conduction electrons are distributed nonuniformly within the metal. Appendix C briefly reviews the salient features of the Overhauser picture and contains an analysis of the most recent data bearing upon this picture. If Overhauser is correct, then there should be a contribution to $\rho(T)$ due to scattering of electrons by phasons—phase excitations of the CDW ground state. Bishop and Overhauser (1979; 1981; see Sec. III.D.4) and Bishop and Lawrence (1985; see Sec. III.J) have developed a model for such scattering which can explain some of the anomalous observations that we shall describe below. Another conclusion of this review is that there is no convincing evidence for the presence of this term in $\rho(T)$.

TABLE II. A_{ee} for alkali metals. Comparison between experiment and theory A_{ee} (fΩ m/K^2) is of $A_{ee}T^2$ and B (fΩ m/K^5) is of BT^5.

| | A_{ee} Experiment | | A_{ee} Theory | | | B Theory | |
	Our proposed values	Range of reported values	MacDonald et al., 1981	Lawrence and Wilkins, 1973	Awasthi and Sathish, 1981	Bloch T^5 estimate MacDonald et al., 1981	Crossing Temperature[a] T_c (K)
K	2.1±0.3	0.5→4	1.7	1.7	2.4	25	1.9
Li	28±3	27→33	2.1			0.02	22
Na	≲1.7	1.7→2.2	1.4	0.15	1.0	5	3
Rb	<25		3.5		4.3	270	1.1
Cs			6.7		3.8	1400	0.8

[a] $A_{ee}T_c^2 = BT_c^5$ defines the estimated crossing temperature.

3. Components of $\rho(T)$ in alloys

a. Inelastic electron-impurity scattering $\rho_{iei}(T)$

Koshino (1960a, 1960b, 1963) and P. L. Taylor (1962, 1963, 1964) first predicted that there should exist a temperature-dependent term in electron-impurity scattering due to higher-order scattering processes involving simultaneous emission or absorption of a phonon. This term is really the difference between two contributions, one due to inelastic electron-impurity scattering, and one to a temperature-dependent component of elastic impurity scattering. The second contribution is similar in nature to the Debye-Waller factor in x-ray scattering; in the alkali metals it reduces the first contribution by about half (Kus and D. W. Taylor, 1980). The net result is a contribution to $\rho(T)$ of the form

$$\rho_{iei}(T) = A_I \rho_0 T^2 . \tag{5}$$

Table III contains values of A_I estimated by several different groups, along with experimental values to be discussed below. We briefly examine these estimates.

P. L. Taylor (1964) derived a generally applicable, order-of-magnitude, expression of the form $A_I = \pi^2 \hbar^2 \langle K^2 \rangle / 2Mk_b \Theta_D^3$, where $\hbar$ is Planck's constant divided by 2π, $\langle K^2 \rangle$ is the average of the square of the change in wave vector due to the scattering, M is the mass of the host ion (assumed equal to the mass of the impurity), and Θ_D is the Debye temperature of the host metal (assumed to have an isotropic Debye phonon spectrum). Specific estimates from this expression are given for KRb and KNa, in the fourth column of Table III. These estimates lie in the range $(10^{-6}-10^{-5})/K^2$. From comparison with Table II, ρ_{iei} should become comparable in size to ρ_{ee} in a K-based alloy containing a few percent impurities.

Kus and D. W. Taylor (1980) calculated $\rho_{iei}(T)$ more realistically for KRb and LiMg, taking into account both pseudopotential and mass differences between the impurity and the host metal. As shown in the fifth column of Table III, they found values compatible with P. L. Taylor's result. For several reasons listed by Kus and Taylor (1980), their results should be considered uncertain by about a factor of 2.

Hu and Overhauser (see Hu, 1987) have argued that the value of $\langle K^2 \rangle$ used with the Taylor formula to obtain

the estimate of $\rho_{iei}(T)$ for KRb given in the fourth column of Table III is too large by a factor of 3. The resulting discrepancy with experiment was used to justify the need for an additional contribution due to a many-body effect in the elastic-scattering resistivity, which we briefly discuss in Sec. IV.E. Their estimate of $\langle K^2 \rangle$ was obtained with a simple Gaussian scattering potential that involved an adjustable parameter chosen to make the combination of ρ_{iei} plus their new term approximately fit the experimental data. A Gaussian potential is not a very good approximation for an isoelectronic impurity such as Rb in K, and no independent justification is given for the choice of the adjustable parameter. Nonetheless, their proposed new term warrants further study.

Finally, Mahan and Wang (1989) recently used a phase-shift analysis to obtain bounds on $\rho_{iei}(T)$ for KRb and for LiMg in its cubic phase. The bounds shown in the seventh column of Table III are in satisfactory agreement both with the previous calculations by Taylor and by Kus and Taylor and with the data for KRb and KNa.

In 1969, experimental capabilities were not sufficient for isolating this small term. We shall see in Secs. III.E and IV.E that modern capabilities, combined with the fact that $\rho_{ep}(T)$ disappears in K below 1 K, due to a combination of partial phonon drag plus the exponential falloff in $\rho_{Uep}(T)$, permitted it to be isolated for the first time in alkali metal alloys.

b. Localization and electron-electron interactions in metals with weak disorder

When an alloy becomes highly concentrated, the electronic mean free path begins to approach the interatomic spacing, and it becomes necessary to correct the Boltzmann transport equation for effects of the disorder due to the impurities. This disorder causes the electronic wave functions to become localized and the electron-electron interactions to be modified because the electrons must diffuse through a disordered potential instead of propagating freely between occasional collisions.

In the weak localization limit $(k_f l \gg 1)$, where k_f is the Fermi momentum and l is the electron mean free path), the correction to $\rho(T)$ takes the form (Lee and Ramakrishnan, 1985)

$$\rho(T) = \rho_0^2 (e^2 / \hbar \pi^3)(T^{p/2}/a) , \tag{6}$$

TABLE III. A_I for alkali-metal-based alloys. Comparison between experiment and theory. A_I $(10^{-6}$ K$^{-2})$ is of $A_I \rho_0 T^2$.

| | Experiment | | | Theory | | | |
	Zhao et al., 1989	Lee et al., 1980	Oomi et al., 1985	Taylor, 1964	Kus and Taylor, 1980	Hu and Overhauser, 1985; Hu, 1987	Mahan and Wang, 1989
KRb	11±1	8.5±0.3		14	13	3.6	9.3→15.8
KNa	7±1			14			
LiMg	1.5±0.1		1.6±0.2		3.1[a]		4[a]

[a]Calculations are for bcc structure of Li, while the data are for the 9R structure.

where a is a constant and the dominant scattering process is assumed to contribute a relaxation time varying as T^{-p}. In our alloy samples, the dominant temperature-dependent term in $\rho(T)$ will be due to inelastic impurity scattering, for which $p = 2$.

The correction to $\rho(T)$ due to electron-electron interactions in the presence of strong disorder takes the form (Lee and Ramakrishnan, 1985)

$$\rho(T) = \rho_0^2(e^2/\hbar)(1/4\pi^2)(1.3/\sqrt{2})(\tfrac{4}{3} + 3\tilde{F}/2)\sqrt{T/D} \ .$$
(7)

Here,

$$\tilde{F} = \tfrac{32}{3}[1 + 3F/4 - (1 + F/2)^{3/2}]F \ ,$$

$F = (1/x)\ln(x + 1)$, $x = (2k_f/k_0)$, k_0 is the Thomas-Fermi screening radius, $D = (v_f^2 T/3)$ is the diffusion constant, v_f is the Fermi velocity, and T is the elastic relaxation time.

Under the conditions we study, Eq. (7) is much larger than Eq. (6). We shall see in Sec. IV.F that data for concentrated LiMg alloys appear to approach the prediction of Eq. (7) as ρ_0 becomes large.

4. Components caused by perturbations

The experimental data to be described in this review force us to consider additional components of $\rho(T)$ caused by three perturbations applied to the alkali metals. Here we briefly describe only previously studied models of these components. New models developed in response to new data on the alkali metals are discussed in conjunction with the appropriate experimental data.

a. Temperature-dependent surface scattering, $\rho_{es}(T)$

The standard models for surface scattering in metallic wires at low temperatures involve a dominant temperature-independent term plus a small temperature-dependent term $\rho_{es}(T)$ that increases with increasing T (see, for example, Bass, 1972; Sambles and Preist, 1982; Kaveh and Wiser, 1984; van der Maas and Huguenin, 1987). A general mechanism for such an increase was proposed by Olsen (1958). He noted that the primary current-carrying electrons were those moving along the axis of the thin wire, and pointed out that the resistance of the wire would increase if small-angle electron-phonon scattering events deflected these electrons toward the wire surface, where diffuse scattering would randomize their momenta. Raising T increases the average angle of deflection during scattering and thus increases $\rho_{es}(T)$. The same phenomenon involving large-angle electron-electron scattering occurs in the limit where an electron is scattered only once before colliding with the surface; this is called the Knudsen limit. In the opposite limit, where electrons are scattered very rapidly by each other,

the scattered electrons diffuse to the wire surface, their average mean free path actually increases, and $\rho_{es}(T)$ decreases with increasing T. This phenomenon is called the Gurzhi effect (Gurzhi, 1963, 1964). A nice discussion of these two limits is given by Kaveh and Wiser (1984). In Sec. IV.C we shall examine a decrease in $\rho_{es}(T)$ with increasing T that does not appear to be due to the Gurzhi effect.

b. Temperature-dependent scattering from dislocations, $\rho_{ed}(T)$

The freedom of the alkali metals from the three problems for other metals listed in the discussion of item (e) in Sec. I.D.1 makes them unique for very-low-temperature studies of scattering of electrons by dislocations. As with point defects and the sample surface, the dominant contribution of dislocation scattering to ρ_t is temperature independent. But two types of excitations associated with dislocations have been predicted to produce temperature-dependent contributions, $\rho_{ed}(T)$. The first involves the possible excitation of quantized vibrations of the dislocations (vibrating dislocation model). For excitation of vibrations having a single characteristic frequency, $d\rho_{ed}/dT$ should increase exponentially well below the temperature corresponding to this frequency and become constant at temperatures well above this temperature (Gantmakher and Kulesco, 1975). The second involves possible excitation of electrons bound to dislocations (bound-state models), for which $d\rho_{ed}/dT$ should also first rise with increasing temperatures, and then fall to zero as $1/T^2$ or faster in K above about 0.5 K (Fulde and Peschel, 1972; Gantmakher and Kulesco, 1975). The detailed form of the vibrating dislocation prediction is given in Sec. IV.D, where we examine how well it and the other alternatives can describe the observed behavior of $\rho_{ed}(T)$ in K.

c. The Kondo effect—scattering from magnetic impurities

The term Kondo effect (Kondo, 1964, 1969) refers to unusual electronic transport behavior found in certain host metals when impurities with localized magnetic moments are present. The characteristics of the Kondo effect include (see, for example, Heeger, 1969) (1) a total resistivity that passes through a minimum value with decreasing temperature and then rises logarithmically with decreasing T below this minimum; (2) an associated thermoelectric anomaly; and (3) sensitivity of both the logarithmic resistivity and the thermoelectric anomaly to application of a small magnetic field. The Kondo resistivity component itself, ρ_K, is constant at temperatures high compared to a characteristic Kondo temperature T_K, assumes its logarithmic form over a broad temperature

range that spans T_K, and ultimately becomes constant again at a higher value for $T \ll T_K$. Section IV.B describes the observation of all three of these Kondo-effect characteristics in K samples that are in contact with polyethylene, a material that some early investigators used to protect the K from atmospheric contamination.

E. Overview of $\rho(T)$ in the alkali metals

With this theoretical background in hand, we now summarize the items that we shall examine and the picture that we propose for $\rho(T)$ in the alkali metals. This picture is based upon the assumption of NFE Fermi surfaces. Such Fermi surfaces permit a quantitative understanding of $\rho(T)$ in pure K and dilute K- and Li-based alloys and a qualitative understanding of all other published data. We do not rule out the possibility that a CDW-based model might be able to describe the same data. However, we will argue that a CDW-based explanation is not necessary for any of the properties of $\rho(T)$ that we now believe we understand quantitatively. The general role that we believe electronic-transport studies can play in the NFE versus CDW debate is described in Appendix C.

The most important single conclusion we reach is that, except for the remaining questions concerning phonon drag in $\rho_{ep}(T)$, alluded to above, $\rho(T)$ in bulk unperturbed K and dilute K-based alloys is quantitatively understood from the melting point of K down to 0.3 K. At temperatures above about 2 K, $\rho_{ep}(T)$ is dominant in pure K and well understood. Between about 1 and 0.3 K, $\rho_{ee}(T)$ is dominant and well understood. Only below 0.3 K is $\rho(T)$ dominated by a term that is not yet adequately understood; this term may be due simply to residual defects such as dislocations in the samples. Addition of a dilute concentration of impurities to K produces some quenching of phonon drag in $\rho(T)$ above 1 K. Below 1 K, $\rho_{iei}(T)$ is dominant and well understood.

In Li, Na, and Rb, and in Li-based alloys, we argue that $\rho(T)$ can also be adequately described in the same way as K. However, for these metals we generally will not be able to make quantitative comparisons with theory at low temperatures: for Li and Na primarily because of the changes in their Fermi surfaces due to crystallographic phase changes, and for Rb primarily because its very low Debye temperature keeps $\rho_{ep}(T)$ dominant to below 0.5 K.

In more concentrated KRb and KNa alloys, $\rho_{ep}(T)$ increases by too much to be explained simply by quenching of phonon drag. The source of this increase is not yet clear. At lower temperatures, the KRb and KNa alloys, as well as more concentrated LiMg alloys, display a completely new, very-low-temperature anomaly. It can be parametrized approximately as $-C\rho_0 T$, with the coefficient C having essentially the same value in all three alloys. The source of this term is also still unclear. For the very high values of alloy residual resistivity, $\rho_0 \geq 10^{-7}$

Ω m, achievable with LiMg alloys, the data approach the behavior expected for electron-electron interactions in the presence of strong disorder.

We shall argue that the KW model of changes in the T^2 coefficient of electron-electron scattering due to anisotropic scattering introduced by dislocations or similar extended defects is not important in $\rho(T)$ in the alkali metals. We shall also argue that there is no need to invoke a CDW ground state to explain $\rho(T)$ in pure, bulk metals or dilute alloys. Instead, we shall attribute the anomalous behaviors that gave rise to these two models to effects of perturbations inadvertently applied to the samples. Some of the anomalies are attributed to a completely unexpected Kondo-like effect which appears in samples encased in polyethylene tubes. Others are attributed to a highly unusual "size effect," which occurs in thin, high-purity wires. This effect is enhanced by, and may also require, the presence of some surface contamination. Finally, we argue that deformation of K does not substantially change the T^2 component of $\rho(T)$ as proposed by Kaveh and Wiser, but rather introduces a new contribution to $\rho(T)$. In the simplest cases, the observed behavior is qualitatively compatible with scattering of electrons from vibrating dislocations; in other cases, scattering from electronic states localized on the dislocation must be included to reproduce the form of the data.

TABLE IV. Two examples of impurities in pure K. Top part: emission spectrographic analysis of potassium (as chloride). This material regularly yielded specimens of residual resistivity about 1 nΩ cm, which corresponds to an impurity of about 10 ppm; one can deduce that either the figures are pessimistic upper limits, or that little of the impurity is in solution. Bottom part: manufacturers chemical analysis of potassium (Callery Chemical Division of MSA).

Element	ppm	Element	ppm
	Gurney and Gugan, 1971		
Si	12	Mo,Ba	<3
Na	4	Al, Mg,	<2
Cu	2	Mn, V, Be	<1
Ca	1	Ag	<1
B, Zr	<10	Li, Rb, Cs	Not detected
Fe, Co, Sn,		O_2,C	Not detected
Pb, Cr, Ti	<5	Total	<88
Ni			
	Haerle et al., 1986		
Fe	<5	Ni	<5
B	<10	Mo	<3
Co	<5	V	<1
Mn	1	Be	<1
Al	<2	Ag	<1
Mg	2	Sr	<1
Sn	<5	Ba	<3
Cu	<1	Ca	8
Cr	<5	Na	15
Si	25	Pb	<5
Ti	<5	Zr	<10

TABLE V. Sample and measurement parameters.

Reference	Metal	Source	Nominal purity	RRR	Gas	Contact material	L(m)
Gugen, 1971	K	MSA[c]	99.95	1000→8000	He	?	0.2
Ekin, 1971; Ekin and Maxfield, 1971	K	MSA[c]	99.95	100→8000	He	Bakelite,	1
Krill, 1971	Li	KLI[d]	99.98	1400	He	Bakelite, Vaseline	0.5
van Kempen et al., 1975, 1976, 1981	K	KLI[d]	99.97	400→8000	He	Polyethylene	1
Rowlands et al., 1978	K	MSA[c]	99.95	1500→6000	He	Teflon	1.8
Levy et al., 1979	K Na	?		2000→14000 5000→6000	He, air, oil, Ar, vacuum	Polyethylene	1
Lee et al., 1980	K KRb	MSA[c]	99.95	20→4000	Ar	Free hanging	0.04
Sinvani et al., 1981	Li	?	99.9	800	He	Bare	4.3
Pratt et al., 1981 Lee et al., 1982, Pratt, 1982	K	MSA[c]	99.95	3500→5000	Ar	Free hanging	~0.05
van Vucht et al., 1982, 1986	K	MSA[c]	99.95	1800→5000	He	Free hanging	0.1
Yu et al., 1983; Yu, 1984	Li Rb	Atomergic Chemicals MSA[c]	99.99 99.95	875→1150 300→400	He	Free hanging	0.04
Haerle et al., 1983, 1986	K, KRb	MSA[c]	99.95	700→5500	He	Free hanging	0.04
Yu, Bass, and Pratt, 1984; Yu, 1984	Na	MSA[c] J. Garland	99.95 99.95	400→4800	He	Free hanging	0.04
Yu, Haerle, et al., 1984b	K, KRb	MSA[c]	99.95	800→6000	He	Free hanging	0.005→0.04
Yu, Haerle, et al., 1984a, Yu et al., 1985, 1989	K KRb	MSA[c]	99.95	2400→7000	He	Polyethylene, Teflon	0.04
Bass et al., 1984, 1986	KRb, KNa, LiMg	MSA[c] Atomergic Chemicals	99.95[a] 99.99[b]	4→1700	He	Free hanging	~0.02
Zhao et al., 1988	K, KRb	MSA[c]	99.95	700→4800	He	Free hanging	0.005→0.04
Yin, 1987; Yin et al., 1989	K, KRb	MSA[c]	99.95	650→4800	Ar	Free hanging	0.04
Zhao et al., 1989	KRb, KNa, LiMg	MSA[c]	99.95	4→1700	He	Free hanging	~0.02

[a]For K, Rb, and Na.
[b]For Li.
[c]MSA=Mine Safety Appliances Co. (Callery Chemical Division)
[d]KLI=Koch Light Industries

II. EXPERIMENTAL BACKGROUND

A. Problems of sample purity and contaminability

Working with the alkali metals involves formidable experimental difficulties.

(1) They are not available in ultrahigh purity. Typical purities quoted are 99.95% and 99.97% (see Table V below). Table IV contains manufacturer-supplied lists of impurities for typical batches of K. However, when the alkali metals are cooled slowly, they can achieve residual resistance ratios [RRR=R(295 K)/R(0 K) =5000–10 000] that are much higher than expected for such purities. For example, using a typical resistivity of 10 nΩ m/at. % impurity (Bass, 1982; Gugan, 1982), a RRR=7000 would correspond to an impurity content of only about 10 parts per million for K [ρ(295 K)=72 nΩ m; Bass, 1982]. Such high RRR's have been attributed to clustering of impurities during the slow cooling (Gugan, 1971; 1982; Gugan et al., 1989), so that the im-

TABLE V. (Continued).

d (mm)	I(A)	Precision	Sensitivity (V)	$T_{minimum}$	Additional information
1	?	5×10^{-5}		1.2	Extruded under oil
1.2, 2.2	< 1	2×10^{-4}	$\sim 10^{-9}$	1.1	Extruded under oil
0.5	?	$\sim 10^{-3}$	10^{-8}	1.3	
0.9	0.3	$\lesssim 10^{-6}$	10^{-12}	1.1	Vacuum pumped, in polyethylene tube
0.8	0.01	$\lesssim 10^{-6}$	$< 10^{-12}$	0.5	
1	0.9	$\geq 10^{-6}$	?	1.1	In polyethylene tubes
3	0.02, 0.05	$\sim 10^{-7}$	10^{-15}	< 0.1	
3	0.9	$\gtrsim 10^{-6}$		1.1	
0.9→3.0	0.02, 0.05	$\sim 10^{-7}$	10^{-15}		Includes one vacuum-pumped sample.
3	0.3	5×10^{-6}	10^{-12}	0.9	Strained by torsion
3	0.05	$< 10^{-7}$	10^{-15}	0.07	
1.5					
0.9	0.05	$< 10^{-7}$	10^{-15}	0.08	Strained by squashing.
1.0	0.05	$< 10^{-7}$	10^{-15}	0.1	
0.09→1.5	0.02	$\leq 10^{-7}$	10^{-15}	0.1	"Size effect"
0.9	0.05	$< 10^{-7}$	10^{-15}	0.1	In polyethylene Kondo-like anomaly
1→3	0.02→0.05	2×10^{-8}	10^{-15}	0.1	Alloy anomaly
0.06→1.0	0.02	2×10^{-8}	10^{-15}	0.1	"Size effect"
2	0.05	$< 10^{-7}$	10^{-15}	0.02	By torsion
1→5	0.02→0.05	2×10^{-8}	10^{-15}	0.1	Alloy anomalies

purities produce a smaller residual resistance R(0 K) than they would if they were separated. Gugan (1982) noted that RRR's for slowly cooled samples from a given batch of K were usually reproducible to within about 10%, but that RRR's for different batches could differ by a factor of 2.

(2) The alkali metals are subject to contamination in air, and thus must either be enclosed in a sample can filled with an inert atmosphere or be encapsulated in an inert material. In Sec. IV, we shall see that few solids appear to be completely inert to K.

(3) Upon cooling, some of the alkali metals undergo martensitic phase transitions to crystal structures with more complex Fermi surfaces than those for the simple bcc structure. Li changes to a $9R$ structure (Overhauser, 1984; Smith, 1987) at about 75 K (Bass, 1982). Na changes to a mixture of fcc and hcp at about 50 K (Bass,

1982; Berliner et al., 1989). Rb may change at 4 K upon deformation (Templeton, 1982). It has even been suggested that at low temperatures K contains premartensitic domains (Wilson and de Podesta, 1986; Blaschko et al., 1988), but this proposal remains controversial.

B. Table of information about sample and measurement parameters

The problems just noted in handling the alkali metals, and the likelihood that perturbations—perhaps even subtle ones—play an important role in a variety of anomalous behaviors that are observed in the very-low-temperature transport properties of the alkali metals, make it of great importance to characterize carefully and fully the the properties of a given set of samples and to

know the conditions under which they were measured. It is also helpful to know the measuring capabilities employed, both to permit choices to be made between competing sets of data on the basis of the quality of the procedures used and to see how these capabilities have evolved. In Table V we list for each experiment the following information, where available: (1) the authors and the year the paper was published; (2) the metal or metals studied; (3) the source of the metal used, and (4) its nominal purity; (5) the range of RRR's for the samples studied; (6) the atmosphere(s) in which the samples were prepared and/or measured (He, Ar, or vacuum); (7) any other material that was in contact with the sample gauge length between the potential leads; (8) the typical sample length L between the potential leads; (9) the sample diameter(s) d; (10) the measuring current(s) I_m; (11) the measuring precision; (12) the measuring sensitivity; (13) the lowest measuring temperature; (14) any additional information that is unusual and thus might be important.

C. Alternative graphs:
$\rho(T)$, $d\rho/dT$ and $(1/T)(d\rho/dT)$

The experimentalist strives to present data in a way that assists the reader to comprehend its form without being misled. Since the only curve that is immediately recognizable is a straight line, coordinates are often chosen to make the data fall on such a line if they conform to a particular equation. Since straight-line behavior can be forced by choice of adjustable parameters, parameter-free graphical presentations are preferred. In this section, we describe the alternative ways in which experimental data are plotted in this review. From $\rho_t = \rho_0 + \rho(T)$ we wish to isolate $\rho(T)$.

At low temperatures, ρ_t is dominated by the unknown parameter ρ_0, even in the highest-purity samples. If ρ_0 is determined approximately by extrapolation to $T = 0$ K, then any uncertainties in this extrapolation appear also as uncertainties in $\rho(T)$, and the quality of the data analysis is limited by the assumptions made in the extrapolation.

ρ_0 can be eliminated from the problem by taking differences between $\rho(T)$ at adjacent temperatures and forming the temperature derivative $d\rho/dT$. The uncertainties in $d\rho/dT$ are then determined only by uncertainties in the measurements of $d\rho$ and dT. Appendix B shows how modern techniques now permit reliable determinations of very small changes in both ρ (parts in 10^8) and T (parts in 10^3 to 10^4).

At very low temperatures, we shall often be interested in the question of whether $\rho(T)$ is dominated by $\rho_{ee}(T)$, which should vary as T^2. For perfect T^2 behavior, a plot of $d\rho/dT$ versus T would yield a straight line passing through the origin. When deviations from a straight line occur at very low temperatures, it is useful also to examine the quantity $(1/T)(d\rho/dT)$, for three reasons. (1) For a purely T^2 variation of $\rho(T)$, $(1/T)(d\rho/dT)$ should yield a horizontal straight line. The presence or absence of a horizontal straight line is often more immediately evident than whether a line with a finite slope is straight and passes through the origin, especially when the lowest-temperature data point is far from the origin. (2) Deviations from T^2 behavior are particularly easy to recognize as deviations from a horizontal line. (3) Such deviations are relatively enhanced as $T \rightarrow 0$ K, due to the divergence of $1/T$. On the other hand, exactly this sensitivity to anomalies can make such a graph deceptive for data taken over too narrow a temperature range.

To demonstrate both the advantages and the pitfalls of these alternative graphs, Fig. 3 compares graphs of $\rho(T)$ versus T^2 with graphs of $d\rho/dT$ and $(1/T)(d\rho/dT)$ versus T, for real data. For the $\rho(T)$ plots, convenient values of ρ_0 have been subtracted from each set of data. (1) The solid lines represent a perfect T^2 variation. In this ideal case, all three plots permit an immediate visual identification of this variation. (2) The open circles are experimental data for high-purity K. $\rho(T)$ for these data is dominated by an exponential temperature variation above about 1.3 K, a T^2 variation between about 1.3 and 0.3 K, and a variation below 0.3 K in which the derivative becomes larger with decreasing temperature than the extrapolation from the T^2 horizontal straight line. Note how the $(1/T)(d\rho/dT)$ plot exaggerates the size of the anomaly relative to the $d\rho/dT$ and $\rho(T)$ plots. (3) The open squares are experimental data for a sample of deformed K. In this case, the $d\rho/dT$ plot gives the most useful information concerning the complex form of these data. Note how, if the data extended down to only about 1 K, one might erroneously conclude from any of these three curves that the low-temperature behavior was simply T^2. We shall encounter examples of such difficulties in early data. (4) Finally, the crosses are experimental data for K in contact with polyethylene. The values of $d\rho/dT$ decrease more rapidly with decreasing temperature than expected for $\rho(T) \propto T^2$ and eventually become negative, corresponding to a resistivity minimum. Again, note that if the data extended down to only 1 K, one might well conclude that the low-temperature behavior is simply T^2.

In this review, we plot whichever of $\rho(T) = \rho_t - \rho_0$, $d\rho/dT$, or $(1/T)(d\rho/dT)$ was published. We occasionally plot more than one form when such additional information helps to clarify a point.

III. REVIEW OF PRIOR DATA AND THEORIES

In this section we review the data on $\rho(T)$ in the alkali metals published prior to 1984–1985, when the three above-mentioned reviews appeared. Data on alkali metals in glass tubing—e.g., measurements of $\rho(T)$ in Cs at low temperatures (Aleksandrov et al., 1968)—are omit-

ted, because encapsulation in glass is known to produce erroneous results (Dugdale and Gugan, 1963). We also review the theories spawned by these data. The presentation begins at high temperatures and works down to below $T = 0.1$ K. It is chronological, except where departures are required for continuity. A list of the ex-

pected components of $\rho(T)$ at low T has been given in Sec. I.D and Table I. An outline of what is required for a realistic calculation of $\rho(T)$ is given in Appendix A, much of which is abstracted from Ziman (1972), to which the reader is referred for additional details, justifications, etc. Appendix A should not be essential for understand-
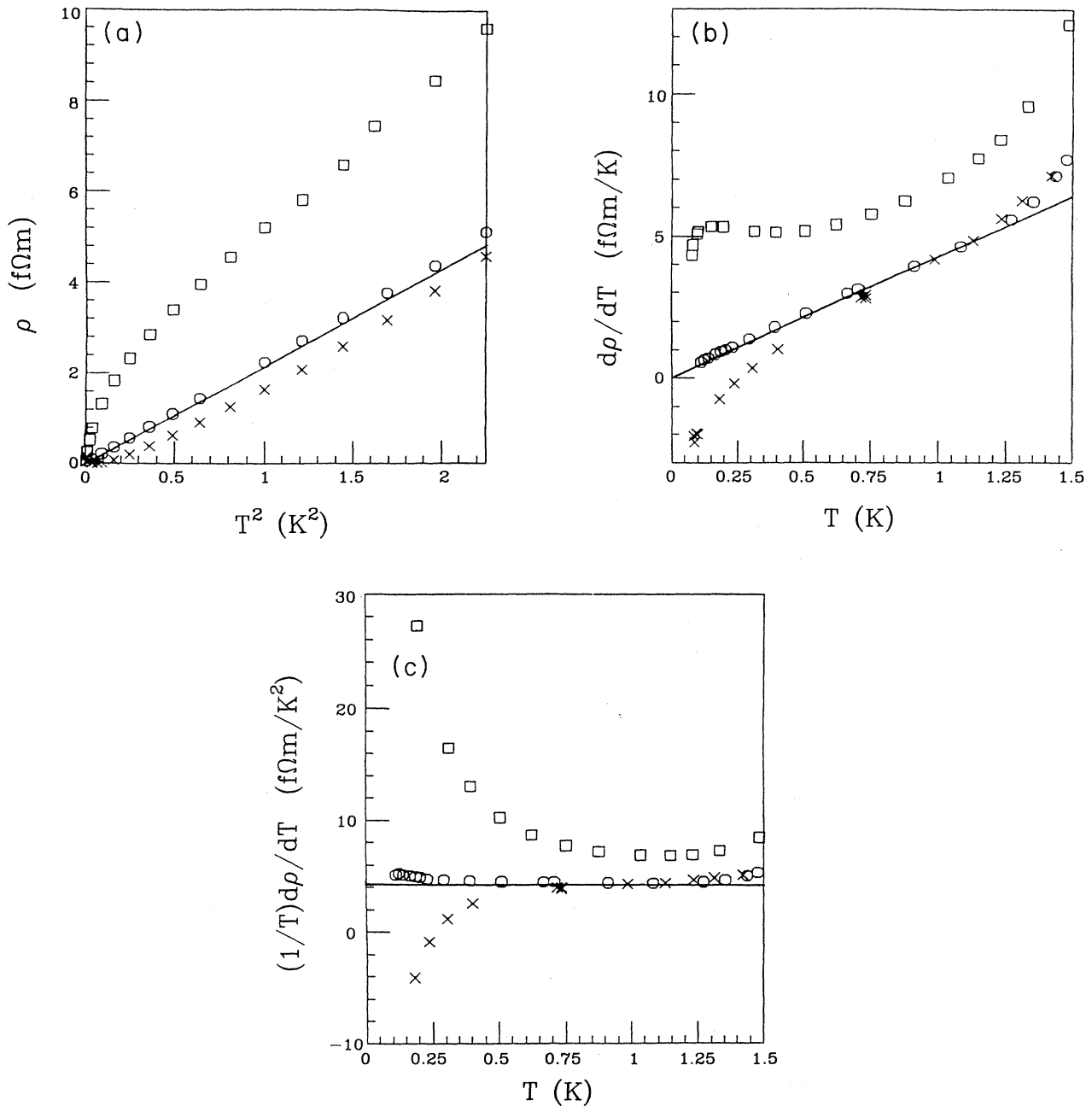

FIG. 3. Comparison of $\rho(T)$ vs T^2 and $d\rho/dT$ and $(1/T)(d\rho/dT)$ vs T: ——, an ideal T^2 variation; ○, a high-purity K sample, □, a strained K sample; ×, a K sample in polyethylene.

ing the main issues to be covered in this review, but will be helpful to the reader who wants to understand the subtleties of sometimes complex theoretical analyses.

A. Overview

As indicated by the quote from Ziman that begins this review, the understanding of $\rho(T)$ in metals in 1969 was qualitative in nature. By 1961, it was known from magnetoresistance measurements (Garcia-Molinar, 1958) that the Fermi surfaces of Na and K were nearly spherical and that those of the other alkali metals were more distorted. But details of the shapes of both these Fermi surfaces and the lattice spectra for the alkali metals were not yet available. Collins and Ziman (1961) investigated what conclusions could be drawn about the Fermi surfaces of the alkali metals from their zero-field transport properties if it was assumed that their lattice spectra were very similar. They concluded that the data were compatible with nearly spherical Fermi surfaces for both Na and K and much more distorted Fermi surfaces for the other metals. But, even in Na, they were unable to fit $\rho(T)$ very well.

During the 1960s, the development of the de Haas–van Alphen effect as a quantitative tool, as well as improvements in inelastic neutron scattering techniques, led to detailed information about the shapes of the Fermi surfaces of the alkali metals (see, for example, Cracknell, 1969) and about their phonon spectra along high-symmetry directions (see, for example, Cowley et al., 1966). Theoretical techniques and computing capabilities also rapidly improved, to where realistic, quantitative calculations of $\rho(T)$ for the alkali metals without adjustable parameters became feasible. $\rho_{ee}(T)$ was calculated for K and Na in 1973, $\rho_{ep}(T)$ was calculated for all of the alkali metals from 1976–1980, and $\rho_{iei}(T)$ was calculated for KRb and for the bcc structure of LiMg in 1980. During this same decade, measuring precisions of resistances improved in stages to 10^{-4}, 10^{-6}, 10^{-7}, and, finally, to almost 10^{-8}. As a consequence, measurements of $\rho(T)$ in the alkali metals with uncertainties of a few percent were successively extended to 2 K, 1 K, 0.5 K, and—by 1980—to below 0.1 K. This section of the review tells the story of the interaction between experiment and theory from 1970 until 1984–1985.

Section III.B.1 covers calculations of $\rho_{ep}(T)$ that fit experimental data on K to within a few percent from its T_m down to 20 K with no adjustable parameters whatever. The fits to the other alkali metals are also described.

Section III.B.2 describes how improvements in measuring sensitivity to 10^{-4} led to observations of the predicted exponential decay of umklapp electron-phonon scattering in K just below 4 K, and of the predicted T^2 electron-electron component in Li below 10 K. The K data also led to a sustained debate over the phenomenon of phonon drag in $\rho(T)$, which is covered in Secs. III.B.3

and III.D.3. Additional physics underlying quenching of phonon drag by dislocations is discussed in Sec. III.D.7.

Section III.C contains a detailed description of the first realistic calculation of ρ_{ee} in simple metals—made in 1973—which formed the basis for analyses of new low-temperature data obtained a few years later. This calculation was not improved until 1980 (Sec. III.D.9).

A series of surprising experimental results on $\rho(T)$ in K in the vicinity of 1 K were obtained when improvement of experimental precision to 10^{-6} allowed accurate measurements of $\rho(T)$ to be extended to $\simeq 1$ K. Two groups (Secs. III.D.1 and III.D.5) reported finding the apparent T^2 variation expected for electron scattering, but with coefficients that varied substantially from sample to sample and even on a single sample subjected to different treatments. A third group (Sec. III.D.2) reported that their data were fit better by a $T^{3/2}$ variation. Two models were quickly developed to explain these results. An initial CDW-based model developed to explain the $T^{3/2}$ behavior is described in Sec. III.D.4; its later generalization to include ρ_{ee} is covered in Sec. III.J. An alternative model to describe the apparent variations in the magnitude of A_{ee} is reviewed in Sec. III.D.6. This latter model was used as the basis for the analyses of $\rho(T)$ in the alkali metals given in three review articles published in 1984–1985. These reviews are discussed in Sec. III.I.

Lastly, the achievement of precisions $\leq 10^{-7}$ permitted the extension of measurements of $\rho(T)$ to $T < 0.1$ K. These measurements led to the isolation of ρ_{iei} and to the beginnings of a clarification of the sources of the surprising behaviors of $\rho(T)$ in K noted in the preceding paragraph. Measurements on pure bulk K and dilute KRb alloys are described in Sec. III.E. Measurements on Li, Na, and Rb are discussed in Sec. III.F. Measurements on thin K wires, described in Sec. III.H, began to clarify the source of the $T^{3/2}$ anomaly reported by Rowlands et al. The first measurements of deformed K and KRb wires are described in Sec. III.G.

We now turn to a more detailed, chronological analysis of this material.

B. Measurements before 1972 and theory outgrowths

1. Measurements with precisions poorer than 10^{-4} and calculations of $\rho_{ep}(T)$

Chi (1979) and Bass (1982) have collected together the best data on $\rho(T)$ in the alkali metals from their melting temperatures T_m down to below 4 K. $\rho(T)$ is dominated by $\rho_{ep}(T)$ over almost all of this temperature range. In this section, we show that $\rho_{ep}(T)$ in K is well understood from the melting point down to below 20 K.

From 1976 to 1980, a group of scientists located in Canada carried out a pioneering set of calculations of

$\rho_{\mathrm{ep}}(T)$ based upon the assumption that the Fermi surfaces of the alkali metals were all perfect spheres. These calculations, which used no adjustable parameters whatever, used a first-principles pseudopotential with sophisticated treatments of both screening and a many-body vertex function designed to take nonlocal effects in the pseudopotential into account. The phonon frequencies for the metal were calculated numerically using this pseudopotential, and effects of umklapp electron-phonon scattering were included. Numerical calculations of $\rho(T)$ used the simple electron trial function [Eq. (A7b)] appropriate to a metal with a spherical Fermi surface.

The first calculation, by Shukla and R. Taylor (1976) for bcc K and bcc Na from T_m down to 20 K, neglected both Debye-Waller and multiphonon processes, both of which are expected to be most important between Θ_D and T_m. As shown in Table VI, the percentage difference between the calculated and measured values of $\rho(T)$ for K at constant density varied from -1.3% at 295 K to $+6\%$ at 20 K. For Na, this difference varied from -5% at 295 K to $+8.5\%$ at 50 K, about where the Na crystal structure transforms from bcc to $9R$. Below 50 K, the difference increased to $+33\%$ by 20 K. Shukla (1980) and Shukla and VanderSchans (1980) later showed that Debye-Waller and multiphonon processes make opposite

TABLE VI. High-temperature data for K and Na compared with calculations. Ideal resistivities of K and Na (bcc) at constant density ρ_i' and at constant pressure ρ_i (units of 10^{-8} $\Omega\,\mathrm{cm/K}$). Experimental data from Dugdale and Gugan (1960, 1962). Calculations from Shukla and Taylor (1976).

T (K)	K		Na	
	Calc.	Exp.	Calc.	Exp.
	ρ_i'/T	ρ_i'/T	ρ_i'/T	ρ_i'/T
20	0.568	0.537	0.110	0.083
30	0.980	0.944	0.301	0.245
40	1.244	1.224	0.509	0.441
50	1.404	1.411	0.682	0.628
60	1.504	1.534	0.812	0.782
70	1.570	1.612	0.909	0.895
80	1.615	1.661	0.980	0.985
90	1.647	1.692	1.034	1.054
100	1.670	1.716	1.075	1.108
120	1.701	1.744	1.132	1.180
140	1.721	1.758	1.168	1.223
150	1.728	1.762	1.181	1.238
160	1.733	1.765	1.193	1.250
180	1.742	1.769	1.209	1.269
200	1.748	1.772	1.222	1.283
250	1.758	1.778	1.242	1.305
295	1.763	1.786	1.252	1.316
	ρ_i/T	ρ_i/T	ρ_i/T	ρ_i/T
90	1.789	1.790	1.074	1.084
160	2.006	2.032	1.317	1.354
295	2.437	2.436	1.580	1.610
330	2.520			
361			1.722	

contributions to $\rho(T)$ and nearly cancel in both K and Na. Inclusion of such effects reduced the differences between calculation and experiment: e.g., at 295 K from -1.3% to -0.2% for K and from -5% to -1% for Na. Given the complexity of transport integrals, these quantitative agreements for K and Na are very impressive.

Highly successful fits with no adjustable parameters were also made to the high-temperature thermopowers S of K and Na (Leavens and R. Taylor, 1978; R. Taylor and MacDonald, 1986), which are also dominated by electron-phonon scattering. Comparable fits to S at low temperatures are not possible because of the presence of very strong effects of phonon drag (see, for example, Blatt et al., 1976) as well as complex higher-order "Nielsen-Taylor" effects (Blatt et al., 1976) and many-body effects (Opsal, Thaler, and Bass, 1976; Thaler, Fletcher, and Bass, 1978) which do not appear in $\rho(T)$ (Opsal, Thaler, and Bass, 1976).

The success of these $\rho_{\mathrm{ep}}(T)$ and S calculations demonstrates that the fundamental physics underlying electron-phonon scattering in K and Na is quantitatively understood—for K down to below 10 K as we discuss further in Sec. III.B.3.

Similar calculations for Rb and Cs were made by Taylor and MacDonald (1980), again neglecting Debye-Waller and multiphonon effects and using no adjustable parameters. In Rb [Fig. 4(a)], the percentage differences ranged from -10% at 100 K to $+10\%$ at 50 K. In Cs [Fig. 4(b)], they were -20% at 100 K and $+35\%$ at 50 K. In both metals the authors attributed the fact that the calculations were too large at low temperatures primarily to DMR due to the energy dependence (and presumably also angular dependence) of the electron distribution function, which were neglected in the calculation (see Appendix A and Sec. III.B.3). They noted that there were several reasons why the calculations might be too low at high temperatures: (a) softening of phonon modes with increasing temperature; (b) incomplete cancellation of Debye-Waller and multiphonon effects; (c) failure to include core-orthogonalization components of the wave functions "since Rb and especially Cs ion cores occupy a significant fraction of the metallic volume"; and (d) distortions of the Fermi surfaces from sphericity, which are especially large in Cs.

Taylor and MacDonald (1980) also examined effects of different crystal structures on $\rho_{\mathrm{ep}}(T)$ in Li and Na by calculating $\rho_{\mathrm{ep}}(T)$ for both bcc and fcc structures. $\rho_{\mathrm{ep}}(T)$ was always larger for the bcc structure. In Na [Fig. 4(c)], the changes were generally modest, both from 300 to 30 K and below 3 K (i.e., $=10–20\%$ estimated from a small graph), but increased to more than 100% near 9 K. In Li [Fig. 4(b)], the changes ranged from a low of 30% at 300 K to well over 100% below 40 K. The calculated $\rho_{\mathrm{ep}}(T)$ for Li in the bcc structure fell below experiment by almost 100% at 300 K, dropping to about 20% at $\simeq 80$ K, where the bcc-to-$9R$ transition occurs. Presumably most of the same complicating effects noted for Rb and Cs are

also present in Li, especially those due to distortion of the Fermi surface from spherical.

Having demonstrated that $\rho_{ep}(T)$ is well understood in K from T_m down to at least 20 K, we turn next to studies
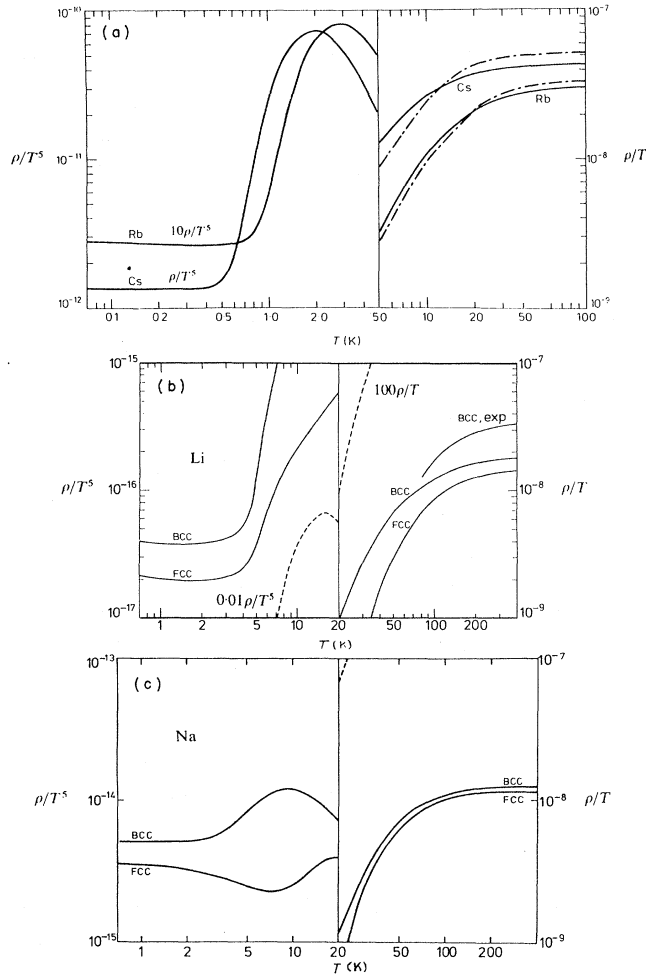

FIG. 4. Calculations of electron-phonon resistivity $\rho_{ep}(T)$ for Rb, Cs, Li, and Na. Units for $\rho_{ep}(T)$ are ohm-cm. The solid curves are the calculations; the dashed or dot-dashed curves give the experimental data recommended by Chi (1979). (a) Rb and Cs. For $T > 5$ K, the quantity plotted is $\rho_{ep}(T)/T$ for both Rb and Cs. For $T < 5$ K, the quantities plotted are $\rho_{ep}(T)/T^5$ for Cs and $10\rho_{ep}(T)/T^5$ for Rb. Note that the limiting T^5 variation at the very lowest temperatures persists only to about 0.7 K in Rb and about 0.4 K in Cs. The rise in $\rho_{ep}(T)/T^5$ above these temperatures is due to the onset of umklapp scattering. After Taylor and MacDonald, 1980b. (b) Li in bcc and fcc phases. For $T > 20$ K, the quantity plotted is $\rho_{ep}(T)/T$. The dashed curve in this region shows recommended experimental data for $100\rho_{ep}(T)/T$ for fcc Li. For $T < 20$ K, the quantity plotted is $\rho_{ep}(T)/T^5$. The dashed curve here is $0.01\rho_{ep}(T)/T^5$ for experimental data for bcc Li. After Taylor and MacDonald, 1980a. (c) Na in bcc and fcc phases. For $T > 20$ K, the quantity plotted is $\rho_{ep}(T)/T$. The dashed curve in this region shows $100\rho_{ep}(T)/T$ for experimental data for fcc Na. For $T < 20$ K, the quantity plotted is $\rho_{ep}(T)/T^5$. After Taylor and MacDonald, 1980a.

of $\rho_{ep}(T)$ below 20 K and, in fact, mostly below 4.2 K. Prior to 1971, resistivity measurements on the alkali metals at temperatures below 4 K were limited by available voltage sensitivities to measuring precisions of 1% to 0.1%. The best such measurements gave conflicting results. Garland and Bowers (1968) reported T^5 variations in both Na and K [Fig. 5(a)] below about 4 K. In contrast, Woods (1956), and Tsoi and Gantmakher (1969) reported faster variations—more like T^6—for Na and K [Fig. 5(a)], respectively. These data were not accurate enough to give detailed guidance for theoretical analysis. Nonetheless, Kaveh and Wiser (1971) claimed that new variational calculations which they had made gave precise agreement with the temperature dependence of the data of Woods on Na, provided that electron-phonon umklapp scattering was properly included, and with the temperature dependence of the data of Garland and Bowers on K, provided that both umklapp scattering and phonon drag were properly included. With historical perspective, we can now see that Kaveh and Wiser's reported agreement with the data of Garland and Bowers for K must have been a fortuitous consequence of approximations that Kaveh and Wiser made, since within a few months new, higher-precision measurements of $\rho(T)$ for K yielded a very different temperature dependence from that reported by Garland and Bowers, as we describe next. These new data showed clearly that Kaveh and Wiser were right that umklapp scattering was present and important in K. It took five more years before additional data showed that their assertion that phonon drag was important in K up to at least 2 K was also correct. We shall see that this assertion remained highly controversial in the interim.

2. Measurements with 10^{-4} precision: umklapp electron-phonon scattering

Gugan (1971), and, independently, Ekin and Maxfield (1971), extended measurements of $\rho(T)$ for high-purity K [values of RRR = $R(300$ K$)/R(0$ K$)$ ranging from 300 to 8000] down to 1.1–1.2 K with measuring precisions of about 1 part in 10^4 [Figs. 5(a) and 5(b)]. Gugan's measurements extended up to 4.2 K, and Ekin and Maxfield's up to 20 K. The two sets of data were in excellent agreement, and both investigators reached very similar conclusions.

(a) To obtain the best RRR's ($= 7000–8000$), both found that they had to cool their samples slowly. Either rapid cooling or deformation caused the RRR's of the samples to decrease, but the decreases were reversible with very modest anneals. After rapid cooling, Ekin and Maxfield found that the highest RRR could be restored by taking an hour to cool the sample from room temperature to 4.2 K. After deformation, Gugan was able to restore a high RRR by a series of anneals at increasing temperatures, concluding with only 10 minutes at 200 K. In a more complete study of the production and annealing out of deformation-induced defects in K, Gurney and

Gugan (1971) found that plastic deformation produced approximately equal increases in ρ_0 due to vacancies and dislocations. Deformation by 25% produced a vacancy concentration of about 1 part in 10^5 (comparable to the

impurity concentration in solution in high-purity K) and a dislocation density of about $10^{14}/m^2$. Free vacancies annealed out below 20 K, detrapping of vacancies by impurities occurred to perhaps as high as 80 K, and disloca-
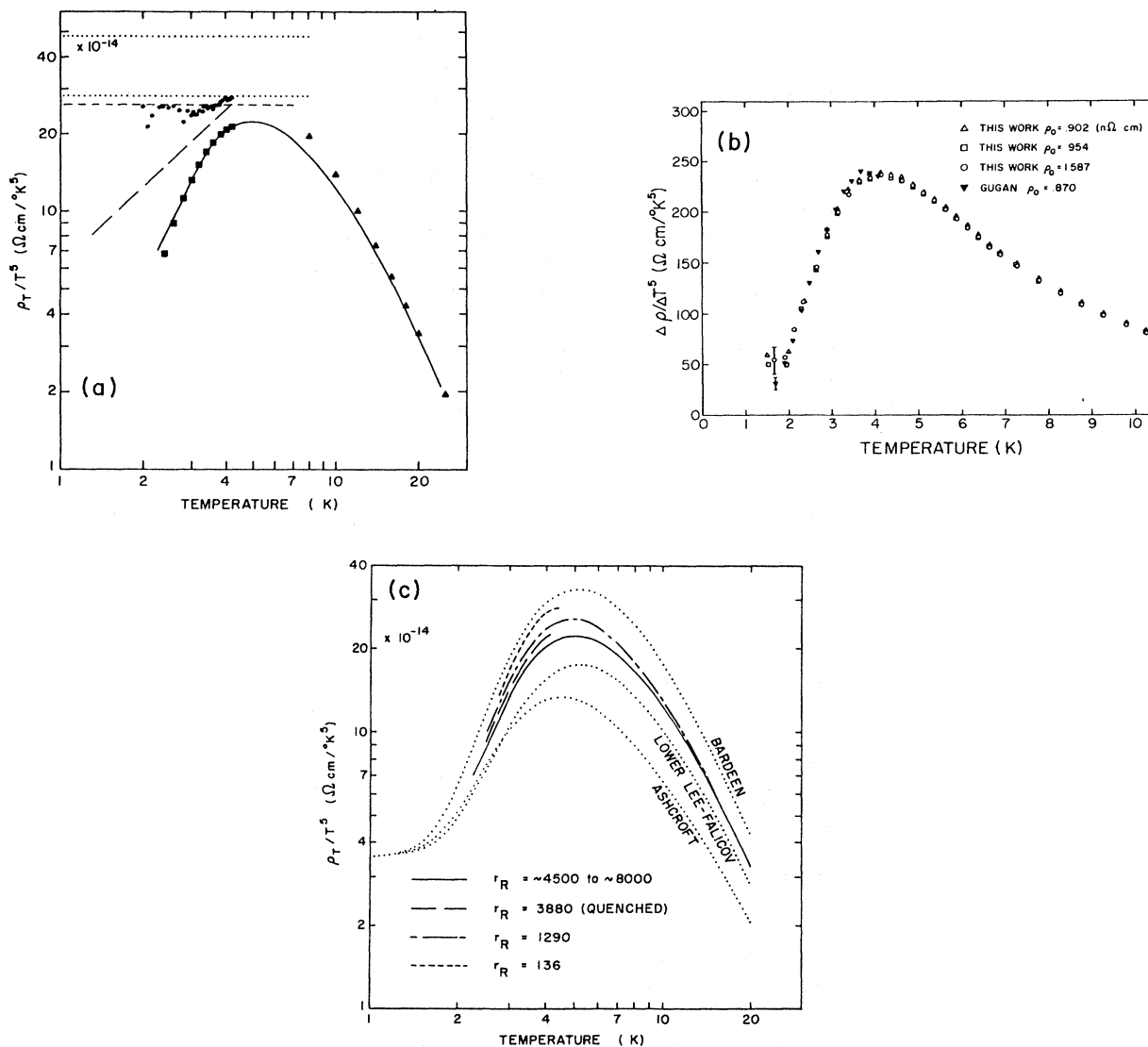

FIG. 5. Electron-phonon resistivities of a variety of K samples from 20 K to 2 K. (a) $\rho(T)/T^5$ vs T, comparing early K data from a variety of sources: ———, Ekin and Maxfield, 1971 ($4500 \leq RRR \leq 8000$); ■, sample K 3(c) of Gugan, 1971 ($RRR=8180$); ▲, Dugdale and Gugan, 1962 ($RRR=1400$); ●, Garland and Bowers, 1968 ($RRR=3800$); long-dashed line, the T^6 dependence reported from 1.3 to 4.2 K by Tsoi and Gantmakher, 1969 ($RRR=5300$); horizontal dashed line, the T^5 dependence reported below 7 K by Natale and Rudnick, 1968 ($1400 < RRR < 2800$); · · · ·, the T^5 coefficients reported below 8 K by MacDonald, White, and Woods, 1956 (upper line, $RRR=512$; lower line, $RRR=532$ and 324). From Ekin and Maxfield, 1971. (b) Temperature-derivative data in the form $\Delta\rho/\Delta T^5=(\rho_i-\rho_j)/(T_i^5-T_j^5)$ (where $i,j=$any two adjacent data points) vs T: open symbols, data of Ekin and Maxfield (1971); ▲, one sample of Gugan (1971). From Ekin and Maxfield, 1971. (c) Comparison of experimental and theoretical results for $\rho(T)/T^5$ vs T in K: · · · ·, theoretical results described in Ekin and Maxfield (1971), Table III; ———, —·—·—·, and — — —, experimental results for samples with the RRR's indicated. From Ekin and Maxfield, 1971.

tions were gone from high-purity K by about 150 K.

(b) For samples with RRR's greater than about 4500, both Gugan and Ekin and Maxfield found only small DMR [Fig. 5(c)]. To isolate $\rho(T)$ for high-purity K independently of any extrapolations or assumptions concerning the unknown quantity ρ_0, they determined the temperature derivatives of their data, which could be done down to about 2 K. Below 4 K, they both found data [Figs. 5(a) and 5(b)] that decreased approximately exponentially with temperature, much more rapidly than either the T^5 predicted by the Debye model or the earlier measurements on K mentioned just above [Fig. 5(a)]. Obviously, they were seeing for the first time the exponential falloff of ρ_{Uep} predicted for the alkali metals. Fitting their data below about 4 K with a T^5 component plus $\rho_{\mathrm{Uep}} \propto T^n \exp(-\Theta/T)$, both found good fits with $n=0$ and $\Theta=23$ K. Gugan noted that alternative fits with different values of n and Θ were almost equally compatible with the data, provided that n and Θ satisfied $(2.8n + \Theta = 23.6$ K$)$. He also noted that the very-low-temperature data could be fit almost as well with an exponential term alone—i.e., with $\rho_{\mathrm{Nep}}=0$—corresponding to complete phonon drag.

Figure 5(c) compares the Gugan and Ekin and Maxfield data on K with variational calculations (dotted curves) of $\rho(T)$ performed by Ekin and Maxfield, assuming a spherical Fermi surface and using various alternative contemporary pseudopotentials (see labels on dotted curves) with no adjustable parameters. The calculations give remarkably good semiquantitative fits to the joint data of Ekin and Maxfield and Gugan all the way up to 20 K. Such agreement was unprecedented, since, for other metals, calculations of $\rho(T)$ with no adjustable parameters were lucky to achieve even order-of-magnitude agreement with experiment. Clearly the simplicity of the Fermi surface of K was crucial to this success. These calculations used an isotropic trial function for the electrons, took the phonon trial function to be zero (i.e., assumed that there was no phonon drag), took the phonon frequencies from neutron scattering results, and assumed a perfectly spherical Fermi surface with only single-plane-wave states for the electron states. We see from Fig. 5 that although the absolute magnitudes of the fits with different pseudopotentials are different, their temperature variations are quite similar. Using the best modern value for ρ_{Nep}, based upon a more modern phonon spectrum (see, for example, MacDonald et al., 1981), and neglecting phonon drag, the calculations of Ekin and Maxfield show that ρ_{Uep} is dominant down to about 3 K, and ρ_{Nep} is never more than about 15% of the total from 4 K up to 20 K. Ekin and Maxfield found that the magnitude of the calculated ρ_{Uep} is very sensitive to the choice of pseudopotential, since it is determined primarily by the magnitude of the pseudopotential near $\mathbf{k}=2\mathbf{k}_f$ ($\mathbf{k}_f$ is the Fermi wave vector), which is small and can differ substantially from one pseudopotential to another. In contrast, ρ_{Nep} is insensitive to choice of pseudopotential, since it is determined primarily by the magnitude of

the pseudopotential near $k=0$, which is large and nearly the same for different pseudopotentials.

(c) For less pure samples, both Gugan and Ekin and Maxfield found significant DMR, in Gugan's case also explicitly for dislocations. From Fig. 5(c) we see that decreasing the RRR of K from 8000 to 136 in Ekin and Maxfield's samples produced a fractional change in $\rho(T)$ of about 30% at 5 K, the maximum in a plot of $\rho(T)/T^5$ versus T. To consider the lower-temperature DMR in more detail, we define $\delta(T)$ to be the fractional increase in $\rho(T)$ at temperature T. Then for point defects (i.e., vacancies and impurities), both found (Fig. 6) that $\delta(T)$ was only about 5% between 2 and 4 K, and had essentially the same temperature dependence as $\rho(T)$ for pure K. For dislocations, in contrast, Gugan found more complex behavior (Fig. 7). In the vicinity of 4 K, $\delta(T)$ was about 20% and nearly temperature independent. However, between 3 and 2 K, $\delta(T)$ grew rapidly, so that by 2K $\delta(T)$ was 50–100%.

In the same year, Krill (1971) measured $\rho(T)$ on high-purity Li down to 1.3 K with a voltage sensitivity of 10^{-8} V and a measuring sensitivity of about 1 part in 10^4. He found (Fig. 8) a closely T^2 term to be dominant between
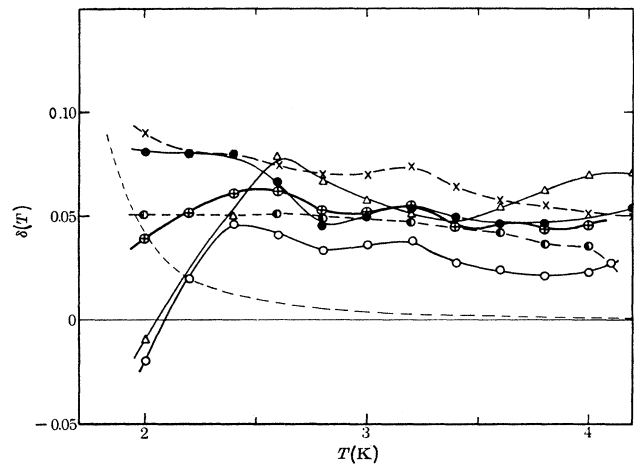

FIG. 6. Deviations from Matthiessen's rule for point defects (chemical impurities and vacancies in potassium), $\delta(T)=\Delta(T)/\rho_i^*(T)$ vs T. $\Delta(T)$ is the difference between the resistivity of the sample of interest and a reference sample, and $\rho_i^*(T)$ is the resistivity of the well-annealed sample with the highest RRR ($\simeq 8300$), chosen to best approximate the ideal resistivity of K. For chemical impurities—○, K 1; ●, K 5(a) and (e); △, K 4(a) and (b)—the reference sample is K 3(c). For vacancies—◐, K 3(a) and ×, K 5(b)—the references are K 3(b) and K 5(c), respectively. Here the references are the same sample after an anneal designed to remove only vacancies. The symbols ⊕, through which the heavy line is drawn, indicate the average of all of the above data. The thin solid line indicates the assumed zero deviation for the standardizing specimen K 3(c), and the dashed line indicates the expected limits of random error in $\delta(T)$. From Gugan, 1971.
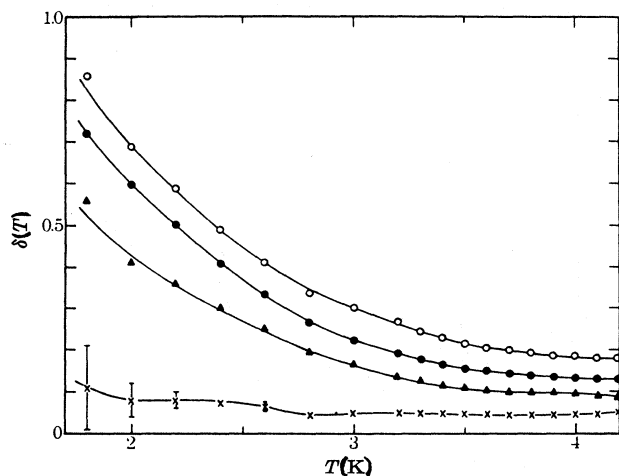
FIG. 7. Deviations from Matthiessen's rule for deformed K sample K 5, $\delta(T) = \Delta(T)/\rho_i(T)$, vs T, where $\Delta(T)$ and $\rho_i^*(T)$ are defined in the caption to Fig. 6: $\bigcirc$, run K 5(b), deformed at 4.2 K, annealed 10 min at 6.5 K; $\bullet$, run K 5(c), further 10-min anneal at 26 K; $\blacktriangle$, run K 5(d), further 10-min anneal at 78 K; $\times$, runs K 5(a) and (e), fully annealed. From Gugan 1971.

3. Controversy among theorists over phonon drag

The following year, Kaveh and Wiser (1972, 1974a, 1974b, 1974c) published the first of four related papers in which they claimed to demonstrate conclusively, by a general variational calculation, that the data of Gugan and of Ekin and Maxfield required the presence of a substantial amount of phonon drag between 1 and 4 K in K. These papers stimulated a spirited debate over this claim, which was later shown by the experimentalists to be correct up to at least 2 K. We discuss these KW papers in detail, and several others which were written in response to them, in order to provide the background necessary to understand why we are not yet sure of the importance of phonon drag in K above about 2 K.

As discussed in Appendix A, variational calculations give an upper bound on $\rho(T)$, the quality of which depends upon many factors, including choices of the interaction potential, the electronic wave functions, and the variational function or functions. Kaveh and Wiser's calculation was very similar to that of Ekin and Maxfield, except that KW assumed complete phonon drag, using the simple phonon out-of-balance function ψ_q given in Eq. (A10), and included in their pseudopotential an adjustable parameter that was determined by fitting the experimental data at one temperature. For the electrons, Kaveh and Wiser considered only electron-phonon and electron-impurity scattering, with electron-impurity scattering dominant. They used the isotropic variational function appropriate to a Φ_k determined by impurity scattering, Eq. (A7b). For the phonons, only phonon-electron scattering was considered. A Born–von Kármán fit to contemporary neutron scattering data was used to determine the phonon spectrum, and they chose a one-parameter Harrison pseudopotential designed to pro-

about 10 and 4.5 K, with a coefficient that we estimate from his graph to be about $A = 33$ fΩ m/K^2. Krill tentatively attributed this term to umklapp electron-phonon scattering, based upon a contemporary calculation suggesting that such scattering could produce a T^2 variation. We shall argue below that his T^2 term arises instead from electron-electron scattering, which is visible to such high temperatures in Li because its high Debye temperature eliminates electron-phonon scattering below about 10 K.
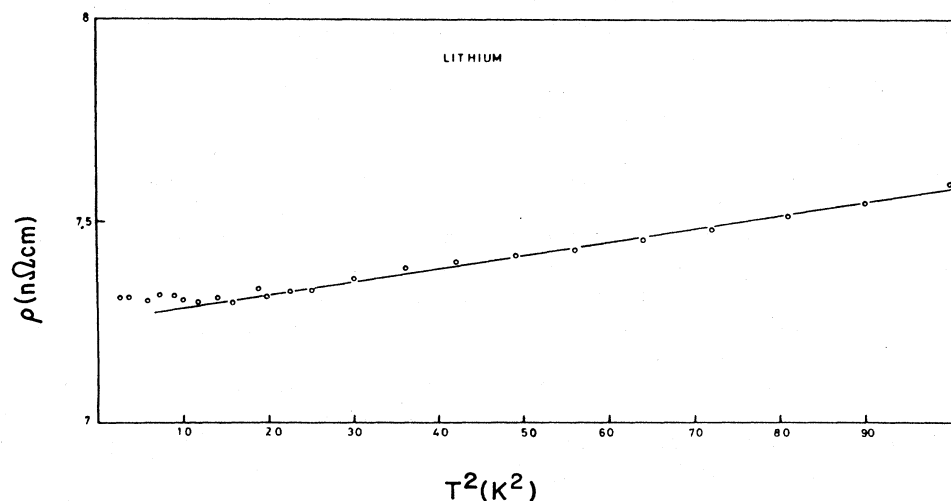

FIG. 8. ρ_t vs T^2 for Li at $T \leq 10$ K. After Krill, 1971.

duce the correct behavior near the important points $k=0$ and $k=2k_f$. When fit to Gugan's data at 14 K, their calculation agreed with the rest of Gugan's data to within 10% from 20 K down to 2 K, a temperature range over which $\rho(T)$ decreased by five orders of magnitude. The calculation also agreed with the data of Ekin and Maxfield to within 10% from 4 K down to 2.4 K. The derived correction due to phonon drag was just over 50% at 2 K, 10 at 4 K, and 5% at 20 K. A debate quickly arose over whether their conclusion concerning the need for phonon drag was required by these data.

Leavens and Laubitz (1974, 1975) argued that Kaveh and Wiser had used an inappropriate trial function for the deviation of the phonon system from equilibrium. They pointed out that, when phonons were assumed to be scattered only by electrons, it was not necessary to choose a separate trial function for the deviation of the phonon system from equilibrium, since the phonon distribution function could be expressed explicitly in terms of the electron distribution function (Bailyn, 1958). For the same electronic trial function used by Kaveh and Wiser, they showed that the correct phonon deviation function (a) depended sensitively upon the details of the electron-phonon scattering; and (b) generally differed substantially from the form assumed by Kaveh and Wiser. Minimizing the resistivity by applying their formalism to the same one-parameter pseudopotential used by Kaveh and Wiser, and extending their calculation up to 20 K without including phonon-phonon scattering, they found (Fig. 9) that their phonon trial function produced values for $\rho_{ep}(T)$ almost 50% smaller than those obtained using the KW trial function. Above about 4 K, where ρ_{Uep} was dominant, the predicted phonon-drag limit became nearly a constant fraction of both the ideal resistivity without phonon drag (called the Bloch limit) and the phonon-drag limit calculated using the KW procedure. This is an important result, because it shows that from 4 K to 20 K both complete phonon drag and the Bloch limit give nearly the same form for $\rho(T)$. These two alternatives can only be distinguished by a correct calculation of the absolute magnitude of $\rho(T)$ or by a calculation that correctly describes how $\rho(T)$ changes from the phonon-drag limit at very low temperatures to the Bloch limit at high temperatures. Below 4 K, ρ_{Nep} becomes increasingly more important in the Bloch limit as the temperature drops—since its T^5 falloff is much slower than the exponential falloff of ρ_{Uep}—and the phonon-drag limit rapidly decreases as a fraction of the Bloch limit. Leavens and Laubitz pointed out that the neglect of phonon-phonon scattering left their calculation with no mechanism for equilibrating the phonon system. They stated that it was quite possible that such scattering becomes important below 20 K and that a proper calculation of $\rho_{ep}(T)$ taking both phonon-electron and phonon-phonon scattering into account was a formidable task, well beyond what they had done. Leavens and Laubitz concluded that their results invalidated Kaveh and Wiser's claim to have made a complete analysis for $\rho(T)$ for the
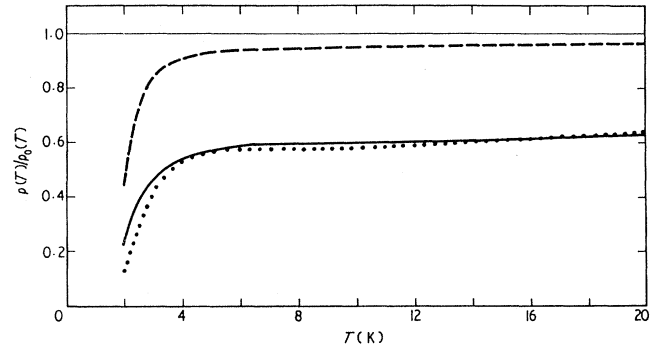

FIG. 9. The ratio $\rho(T)/\rho_0(T)$ of the ideal electrical resistivity of K calculated with the inclusion of phonon drag to that without, vs T. The dashed curve was calculated using the simple variational formula for $\rho(T)$ used by Kaveh and Wiser (1974); the solid and dotted curves were calculated taking phonon drag into account more correctly. The solid and dashed curves were calculated with the one-parameter Harrison pseudopotential fitted to the experimental resistivity by Kaveh and Wiser; the dotted curve was calculated with the Ashcroft pseudopotential used by Hayman and Carbotte (1973). From Leavens and Laubitz, 1975.

alkali metals at low temperatures and remarked that there was still a great deal of theoretical work to be done before $\rho(T)$ in K could be rigorously calculated.

Included in the required work were estimates of corrections to $\rho(T)$ due to the fact that the electronic distribution function Φ_k varies with energy and is also anisotropic in k space. Their analysis suggested that such effects might be important, especially in that they might cause different changes with and without phonon drag. Leavens and Laubitz (1976), Leavens, (1977), and Jumper and Lawrence (1977) soon found that including both energy dependence and scattering anisotropy in Φ_k produced only modest changes in $\rho(T)$ for pure K at low temperatures, with the corrections due to energy dependence being about twice as large as those due to anisotropy. The fractional changes from the two combined were only slightly larger in the Bloch limit than in the phonon-drag limit, with a maximum value in the former of about 30% near 6 K, 20% at 4 K, and less than 5% by 2 K. Such changes nicely explained the DMR due to point defects in the less pure K samples shown in Fig. 5, but did not fundamentally change the form of $\rho(T)$ for pure K. The fact that these calculations found DMR due to energy dependence and anisotropy to be small below 4 K will figure importantly in the analyses of phonon drag and quenching of phonon drag to be given below.

Kaveh and Wiser (1975b) responded to Leavens and Laubitz (1974, 1975) by performing a new calculation using the procedure of Bailyn, and found, in general agreement with Leavens and Laubitz, a reduction in their previously calculated $\rho(T)$ of somewhat over 50% between

4.2 and 2.6 K. However, they noted that the reduction itself changed by only about 15% from 4.2 K down to 2.6 K. Since this was a small change compared to the factor-of-30 increase in the exponential component of $\rho(T)$, they argued that the form of the new calculated $\rho(T)$ was practically the same as that of the old one. They asserted that the new calculation thus fit the data below 4.2 K just as well as the old one, simply requiring a different value for the adjustable parameter. They reiterated their claim for the importance of phonon drag up to at least 4.2 K. Recognizing the importance for $T > 4.2$ K of the Leavens and Laubitz result shown in Fig. 9, they reserved consideration of phonon drag at higher temperatures for a later paper.

Taylor et al. (1976) then reported the extension to lower temperatures of a calculation of $\rho(T)$ for K based upon the same first-principles pseudopotentials that had been very successful at fitting data above 20 K in both K and Na using no adjustable parameters (see Sec. III.B.1 above). Upon introducing the pseudopotential for K into the formulation of Leavens and Laubitz and applying the variational procedure including an energy dependence in Φ_k, they found good agreement with the experimental data of Gugan and Ekin and Maxfield, provided that there was little or no phonon drag (i.e., $\Psi_q = 0$). Inclusion of phonon drag disrupted this agreement by a factor of 4 at the lowest temperatures. Taylor et al. argued that their calculation was superior to Kaveh and Wiser's in several ways, the most important of which were the superiority of their first-principles pseudopotential and the fact that Kaveh and Wiser had required an adjustable parameter to fit the data. They asserted that Kaveh and Wiser's claim that phonon drag is present in K was based solely upon their ability to fit the data over a limited temperature range with a model in which phonon drag was complete. They argued that their own ability to fit data over a much wider temperature range with no adjustable parameters, and no phonon drag, clearly opened to question the basis for Kaveh and Wiser's conclusion. These authors did not, however, claim to have proved that phonon drag was absent, noting that their calculation was also only approximate. They argued that still better calculations were needed to demonstrate conclusively the presence or absence of phonon drag on theoretical grounds alone.

Later that same year, the debate over the existence of phonon drag in K up to about 2 K was settled by more precise new measurements, which vindicated the claim of Kaveh and Wiser for this temperature range, as we describe in Secs. III.D.1 and III.D.2.

The debate, however, continued with several additional papers.

Frobose (1977) presented an alternative analysis of $\rho_{ep}(T)$ for K, which fit the data of van Kempen et al. well taking phonon drag into account. He pointed out that the only phonons that contribute to $\rho(T)$ in the presence of phonon drag are those which can undergo not one, but two different umklapp scattering processes.

Kaveh and Wiser (1977) responded to Taylor et al. (1976) by challenging the local-screening approximation for the pseudopotential used in that paper. They asserted that the first-principles form factors used by Taylor et al. (1976) were simply not accurate enough at the crucial point $k = 2k_f$ to properly determine $\rho_{Uep}(T)$ for K at very low temperatures. They pointed out that their own empirical form factor, in contrast, was fit to experimental data at $2k_f$, a procedure that, they argued, automatically ensured the high accuracy required at this point. In this paper they reported the extension of their calculation of $\rho(T)$ based upon this empirical form factor to above 4 K using a single relaxation-time approximation to treat phonon-phonon scattering and assuming a coefficient for the magnitude of this scattering which they described as "reasonable," but which they did not specify. They thus appear to have had two adjustable parameters in this calculation, the magnitude of the phonon-phonon relaxation time and the parameter in their form factor. They showed that their empirical form factor could then fit the $\rho(T)$ data for K all the way up to 300 K, with a phonon-drag contribution that was essentially complete below 3 K and did not disappear until 30 K (Fig. 10). Given the approximate relaxation-time treatment of phonon-phonon scattering, the lack of a rigorous justification for the chosen magnitude for the relaxation time, and the fact that neither angular nor energy dependences of Φ_k were taken into account, it is difficult to accept this calculation as definitive concerning phonon drag. For this reason, we shall base our conclusions concerning the temperature range over which phonon drag is important in K on the complete combination of theoretical analysis
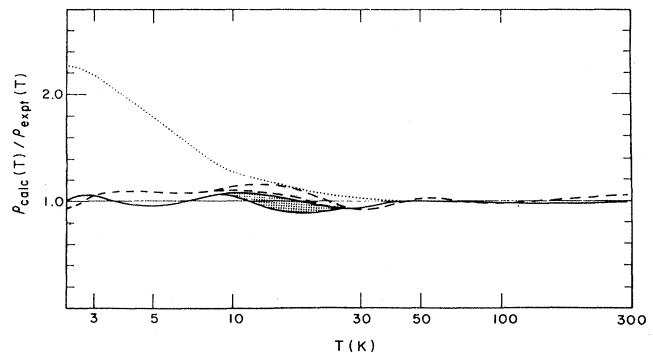
FIG. 10. The ratio $\rho_{calc}(T)/\rho_{exp}(T)$ for K from the one-parameter fit of Kaveh and Wiser (1977) using two different empirical form factors, one based on Hartree screening (solid curve) and the other on many-body Taylor-Leavens-Schukla screening (dashed curve). The width of the hatched portion indicates the authors' estimated error resulting from the uncertainty in the phonon-phonon scattering relaxation time. The dotted curve gives the results of this calculation without phonon drag. From Kaveh and Wiser, 1977.

and experimental data covered in the present review.

Taylor (1978) accepted Kaveh and Wiser's specific criticism of the screening procedure used by Taylor *et al.* (1976). However, he reported that he and his colleagues had examined this issue in more detail and found that appropriate corrections to this screening procedure produced only small changes in $\rho(T)$. He asserted that Kaveh and Wiser's more general criticism of the accuracy of the first-principles form factor at $2\mathbf{k}_f$ was simply erroneous. In addition, Taylor proposed that phonon-dislocation scattering could eliminate phonon drag by equilibrating the phonon system at low temperatures, noting that he and his colleagues had recently calculated that such scattering could explain brand new data $\rho(T)$ on K which we describe in Sec. III.D.1 below. We shall consider this calculation by Taylor and colleagues in Sec. III.D.3, where we shall see that the dislocation density that they required is unphysically large.

Because evaluation of the few papers that concluded this debate requires knowledge of new high-precision measurements of $\rho(T)$ for K below 2 K, published in 1976 and 1978, we postpone discussion of these papers to Sec. III.D.3, after the presentation of the new data. Before turning to these data, we discuss the first calculation of electron-electron scattering in the alkali metals, the results of which were used to help interpret the new data.

C. Lawrence and Wilkins: the first calculation of A_{ee}

In the same letter that described their observations of T^5 behavior in K and Na below 4 K, noted in Sec. III.B.1, Garland and Bowers (1968) also reported that $\rho(T)$ for Al and In varied closely as AT^2 at these same temperatures. They attributed this T^2 variation to the dominance of electron-electron scattering in these two metals at these low temperatures.

This report stimulated Lawrence and Wilkins (1973) to make a pioneering detailed analysis of $\rho_{ee}(T)$ in simple metals to see whether they could reproduce the magnitude of the coefficient A reported by Garland and Bowers for Al. Their calculation led them to two conclusions: first, that Garland and Bowers could not be seeing electron-electron scattering, since their measured A was about 30 times larger than the A_{ee} that Lawrence and Wilkins calculated; second, that A_{ee} for the alkali metals should be of order 1 fΩ m/K^2, quite comparable to its values for metals with much more complex Fermi surfaces, such as Al and the noble metals. This latter conclusion was rather a surprise, because A_{ee} for the alkali metals contains a contribution [called the umklapp fraction Δ—Eq. (9) below] that depends primarily on the geometry of the Fermi surface and is more than an order of magnitude smaller for the nearly spherical Fermi surfaces of the alkali metals than for the more complex Fermi surfaces of other metals. The resolution of this apparent paradox lies in that fact that A_{ee} is inversely proportional to the electron-electron scattering time τ_0, and

τ_0 turns out to be roughly proportional to the electron density. The electron densities in the alkali metals are unusually low and largely cancel the effect of a small umklapp fraction.

To quantify these two points, Lawrence and Wilkins started with the linearized Boltzmann transport equation (LBTE) for electrons scattered by other electrons and by impurities. They used the electronic trial function $\Phi_{\mathbf{k}}$ given in Eq. (A6c) as the starting point for the calculation of A_{ee}, explicitly taking into account its energy dependence. Following Smith and Wilkins (1969), they showed that when both electron-electron and electron-impurity scattering are present, $\rho_{ee}(T) = A_{ee}T^2$ can be written in the standard form of Eq. (A8), except that this equation has to be multiplied by a quantity they called the "umklapp fraction" Δ, times a correction factor that is nearly unity, i.e.,

$$A_{ee}T^2 = (2\pi^2/3)(m_{opt}/ne^2\tau_0)$$
$$\times \Delta[1 - \Delta/(10.4 + \Delta + 5\beta)] . \qquad (8)$$

In Eq. (8), m_{opt} is the electron optical mass—which they approximated as the free-electron mass—and $\beta = (2/\pi^2)(\tau_0/\tau_{imp})$, where τ_{imp} is the relaxation time due to scattering from impurities. For τ_0, Lawrence and Wilkins used values calculated by Jensen, Smith, and Wilkins (1969), corrected for electron exchange. This correction multiplied the previous τ_0's by about $\frac{3}{2}$.

The umklapp fraction Δ is given by

$$\Delta = \frac{[(\mathbf{v}_{\mathbf{k}_1} + \mathbf{v}_{\mathbf{k}_2} - \mathbf{v}_{\mathbf{k}_3} - \mathbf{v}_{\mathbf{k}_4})^2 W]}{4[(v)^2 W]} , \qquad (9)$$

where the parentheses indicate absolute values, the square brackets indicate averages over the Fermi surface, $\mathbf{v}_{\mathbf{k}_i}$ is the velocity of an electron with wave vector $\mathbf{k}_i$, and W is the matrix element for scattering from $\mathbf{k}_1, \mathbf{k}_2$ to $\mathbf{k}_3, \mathbf{k}_4$. For a perfectly spherical Fermi surface, $\mathbf{v}_{\mathbf{k}}$ is simply proportional to $\mathbf{k}$, and conservation of crystal momentum $(\mathbf{k}_1 + \mathbf{k}_2 - \mathbf{k}_3 - \mathbf{k}_4 = 0)$ makes $\Delta = 0$ for the normal component A_{Nee}, since the only reciprocal lattice vector that contributes to A_{Nee} is $\mathbf{G} = 0$. Nonsphericity of the Fermi surface makes A_{Nee} nonzero, but typically small. For umklapp scattering processes $(\mathbf{k}_1 + \mathbf{k}_2 - \mathbf{k}_3 - \mathbf{k}_4 = \mathbf{G})$, Δ is not zero, and such processes are expected to dominate A_{ee} in the alkali metals.

To estimate Δ, Lawrence and Wilkins used two plane-wave representations of the electron eigenstates. As described in the original paper, they also took account of a variety of important subtleties, such as interference effects in Δ due to scattering involving different reciprocal lattice vectors. For K and Na they found Δ to be 0.06 and 0.015, respectively. In contrast, Δ for Al, In, Mg, Cd, and Zn varied from 0.4 to 0.6. The values of A_{ee} that Lawrence and Wilkins predicted for the alkali metals are listed as the fifth column of Table II. These predictions played an important role in the interpretations of the alkali metal data that we describe in the

remainder of this review.

For Al, as indicated above, Lawrence and Wilkins predicted A_{ee} to be about 30 times smaller than the value Garland and Bowers had derived from their measurements. Because the resolution of that discrepancy had important ramifications for our current understanding of A_{ee} in the alkali metals, we briefly digress to discuss the history of A_{ee} in Al.

The experimental situation in Al became confused when new measurements below 4 K disagreed with the T^2 form of $\rho(T)$ reported by Garland and Bowers for Al below 4 K. These new data were fit better by a T^3 dependence (see, for example, Senoussi and Campbell, 1973). It was initially assumed that this different behavior was due either to a complex contribution of $\rho(T)$ from umklapp electron-phonon scattering, or to DMR (Bass, 1972; Cimberle et al., 1974). Kaveh and Wiser (1975a), however, argued that this apparent T^3 behavior was due to the combination of two terms: a T^2 term due to electron-electron scattering, the magnitude of which was about 10% smaller than the value reported by Garland and Bowers (1968), and a term varying approximately as T^5 due to electron-phonon scattering. Given its continuing disagreement with the Lawrence-Wilkins calculation, such a large value for A_{ee} in Al did not achieve general acceptance until four years later, when a reconsideration of the Lawrence-Wilkins calculation was finally spurred by results from two additional studies. (1) New, higher-precision measurements were made of $\rho(T)$ in Al by Ribot et al. (1979, 1981), as we briefly discuss next. (2) MacDonald and co-workers in Canada (1980) found a large discrepancy between the new Ribot et al. value for A_{ee} in Al and the value for A_{ee} that they derived from analysis of the electron-electron scattering contribution to the high-temperature thermal conductivity of Al. We shall discuss the relation between W_{ee} and A_{ee}, as well as the MacDonald et al. calculations, in Sec. III.D.9.

The new measurements by Ribot et al. (1979, 1981) showed that below 2 K, $\rho(T)$ in Al was clearly dominated by a T^2 term, the size of which was insensitive to various perturbations, just as would be expected for electron-electron scattering. This T^2 term was about 30% and 20% smaller, respectively, than the estimates by Garland and Bowers and by Kaveh and Wiser, which reduced the discrepancy with the Lawrence-Wilkins theory to a factor of 20. The remaining portion of $\rho(T)$ below 2 K was compatible with both the form and the magnitude expected for electron-phonon scattering in Al at these temperatures. Ribot et al. argued strongly that the behavior they observed in Al had to be due either to electron-electron scattering or to some scattering process not yet considered.

These new results stimulated MacDonald (1980) to reexamine the nature of the electron-electron scattering process. He developed a way to calculate the contribution to A_{ee} of phonon-mediated electron-electron scattering, a higher-order scattering process that had been known to exist, but which crude estimates had suggested would make only a small contribution to A_{ee} in metals. MacDonald noted that this process must be worth examining carefully in Al, since it was strong enough to cause superconductivity at about 1.2 K. He was able to show that the process dominated A_{ee} for Al and increased its calculated value to where it agreed with the measurements of Ribot et al.

Although the alkali metals do not superconduct, this higher-order scattering process turns out to play an extremely important role in A_{ee} for these metals too, as we shall see in Sec. III.D.9, where we examine calculations of A_{ee} for the alkali metals by MacDonald et al. (1981) that include this process. For K, these new calculations turn out, fortuitously, to agree exactly with the Lawrence-Wilkins value. For Na, in contrast, they predict a much larger value of A_{ee}, as shown in Table II.

D. Measurements with 10^{-6} precision and resulting theories

In 1975–1976, van Kempen et al. (1975, 1979) and Rowlands and Woods (1976) started a revolution in low-temperature resistivity measurements by showing that the resistances of metallic samples could be measured with a precision of better than 1 part in 10^7 using a current comparator (Kusters and MacMartin, 1970). It took several more years to actually reach a precision of 10^{-7} with the low resistances (10^{-5}–10^{-7} Ω) of high-purity K samples at low temperatures. But the precisions of 10^{-6} that van Kempen et al. (1976) and Rowlands et al. (1978) achieved represented a 10^2 improvement over previous measurements and allowed them to discover surprising behavior, the sources of which are only now becoming properly understood.

1. Van Kempen et al.: phonon drag and an anomaly in K below 1.4 K

Van Kempen et al. (1975, 1976) published the first high-precision data on K samples from 4.2 K down to 1.1 K. Their achieved precision of 1 ppm was limited by their voltage sensitivity of 10^{-12} V. To within their measuring uncertainty, they found no current-dependent effects on $d\rho/dT$ for measuring currents up to 0.3 A. To cleanse their K of possible dissolved gases, van Kampen et al. liquified it at 373–383 K and pumped it for half an hour in a small vacuum chamber inside a glove box. They then used He gas to force the molten K into a protective polyethylene tube, where it was solidified carefully to eliminate contraction voids. Polyethylene was chosen as the protective material because it has a coefficient of expansion not too different from that of K and because tests showed that the surface of the K remained shiny in such tubing for several days in air if the tubing was wrapped with plastic tape to keep oxygen and water vapor from diffusing through the polyethylene to the sample surface. Van Kempen et al. demonstrated that po-

lyethylene did not produce the erroneous stress-induced effects of glass, by showing that in the overlapping temperature range from 4.2 to 2 K their data for $\rho(T)$ were in good agreement with the data of Gugan (1971) and Ekin and Maxfield (1971) taken on free-hanging samples. To minimize cooling stresses, the sample in its tube was first slowly cooled in vacuum inside the measuring cryostat to liquid-nitrogen temperature for over 10 h, and then cooled to 4.2 K by transfer of liquid helium directly into the inner cryostat chamber containing the sample.

Van Kempen *et al.* found several interesting results.

(a) When measured within a day of preparation, the RRR of one of their samples was as low as 3000. However it increased to 8000 when the sample was held at room temperature for several days to several weeks [Fig. 11(a)]. This unusual behavior was contrary to what had been seen by Gugan and by Ekin and Maxfield, both of whom found RRR's of 5000–6000 upon first cooling. Van Kempen *et al.* proposed that the increases in RRR with annealing time at room temperature were due to annealing out of some unknown defect initially in the as-cooled samples. Based upon the work of Gurney and Gugan (1971), which showed that dislocations annealed out of K below 200 K, they noted that it was highly unlikely that these defects could be dislocations.

(b) Compatible with the data of Gugan (1971) and Ekin and Maxfield (1971), van Kempen *et al.*'s data were also dominated by an exponential term [Fig. 11(a)] from 4.2 K down to about 1.8 K. They fit their data to the form $BT^n\exp(-\Theta/T)$ and found best values $n = 0.9 \pm 0.2$ and $\Theta = 19.9 \pm 0.2$ K. The magnitude of this exponential term was essentially independent of ρ_0 for RRR's above 5000. Below about 1.8 K, they found an additional term in $\rho(T)$. If they chose a T^2 form for this term, then they could fit their data nicely with only this T^2 term plus the exponential term; there was no need for any Bloch T^5 term. They concluded that the absence of any T^5 term provided clear evidence of the presence of phonon drag in K. In a more detailed presentation of their results, van Kempen *et al.* (1980) showed that, in the vicinity of 2 K, $\Delta\rho/(5T^4\Delta T)$ for their highest-purity samples actually fell well below both the Bloch T^5 upper bound used by Gugan (1971) and the best new estimates of the Bloch limit (Taylor, Leavens, and Shukla, 1976; MacDonald and Geldart, 1980), thereby confirming unambiguously the presence of a large amount of phonon drag below about 2 K. Residual resistance ratio values less than 5000 led to increased values for $\rho(T)$. They tentatively attributed these increases to partial quenching of phonon drag by the defects that reduced the RRR. However, if the low-temperature anomalies were assumed to vary as T^2, then these higher values of $\rho(T)$ remained consistent with exponential forms, with no need in any of their samples for the T^5 term that was expected to reemerge when phonon drag was partially quenched.

(c) Below about 1.8 K, van Kempen *et al.* found clear deviations from exponential behavior. Fitting $\rho(T)$ to

$$\rho(T) = AT^2 + BT\exp(-\Theta/T) , \qquad (10)$$

they found the coefficients A to be of the same order of magnitude as the Lawrence-Wilkins prediction for electron-electron scattering in K: $A_{ee} = 1.7$ fΩ m/K^2 (Table II). they thus tentatively attributed the deviations
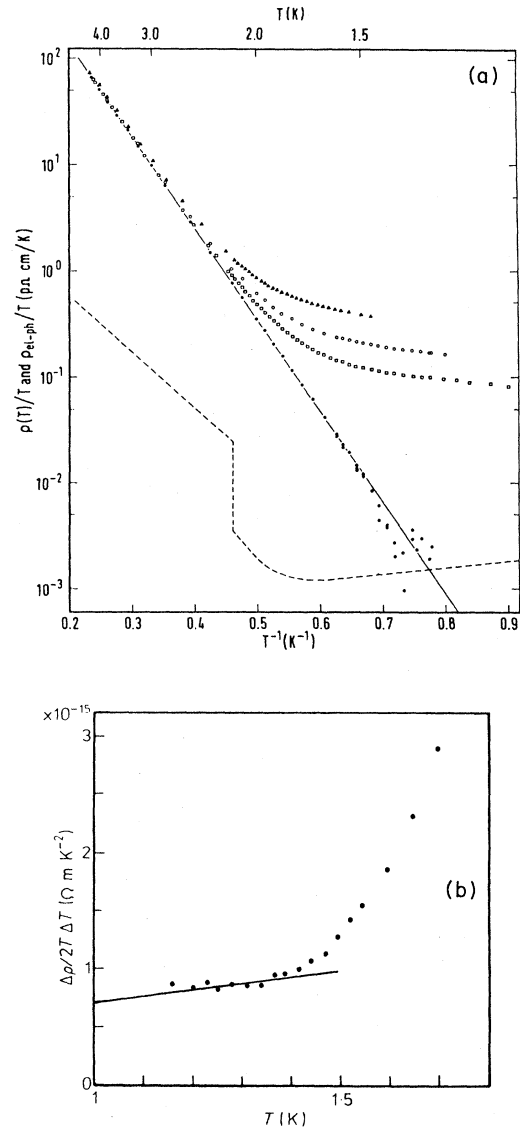

FIG. 11. The first high precision K data down to 1.1 K. (a) $\rho(T)/T$ and $\rho_{ep}(T)/T$ vs $1/T$. The difference between $\rho(T)$ and $\rho_{ep}(T)$ is the AT^2 term. For clarity, only $\rho_{ep}(T)$ for sample 2b (RRR = 6300) is given; the other samples practically coincided with 2b: ▲, $\rho(T)/T$ for sample 1 (RRR = 3100); □, $\rho(T)/T$ for sample 2c (RRR = 8000); ○, $\rho(T)/T$ for sample 2b; ●, $\rho_{ep}(T)/T$ for sample 2b; ———, $\rho_{ep}/T = 7.34\exp(-19.9/T)$; – – –, the estimated measuring error in $\rho(T)/T$ taking into account errors in the standard resistance and in T, but not in the sample form factor. Note that values of ρ_0 had to be assumed to obtain the values of $\rho(T)$ shown. From van Kempen *et al.*, 1976. (b) The derivative $\Delta\rho/2\Delta T$ vs T for sample 2c. Note that only below 1.35 K is $\rho(T) \propto T^2$ to within experimental error. After van Kempen *et al.*, 1981. The solid line, added by the present authors, indicates how a T^3 variation would appear in this figure.

to such scattering. However, they noted that the predicted A_{ee} was expected to be constant for a given metal, whereas their experimental values for A varied dramatically, from 2.7 to 0.8 fΩ m/K^2 [Fig. 11(a)]. In one sample, A dropped from 1.6 to 0.8 fΩ m/K^2 when the sample was simply held at room temperature for several weeks between measurements. Generalizing Eq. (10) to

$$\rho(T) = AT^m + BT^n \exp(-\Theta/T) , \qquad (11)$$

they found that alternative choices for n permitted their data to be fit with values of m ranging from 0.9 to 2.1. They tried to pin down the value of m better by subtracting the data for one sample from another, arguing that the exponential term was practically the same for all of their samples. This procedure yielded data that varied more closely as T^2 than as T. They also examined the data in the form $(1/T)(d\rho/dT)$, as shown in Fig. 11(b). We see that below about 1.35 K the data are compatible with a T^2 variation. But the large scatter and the short temperature range over which $\rho_{ep}(T)$ is negligible permit considerably different alternative forms too. For example, $\rho(T) \propto T^3$ is also compatible with the data, as shown by the solid line in Fig. 11(b), which extrapolates to the origin.

2. Rowlands et al.: phonon drag and a $T^{3/2}$ variation

Rowlands et al. (1978) soon extended measurements of $\rho(T)$ down to 0.5 K in order to better establish the temperature dependence of the anomaly discovered by van Kempen et al. Their samples were wrapped around a grooved Teflon holder and enclosed inside a vacuum can filled with a little ^{4}He exchange gas. Combining a current comparator with a SQUID null detector and a carefully fabricated reference resistor held at 1.1 K, they achieved precisions of better than 1 part in 10^6 with a measuring current of 10 mA. Because they found changes in ρ_0 by parts in 10^5 as they changed their measuring current from 0 to 10 mA, they held their measuring current carefully constant for a given sample.

(a) As had van Kempen et al., Rowlands et al. found the surprising result that the RRR's of their samples increased from as low as 1500 to as high as 6000 when the samples were held at room temperature for several weeks. They tentatively attributed these increases in RRR to a combination of secondary recrystallization and possible void formation, noting that the data of Gugan (1971) indicated that impurity clustering and dislocation loss both occurred too rapidly to be at fault.

(b) In the vicinity of 2 K, they found (Fig. 12) that $\rho(T)$ for their highest-purity sample fell well below the Bloch (non-phonon-drag) limit predicted by Taylor et al., 1976. This behavior was clear evidence of phonon drag. Below 1.5 K, their data rose again to far above the Bloch limit, a behavior that they noted could not be produced simply by quenching of phonon drag. Figure 12 shows that by 3 K the data for both annealed and unannealed samples

had risen too close to the Bloch limit, thereby suggesting substantial quenching of phonon drag.

(c) Since Rowlands et al. could reach lower temperatures than van Kempen et al., they could more accurately determine the temperature variation of their data. To their surprise, they found this variation to be closer to $T^{3/2}$ than T^2 (Fig. 13). As had van Kempen et al., they also found that the magnitude of this component of $\rho(T)$ decreased systematically with decreasing ρ_0 as their samples were annealed at room temperature. They considered three models to describe this $T^{3/2}$ behavior with a varying coefficient. (1) $\rho(T)$ was composed of two components: a small electron-electron component varying as T^2 and independent of ρ_0; and a larger one, due perhaps to scattering from resonant electron states on disloca-
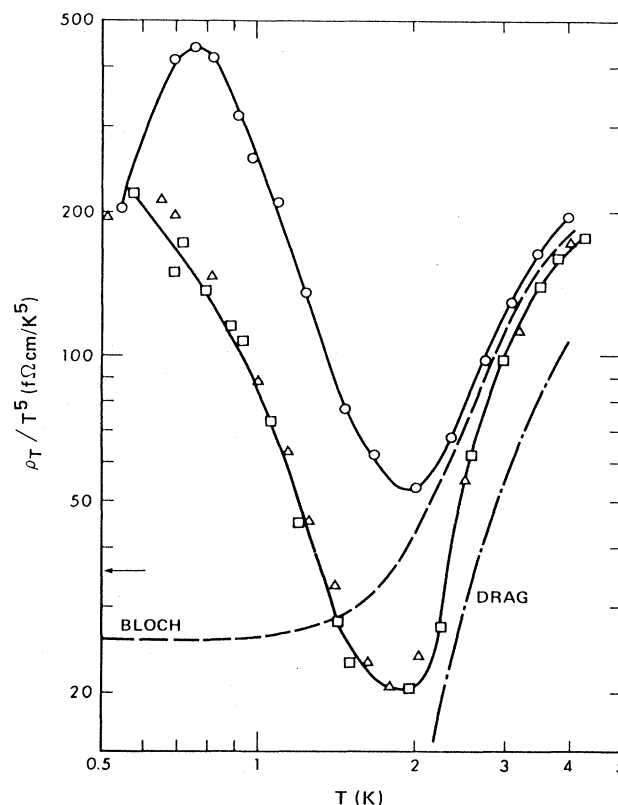

FIG. 12. Lower bound on $\rho(T)/T$ vs T for K in unannealed and annealed states: $\bigcirc$, unannealed K1a; $\square$, annealed K1b; $\triangle$, annealed K2c. The $\rho(T)$'s given in Fig. 12 were defined as the difference between a given value of ρ_t and the lowest temperature value of ρ_t for the same measuring run, so as to emphasize that even the largest possible choice of ρ_0 would not eliminate the rise in $\rho(T)$ with decreasing T seen below about 2 K. Theoretical predictions from Taylor, Leavens, and Shukla (1976) are shown as a dot-dashed curve for the phonon-drag limit and a dashed curve for the Bloch (no-phonon-drag) limit. The arrow on the ordinate indicates the Bloch limit as $T \to 0$ K calculated by Frobose (1977) and Ekin and Maxfield (1971). From Rowlands et al., 1978.
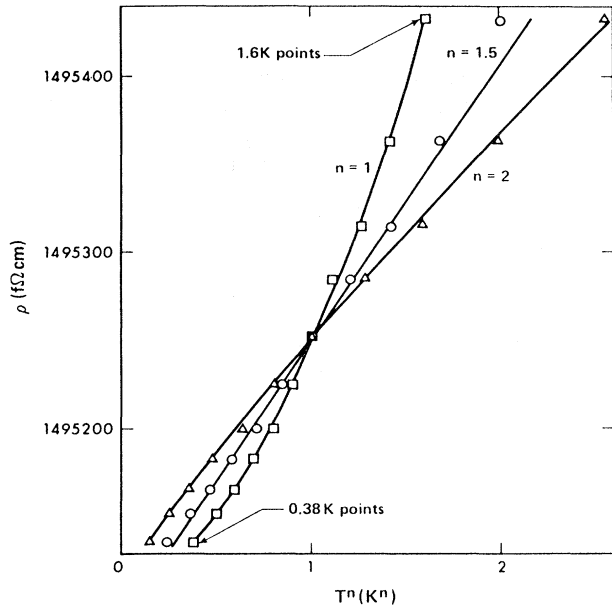
FIG. 13. ρ_i for specimen K 2b of Rowlands *et al.* (1978) plotted vs T^n with $n = 1$, 1.5, and 2. From Rowlands *et al.*, 1978.

the existence of some phonon drag in well annealed K below 2 K. But they argued that phonon-dislocation scattering would eliminate phonon drag in unannealed samples and also in annealed samples at higher temperatures. To demonstrate their point, they compared (Fig. 14) a calculation of $\rho_{ep}(T)$ involving a crude single relaxation-time treatment (Klemens, 1969) of phonon-dislocation scattering with one set of data from van Kempen *et al.*, as initially published (open circles in Fig. 14), and with two sets (filled circles and crosses) after increasing the values of ρ_0 assumed by van Kempen *et al.* by 1 part in 10^4. As shown in Fig. 11(a), these data were originally published in the form $\rho(T)$, which required values to be chosen for ρ_0. To obtain the changes shown in Fig. 14, the approximate calculation made by Taylor *et al.* required dislocation densities of $10^{15}/m^2$. They argued

tions, which varied strongly with ρ_0. (2) The data were due to inelastic impurity scattering—which they immediately rejected on the grounds that their term was too large. (3) The data were due completely to a size effect, in which electron-electron scattering was modified in the Knudsen flow regime of motion of the electrons through their thin wires. This model predicted a $\rho(T)$ of the form

$$\rho(T) = \rho_0[(d/2\lambda) - C(d/2\lambda)^2] , \qquad (12)$$

which is proportional to ρ_0 and depends directly upon sample diameter d. In Eq. (12), λ is the nonresistive electron mean free path for normal (N) electron-electron scattering. Since $(1/\lambda)$ was expected to vary as T^2, the combination of the two terms in Eq. (12) provided a potential explanation for the deviation of the Rowlands *et al.* data from a simple T^2 dependence, but they concluded that additional measurements, including samples of different diameters, were needed to choose between the first and third alternatives or to bring still others to the fore.

We shall see in Sec. IV.C that surface contamination may play an important role in "size effects" in K. We thus note that one of Rowlands *et al.*'s two samples showed a large change in room temperature resistance over 25 days, which they attributed to surface oxidation or similar deterioration.

These measurements by van Kempen *et al.* and Rowlands *et al.* quickly stimulated theoretical analysis.

3. The conclusion of the phonon-drag debate

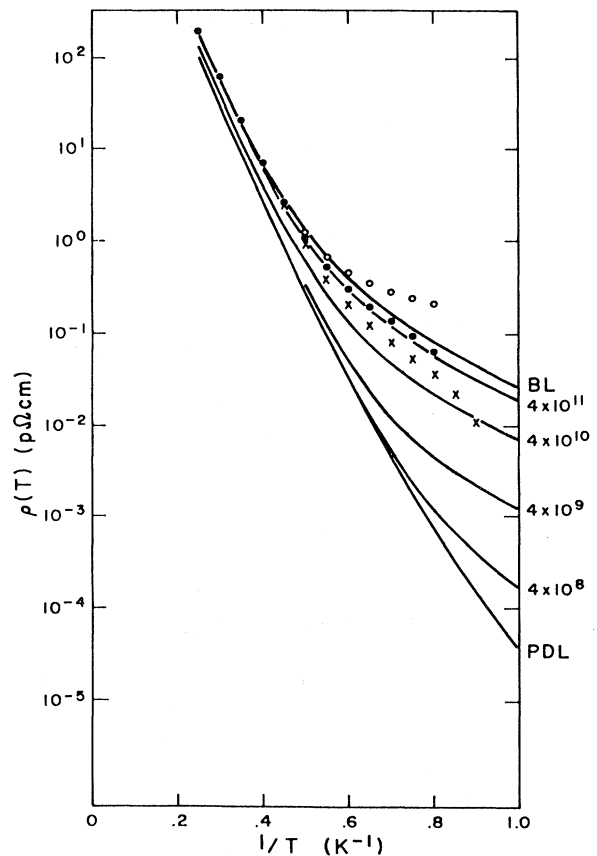Based upon the newly published initial data of van Kempen *et al.* (1975, 1976), Taylor *et al.* (1978) accepted

FIG. 14. $\rho(T)$ for K calculated for a range of dislocation densities. The experimental points are taken from van Kempen *et al.* (1976): ○, sample 2b unadjusted; ●, sample 2b and ×, sample 2c, both after adjustment by increasing ρ_0 by 1 part in 10^4 over the values presented in van Kempen *et al.* (1976). From Taylor *et al.*, 1978.

that such densities were not unreasonable, and that the data of Fig. 11(a) could thus be understood without the need for electron-electron scattering. In further support of their analysis, they noted that they had reason to believe that the Lawrence-Wilkins calculation overestimated the size of electron-electron scattering in K by more than an order of magnitude. In Sec. III.D.7, we shall see that the dislocation densities proposed by Taylor *et al.* are unrealistically high. In Sec. III.D.9, we shall see that, while Taylor *et al.* were correct that the Lawrence-Wilkins calculation involved a large overestimate, when a correction of this overestimate was combined with the inclusion of phonon-assisted electron-electron scattering, the calculation of A_{ee} for K returned to exactly the Lawrence-Wilkins value. Taylor *et al.* were thus incorrect in their expectation that a proper calculation of A_{ee} would yield a value much smaller than the T^2 coefficients reported by van Kempen *et al.*

Kaveh and Wiser (1979) quickly responded to Taylor *et al.* that phonon-dislocation scattering did not limit phonon drag simply to $T \leq 2$ K in annealed high-purity K. They performed an approximate calculation of $\rho_{ep}(T)$, in which both phonon-electron and phonon-dislocation scattering were included. Phonon-dislocation scattering was treated within the same single relaxation-time approximation used by Taylor *et al.*, and electron-dislocation scattering was assumed to be isotropic in **k** space. This calculation confirmed that, within this model, dislocation densities of about $10^{15}/m^2$ were needed before phonon-dislocation scattering became effective in quenching phonon drag. Kaveh and Wiser argued that such high dislocation densities were unrealistic in well annealed K samples and reaffirmed their previous contention (Kaveh and Wiser, 1977) that phonon drag was large in such samples to well above 2 K.

Later the same year, Stinson *et al.* (1979) showed how the presence of phonon drag in K, combined with partial quenching of this phonon drag by the phonon-dislocation scattering mechanism proposed by Taylor *et al.* (1978), could (1) resolve an order-of-magnitude discrepancy between the low-temperature lattice thermal conductivity κ of K measured below 4 K and the values previously calculated by Ekin (1972) assuming that the phonon system was completely equilibrated (i.e., no phonon drag) by phonon-phonon scattering; and (2) simultaneously explain both the form and the magnitude of the Nernst-Ettingshausen coefficient ϵ_{xy} of K from 1 to 4.2 K. Using the same Klemens relaxation-time approximation as was used by Taylor *et al.* and by Kaveh and Wiser (1979), Stinson *et al.* found that a single dislocation density of $\simeq 10^{14}/m^2$ permitted a consistent interpretation of the forms and magnitudes of both λ and ϵ_{xy}. They cautioned that this particular dislocation density should not be taken too seriously, both because of the rough nature of the Klemens formula and because they had no independent method for estimating this density. Since $\rho(T)$ is more sensitive than either ϵ_{xy} or λ to subtle details of the scattering of phonons by both electrons and dislocations,

these results do not permit a definitive conclusion concerning the magnitude of quenching of phonon drag in $\rho(T)$ in annealed high-purity K above 2 K. But they do strongly suggest that phonon-dislocation scattering will play an important role in quenching of phonon drag in $\rho(T)$ whenever enough dislocations are present. The major unresolved issue remains the magnitude of the relaxation time for phonon-dislocation scattering, since as we have already indicated, and will see in more detail in Sec. III.D.7, the dislocation density required by Stinson *et al.* is unrealistically high for annealed high-purity K.

Taylor (1982) later reviewed the successes of the first-principles form factor that he and his colleagues had developed, including the impressive agreements between theory and experiment described in Sec. III.B.1 above, and reaffirmed his confidence in it as a fundamental way of understanding phonon structure and transport properties in the alkali metals. He reiterated that all existing calculations of $\rho_{ep}(T)$ at low temperatures were only approximate, and he attributed the failure of their calculation to reproduce the data for K in the vicinity of 2 K, including phonon-drag, to limitations not yet adequately addressed in any calculation. He continued to question whether phonon drag was significant above about 2.5 K in K.

By 1980, it was agreed that phonon drag existed in K up to at least 2 K. But there was no clear understanding of how phonon drag was quenched by dislocations and impurities. As we just noted, Keveh and Wiser (1979) had used the argument that phonon-dislocation scattering was ineffective in quenching phonon drag to strengthen the theoretical case for the presence of phonon drag in K. One was thus faced with the problem of having to account for the substantial changes in $\rho(T)$ from 2 to 4 K that Gugan (1971) had observed in deformed samples of K, with dislocation densities that Gugan argued were smaller than $10^{15}/m^2$. We shall return to this topic in Sec. III.D.7, with still more experimental data to explain.

4. The CDW-based model of Bishop and Overhauser

Bishop and Overhauser (1979; 1981) proposed that the $T^{3/2}$ form of $\rho(T)$ reported by Rowlands *et al.* was due to scattering of electrons in K by phasons—quantized collective excitations of the CDW ground state (see Appendix C). Their calculation yielded basically an anisotropic Bloch-like behavior for $\rho(T)$, but with a characteristic temperature$= 6$ K instead of $\Theta_D = 100$ K for K (Kittel, 1976). Using parameters compatible with those previously estimated for K (Overhauser, 1978), they showed that this model could fit the $T^{3/2}$ temperature dependence reported by Rowlands *et al.* between 1.3 and 0.5 K as a transition between a high-temperature T dependence and an ultimate T^5 dependence as $T \rightarrow 0$ K. The model was also consistent with both the magnitude and the form of the van Kempen *et al.* (1976) data, since the uncertainties in those data permitted a $T^{3/2}$ fit. With

a suitable choice of parameters, the model could account for the magnitude of the $T^{3/2}$ term seen by Rowlands et al. Finally, since the coefficient of the electron-phason term was highly anisotropic with respect to the CDW domain axis, the model could qualitatively account for the large changes in magnitude of $\rho(T)$ that both Rowlands et al. and van Kempen et al. has found upon annealing, in terms of changes in the CDW domain structure of the samples. Bishop and Overhauser indicated the need for measurements to still lower temperatures to see whether $\rho(T)$ would transform to the ultimate T^5 form that they predicted.

5. Levy et al.: more on K and new measurements on Na

A year after the measurements of Rowlands et al., Levy et al. (1979) reported additional measurements from 4.2 K down to 1.1 K on K, and the first high-precision measurements on Na samples. Their samples were encased in $d = 1.0$ mm polyethylene tubes. Although they were only able to achieve precisions of a few parts in 10^6, not quite as good as van Kempen et al. and
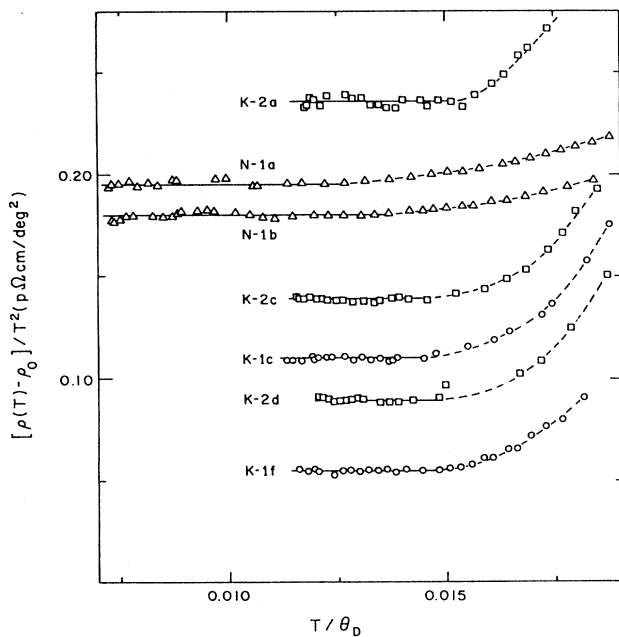
Rowlands et al., their data are unique in that they developed a technique (the details of which have not been published) for achieving very high RRR's in K samples. They interpreted the high RRR for one specially prepared sample as indicating that this sample was essentially strain free, with a very low dislocation content, and they used this sample as the baseline from which to estimate dislocation contents in their other samples. Below about 1.5 K they were able to fit their data with an AT^2 form (Fig. 15) by choosing appropriate values of ρ_0, and they quoted an uncertainty for this fit of $T^{2.0\pm0.1}$. Figure 16 shows their data for one sample replotted as $(1/T)(d\rho/dT)$ by Kaveh and Wiser (1984) to show that if the data were assumed to vary as T^2 then the magnitude of the T^2 coefficient was very low. The data are certainly compatible with a T^2 variation. However, as with the data of van Kempen et al, their scatter is too large, and the temperature range much too short, to delimit the form of the data very well. Thus, repeating the example of Fig. 11(b), the dotted line in Fig. 16 corresponds to $\rho(T) \propto T^3$.

For Na, Levy et al. also proposed an AT^2 fit at low temperatures (Fig. 15), and in this case the low-temperature term was dominant over a large enough temperature range to provide somewhat more confidence in a T^2 power law. Even here, however, as we shall see in Sec. III.F, Na data extended to much lower temperatures

FIG. 15. $(\rho_i - \rho_0)/T^2$ vs reduced temperature (T/Θ_D), with the Debye temperatures taken as 160 K for Na and 100 K for K. A horizontal line is drawn through the flat portion of the data to show the value of A obtained for each sample. The dashed lines showing the deviations from T^2 behavior are drawn free-hand simply to guide the eye: $\triangle$, Na; $\bigcirc$, sample 1 of K; $\square$, sample 2 of K. Note that the values of ρ_0 used to obtain the data points shown in this figure were adjustable parameters. From Levy et al., 1979.
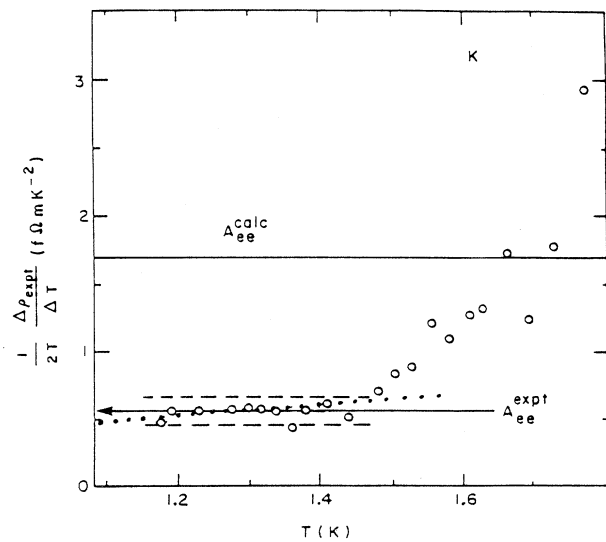

FIG. 16. $(1/2T)(\Delta\rho/\Delta T)$ vs T for sample K 2e of Levy et al. (1979). The horizontal straight line between the two dashed lines gives the experimental value for the coefficient A_{ee}^{exp} for this sample, together with the estimated error, $A_{ee}^{exp} = 0.58\pm0.1$ fΩ m/K^2. The horizontal straight line across the entire figure gives the calculated value $A_{ee}^{calc} = 1.7$ fΩ m/K^2 by MacDonald et al. (1981). After Kaveh and Wiser, 1984. The dotted straight line, added by the present authors, indicates how a T^3 variation would appear in this figure.

raises a question about the T^2 form for temperatures in the range 1–2 K. For Na, Levy et al. found that ρ_0 and A both decreased slightly upon annealing at 328 K for 14 d, and then both increased slightly upon simple cycling to room temperature. The three measurements of A were all consistent with the single value 1.9 ± 0.1 fΩ m/K^2.

For K, in contrast, Levy et al. found much more complex behavior of A_{ee} as ρ_0 changed. They deliberately contaminated their encapsulated samples by heating them in the presence of air to temperatures from 295 to 329 K to produce white contaminant on the sample surface. They also lightly cold-worked one of their samples by rolling a steel cylinder over the outside of the polyethylene tube to mix the surface contaminant into the body of the sample. The processes of contamination caused both the RRR's and the magnitudes of their T^2 terms to decrease. They interpreted these apparently coupled decreases in terms of a model involving anisotropic scattering of electrons by dislocations, which was developed concurrently with their measurements by their colleagues Kaveh and Wiser. To avoid redundancy, we describe that model before considering Levy et al.'s interpretation of their data.

6. The anisotropic scattering model of Kaveh and Wiser

Kaveh and Wiser (1980, 1982) put forward a consistent non-CDW-based explanation for the varieties of different behaviors that had been reported by van Kempen et al., Rowlands et al., and Levy et al. for K in the vicinity of 1 K. They proposed that all three sets of data should be fit with the AT^2 form associated with electron-electron scattering. They then ascribed the observed changes in the magnitude of A to changes in the relative amounts of isotropic and anisotropic (in k space) scattering, which they assumed varied systematically with holding time at room temperature or with changes in impurity content. For the samples of Rowlands et al., they forced a T^2 fit to each data set, ascribing the observed $T^{3/2}$ behaviors to the presence of some small additional effect in each sample, the source of which was not known.

Their model is as follows. They argued that if the relaxation time τ_k varied with wave vector k, then for a metal with a spherical Fermi surface Eq. (A6) should be replaced by Eq. (A7a), and the multiplicative factor in Eq. (9) becomes

$$A_{ee} \propto [\tau_{k_1}k_1 + \tau_{k_2}k_2 - \tau_{k_3}k_3 - \tau_{k_4}k_4] \ . \tag{13}$$

Here k_1 and k_2 are the wave vectors of the incoming electrons, k_3 and k_4 are those of the outgoing electrons, and τ_{k_i} $(i=1,2,3,4)$ is the relaxation time appropriate to the scattering of the electron with wave vector k_i by whatever scatterer dominates ρ_0. They argued that when ρ_0 is determined primarily by scattering of electrons by impurities, τ is isotropic (i.e., $\tau_{k_1}=\tau_{k_2}=\tau_{k_3}=\tau_{k_4}$). Since normal

electron-electron scattering involves only $G=0$, conservation of crystal momentum requires the right-hand side of Eq. (13) to be zero, and $A_{Nee}=0$. In such a case, only A_{Uee} (i.e., $G\neq0$) remains. They asserted that A_{Uee} is small in K, because the electronic states are well described by single plane waves. If, in contrast, ρ_0 is determined by scattering that is highly anisotropic in k space (i.e., $\tau_{k_i}\neq\tau_{k_j}$ for $i\neq j$) then, from Eq. (13), A_{Nee} would not be zero. The total T^2 coefficient would then contain two components, $A_{ee}=A_{Uee}+A_{Nee}$, and the magnitude of the anisotropic component A_{Nee} would vary with the amount of scattering anisotropy in τ. Kaveh and Wiser argued that the anisotropic component A_{Nee}, call it A_{Oee}, could be much larger than A_{Uee}, thereby leading to large increases in A as the scattering became more anisotropic.

To produce the highly anisotropic scattering their model required, Kaveh and Wiser (1980) initially invoked dislocations, postulating that the samples of van Kempen et al., Rowlands et al., and Levy et al. all contained a large number of dislocations when initially prepared. For the data of van Kempen et al. and Rowlands et al. they argued that the dislocation content decreased upon annealing, so that both ρ_0 and A_{Nee} decreased with annealing time. The experimental coefficient A thus decreased systematically with decreases in ρ_0 (i.e., with increases in RRR). For the data of Levy et al., in contrast, they argued, as did Levy et al. (1979), that heating the samples in air and rolling the samples both introduced more isotropic impurity scattering. This process caused A to decrease as ρ_0 increased.

Defining ρ_{0i} as the impurity residual resistivity (isotropic) and ρ_{0d} as the dislocation residual resitivity (anisotropic), with the requirement that $\rho_{0i}+\rho_{0d}=\rho_0$, the total residual resistivity, Kaveh and Wiser derived the following equivalent forms of the equation for A_{ee}:

$$A_{ee} = A_{Uee} + A_{Oee}[\rho_{0d}/\rho_0)]^2$$
$$= A_{Uee} + A_{Oee}[1+(\rho_{0i}/\rho_{0d})]^{-2} \ . \tag{14}$$

When $\rho_{0d}=0$, $A_{ee}=A_{Uee}$. When $\rho_{0d}\gg\rho_{0i}$ (i.e., when $\rho_0=\rho_{0d}$), $A_{ee}=A_{Uee}+A_{Oee}$.

Levy et al. analyzed their data on both K and Na using the first form of Eq. (14). For K, all the treatments to which they subjected their samples caused ρ_0 to increase. They assumed that these treatments increased only ρ_{0i} and not ρ_{0d}, arguing that in most cases they were very careful to avoid mechanical stresses on the sample, and that in the few cases where the samples were cold-worked the increases in ρ_0 were due mainly to mixing of impurities into the body of the sample rather than to the production of dislocations. The constant value for ρ_{0d} for each of their two samples was chosen to be the difference between the ρ_0 for that sample as initially prepared and the ρ_0 for an independent sample that they argued was produced virtually strain-free. For each sample, this ρ_{0d} defined a unique ρ_{0i} for any given value of ρ_0. Since ρ_{0d}

was nearly the same for the two samples, the first form of Eq. (14) allowed them simply to plot the T^2 coefficients for all of their data against $(\rho_{0d}/\rho_0)^2$, with ρ_{0d} fixed. As shown in Fig. 17, this plot yielded a straight line, as predicted by Eq. (14). For Na, in contrast, ρ_0 decreased when Levy et al. followed the same annealing procedure as for K. Since they did not wish to permit ρ_{0i} to decrease, they could not require ρ_{0d} to remain constant. Instead, they assumed a constant value for ρ_{0i} and attributed the decrease in ρ_0 to a decrease in ρ_{0d}. The value of ρ_{0d} was chosen to make the Na data fall on the same line (Fig. 17) as the K data. Presumably, the placement of the Na data on the line in Fig. 17 indicates that Levy et al. intended that the data for Na be interpreted in the same way as the data for K.

Kaveh and Wiser used the second form of Eq. (14) to describe the K data of van Kempen et al., Rowlands et al., and Levy et al. Their procedure for determining the unknown parameters A_{Uee}, A_{Oee}, and ρ_{0d} for the various samples was as follows. For A_{Uee}, they chose the lowest value of A reported in any of the three studies— Levy et al.'s value of $A_{Uee} = 0.5$ fΩ m/K^2. For the data of Levy et al., they followed the procedure used by Levy et al. to define ρ_{0d} and ρ_{0i}, involving the assumption of a constant value of ρ_{0d}. For the data of van Kempen et al. and Rowlands et al., in contrast, they chose the separate, but fixed, values of $\rho_{0i} = 60$ pΩ m and 80 pΩ m, respectively, and defined ρ_{0d} to be the deviation of ρ_0 from the appropriate one of these two values. This procedure assumed that the dislocation content of the samples slowly decrease over months. Kaveh and Wiser did not
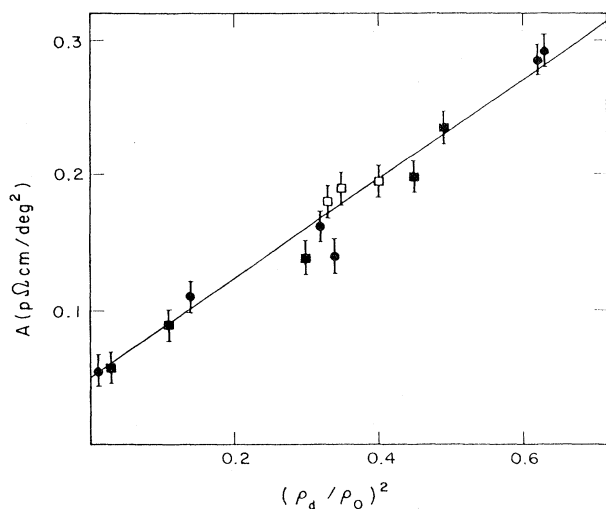
specifically justify the values of ρ_{0i} chosen to fit the data of van Kempen et al. and Rowlands et al., and it seems clear that these were simply picked to make the data fall near the curve determined by Kaveh and Wiser's choice of the only remaining empirical factor, A_{Oee}. They chose this parameter to be 3.5 fΩ m/K^2, close to the value determined by the straight-line fit in Fig. 17. These choices yielded the fit to the three sets of data shown in Fig. 18. At the bottom of this figure are listed what KW described as uncertainties in the values of ρ_{0i}/ρ_{0d}. These appear to have been chosen simply as an arbitrary fraction of the assumed values of ρ_{0i}/ρ_{0d}.

The initial KW (1980) letter did not mention Levy et al.'s Na data. Between publication of that letter and the subsequent longer paper (Kaveh and Wiser, 1982), MacDonald et al. (1981) published new calculations of A_{ee} for Na that increased the predicted value from Lawrence and Wilkins' estimate of 0.15 fΩ m/K^2 to 1.4 fΩ m/K^2—i.e., from less than 10% to over 75% of the A_{ee} measured by Levy et al. Kaveh and Wiser (1982) noted that the experimental value of Levy et al. was in good agreement with this prediction.

In a subsequent longer paper, van Kempen et al. (1981) included $\rho(T)$ data for a rapidly quenched sample (sample No. 3) measured only down to 1.3 K. This sam-
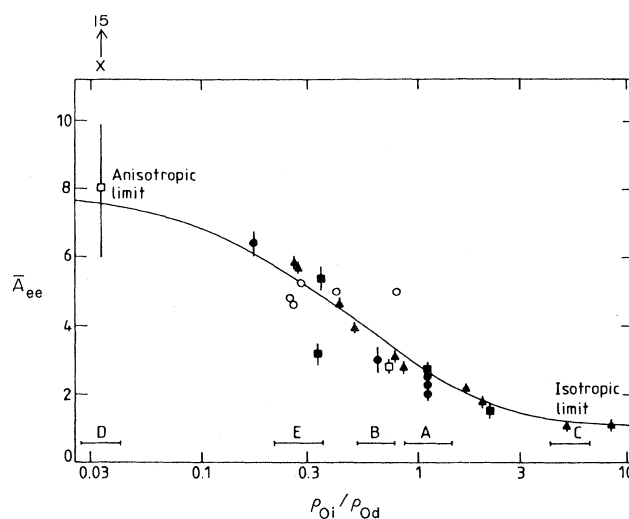

FIG. 17. Plot of A_{exp} vs $(\rho_d/\rho_0)^2$ for various samples of K and Na: ●, sample K-1 of K; ■, five treatments of sample K-2 of K; □, three treatments of sample N-1 of Na. The straight line is from the theory of Kaveh and Wiser (1982). From Levy et al., 1979.

FIG. 18. Values for $\overline{A}_{ee} = A_{ee}/A_{ee}^{iso}$ (where $A_{ee}^{iso} \approx 0.5$ fΩ m/K^2) for K is a function of the ratio ρ_{0i}/ρ_{0d}. The various symbols represent the data as follows: A (■), van Kempen et al., 1976; B (●), Rowlands et al., 1978; C (▲), Levy et al., 1979; D (□), van Kempen et al., 1981; E (○), Lee et al., 1981. The five horizontal error bars give Kaveh and Wiser's estimate of the uncertainty of the value of ρ_{0i}/ρ_{0d} for a typical point for each of the five sets of data. The open square at the left of the graph indicates the value for the sample from van Kempen et al. (1981) as derived by Kaveh and Wiser; the (×) represents the value as originally derived by van Kempen et al. After Kaveh and Wiser, 1982.

ple had a very low RRR (RRR $=368$; $\rho_0 = 186$ pΩ m). It also displayed both an unusually large T^2 coefficient ($A = 7.5$ fΩ m/K^2)—almost twice as large as the anisotropic KW limit—and a very large DMR in $\rho_{ep}(T)$. We consider here only the value of A, deferring consideration of the DMR in $\rho_{ep}(T)$ to the following section (III.D.7), where they can be examined along with other DMR in K. Danino, Kaveh, and Wiser (1981a) quickly reanalyzed the data for A in van Kempen et al.'s sample No. 3, using the calculation of Kaveh and Wiser (1979) to obtain a different form for $\rho_{ep}(T)$ than van Kempen et al. had used. They obtained the value $A_{ee} = 4 \pm 1$ fΩ m/K^2, which they argued was consistent with the predicted isotropic limit of the KW model. To obtain values of ρ_{0i} and ρ_{0d} for this sample, they assumed that the increase in ρ_0 produced by rapid cooling was due entirely to the introduction of dislocations. In Fig. 18 we plot both of these proposed values for this data point, located at the value of ρ_{0d}/ρ_{0i} chosen by Kaveh and Wiser. The discrepancy between the two values shows how large a change in the inferred A_{ee} can be produced by different assumptions concerning the form of ρ_{ep} when the experimental data extend down to only 1.3 K.

Bishop and Overhauser (1981), and Gugan (1982) soon pointed out that the dislocation densities n_d required by Kaveh and Wiser for their anisotropic scattering model were unrealistically large by 2 to 4 orders of magnitude. They noted that it was extremely difficult to produce even 10^{13}/m^2 dislocations in K by deformation, and that the data of Gurney and Gugan (1971) showed that dislocations annealed away in less than an hour at room temperature. Gugan also pointed out that his prior data on DMR in rapidly cooled samples (see Sec. III.B.2) were much more compatible with retention of point defects in solution than with production of dislocations, and indicated that this was likely also to be true for van Kempen et al.'s sample No. 3. Thus a model that required most of the increase in ρ_0 in van Kempen et al.'s sample No. 3 to be due to dislocations was unlikely to be viable.

Accepting the objection just noted concerning the number of dislocations in K samples, Kaveh and Wiser (1982) modified their model to apply to "extended defects," which included dislocations, stacking faults, and grain boundaries. They argued that the highly anisotropic phonon spectrum of K made it likely that all extended defects would produce strongly anisotropic scattering.

Because of the importance of this imaginative model in guiding subsequent experiments, and as the focus of the three previous review articles, it is important to recognize its fundamentally heuristic nature and to remember that it contains unknown parameters for which no fundamental justifications are given. Rather, the parameters of the master curve (Fig. 18) were determined from the fit of the data of Levy et al. shown in Fig. 17, under the assumption that ρ_{0d} was constant for Levy et al.'s samples and that ρ_{0i} varied from measurement to measurement. Data from each other group (including later data from the MSU group presented in Sec. III.E below) were then

fit to the master curve by making the opposite assumption that ρ_{0i} was constant for the complete set of measurements from that group, at a value that caused the data of that set to fall most closely around the curve.

7. Quenching of phonon drag

We noted in Sec. III.D.3 that Kaveh and Wiser (1979) had disputed the proposal of Taylor et al. (1978) that sufficiently large dislocation densities ($\simeq 10^{15}$/m^2 from an approximate calculation) might exist in annealed high-purity K to equilibrate the phonon system above about 2 K by the mechanism of phonon-dislocation scattering and thus to quench phonon drag.

Danino, Kaveh, and Wiser (1981b, 1981c) subsequently revived this mechanism to try to understand the unusually large value of $\rho_{ep}(T)$ for van Kempen et al.'s (1981) rapidly quenched sample No. 3 discussed near the end of Sec. III.D.6. They argued that quenching produced a large dislocation density. To explain the data with the same Klemens relaxation-time model used previously, they had to attribute all of the increase in ρ_0 to the introduction of dislocations. They used an "experimental" estimate of $\rho_{0d} = (4 \times 10^{-25} \; \Omega \, \text{m}^3)n_d$ [referenced to Brown (1977) but from original data from Basinski et al. (1963)] to relate the increase in ρ_0 to a dislocation density n_d, and obtained a value of $n_d = 5 \times 10^{14}$/m^2 for the van Kempen et al. sample. Their model yielded an expression for the ratio $\rho_{ep}(n_d, T)/\rho_{ep}(0, T)$, in which $\rho_{ep}(n_d, T)$ was the electron-phonon resistivity with phonon drag partially quenched by n_d dislocations, and $\rho_{ep}(0, T)$ was the resistivity of the same sample with complete phonon drag. The magnitude of $\rho_{ep}(n_d, T)$ for the rapidly quenched sample of van Kempen et al. (1981) was compatible with this model for $n_d = 5 \times 10^{14}$/m^2.

The paper by Gugan (1982) mentioned at the end of the preceding section (III.D.6) made three points concerning the dislocation content of K that are relevant to the Danino et al. model. First, that any estimate of n_d in K was highly uncertain; for example, Brown (1977) had calculated a value of $\rho_{0d}/n_d = 8 \times 10^{-25} \; \Omega \, \text{m}^3$ for dislocations in K, twice as large as the "experimental" estimate of $4 \times 10^{-25} \; \Omega \, \text{m}^3$ derived from the data of Basinski et al. Second, that the Danino et al. (1981b, 1981c) model could not produce the large changes in $\rho_{ep}(T)$ that Gugan (1971) had previously found on deliberately deformed K, even with the uncertainties just noted concerning the number of dislocations introduced by the deformation. Third, that the large value of ρ_0 in van Kempen et al.'s rapidly cooled sample was much more likely to be due to a supersaturation of impurities in solution than to the dislocations required by Danino et al.

Engquist (1982), and Danino, Kaveh, and Wiser (1982, 1983), soon independently proposed a qualitative mechanism, involving anisotropic electron-dislocation scattering, to make dislocations more effective in reducing phonon drag. Their argument extended the reasoning under-

lying the KW analysis for A_{ee} in K. Danino *et al.* described the mechanism as follows. Phonon drag is only fully operative if the electron distribution function is characterized by an isotropic relaxation time in **k** space. In this case, there is a coherent exchange of momentum back and forth between the electron and phonon systems, and the dislocations are ineffective in equilibrating the phonon system. If, instead, the dominant electron relaxation time τ_k is anisotropic, then certain portions of the Fermi surface dominate electron-phonon scattering, the mutual transfer of momentum between the electrons and the phonons becomes "random," and phonon drag is reduced. A much smaller number of dislocations can then quench phonon drag.

Engquist examined the data of Rowlands *et al.* (1978), and concluded that this mechanism provided a plausible explanation for the facts that the data for their unannealed sample in Fig. 12 were approximately in the Bloch limit from 2–3 K, whereas their data for an annealed sample shifted from near the phonon-drag limit at 2 K to near the Bloch limit by 3 K. No quantitative fits were given.

Danino *et al.* examined the data for one of Gugan's (1971) samples. They simply assumed that the scattering anisotropy varied as $(k_2)^n$, where **k** is the change in the wave vector upon scattering, and the power n was an adjustable parameter chosen to give the best fit to the experimental data. With $n = 2$, they obtained the fit shown in Fig. 19. Including effects of both electron-dislocation scattering and phonon-dislocation scattering, they predicted the ratios of $\rho_{ep}(n_d, T)/\rho_{ep}(0, T)$ for K at 3 K to be those shown in Fig. 20. At 3 K, Danino *et al.* required dislocation densities of $n_d = 10^{13}/\mathrm{m}^2$ to start to quench

FIG. 20. The ratio $\rho_{ep}(n_d, T)/\rho_{ep}(0, T)$ as a function of the dislocation density n_d for K at 3 K, as predicted by Danino *et al.*, 1983. $\rho_{ep}(n_d, T)$, and $\rho_{ep}(0, T)$ are defined in the caption to Fig. 19. The dashed and dot-dashed curves give, respectively, the predictions including only phonon-dislocation scattering or only electron-dislocation scattering. The solid curve indicates the effect of combining both types of scattering. The arrows labeled "el-dis" and "ph-dis" show the value of n_d at which the indicated scattering process begins to contribute significantly. From Danino *et al.*, 1983.

phonon drag in K, and $n_d = 10^{16}/\mathrm{m}^2$ to fully quench it. Danino *et al.* (1983) also estimated the relative effects of anisotropic scattering on phonon drag in the other alkali metals. For these predictions, we refer the interested reader to their paper.

While the proposal that anisotropic electron-dislocation scattering enhances the effectiveness of quenching of phonon drag by dislocations provides a plausible heuristic explanation for the data of the samples chosen, it has not yet been converted into a quantitative theory involving no adjustable parameters. We shall see in Sec. III.G that it fails even qualitatively to describe some later data. Moreover, we note that the parameters derived by Danino *et al.* do not produce the behavior of Rowlands *et al.*'s data attributed to this same mechanism by Engquist.

8. Sinvani *et al.*: Li

The next study of $\rho(T)$ in an alkali metal was made by Sinvani *et al.* (1981), who measured $\rho(T)$ for Li from 4.2 K down to 1.1 K with the same procedures used by Levy *et al.* for K and Na. They found $\rho(T)$ to vary closely as T^2 over the whole temperature range (Fig. 21), with a coefficient $A = 30 \pm 1$ fΩ m/K^2 in good agreement with the value of $A \simeq 33$ fΩ m/K^2 found by Krill (1971) almost 10 years before at temperatures between 4 and 10 K. Sinvani *et al.* attributed this T^2 variation to the dominance of electron-electron scattering in Li all the way up to 10 K. Noting that this value of A was an or-
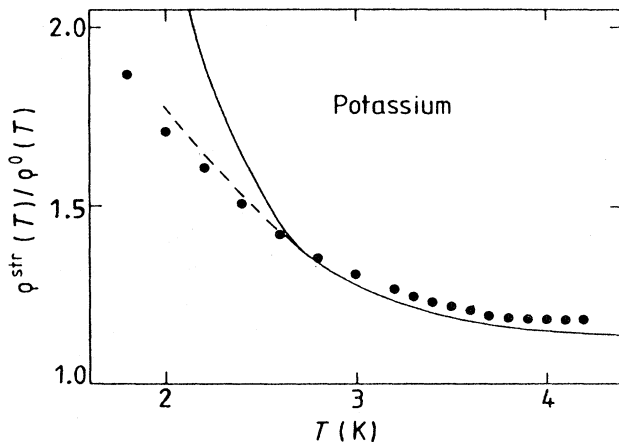

FIG. 19. $\rho_{ep}(n_d, T)/\rho_{ep}(0, T)$ (solid circles) for strained sample 5b of Gugan (1971). $\rho_{ep}(n_d, T)$ and $\rho_{ep}(0, T)$ are, respectively, the resistivities of strained K (containing n_d dislocations) and of fully annealed K. The dashed and solid curves give, respectively, the theoretical values calculated by Danino *et al.* (1982) with and without an electron-electron scattering term. From Danino *et al.*, 1982.
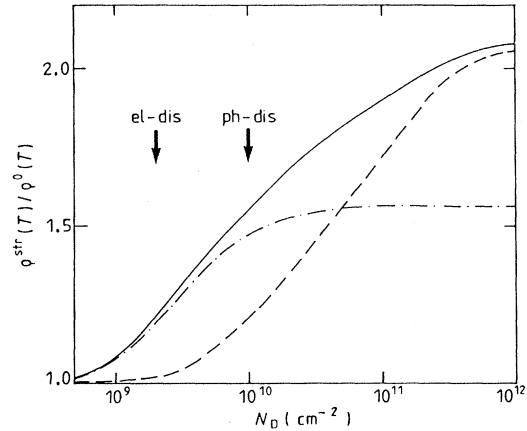
der of magnitude larger than the best prediction for bcc Li (see Table I), they proposed that their Li samples were in the anisotropic scattering limit of the KW model, with $A_{Nee} \simeq 10 A_{Uee}$. They argued that Li would be forced into this limit by the multiple-plane-wave nature of its wave functions and—even more importantly—by defects introduced during its phase transformation from a bcc structure to a more complex structure upon cooling to below 75 K. This model was purely heuristic; the value $A_{Nee} \simeq 10 A_{Uee}$ was justified solely on the ground of need and similarity to the ratio developed by Kaveh and Wiser for K (Sec. III.D.6).

9. Electron-electron scattering from high-temperature Lorenz ratio measurements, and new calculations of A_{ee}

While evidence for the presence of electron-electron scattering in $\rho(T)$ in simple metals was growing, thought was also being given to other ways of obtaining informa-
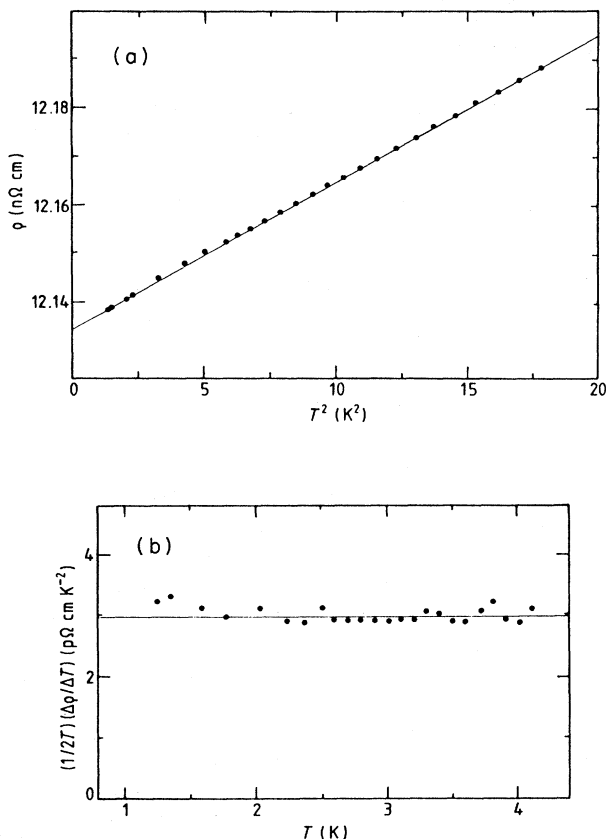

FIG. 21. Additional evidence of electron-electron scattering in Li. (a) ρ_t vs T^2 for Li: ●, the measured data points; solid line, the best straight-line fit to the data points. (b) The data of (a) for Li replotted as $(2T)^{-1}(\Delta\rho/\Delta T)$ vs T: ●, the measured data points, ———, the best horizontal straight-line fit to the data points. From Sinvani et al., 1981.

tion about electron-electron scattering in these metals.

The possibility of studying electron-electron scattering in the thermal resistivities W_{ee} of simple metals at low temperatures was ruled out on the grounds that the expected effects were smaller than anticipated experimental uncertainties. Kaveh and Wiser (1984) discuss the considerations involved.

Laubitz (1970) pointed out, however, that the contribution of electron-electron scattering to W_{ee} should be observable at high temperatures as a negative deviation of the Lorenz number, $L(T) = \rho(T)/[TW(T)]$, from its Sommerfeld value of $L_0 = 2.44 \times 10^{-8}$ WΩ/K². Cook, Van der Meer, and Laubitz subsequently measured W_{ee} for the noble metals, Al, and the alkali metals. The results for the alkali metals are given in Cook (1979a, 1979b; 1981; 1982) and Cook, Van der Meer, and Laubitz (1972), and are very nicely summarized along with additional data in Kaveh and Wiser (1984). We consider in detail only the alkali metals data, focusing mainly on their relation to A_{ee}.

The availability of data on W_{ee} for the simple metals stimulated MacDonald and Geldart (1980) to calculate W_{ee} for these metals. They noted that W_{ee} should be easier to calculate than A_{ee}, because all scattering events contributed to W_{ee}, not only those described by the umklapp fraction Δ [Eq. (9)]. One thus needs to calculate only the electron-electron scattering time τ, and not Δ, to determine W_{ee}. For the alkali metals, they calculated τ using the approximate quasiparticle scattering function developed by Lawrence and Wilkins (1973), but with added corrections for band structure and for DMR. Their calculations yielded rather good agreement with experiment for the alkali metals. For the noble metals, the predicted values were two to three times larger than experiment, but here the combined uncertainties in theory and experiment were so large that these values were not considered to be in conflict.

Soon afterward, new measurements of A_{ee} in Cu and Au by Khoshnevisan et al. (1979) stimulated MacDonald and Laubitz (1980) to estimate values of A_{ee} for the simple metals from the high-temperature experimental data for W_{ee}^{exp}. Following a procedure proposed by Lawrence (1978), they related A_{ee} to the quantity $X_{ee} = (-\rho_{ee}/T^2 + W_{ee}L_0/T)$, $T \gg \Theta_D$ by the equation

$$A_{ee}^{calc} = 5\Delta X_{ee}^{exp}/(8-2\Delta) , \qquad (15)$$

in which the only unknown quantity is the umklapp fraction Δ. Although this equation was not exact, they expected it to be rather good. Combining the W_{ee} measurements of Cook and co-workers, noted just above, with the Lawrence-Wilkins (1973) calculations for Δ, they derived values for A_{ee}^{calc} from Eq. (15) to compare with A_{ee}^{exp}.

For the noble metals, MacDonald and Laubitz found reasonable agreement between A_{ee}^{calc} and A_{ee}^{exp}, given the mutual uncertainties, i.e., $A_{ee}^{calc} \simeq 0.6-0.8 A_{ee}^{exp}$. For Al, in contrast, they found A_{ee}^{calc} to be a factor of 15 smaller

than the new A_{ee}^{exp} of Ribot *et al.* (1979). For K, Mac-Donald and Laubitz derived the value $A_{ee}^{calc} \leq 2.5$ $f\Omega \, m/K^2$. They viewed this value as an upper bound on the true A_{ee}, because they believed that the Lawrence-Wilkins value of Δ for K was an overestimate. The only experimental data they had to compare with this prediction were those of van Kempen *et al.* (1976), the T^2 coefficients of which varied from sample to sample. Since such a variation was contrary to expectation for simple electron-electron scattering, MacDonald and Laubitz assumed that there must be two different effects present, and that the lowest T^2 coefficient of van Kempen *et al.* would provide an upper bound on A_{ee}^{exp}. This value, $A_{ee}^{exp} \leq 0.8$ $f\Omega \, m/K^2$, was only about one-third of their prediction. K thus joined Al as a metal for which it appeared that $A_{ee}^{calc} \neq A_{ee}^{exp}$.

MacDonald (1980) was stimulated by this disagreement between A_{ee}^{calc} and A_{ee}^{exp} for Al to reexamine electron-electron scattering in Al. He found that A_{ee} in Al was dominated, not by Coulomb scattering, but rather by phonon-mediated scattering, a type of scattering that had been completely neglected in the previous calculations of A_{ee}. Including this term increased A_{ee}^{calc} for Al by the factor of almost 20 needed to bring it into agreement with the data of Ribot *et al.*

Kaveh and Wiser (1981) quickly used MacDonald's new result for Al to propose a general qualitative framework for understanding why MacDonald and Laubitz's values of A_{ee}^{exp} and A_{ee}^{calc} agreed with each other for the noble metals but differed for Al and K. They argued that two different contributions should each cause A_{ee} to decrease with increasing temperature: anisotropic dislocation scattering and phonon-mediated scattering. The contribution from anisotropic dislocation scattering should be large for the alkali metals but small for the noble and polyvalent simple metals. In contrast, phonon-mediated electron-electron scattering should be important in the polyvalent metals, which become superconducting, but relatively unimportant in the alkali and noble metals, which do not. Combining these two effects, they concluded that one would expect $A_{ee}^{exp} = A_{ee}^{calc}$ for the noble metals, but $A_{ee}^{exp} < A_{ee}^{calc}$ for both Al and K. To explain the K data semiquantitatively, they also had to postulate that Lawrence and Wilkins's value of A_{ee}^{calc} was too large by about a factor of 2.

MacDonald's (1980) demonstration of the importance of phonon-mediated electron-electron scattering in Al stimulated MacDonald, Taylor, and Geldart (1981) to recalculate A_{ee} for the alkali metals with this new contribution. They improved the previous estimate of Δ for the alkali metals by using a four-plane-wave Fermi surface, made a new estimate of the phase space available for umklapp scattering, used a nonlocal first-principles pseudopotential, and took into account many-body effects on the electron-ion interaction. Comparison of the third and fourth columns in Table II shows that their calculated A_{ee} for Na was about 10 times larger than the Lawrence-Wilkins value, but their A_{ee} for K was exactly

the same as Lawrence and Wilkins had found. This agreement for K occurred, however, by means of a cancellation of two very large effects. For Coulomb scattering alone, the combination of four-plane-wave Fermi surfaces with the new estimates of MacDonald *et al.* for the phase space available for umklapp scattering reduced Δ in K by about a factor of 100 compared to the Lawrence-Wilkins calculation. However, including phonon-mediated electron-electron scattering caused A_{ee} for K to return to the Lawrence-Wilkins value.

For K, this importance of phonon-mediated scattering in K, and the lack of change in A_{ee}^{calc}, were both contrary to the assumptions made by Kaveh and Wiser in their analysis described just above. The puzzle concerning the difference between $A_{ee}^{calc} = 1.7$ $f\Omega \, m/K^2$ and Kaveh and Wiser's value of $A_{ee}^{exp} = 0.5$ $f\Omega \, m/K^2$ thus remained. We note that our picture completely resolves this puzzle, since our proposed constant value for K of $A_{ee}^{exp} \simeq 2.1$ $f\Omega \, m/K^2$ (Table II) agrees well with the calculated value of 1.7 $f\Omega \, m/K^2$.

E. Initial measurements on K and KRb with 10^{-7} precision: inelastic electron-impurity scattering and a new anomaly below 0.3 K

An important limitation on all of the measurements on K that we have described so far was that they contained residual effects of electron-phonon scattering down to their lowest temperatures. It was thus necessary to know the form of the contribution due to electron-phonon scattering to properly extract the form of the new low-temperature term that was being attributed to electron-electron scattering. The theorists tackled this issue seriously and proposed various values for the quantities n and Θ in Eq. (11) for different temperature ranges. Kaveh and Wiser (1974a) derived the values $n = 2$ and $\Theta = 10$ K for $T < 0.6$ K, but $n = \frac{7}{2}$ and $\Theta = 8$ K for 3 K $< T < 6$ K. Orlov (1975) derived $n = 1$ and $\Theta \simeq 20$ K for 2 K $< T < 5$ K. Frobose (1977) derived $n = \frac{3}{2}$ and $\Theta = 17.6$ for 2 K $< T < 6$ K, but with an extra temperature-dependent term also present. Finally, Kaveh, Leavens, and Wiser (1979) carefully examined the complete temperature range from 0 to 6 K. For 2.5 K $< T < 4$ K, they found $n = 1$ and $\Theta = 20$ K. They concluded, however, that (1) no single pair of values for n and Θ in Eq. (11) is valid over the entire range from 0 to 6 K; (2) between 2 and 4 K, a variety of alternatives give fits of comparable quality—as initially observd by Gugan (1971); (3) any given fit should be used over only a few K at most; and (4) Eq. (11) is not valid for the temperature range 1–2 K, exactly where the experimentalists needed it most. This last point made it clear that measurements to still lower temperatures were essential for establishing the detailed temperature dependence of the additional term.

The group that finally succeeded in extending ultrahigh-precision resistivity measurements on the alkali

metals to below 0.5 K with the capabilities described in Appendix B was the Michigan State University (MSU) group of the authors of this article, with important initial assistance from J. A. Rowlands as a visitor. Because of the higher measuring sensitivity and precision available to this group, it was able, for the first time, to measure free-hanging samples only a few centimeters long. It was also able to reproduce most of the conditions used by others (thin samples, samples in polyethylene, etc.) and to study deformed samples with high precision, abilities of great importance in understanding $\rho(T)$ in the alkali metals. With only one exception—a study by van Vucht et al. (1982; 1986) of deformed K and KRb down to 0.9 K—all the remaining data we describe were obtained by the MSU group. We shall see that their first studies yielded results much simpler than those reported by van Kempen et al., Rowlands et al., and Levy et al..

The experimental techniques and capabilities of the MSU group are described in Appendix B. The samples were extruded in a glove box and mounted in pairs on a sample holder, which permitted each to be used as the reference for the other. Bulk samples were typically 5 cm long between the potential leads and had $d \geq 1$ mm. The first measurements were made with Ar in both the glove box and the sample can. These measurements were made with a precision of about 1 part in 10^{7} using a preliminary sample can, which was subsequently discovered to produce temperature errors below about 0.2 K (Pratt, 1982). Later measurements were made with an improved sample can, in which absolute uncertainties in dT at the lowest temperatures were reduced to about one percent. In addition, the measuring precision was improved to about 2 parts in 10^{8}. We shall see that data below 0.3 K obtained with the new can differed little from those found with the old one.

Data taken with the unimproved sample can were presented in three papers.

In the first, Lee et al. (1980) reported measurements of the resistivities of free-hanging K(Rb) alloys containing 0.077–2.24 % Rb, which permitted the first isolation of the term $\rho_{iei} = A_{I}\rho_{0}T^{2}$ [Eq. (5)]. To eliminate unwanted effects of electron-phonon scattering, they limited their analysis to temperatures below 1.1 K. From 1.1 K down to 0.2 K, their data were consistent to within experimental uncertainty with a simple T^{2} variation (Fig. 22), and the coefficient of this T^{2} term increased linearly with ρ_{0} (Fig. 23). Since their experimental coefficient of $A_{I} = (8.5 \pm 0.3) \times 10^{-6}/\mathrm{K}^{2}$ was in good agreement with the predictions of about $13 \times 10^{-6}/\mathrm{K}^{2}$ by Taylor (1964) and Kus and Taylor (1980) listed in Table III, they concluded that they must be seeing inelastic electron-impurity scattering. Importantly, their data on KRb alloys also extrapolated to the value $A_{ee} = 2.1 \pm 0.2$ fΩ m/K^{2} for pure K.

Pratt et al. (1981) and Lee et al. (1982) then described measurements extending from 4.2 K down to 0.5 K on free-hanging high-purity K samples with diameters 0.9, 1.5, and 3.0 mm, prepared and cooled in Ar gas. Above
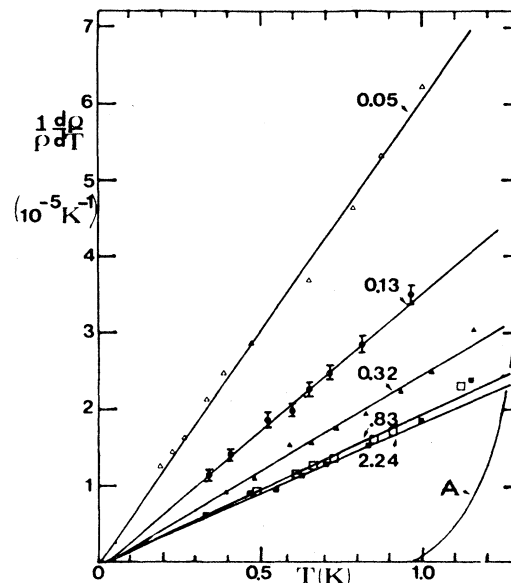

FIG. 22. $(1/\rho)(d\rho/dT)$ vs T for KRb alloy samples for $T < 1.3$ K. Numbers appended to curves are nominal Rb concentrations. Typical errors are shown for the 0.13% sample. Curve A represents $\rho^{-1}(d\rho/dT)$ for electron-phonon scattering in units of 10^{-7} K^{-1} (0.32% sample). After Lee et al., 1980.

1.3 K, their data were in excellent agreement with those found by previous investigators (Fig. 24). Between 1.3 and 0.5 K they found simple AT^{2} resistivities, with a coefficient A that was nearly independent of modest
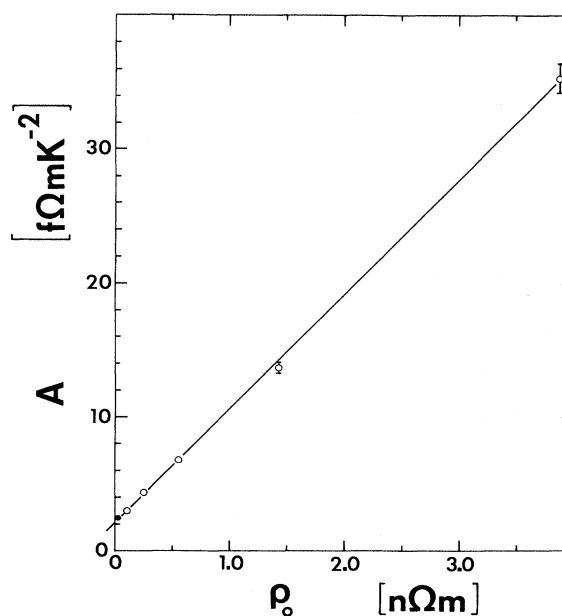

FIG. 23. A vs ρ_{0} for KRb alloys and for pure K: ○, KRb alloys; ●, pure K. A is the coefficient of the T^{2} term in $\rho(T)$ below 1 K. From Pratt et al., 1981.

van Kempen *et al.*,[2]
☐ sample no. 2b, RRR ≃ 6000

Rowlands *et al.*,[3]
+ sample no. K1b, RRR ≅ 4800
× sample no. K2B, RRR ≅ 4800

Ekin and Maxfield,[4]
△ sample, RRR ≅ 8000
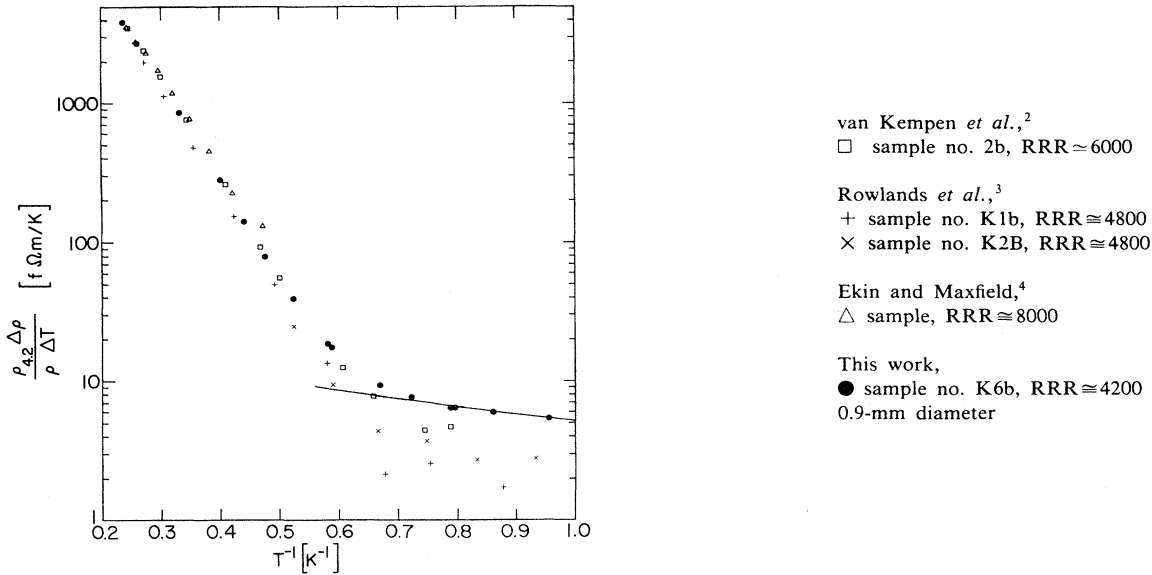
This work,
● sample no. K6b, RRR ≅ 4200
0.9-mm diameter

FIG. 24. Log of $(\rho_{4.2\,K}/\rho)(\Delta\rho/\Delta T)$ vs T^{-1} for data from a variety of sources. A straight-line behavior for smaller values of T^{-1} indicates a dominant exponential dependence of $\rho(T)$. The smooth curve at large values of T^{-1} is an extrapolation to higher temperatures of the observed AT^2 behavior between 0.5 and 1 K in sample K 6b. After Pratt *et al.*, 1981.

changes in both ρ_0 and sample thickness (Fig. 25). They reported being unable to reproduce the $T^{3/2}$ variation found by Rowlands *et al.*; the dashed curve in Fig. 25 corresponds to a $T^{3/2}$ variation. They argued that the
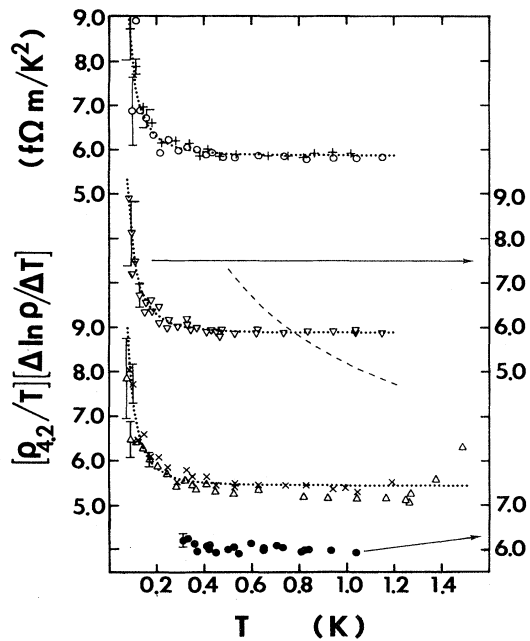

FIG. 25. $(\rho_{4.2\,K}/\rho T)(\Delta\rho/\Delta T)$ vs T for various samples: +, K4a; ○, K4b; ▽, K5; ×, K6a; △, K6b; ●, K7c. The dashed curve represents a $T^{3/2}$ variation of $\rho(T)$. The dotted curves are fits to the data of a T^2 term plus a term varying as $T^{-0.3}$. From Pratt *et al.*, 1982.

absence of a size effect in their data ruled out the Knudsen limit size-effect model of Rowlands *et al.* as an explanation for their data, and that the absence of a $T^{3/2}$ variation made any CDW-based model unnecessary. They noted that their value of the T^2 coefficient $A = (2.2 + 0.3)$ fΩ m/K^2 for high-purity K was nicely consistent with an extrapolation to $\rho_0 = 0$ of the K(Rb) alloy data of Lee *et al.* (1980) and also in good agreement with the calculations of A_{ee} (dominated by A_{Uee}) for K listed in Table II. Pointing out that the data of Gugan (1971) made it highly unlikely that their samples could have the large dislocation densities needed to make their results compatible with the KW model, Lee *et al.* concluded that simple electron-electron scattering provided the best available explanation for their data from 1.3 K down to 0.3 K. They noted that additional mechanisms were then needed to explain the more complicated behaviors reported by other investigators.

Lee *et al.* (1982) extended measurements of $d\rho/dT$ for pure K down to below 0.1 K. Below 0.3 K, they discovered a new anomaly, involving a strong deviation from T^2 behavior (Fig. 25). This anomaly was neither predicted nor explained by any of the existing models for $\rho(T)$ in K. They presented alternative fits to this anomalous term varying as $T^{-0.3}$ or as $\ln T$. They ruled out a Kondo effect as the source of the anomaly on the grounds that they observed no related thermoelectric anomaly (Blatt *et al.*, 1976)—i.e., the G data went smoothly to a constant value at low temperatures (Fig. 26). Lee *et al.* argued that this deviation from T^2 behavior in $\rho(T)$ might indicate (a) a change in the T^2 coefficient below 0.3 K; (b) the appearance of a completely new phenomenon below 0.3 K; or (c) that the success of the simple free-
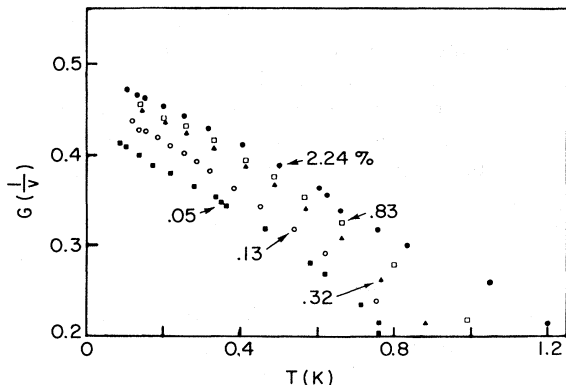
FIG. 26. Thermoelectric ratio G vs T for KRb samples. $G = S/LT$, where S is the thermopower and L the Lorenz ratio. After Yu, 1984.

electron model above 0.3 K was fortuitous—based on the possibility of an alternative fit involving a different form for the low-temperature anomaly combined with something other than a simple T^2 term above 0.3 K.

These MSU results were soon reviewed by Schroeder (1982) and Pratt (1982) at conferences. Schroeder briefly

ρ (pΩm)		ρ (pΩm)	
X K−8	12.2	▽ K−H3	16.9
⋈ K−9	14.4	▼ K−H4	9.4
● K−10	11.9	▲ K−H5a	10.2
★ K−11	10.1	△ K−H5b	11.1
○ K−H1	14.2	• K−H6a	9.5
□ K−H1b	13.7	■ K−H6b	10.5
◇ K−H2	9.9	◆ K−H6c	11.0
——— K−4a	} of Lee		
- - - - K−6a			

FIG. 27. $(\rho_{4.2\,K}/\rho T)(\Delta\rho/\Delta T)$ vs T for free-hanging, bare, high-purity, thick K wires. Note that the magnitudes of the horizontal portions of the data vary by only about ±15% about the average value. From Yu et al., 1989.

reviewed all of the known data on K, but focused upon the fact that the MSU group did not find the large variations in A reported by previous groups. Pratt described the problems with the initial sample can that we noted above, and indicated that these problems generated uncertainty concerning the magnitude of the anomalous behavior in K seen below 0.3 K. Subsequently, Yu et al. (Yu et al., 1983; Yu, Yin, et al., 1989) took more complete data on pure K measured in the improved sample can and found that the anomaly below 0.3 K continued to be seen in all pure-K samples measured. Figure 27 shows, however, that the magnitude of this anomaly varied considerably from sample to sample, with both larger and smaller anomalies than those reported by Lee et al. (1982).

Pratt (1982) also described a new set of data in which K had been outgassed in vacuum for 12 h before being placed in the sample can in a He atmosphere. Above 0.3 K the results obtained with this sample (filled symbols in Fig. 25) were consistent with those obtained with non-outgassed samples in Ar gas. Outgassing the samples was thus not necessary for obtaining reproducible results.

Both Pratt and Schroeder concluded that the MSU group was finding much simpler behavior for $\rho(T)$ in K between 0.3 and 1.3 K than had been reported by previous researchers and that the reasons for these differences were not yet understood.

At the same conference, Wiser (1982) reviewed the experimental data on $\rho(T)$ for K at low temperatures, emphasizing the large variations in magnitude that were observed in $\rho_{ep}(T)$ and—by most groups—also in $\rho_{ee}(T)$. He showed how the KW models for quenching of phonon drag and electron-electron scattering could explain these variations. The nonvarying A_{ee} data of Lee et al. (1982) were incorporated into the KW model by simply choosing for all of Lee et al.'s samples a single value for $\rho_0 d$ that caused their T^2 components to span the KW curve (Fig. 18). Following Danino et al. (1981a) the A_{ee} data for the rapidly cooled K sample of van Kempen et al. (1981) were incorporated as representing the anisotropic limit of the KW model. These were the last K data that Kaveh and Wiser compared quantitatively with their model for A_{ee} in their later review articles (Wiser, 1984; Kaveh and Wiser, 1984).

F. Li, Na, and Rb below 1 K: very-low-temperature anomalies

The MSU group subsequently extended measurements of $\rho(T)$ on Li (Yu et al., 1983), Rb (Yu et al., 1983), and Na (Yu, Bass, and Pratt, 1984, 1985) to temperatures down to 0.1 K. In all three cases they discovered anomalous upturns in $(1/T)(d\rho/dT)$ at temperatures lower than previous experimenters had reached. These anomalies are illustrated together in Figs. 28(a) and 28(b) in the alternative forms $(1/T)(d\rho/dT)$ and $d\rho/dT$, respectively, along with K data for comparison. We discuss each metal separately.
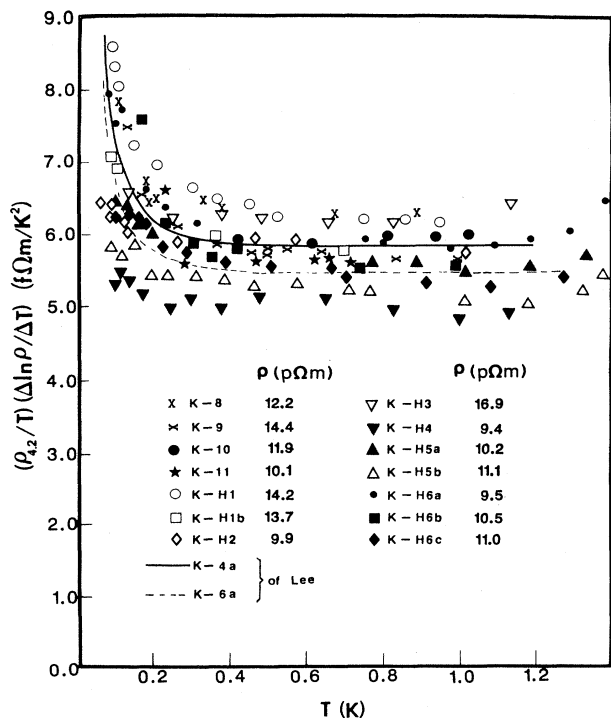
For Li, the anomalous behavior began at about 1.3 K, just at the low end of the data of Sinvani et al. (1981). Above 1.3 K, the new Li data were in good agreement in both form and magnitude with the T^2 behaviors found by Sinvani et al. and by Krill (1971). Since these combined sets of data produce AT^2 behavior from 1.3 K up to 10 K, with coefficients that fall within the range $A = 30 \pm 3$ fΩ m/K^2 for all three studies, we conclude that electron-electron scattering dominates $\rho(T)$ in Li from 1.3 to 10 K. We follow Sinvani et al. in noting that the magnitude of this T^2 term is about 10 times larger than the predictions (Table II) for Li in a bcc structure. We shall consider the significance of this discrepancy in Sec. IV.E.

In contrast to Li and K, the Rb data of Yu et al. (1983) showed no T^2 regime at all; the low Debye temperature of Rb caused electron-phonon scattering to remain large right down to where the very-low-temperature anomaly became important (about 0.4 K). Since no T^2 regime was observed, it was only possible to estimate an upper bound on the AT^2 term in Rb. From Fig. 28(a), this bound is 25 fΩ m/K^2, a value about eight times larger than the best theoretical estimate (Table II).

Above 0.4 K, $(1/T)(d\rho/dT)$ for Rb [Fig. 29(a)] initially rises much more rapidly with increasing temperature [see Fig. 3(a)] than Taylor and MacDonald (1980b) had predicted for $\rho_{ep}(T)$ assuming a spherical Fermi surface, but eventually slows down to where it increases less rapidly than predicted [see insert in Fig. 29(a)]. Thus either the experimental $\rho_{ep}(T)$ for Rb contains a much larger normal (i.e., T^5) component than predicted, or else the umklapp component does not assume its ultimate exponential form until much lower temperatures than predicted. The first alternative seems unlikely. The second, in contrast, would be a natural consequence of a distorted Fermi surface. Calculations with a more realistic Fermi surface are needed to clarify the form and magnitude of $\rho_{ep}(T)$ without phonon drag before we can address the issue of phonon drag in Rb.

The data for Na were intermediate in behavior between Li and Rb. For Na samples from two different sources, and with two different RRR's, the anomalous behavior at very low temperatures extended up to above 1 K. Between 1.2 and 2.3 K, the new Na data (Fig. 30)
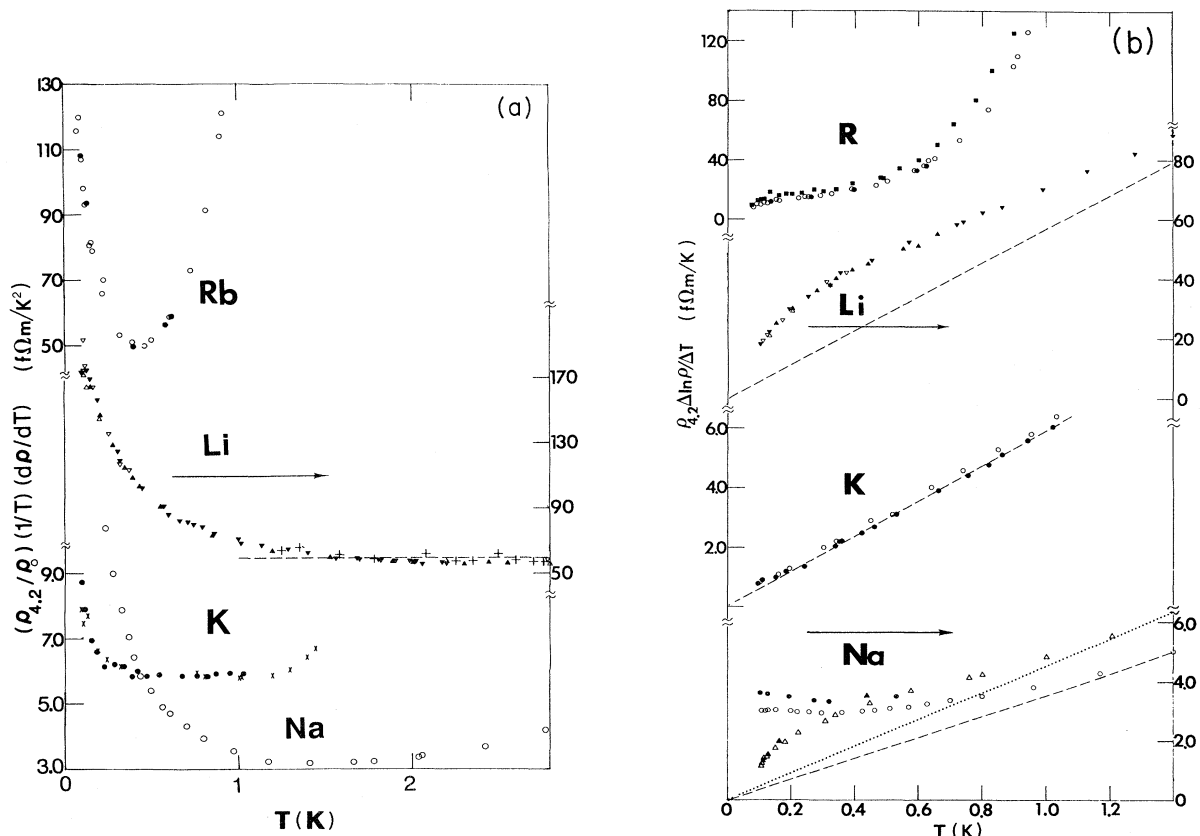

FIG. 28. Low temperature resistivity anomalies in K, Li, Na, and Rb. (a) $(\rho_{4.2\,K}/\rho T)(\Delta\rho/\Delta T)$ vs T for K, Li, Na, and Rb samples showing the appearance of low-temperature anomalies in all four metals. From Zhao, 1988. (b) The data of Fig. 28(a) plus additional samples, plotted as $(\rho_{4.2\,K}/\rho)(\Delta\rho/\Delta T)$ vs T. The dashed and dotted lines indicate the T^2 resistivities inferred from the flat portions of curves plotted as in Fig. 28(a). From Yu, Bass, and Pratt, 1985.

bounded the Na data of Levy et al. (1979). The data for Yu et al.'s Na samples with RRR ≃ 4700—comparable to Levy et al.'s samples—fell slightly below the data of Levy et al. The data for Yu et al.'s Na samples with a

lower RRR ≃ 400 fell above Levy et al.'s data. From Fig. 28(b), it appears that these differences in behavior for different RRR's are at least partly attributable to the anomalous portion of $\rho(T)$ below 1.2 K. But they could also reflect different percentages of bcc and fcc-hcp Na, since Taylor and MacDonald (1980a) predict significant differences (e.g., 20–50 % depending upon the temperature) between the values of $\rho_{ep}(T)$ of these two different crystal structures. To within experimental uncertainties, all of the Na data were compatible with a T^2 behavior between about 2 and 1.2 K, and any horizontal line in the vicinity of the Levy et al. data and the new higher RRR data yields a value of A_{ee} in good agreement with the best prediction in Table II. Yu et al. noted, however, that the new Na data were better described by a smooth curve in a plot of $(1/T)(d\rho/dT)$ than by a flat region bounded by upturns. Given the absence of a clear flat region in Fig. 30, Yu et al. concluded on the basis of their new data that Levy et al.'s data for Na probably defined only an upper bound on the real A_{ee}.

Above 2 K, the form of $(1/T)(d\rho/dT)$ for Na [Fig. 29(b)] is compatible with the T^3 variation predicted [see Fig. 4(c)] by Taylor and MacDonald (1980a), but the magnitudes are only about half those predicted. If we take the calculation at face value, these magnitudes sug-
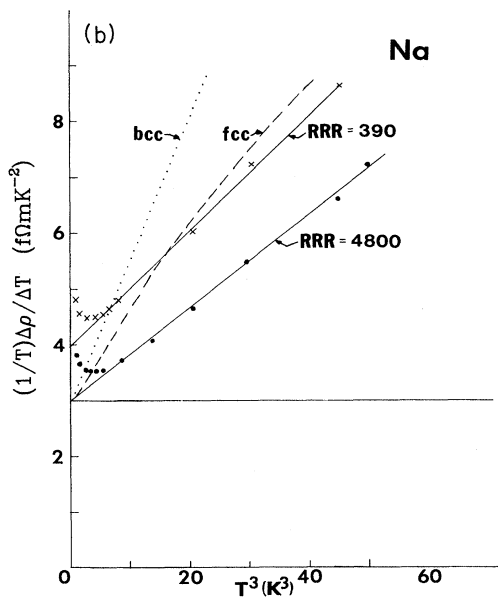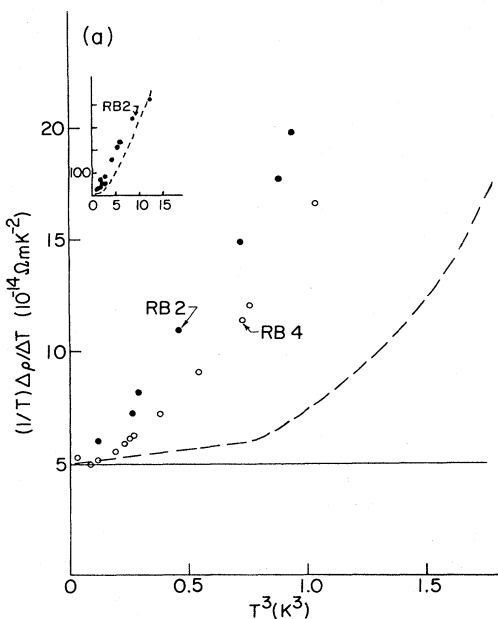

FIG. 29. Measured and predicted values of $d\rho_{ep}/dT$ for Rb and Na. (a) $(1/T)(d\rho/dT)$ vs T^3 for two Rb samples above the "minima" in the curves of Fig. 28(a). Straight-line behavior indicates a T^5 variation of $\rho_{ep}(T)$. The dashed curves are estimates, taken from Fig. 4(a), of the predictions of Taylor and MacDonald, 1980a. (b) $(1/T)(d\rho/dT)$ vs T^3 for two Na samples above the "minima" in the curves of Fig. 28(a). Straight-lines behavior indicates a T^5 variation of $\rho_{ep}(T)$. The dashed and dotted curves are estimates, taken from Fig. 4(c), of the predictions of Taylor and MacDonald, 1980b for fcc and bcc Na, respectively.
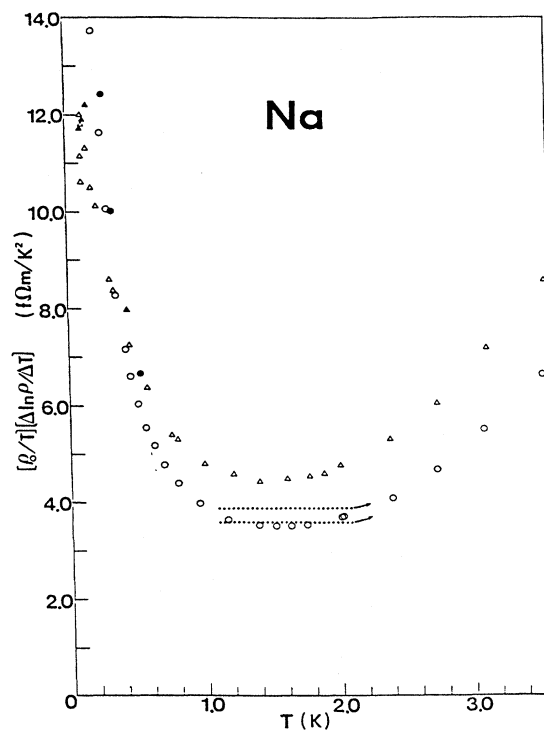

FIG. 30. $(\rho_0/\rho T)(\Delta\rho/\Delta T) \simeq d\rho/dT$ vs T for Na samples from 0.1 to 3.6 K. The dotted lines represent $\rho(T) \propto T^2$ fits to Na data from Levy et al. (1979). This figure corrects data for one Na sample given in Yu, Bass, and Pratt, 1984, 1985.

gest the possibility of partial phonon drag. However, we are unable to quantify the amount of phonon drag in Na, since Taylor and MacDonald used only an energy-independent, isotropic distribution function, and inclusion of energy and angular dependences could well cause the calculated $\rho_{\mathrm{ep}}(T)$ to decrease significantly.

In his Ph.D. thesis, Yu (1984) also examined two other possible effects in Na, the data for which are published for the first time in this review.

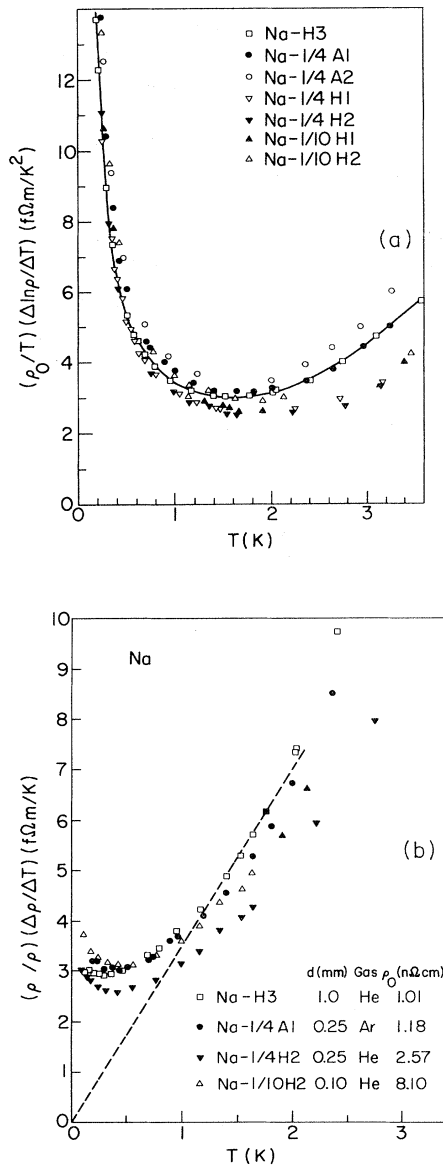To check for any size effect in Na wires, Yu examined

whether $d\rho/dT$ would change significantly in thinner wires of his highest-purity Na. As shown in Fig. 31, the thinned samples displayed behavior somewhat different from that of the $d=1$ mm Na, especially above about 2 K, but there was no systematic variation with sample thickness. Whether this absence of a systematic size effect is intrinsic, or simply due to the lack of sufficiently pure bulk samples (see Sec. IV.C), is not yet clear. We tentatively attribute the differences between data for different samples shown in Figs. 30 and 31 to different mixtures of the bcc and hcp phases of Na in different samples—such as samples with different thicknesses—assuming that these two phases have somewhat different values of the coefficient A_{ee}.

Stimulated by his study of a "Kondo-like" anomaly in K in polyethylene tubing, which we will discuss in Sec. IV.B, Yu examined whether encasing Na in polyethylene tubing might produce a similar anomaly. As shown in Fig. 32, the values of $(1/T)(d\rho/dT)$ for the samples in polyethylene were similar to those for bare samples with, perhaps, a slightly more rapid rise with increasing temperature above 2 K for the samples in polyethylene. No "Kondo-like" anomaly was found.

We conclude this discussion of $\rho(T)$ for Li, Rb, and Na by examining in more detail the anomalous behavior at the lowest temperatures illustrated in Fig. 28(b). We see

FIG. 31. Low temperature resistivities of thin Na samples. (a) $(\rho_0/\rho T)(\Delta\rho/\Delta T)\simeq(1/T)(d\rho/dT)$ vs T for thin Na samples. (b) The data of (a) replotted as $(\rho_0/\rho)(\Delta\rho/\Delta T)\simeq d\rho/dT$. After Yu, 1984.
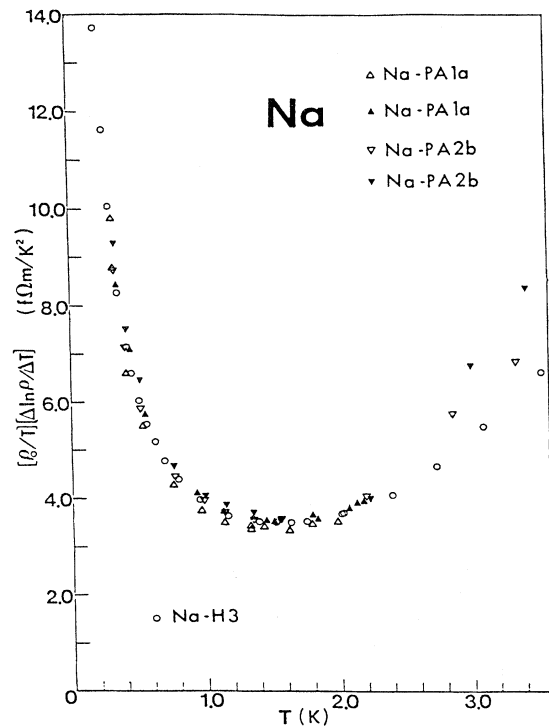

FIG. 32. $(\rho_0/\rho T)(\Delta\rho/\Delta T)\simeq(1/T)(d\rho/dT)$ vs T for Na samples encased in polyethylene tubes. From Yu, 1984.

that the low-temperature anomalies in Li, Na, and probably also in Rb display a peaked form in $d\rho/dT$. We shall see in the following section (III.G) that similar peaks in $d\rho/dT$ are seen in deformed K samples. Since the Li data extended over the widest temperature range and also had the best defined T^2 component from higher-temperature data, Yu tried fits to these data using four alternative models: scattering of electrons by vibrating dislocations with one or two local phonon modes, and scattering of electrons by bound electron states with one or two bound states. The two bound-electron states gave the best fits, but it is not clear whether these fits have any physical significance.

G. Initial measurements on deformed K and KRb: a new anomaly

We have seen that dislocations play an important role in the KW model of the behavior of $\rho(T)$ in K in the vicinity of 1 K. To check explicitly how dislocations affect $\rho(T)$, van Vucht et al. in 1982 and Haerle et al. in 1983 measured deformed samples of K. The measurements of van Vucht et al. extended down to 0.9 K, those of Haerle et al. to 0.1 K. Three important results came

from these measurements. (1) Above 1.3 K, both van Vucht et al. and Haerle et al. found large DMR in $\rho(T)$. We shall see, however, that they disagreed concerning the temperature dependence of these DMR. (2) For $T \leq 1.3$ K, both found increases in $\rho(T)$ much larger than those predicted by Kaveh and Wiser. (3) van Vucht et al. were unable to determine independently the form of the increases in $\rho(T)$ below 1.3 K and assumed that it was simply T^2. Haerle et al., with their wider temperature range, discovered a form that was much more complex than T^2. They analyzed their data in terms of a completely new contribution, scattering of electrons from vibrating dislocations.

1. van Vucht et al.

van Vucht (1982) measured $\rho(T)$ down to 0.8 K on three $d=3$ mm samples twisted at 4.2 K. The characteristics of their samples (K4, K5, K7), as well as those of a later measurement (van Vucht et al., 1986) (K8, K12), to be considered in Sec. IV.D, are given in Table VII. We note that extended annealing at room temperature always restored the coefficient A to approximately its pre-

TABLE VII. Characteristics of deformed samples of van Vucht et al., 1982 and 1986.

Sample		State	ρ_0 (pΩ m)	A (fΩ m K^{-2})	B (pΩ m K^{-1})
K4	1	Annealed at room temperature 3d in He	27.63	3.1±0.3	
	2	Deformed 180°	28.59	3.6±0.3	
K5	1	Annealed at room temperature 3d in He	14.38	2.7±0.1	43±2
	2	Deformed 360°	15.63	3.6±0.1	53±2
	3	Annealed at room temperature 3 weeks *in vacuo*	14.82	2.6±0.1	45±2
K7	1	Annealed at room temperature 3d in He	15.63	2.6±0.1	46±2
	2	Deformed 360° clockwise	16.96	3.8±0.1	53±2
	3	Deformed 360° counterclockwise	18.24	4.2±0.1	56±2
	4	Annealed at 18 K for 10 min	17.54	3.6±0.1	53±2
	5	Annealed at 78 K for 6 h	16.17	3.1±0.1	51±2
	6	Annealed at room temperature 30 h *in vacuo*	13.18	2.78±0.1	48±2
	7	Deformed 180°	13.91	3.35±0.1	54±2
	8	Deformed 360°	14.81	3.75±0.1	57±2
	9	Deformed 540°	15.75	4.15±0.1	60±2
	10	Annealed at room temperature 4 d *in vacuo*	15.76	3.0±0.3	53±2
	11	Deformed 10×360°	28.17	6.0±0.3	73±2
	12	Deformed 30×360°	36.55	7.2±0.3	80±2
	13	Deformed 60×360°	40.58	8.09±0.05	78.0±0.5
K8	1	Annealed at room temperature 1 d in He	18.31	2.9±0.2	52±3
	2	Deformed 2×360°	21.72	4.2±0.5	84±10
	3	Deformed 4×360°	24.12	5.1±0.4	60±3
	4	Deformed 8×360°	28.66	5.4±0.2	68±3
K12	1	Annealed at room temperature 1 d in He	146.3	4.8±0.2	65±5
	2	Deformed 5×360°	158.7	7.5±0.3	82±10
	3	Deformed 6×360°	170.9	8.4±0.5	110±20
	4	Annealed at 6 K for 10 min	165.3	8.1±0.2	77±5
	5	Annealed at 20 K for 20 min	163.0	7.7±0.3	81±5
	6	Annealed at 110 K for 20 min	150.8	4.8±0.3	111±20

deformation value; the effects of deformation were thus reversible.

Because their samples were thick and their voltage sensitivity was limited, van Vucht et al. were able to achieve a precision of only $\simeq 5 \times 10^{-6}$. Combined with their limited temperature range, this limited precision made it impossible for them to determine reliably the form of their data at low temperatures. They fit their data to the sum of two terms,

$$\rho(T) = \rho_{ee}(T) + \rho_{ep}(T) = AT^2 + BT \exp(-\Theta/T) .$$

Figure 33 shows that van Vucht et al. found the coefficient B to increase by up to a factor of 2 after deformation. The abscissa in Fig. 33 is the value of the dislocation resistivity ρ_{0d} derived from analysis of their coefficients A, as we describe next. Interestingly, the values of B that van Vucht et al. obtained for their unstrained samples are considerably smaller than those reported by van Kempen et al. (1976, 1981) or by other investigators, even taking into account that van Vucht et al. found a best fit $\Theta = 18.8$ K rather than the 19.9 K found by van Kempen et al. The reason for this discrepancy is not known, and its significance for evaluating the changes in their data is unclear.

Taking guidance from the KW model (1981), van Vucht et al. fit their values of the coefficient A to the first form on the right-hand side of Eq. (14)—i.e., $A = A_0 + A_I(\rho_{0d}/\rho_0)^2$—with values of $A_0 = A_{Uee}$ and $A_I = A_{Oee}$ common to all of their samples. In practice,
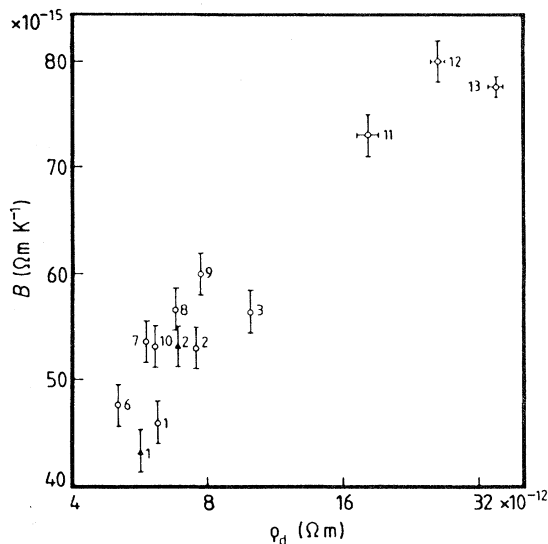
the contributions due to A_0 were found to be so small that A_0 was neglected. Using the fact that $\rho_{0d} = \rho_0 - \rho_{0i}$, the operative equation then becomes

$$A = A_I[(\rho_0 - \rho_{0i})/\rho_0]^2 , \tag{16}$$

and a plot of $\rho_0 A^{1/2}$ versus ρ_0 should yield a straight line for samples with the same ρ_{0i}. Figure 34 is such a plot for the van Vucht et al. data, data from the earlier paper by van Kempen et al. (1981), and some later data to be discussed in Sec. IV.D.1.

van Vucht et al. separated their new data into five groups, each assumed to have a constant value of ρ_{0i}. Two of these groups had only two data points, one had three, and two had four. Four of these groups were compatible in form with Eq. (16) with a single slope of $A_I = 19 \pm 2$ fΩ m/K^2 (solid lines in Fig. 34). van Vucht et al. noted with surprise that this coefficient was five times larger than the value of 3.5 fΩ m/K^2 that had been derived by Kaveh and Wiser (1981) from the data of Levy et al., van Kempen et al., and Rowlands et al. The four data points for the fifth group, in which a sample was subjected to much larger deformations than for the other groups, also fell on a straight line, but with a slightly smaller slope (dashed line in Fig. 34). We note that each of the straight lines just described defines a unique value of $\rho_{0d} = \rho_0 - \rho_{0i}$ for every data point in the group to which that line applies.

In contrast to the behavior of van Vucht et al.'s data on deformed samples, the older data of van Kempen et al. (1981) fell along a line with a much smaller slope (chain line in Fig. 34), closer to the value derived by Kaveh and Wiser (1981) from the data of Levy et al., van Kempen et al., and Rowlands et al. The data for van Vucht et al.'s annealed samples also fell along a single line with a slope similar to that for van Kempen et al.'s data. In Sec. III.I.3, we describe how van Vucht et al. (1985) in their subsequent review article proposed making the KW model consistent with both the old and the new data simply by rescaling the constants in the KW model. The data of Haerle et al., which we describe next, shows that the actual situation is more complex than this proposal anticipated.

van Vucht et al. also found, to their surprise, that when they annealed one of their samples at 18 K, which according to Gugan eliminates only point defects, A decreased. On its face, this behavior was contrary to the KW model, in that an increase in the fraction of ρ_0 due to dislocation scattering should lead to an increase in A. In an attempt to resolve this discrepancy, van Vucht et al. postulated that vacancies in K were generated in strings, which scattered electrons with an anisotropy similar to that for dislocations.

FIG. 33. The coefficient B of the exponential electron-phonon component of strained K vs ρ_0 for samples K5 (▲) and K7 (○). This graph shows the influence of lattice imperfections on the electron-phonon component of $\rho(T)$ in K. From van Vucht et al., 1982.

2. Haerle et al.

Haerle et al. (1983) extended measurements to below 0.1 K on K and KRb samples of diameter $d = 0.9$ mm
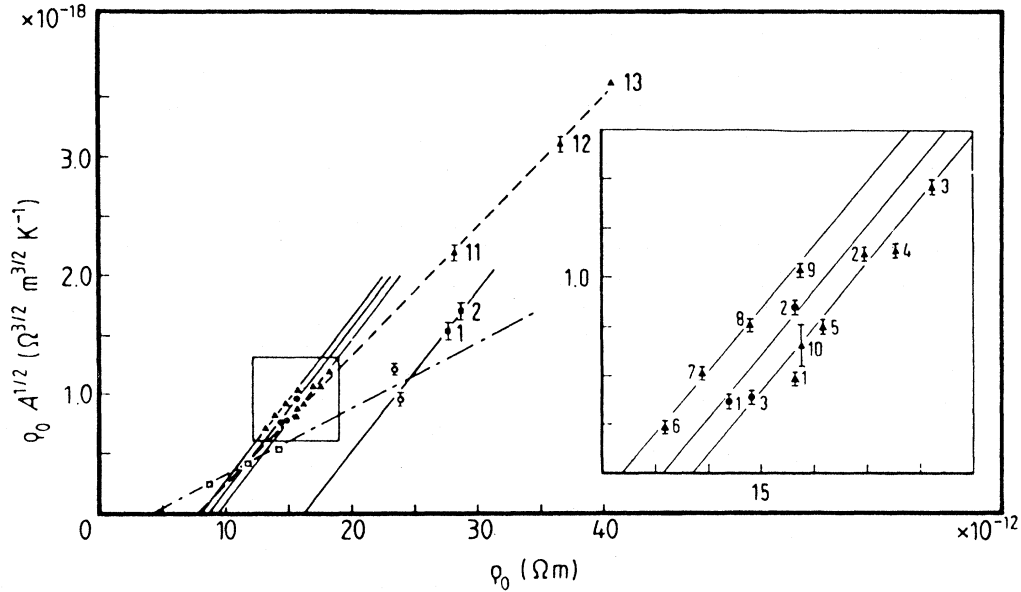
FIG. 34. $\rho_0 A^{1/2}$ vs ρ_0, where A is the coefficient of an assumed T^2 term in strained K samples. This graph shows the inferred influence of lattice imperfections on electron-electron scattering in K: $\blacksquare$, sample K4; $\bullet$, sample K5; $\blacktriangle$, sample K7; $\bigcirc$ and $\square$, data from van Kempen et al., 1981. The continuous lines represent a least-squares fit to the data of van Vucht et al. (1982). The dashed line is a similar fit to the most heavily deformed data of sample K7 (see Table VII). The dot-dashed line is a least-squares fit to the data of van Kempen et al., 1981. From van Vucht et al., 1982.

deformed at 60 K by squashing them between two metal plates. Because it was not feasible to have two identical samples, only one of which was squashed, the measurements were made against a reference resistor fabricated from an oxygen-annealed dilute Cu(Ag) alloy with a resistance of $R = 1.6$ $\mu\Omega$ that varied very little with either temperature or measuring current. The samples were electrically insulated from the two metal plates by thin plastic sheets. The choice of plastic for these sheets turned out to be very significant. Initial tests with Teflon on undeformed samples showed that the K surface blackened, but that no anomalies appeared. Preferring a plastic that did not react with K, the experimentors carried out tests with polyethylene. The K in contact with the plastic remained shiny, but there appeared an unexpected Kondo-like anomaly at very low temperatures (Haerle et al., 1986), in which $d\rho/dT$ became negative (Fig. 35), corresponding to a resistivity minimum. We shall discuss further studies of this anomaly in Sec. IV.B. Teflon was thereafter used as the insulating plastic.

The diameter $d = 0.9$ mm was chosen to be small enough to permit heavy deformation in a convenient geometry. From the data of Lee et al. (1982; see Sec. III.E), for samples measured in Ar gas, this thickness was expected to be large enough to eliminate any size effect on $\rho(T)$. Unfortunately, this assumption was erroneous for Haerle et al.'s samples measured in He gas. In fact, Haerle et al. were the first people to reproduce the smaller values and curvature of $d\rho/dT$ reported by Rowlands et al. (1978) on thin samples made and cooled in He.

Haerle et al. did not discover this fact until measurements were well underway in a system in which thicker wires could not be used. We shall see that the behavior of $d\rho/dT$ for the undeformed pure K complicated the in-
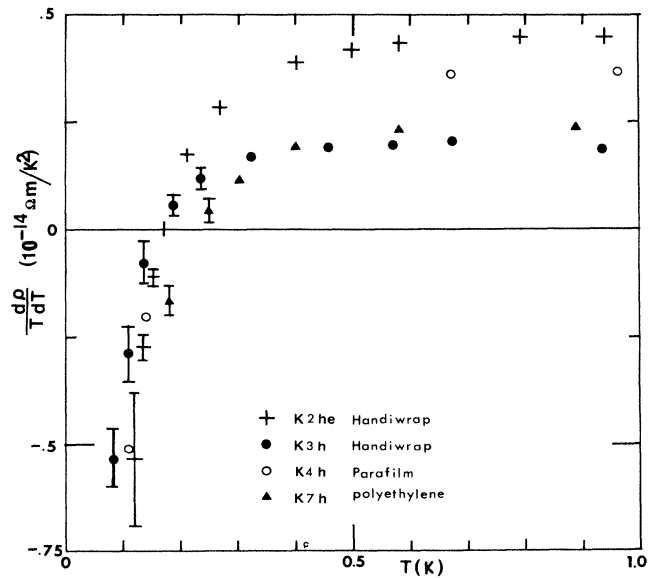

FIG. 35. $(1/T)(d\rho/dT)$ vs T for several K specimens in contact with the indicated plastics. From Haerle et al., 1986.

terpretation of their data.

Haerle *et al.* were able to make a direct test of the KW model by comparing two particular samples among those they had deformed. The first was a pure-K sample in which the deformation-induced increase in ρ_0 due to dislocations was arranged to be comparable to the initial ρ_0 due to impurities alone. For this sample, the KW model predicted substantial changes in A, due to the increase in the amount of anisotropic scattering. The second was a dilute K alloy (0.077 at. % Rb), in which the initial value of ρ_0 due to the Rb was so large that the fractional increase due to dislocations produced by the deformation was less than 10%. For this sample, the KW model predicted little change in A, since the dominant scatterer remained isotropic.

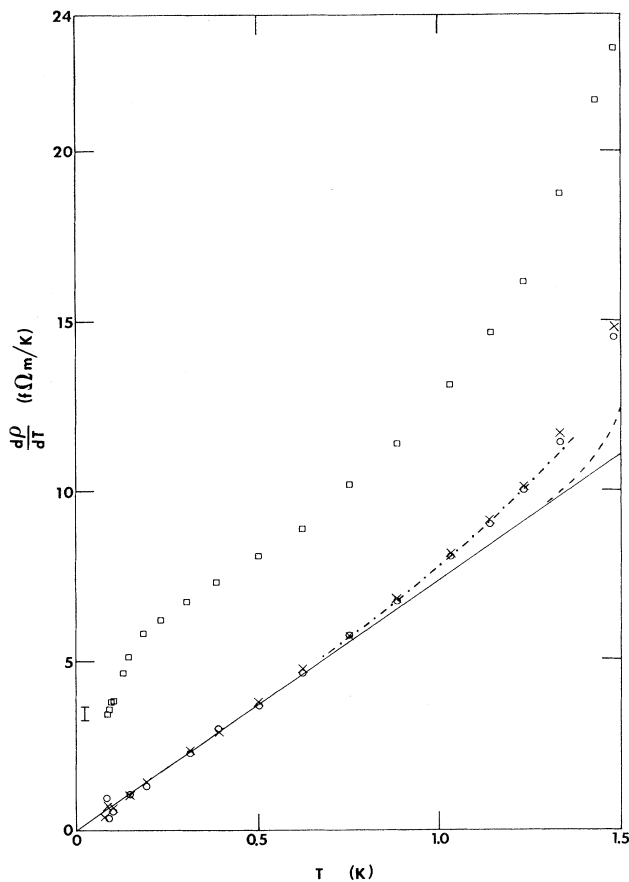For both K and KRb, Haerle *et al.* used the conver-

sion factor 4×10^{-25} Ω m^3 to derive deformation-induced dislocation densities of about 2×10^{13}/m^2 from the measured increases in ρ_0 due to deformation. Both these increases in ρ_0 and the concurrent increases in $d\rho/dT$ due to the presence of the dislocations were completely reversed by annealing for several minutes at 160–200 K.

Haerle *et al.* found several interesting results.

(1) At temperatures above 1 K, they confirmed van Vucht *et al.*'s observations that deformation caused $\rho_{ep}(T)$ to increase, as illustrated in Figs. 36 and 37. However, in disagreement with van Vucht *et al.*, they found that they could attribute this increase solely to the growth of a T^5 term.

(2) At all temperatures, they found that similar deformations of K and KRb gave similar increases in both ρ_0 and $d\rho/dT$, despite the fact that the fractional increase in ρ_0 was 100% in K but only 7% in KRb. Above 1.3 K this similarity for $d\rho/dT$ is qualitatively incompatible with the Engquist (1982) and Danino *et al.* (1982) models of quenching of phonon drag due to anisotropic electron-dislocation scattering. Below 1.3 K it is similarly incompatible with the KW model for effects of anisotropic scattering on A_{ee}.

(3) For the KRb alloy, they found (Fig. 36) that a deformation-induced increase in ρ_0 of only 7% caused a large change in $d\rho/dT$ below 1 K, completely at variance with the KW prediction that such a small change in total ρ_0 should produce only a small effect on A_{ee}.

(4) Lastly, but importantly, they found that the form of the additional low-temperature resistivity deviated strongly from a simple T^2 behavior. They fit their data with the equation

FIG. 36. $d\rho/dT$ vs T for a K(0.077 at. % Rb) alloy: $\bigcirc$, KRbHa (unstrained); $\square$, KRbHb (strained); $\times$, annealed at 160 K; ———, an assumed T^2 variation of $\rho(T)$ fit to the data below 0.5 K; — — — above 1.3 K, the $\rho_{ep}(T)$ expected for pure K; —·—·—·, a fit to the data of Eq. (10) plus a CT^5 term with a nonzero coefficient C. The error bar next to the ordinate represents the random uncertainty in the data points at the lowest temperatures. From Haerle *et al.*, 1983.
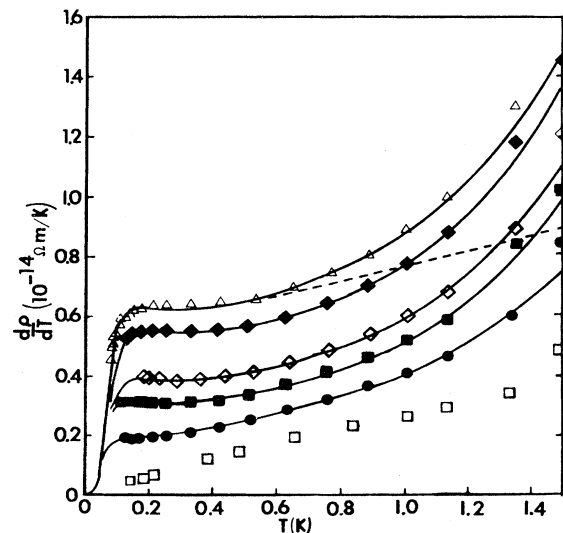

FIG. 37. $d\rho/dT$ vs T for sample K8H subjected to increasing strains. ———, fits to Eq. (17); — — —, the same fit but with the CT^5 term eliminated for K8Hf to illustrate the behavior with no increase in ρ_{ep}. From Haerle *et al.*, 1986.

$$\rho(T) = AT^2 + CT^5 + (D/4T)\sinh^{-2}(\epsilon/2T) . \quad (17)$$

The first term on the right-hand side of Eq. (17) corresponds to electron-electron scattering, the second to partial quenching of phonon drag, and the third has the form predicted by a model of Gantmakher and Kulesco (1975), in which electrons are scattered by vibrating dislocations with a characteristic frequency $\omega = (\epsilon k_B)/\hbar$. The solid curves in Figs. 37 and 38 show that Eq. (17) was able to fit the data of Haerle et al. quite satisfactorily, with little or no change in the coefficient A.

To focus attention upon the new component of $\rho(T)$ due to deformation, and to correct, to the extent possible, for the anomalous behavior of the pure-K data noted above, Haerle et al. replotted (Fig. 38) the data of Figs. 36 and one sample from Fig. 37 with assumed AT^2 coefficients for the undeformed samples subtracted away, and with a comparison sample consisting of a similarly treated set of data for an undeformed pure-K sample of Lee et al. (1982) which showed no Rowlands-like anomaly. For Haerle et al.'s two samples in Fig. 38, the AT^2 terms subtracted off are indicated by the solid line in Fig. 36 and by the dashed line in Fig. 37.

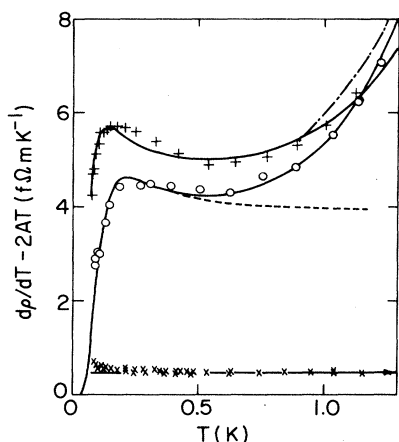For the KRb sample, the solid line in Fig. 36 falls below the data. This behavior is most likely due to a partial quenching of phonon drag by the impurities, which restores part of the T^5 Bloch term that had been essentially eliminated in pure K below 1.5 K by phonon drag. The dot-dashed curve in Fig. 36 is the sum of assumed T^2 and T^5 components for the KRb alloy. The dashed curve in Fig. 36 indicates the much smaller $\rho_{ep}(T)$ component for a typical pure, bulk K sample, corresponding to almost complete phonon drag. The slope of the line in Fig. 36 agrees well with expectation for $A_{ee} + A_I\rho_0$ for a bulk KRb alloy with the specified Rb concentration of 0.077 at. %.

For the pure-K sample, in contrast, the chain line in Fig. 37 falls above the experimental data at higher temperatures, and the slope of the line ($\simeq 1.6$ fΩ m/K^2) is considerably smaller than the typical value ($\simeq 2.2$ fΩ m/K^2) seen in bulk, free-hanging pure K (see Sec. III.E above). A smaller slope and downward curvature on a plot of $d\rho/dT$ were exactly the features seen by Rowlands et al. on $d = 0.9$ mm K samples prepared and cooled in He gas (Sec. III.D.2 above).

The changes in $d\rho/dT$ after deformation, shown in Fig. 38, clearly manifest a completely different form from that predicted by Kaveh and Wiser. Haerle et al. found that any changes in the T^2 coefficient due to anisotropic scattering were too small to be isolated.

In the longer, more detailed presentation of these results, Haerle et al (1986) described effects of a series of increasing deformations on one pure-K sample (data shown in Fig. 37) and of annealing studies on another (data to be presented in Sec. IV.D). They also presented complementary measurements of the thermoelectric ratio G. Since that paper was published after the three previous reviews were written, we defer further discussion of its results to Sec. IV.D. However, we briefly note that three phenomena mentioned above that Haerle et al. saw in their unstrained samples gave impetus to the study we describe next and to additional studies presented in Sec. IV. These were the following. (1) The evidence of an increase in the electron-phonon contribution to $\rho(T)$ in the KRb alloy over its value for pure K shown in Fig. 36, which Haerle et al. attributed to partial quenching of phonon drag by the Rb impurities. (2) The first independent evidence for curvature in a plot of $d\rho/dT$ versus T (Fig. 37) similar to that reported by Rowlands et al. (1979) for thin wires prepared and cooled in He gas. Since this behavior was different from that found by Lee et al. on $d = 0.9$ mm samples prepared and cooled in Ar, it stimulated a more complete study of size effects in K prepared and cooled in He, in Ar, and in vacuum, which we describe next. In our discussion in Sec. IV.D of Haerle et al.'s more detailed studies of deformation-induced behavior, we shall see that this size effect perturbed the detailed behavior they observed for $d\rho/dT$ due to dislocations in pure K. (3) The first evidence of anomalies in $d\rho/dT$ and G below 1 K for samples in contact with polyethylene. The followup studies of these three phenomena are described in Secs. III.H.2, IV.F, IV.C, and IV.B, respectively.

FIG. 38. $(d\rho/dT - 2AT)$ vs T for three samples: ○, KRbHb; +, K8Hf; ×, K5. A was assumed to remain constant at the value determined by straight lines through the lowest-temperature data. The data for sample K5 taken from Lee et al. (1982), through which a horizontal straight line is drawn, are plotted on the same ordinate scale except for a displaced zero. ——, fits of the data to Eq. (17) with the T^2 term removed; — — —, the fit to sample KRbHb but with the CT^5 component omitted; —·—·—·, the parametrized fit by van Vucht et al. (1982) to the data of one of their samples with the T^2 component removed (this curve indicates that the data of van Vucht et al. and the data of Haerle were very similar in the temperature region of overlap). After Haerle et al., 1983.

H. Initial measurements on thin K wires
in He gas: the Rowlands *et al.* anomaly revived

To try to understand why Rowlands *et al.* (1978) and Haerle *et al.* (1983) found curved lines in plots of $\rho(T)$ versus T^2 for K wires of $d = 0.8$ or 0.9 mm cooled in He gas, whereas Lee *et al.* (1982) found straight lines in similar plots for $d = 0.9$ mm wires cooled in Ar, Yu, Haerle, *et al.* (1984b) examined $\rho(T)$ for K wires with 0.1 mm $\leq d \leq 3.0$ mm, cooled in He, in vacuum, and in Ar.

For samples cooled in He, Yu, Haerle, *et al.* found reproducible data (Fig. 39) that showed systematic changes in $\rho(T)$ with decreasing sample diameter. For $d \simeq 0.8–0.9$ mm, the data were nicely compatible with both the curvature and the magnitudes of the data of Rowlands *et al.* and of Haerle *et al.* for wires with these

diameters cooled and measured in He. Figure 40 shows a comparison with one of Rowlands *et al.*'s samples. For wires thinner than 0.8 mm, the curvature became still greater, and for wires thinner than the bulk electron mean free path ($l = 0.2$ mm in a sample with bulk RRR = 6000), $d\rho/dT$ actually became negative— corresponding to a resistance minimum in $\rho(T)$. When Yu, Haerle, *et al.* added 0.077% Rb to their K, to reduce l to about 0.05 mm, they found a simple AT^2 behavior in samples with $d = 0.1$ mm, with no evidence of any curvature and with the proper magnitude of A for such an impurity concentration in bulk material. They thus concluded that they were seeing a true size effect.

For samples cooled in Ar or vacuum, Yu, Haerle, *et al.* found behaviors (Fig. 41) that were qualitatively similar to those observed in He, but with both smaller
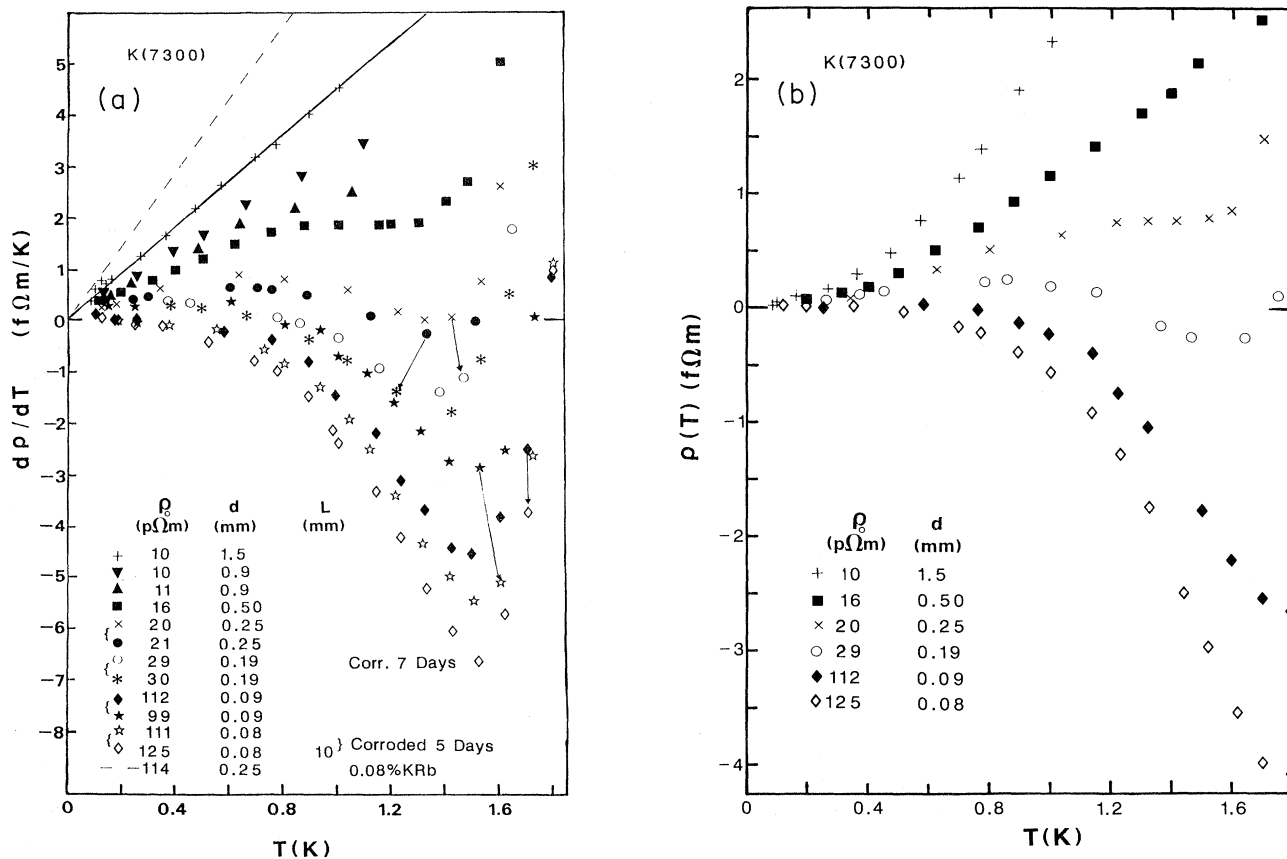

FIG. 39. $d\rho/dT$ and $\rho(T)$ for thin K(7300) samples. (a) $d\rho/dT$ vs T for the K(7300) samples, which were prepared and cooled in a He atmosphere. ——— indicates bulk behavior for the pure K; — — —, the behavior seen in a d=0.25 mm wire of K (0.08 at. % Rb). Two nearly identical samples were always prepared and measured together; for the samples in this figure, the data for both wires in a pair were always fairly close. Two pairs of samples were annealed at room temperature to thin them further after their initial measurements; the arrows indicate the changes that occurred due to these annealings. (b) $\rho(T)$ vs T for selected data from (a); the data of (a) were integrated by hand. Note that the integrated data have qualitatively similar forms to the data of (a). From Zhao *et al.*, 1988.

anomalies and larger scatter for a given sample diameter. In view of the apparently consistent data of Rowlands *et al.*, Lee *et al.*, Haerle *et al.*, and Yu, Haerle, *et al.*, that larger size effects occurred in He than in Ar, Yu, Haerle, *et al.* presumed that the atmosphere affected the data in some as yet unknown fashion. We shall see in Sec. IV.C that additional experiments showed that this was too simplistic a view of the effect of the atmosphere.

To explain the size effect, Yu, Haerle, *et al.* took $\rho(T)$ to be the sum of two terms. The first term was simple electron-electron scattering with a coefficient $A \simeq 2.2$ fΩ m/K^2, as proposed by the MSU group for pure K (see Sec. III.E and Pratt, 1982). This term was strictly positive and independent of sample diameter d. They assumed that the second term generated a negative contribution to $d\rho/dT$, which began to appear in high-purity K for $d \leq 1$ mm and became so large for $d \leq l$ that it made the total $d\rho/dT$ negative. They tentatively attributed this term to a phenomenon predicted by Gurzhi (1963), that had not previously been observed. This phenomenon involved a reduced contribution of diffuse surface scattering with increasing temperature, due to an increase in the average distance an electron initially moving along the wire axis had to travel before colliding with the wire surface.
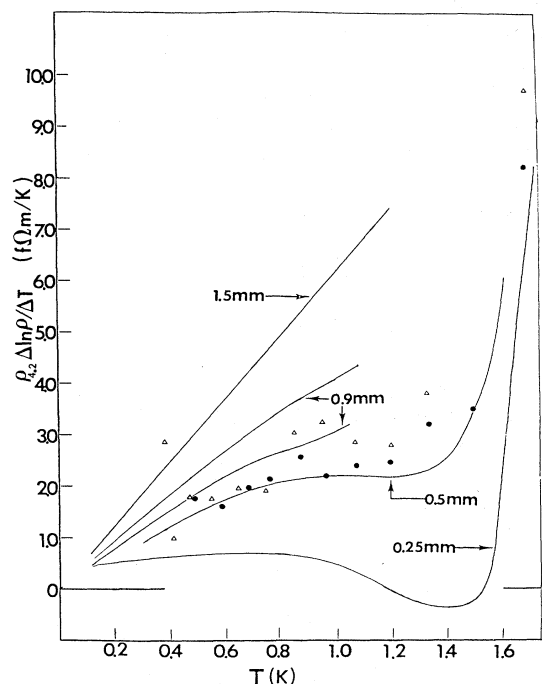
Theoretical analysis, both numerical (Movshovitz and

Wiser, 1987) and analytical (Stump, 1986) subsequently showed that the Gurzhi effect could not be the correct explanation for the size-effect data of Yu, Haerle, *et al.* in samples cooled in He gas. Several alternative explanations were then put forward.

De Gennero and Rettori (1984; 1985) proposed an explanation for the data of Yu, Haerle, *et al.* in terms of interference between normal electron-electron scattering and surface scattering. This model succeeded in explaining the qualitative features of the data, and the authors were able to choose parameters that produced changes in magnitude comparable to those observed. With these parameters, the model predicted that if wires were made still thinner, the size-effect anomaly would disappear. This model had the problem as a complete explanation for the data that it predicted a strict T^2 variation of $\rho(T)$, whereas the data showed clear deviations from T^2.

Kaveh and Wiser (1985) proposed that the behavior shown in Fig. 39 was due to a reduction in the effect of surface scattering due to normal electron-phonon scattering. With a judicious choice of parameters, this model also yielded predictions at 1 K roughly comparable in size to those observed. However, this model predicted a T^5 temperature dependence, which decreased much too

FIG. 40. $(\rho_{4.2\,K}/\rho)(d\rho/dT)$ vs T for two K samples of Rowlands *et al.* (1978) with $d=0.08$ mm cooled in a He atmosphere. For comparison, the solid curves represent data from Fig. 39(a) for K samples having the diameters indicated. From Yu *et al.*, 1984.
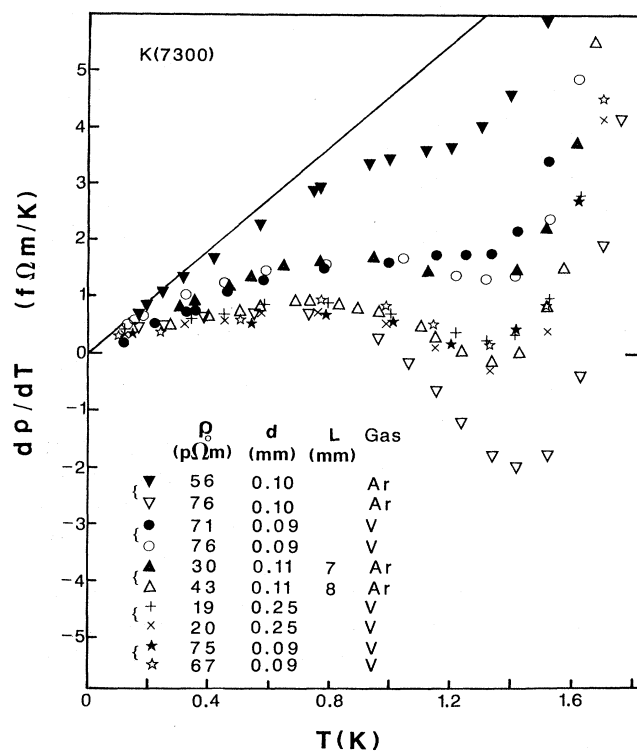
FIG. 41. $d\rho/dT$ vs T for thin K(7300) wires cooled in an Ar atmosphere or in partial vacuum. The solid straight line indicating bulk behavior is the same as the solid line in Fig. 39(a). The samples connected by brackets were prepared and measured together. From Zhao *et al.*, 1988.

quickly with decreasing temperature to explain the data at temperatures below 1 K.

Farrell *et al.* (1985) made the most dramatic proposal, that the negative values of $d\rho/dT$ seen in the thinnest samples were due to strong localization effects in these wires. They considered such localization both with and without a CDW ground state. Assuming a single localization channel, they were able to fit the form of the experimental data. However, using only a single localization channel gave a predicted size effect about two orders of magnitude smaller than the data. Including enough channels to explain the magnitude of the data caused the temperature dependence to change for the worse. This interpretation also had the problem that it explained only data for which $d\rho/dT$ was negative. The smooth change from a T^2 behavior to negative values of $d\rho/dT$ had to be attributed to a second mechanism—CDW-based effects—that had not been shown to produce the behavior observed. On the other hand, this model made a clear testable prediction, that $d\rho/dT$ would depend strongly on the sample length under conditions where $d\rho/dT < 0$.

I. The three reviews of 1984–1985

In their discussions of $\rho(T)$ for the alkali metals, all three of the reviews mentioned in Sec. I.B. were structured around the KW models for (a) phonon drag; (b) quenching of phonon drag by anisotropic electron-dislocation scattering and phonon-dislocation scattering; and (c) effects upon A_{ee} of anisotropic scattering due to extended defects. The Wiser and the KW reviews naturally focused upon showing how the KW model of anisotropic scattering could simultaneously explain both the complex behaviors seen in K and the simple behavior seen in Li (which they placed in the anisotropic limit of the model). The KW review also placed Na in the anisotropic limit of the model. Below 1 K, the KW model is based upon the following three assumptions: (1) that all of the published measurements of $\rho(T)$ for high-purity K, Li, and Na represented the behavior of bulk samples not affected by any significant perturbations other than an unavoidable concentration of extended defects; (2) that $\rho(T)$ in the vicinity of 1 K was always dominated by a term varying as AT^2 that was due to electron-electron scattering; and (3) that all the variations in A had to be explained by a single model. As we have indicated above, by the time these reviews were published, potential difficulties with all three assumptions had become visible. Only the review by van Vucht *et al.* seriously tried to address these difficulties.

1. Wiser

The Wiser (1984) review is a clear and well written presentation of the KW models for electron-phonon scattering, phonon drag, and anisotropic electron-electron scattering in Al, the noble metals, and the alkali metals.

The review begins with a listing of ten new theoretical results that Wiser contended had been confirmed experimentally and that formed the basis for the review. He referred back to these same ten results to summarize the review and concluded that "Although there certainly exist resistivity data that are currently unexplained, I think that it is fair to say that, on the whole, the low-temperature resistivity of the simple metals is now basically understood." Since almost all of the detailed points made in Wiser's review relating to the alkali metals have already been described and analyzed above, we limit ourselves simply to listing his ten general results and briefly commenting upon the ones that apply to the alkali metals. Those items (4, 7, and 8) that do not apply to the alkali metals are included to give an overview of the KW analysis of the behavior of $\rho(T)$ at low temperatures in simple metals.

1. "The Bloch T^5 law for the low-temperature electrical resistivity is never observed for any metal over any temperature range. There are different reasons for the failure of the Bloch law for the alkali metals and polyvalent metals."

2. "Phonon drag has a dramatic effect on the low-temperature electrical resistivity of the alkali metals. It alters the temperature dependence, completely eliminating the normal-scattering T^5 term (Bloch law) and leaving only the umklapp-scattering term, which decays exponentially with temperature for the alkali metals."

3. "The large strain dependence observed for the electrical resistivity of the alkali metals is due to the partial quenching of phonon drag by electron-dislocation scattering and by phonon-dislocation scattering."

4. "Phonon drag is negligible for the noble and polyvalent metals and may be totally ignored. This is because the Fermi surface is not spherical for these metals."

5. "Electron-electron scattering makes an important contribution to the electrical resistivity of the simple metals at low temperatures, typically below about 2–3 K."

6. "The electron-electron scattering contribution to the electrical resistivity exhibits a marked sample dependence for many simple metals. This is due to the large enhancement of normal electron-electron scattering that results from the presence of anistropic scattering centers in the sample. The degree of anisotropy for any particular sample depends on the relative contributions to the residual resistivity arising from electron-dislocation scattering and electron-impurity scattering."

7. "There is a complete breakdown of Matthiessen's rule at low temperatures for the noble and polyvalent metals. This results from the existence for these metals of small regions of the Fermi surface of extremely strong electron-phonon scattering at low temperatures. These regions lie near the intersections of the Fermi surface and the Brillouin zone boundaries."

8. "The deviations (DMR) from Matthiessen's rule for the noble and polyvalent metals may be of either sign.

For impure samples, the DMR are positive. For strained samples, the DMR can be positive, negative, or even absent altogether. The results for any particular strained sample depend on the temperature, on the metal, and on the value of the residual resistivity before straining. There are also important low-temperature DMR, negative in sign, for ultra-pure samples of the noble and polyvalent metals."

9. "For the alkali metals, the DMR for annealed samples are small even at low temperatures. This is due to the sphericity of the Fermi surface for the alkali metals, with the lack of any intersection of the Fermi surface with the Brillouin zone boundaries."

10. "Dislocations and other anisotropic scattering centers play a central role in determining the low-temperature electrical resistivity of the simple metals. The primary effect of dislocations is to increase the electron-electron scattering resistivity of all the simple metals, to decrease the electron-phonon scattering resistivity of the noble and polyvalent metals, and to increase the electron-phonon scattering resistivity of the alkali metals."

We agree with item 9. We also generally accept items 1, 2, 3, and 5, but would make the following modifications. A more precise statement of item 1 is that the Bloch T^5 term is never found to be the only temperature-dependent term at very low temperatures. It is always accompanied by—and usually overshadowed by—some combination of umklapp electron-phonon scattering, electron-electron scattering, and—in the alkali metals—phonon drag. Unless phonon drag is complete, the Bloch T^5 term is still present, and we describe circumstances in which it seems to be observed. In item 2 we agree that phonon drag is both present and large in K from 2 K downward. However, the experimental data do not prove that it completely eliminates the T^5 term at any temperature, and we are not sure as to how high a temperature it extends in K. The importance of phonon drag in the other alkali metals has not yet been demonstrated experimentally. In item 3, we agree that the two mechanisms specified must be operating, but we do not believe that we yet adequately understand either their relative importance or how they produce the large effects that are observed. In item 5, we agree that electron-electron scattering is important under the conditions specified, but will argue that other processes not considered by Kaveh and Wiser also become important when the alkali metals—especially K—are subjected to a variety of perturbations.

We disagree with items 6 and 10 as applied to electron-electron scattering in the alkali metals. We have already indicated in Sec. III.G.2, and will show further in Sec. IV, that dislocations produce a contribution to $\rho(T)$ that has a more complex temperature dependence than simply T^2. We have also already noted, and will argue further, that the sample dependences observed in K are not primarily associated with variations in A_{ee}, but rather result mainly from a variety of perturbations.

2. Kaveh and Wiser

The KW (1984) review limits itself to electron-electron scattering, but ranges very widely over this topic. It extends well beyond simply electron-electron scattering in the alkali and other simple metals, by also covering effects of dimensionality on electron-electron scattering; electron-electron scattering in very impure metals; quantum corrections to the electron-electron scattering rate; electron-electron scattering in transition metals, semimetals, and semiconductors; electron-electron scattering contributions to surface impedance and optical relaxation; and effects of a magnetic field on electron-electron scattering. As was the Wiser review, this review is highly readable and exemplifies one of the special strengths of Kaveh and Wiser, the ability to provide simple physical pictures that greatly aid the understanding of sometimes complex mathematical phenomena. We refer the reader especially to Kaveh and Wiser's nice discussions of contributions of electron-electron scattering to thermal conductivity and of size effects in electron-electron scattering. They treat these topics in more detail than we do.

Since we have already discussed most of the individual items concerning the alkali metals covered in this review, we limit ourselves to correcting one minor error. Kaveh and Wiser erroneously claimed that the MSU group first argued (Lee et al., 1982) that the behavior of the data of Rowlands et al. (1978) was not due to a size effect, and then later reversed themselves and argued that it was (Yu, 1984b). We believe that a careful reading of the papers concerned will reveal that this statment is incorrect for two separate reasons. First, Lee et al. simply asserted that their own data were incompatible with the model [Eq. (12)] that Rowlands et al. had proposed; no interpretation of Rowlands et al.'s data was presented. Second, while Yu et al. (1984b) did propose an interpretation for the Rowlands et al. data, this interpretation was based primarily upon simple electron-electron scattering, with only a small contribution from a size effect that was completely unrelated to the Rowlands et al. model. The claimed reversal in interpretation never occurred.

3. van Vucht et al.

The review of van Vucht et al. (1985) provides a clear picture of the state of understanding of $\rho(T)$ in simple metals at the end of 1984, with a natural emphasis on the important contributions made by the group in the Netherlands headed by van Vucht's co-authors Wyder and van Kempen. The review discussed not only electron-electron and electron-phonon scattering in the simple metals at temperatures below 4 K, but also the influence of the lattice thermal conductivity on thermal transport in the simple metals, linear magnetoresistance, and the likelihood and possible effects of a CDW ground state in the alkali metals.

Again, as with the two previous reviews, we have al-

ready discussed most of the items concerning the alkali metals that were covered by van Vucht *et al.* However this review did break new ground in some of its analyses, which we now discuss.

(1) van Vucht *et al.* argued that the data of van Kempen *et al.* (1981) conflicted with the claim of Kaveh *et al.* (1979) that Eq. (11) could not be applied with a constant Θ to temperatures below 2 K. They argued that since the data of Lee *et al.* (1982) had shown that $\rho(T)$ in pure K varied precisely as T^2 from 1.3 K down to 0.3 K, then subtracting a T^2 term from $\rho(T)$ should provide a reliable measure of $\rho_{ep}(T)$. When van Kempen *et al.* did this, they found that Eq. (11) could describe their data all the way down to their lowest temperature of almost 1 K. We shall consider this issue in detail in Sec. V, after presenting new data in Sec. IV.A for K samples in polyethylene tubing that calls into question the applicability of a simple T^2 form to the van Kempen *et al.* data.

(2) To try to remove the inconsistency between the KW model and the more complex temperature dependence of the Haerle *et al.* (1983) data for deformed K and KRb described in Sec. III.G.2 above van Vucht *et al.* proposed that the A_{ee} coefficient of deformed K might change with decreasing temperature due to sequential "freezing out" at different temperatures of T^2 contributions from different scattering entities such as point defects, defect clusters, and dislocations. No mechanism was proposed by which such freezing might occur, and this proposal has subsequently been shown to have two severe problems: (a) Yin *et al.* (Yin, 1987; Yin *et al.*, 1990) found even more complex forms of $d\rho/dT$ that are incompatible with simple changes in T^2 coefficients with decreasing temperature. (b) Haerle *et al.* (1986) found that $d\rho/dT$ retains a complex form even after annealing to temperatures at which point defects are completely eliminated.

(3) van Vucht *et al.* pointed out that there were problems with the Danino *et al.* (1981b, 1981c) model of phonon drag due to phonon-dislocation scattering for explaining the data for a rapidly quenched sample of van Kempen *et al.* (1981). In particular, the data did not seem to contain the T^5 component predicted by Danino *et al.*, and the dislocation density n_d appeared to be much smaller than they required. Similarly, van Vucht *et al.* noted that twisted samples, for which n_d was clearly established to be much smaller than required by Danino *et al.*, also produced very large changes in the exponential component of $\rho(T)$ with no evidence of a T^5 term. van Vucht *et al.* noted that the later models by Engquist (1982) and Danino *et al.* (1982, 1983), of phonon drag due to anisotropic electron-dislocation scattering, reduced the required n_d to more realistic values, but still failed to predict the simple exponential temperature dependence inferred by van Kempen *et al.* and van Vucht *et al.*

(4) As illustrated in Fig. 42, van Vucht *et al.* noted that the KW anisotropic scattering model with the parameters given by Kaveh and Wiser could not describe
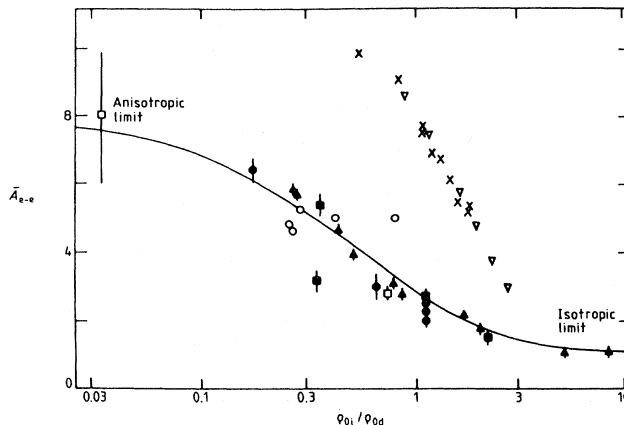

FIG. 42. $\overline{A}_{ee}$ of a large number of K samples from different authors plotted as a function of ρ_{0i}/ρ_{0d} to compare the data with the theory of Kaveh and Wiser (1982). The data are scaled to the value of A_{ee} in the anisotropic limit; otherwise the solid curve and the symbols falling around it are the same as in Fig. 18. For most of the symbols, ρ_{0i} and ρ_{0d} were inferred by Kaveh and Wiser. But for the $\times$'s (samples of van Vucht *et al.*, 1982) and the $\triangle$'s (Haerle *et al.*, 1983), these two quantities were extracted from a plot like that shown in Fig. 43. The $\times$'s and $\triangle$'s manifest a serious discrepancy with the original theoretical curve (solid curve). This discrepancy can be removed by increasing the magnitude of A_{ee} in the anisotropic limit by a factor of about 4 and simultaneously changing the assumed values of ρ_{0i} and ρ_{0d} for the earlier data. From van Vucht *et al.*, 1985.

the magnitudes of either the data of van Vucht *et al.* (1982) or the data of Haerle *et al.* (1983) if the Haerle *et al.* data were forced to a T^2 form. van Vucht *et al.* tried to save the model by proposing that both the parameters derived by Kaveh and Wiser for Eq. (14) and the specific values of $\rho_0 d$ used by Kaveh and Wiser to fit the data of van Kempen *et al.* (1976), Rowlands *et al.* (1978), Levy *et al.* (1979), and Lee *et al.* (1982) should be changed to make the older data consistent with the new. van Vucht *et al.* reanalyzed all of the available data in terms of Eq. (16) as shown in Fig. 43. For the data of van Vucht *et al.* and Haerle *et al.*, this analysis produced the values of A_{ee} that are shown in Fig. 42. For the other data, examination of Fig. 43 shows that, while values of the necessary constants can be chosen for each data point by assuming that the point lies on some line, in most cases, the choice of this line is either arbitrary or subject to large uncertainty.

(5) Finally, carrying the anisotropic scattering model to its logical conclusion for alloys, van Vucht *et al.* considered the possibility of reinterpreting the very dilute KRb alloy data of Lee *et al.* (1980) in terms of anisotropic scattering by the Rb impurities, rather than the inelastic impurity scattering proposed by Lee *et al.* They concluded, however, that the linearity of the increase in A_{ee}
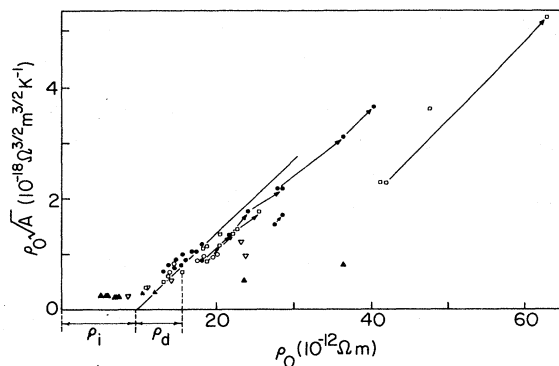
FIG. 43. $\rho_0\sqrt{A_{ee}}$ vs ρ_0 for a large number of K samples from different authors. Data of the same sample after different stages of deformation are linked by arrows. The theory of Kaveh and Wiser (1982) predicts that if only ρ_{0d} varies during such deformation, the data should lie on a straight line with slope $\sqrt{A_I}$ and intercept ρ_{0i} with the ρ_0 axis. All data of van Vucht et al., 1982 (●) and Haerle et al., 1983 (□) are approximately consistent with this theory and give an A_I of about $190\pm20\times10^{-16}$ Ω m/K^2 for most data. When a specific A_I is assumed, this plot enables one to determine the ρ_{0d} portion of ρ_0 from A_{ee}. △, from van Kempen et al., 1981; ▲, from Levy et al., 1979; ○, from Lee et al., 1982. After van Vucht et al., 1985.

with ρ_0, as well as the lack of saturation of the T^2 coefficient A for large values of ρ_0, made such an interpretation untenable as a complete explanation for the data.

J. Bishop and Lawrence: a more general CDW-based model for $T \leq 1$ K

Soon after the completion of these three review articles, Bishop and Lawrence (1985) extended the work of Bishop and Overhauser (1979, 1981) to propose an alternative to the KW model for explaining the behavior of all of the published data for pure K. Their model was based on a CDW ground state. They argued that below 1.3 K, $\rho(T)$ in K consisted of two terms, the electron-phason term proposed by Bishop and Overhauser and a T^2 term due to electron-electron scattering. Bishop and Overhauser had already indicated that the magnitude of the CDW contribution should be highly anisotropic with respect to the axis of a given CDW domain. Bishop and Lawrence now argued that the presence of the CDW also made the electron-electron term highly anisotropic with respect to the CDW domain axis. Different CDW domain structures thus naturally gave rise both to large variations in the coefficient of the T^2 term—e.g., the data of van Kempen et al. (1976), Levy et al. (1979), and Lee et al. (1982)—and to deviations from T^2 behavior when the electron-phason term became important—e.g., the data of Rowlands et al. (1978). This model had the ad-

vantage over the KW model of being able to incorporate directly the $T^{3/2}$ behavior reported by Rowlands et al.

In Sec. V we shall reexamine both the Bishop and Lawrence and the KW models in the light of all of the experimental data now available.

IV. NEWER DATA WITH PRECISIONS BETTER THAN 10^{-7}

A. Overview and significance of results to be discussed

In this section we deviate from chronological order so as to focus separately on each of several different topics. We start in Sec. IV.B with the most surprising and important new result, the discovery that contact of K with polyethylene produces a large Kondo-like anomaly in $d\rho/dT$ for K below 1 K. This anomaly provides a plausible explanation for most of the apparent changes in A_{ee} reported by van Kempen et al. and by Levy et al. It is also interesting in its own right, since no Kondo effect has previously been seen in any alkali metal. In Sec. IV.C we describe further studies of thin K samples which reveal that the situation in thin K wires is more complex than the first studies suggested; surface contamination certainly enhances the "size-effect" anomaly and may be fundamental to its presence. No similar anomaly has yet been seen in thin K foils prepared in high vacuum. In Sec. IV.D we describe new studies of deformed K and KRb samples which confirm the complex form of $\rho(T)$ reported by Haerle et al and which expand our knowledge of the magnitudes of the changes produced under different experimental conditions. In Secs. IV.E and IV.F we describe new measurements on dilute and concentrated alloys, respectively, of KRb, KNa, and LiMg. The dilute alloy studies confirm previous results on ρ_{iei} in KRb alloys and extend measurements to KNa and LiMg alloys. The fact that the T^2 components of the alloy data extrapolate to the same values as for pure K and pure Li provides powerful evidence that the A_{ee} coefficients in these metals are intrinsic and do not vary substantially under perturbation. More concentrated alloys display a new, apparently universal anomaly, which varies approximately as $-C\rho_0 T$, with C having essentially the same value for KRb, KNa, and LiMg alloys. In very concentrated LiMg alloys, $\rho(T)$ seems to approach the behavior expected for quantum corrections to the Boltzmann transport equation. Lastly, in Sec. IV.G we reexamine the behavior of $\rho(T)$ for pure, bulk K in light of the data contained in Secs. IV.B–IV.E. We show that, when K samples from all the different research groups are carefully chosen to eliminate or minimize the nonintrinsic effects described in Secs. IV.B–IV.E, the resulting values of A_{ee} vary by only 60% from maximum to minimum, an order of magnitude smaller than the 500% variations that gave birth to the KW model. When only the most precisely determined values are used, the data

show only a 30% variation—i.e., $\pm 15\%$ around the average. We conclude that A_{ee} for K can be determined to within this uncertainty. The presentation of each topic begins with a brief rationale for the measurements and an overview of the results obtained, so as to provide context for the more detailed analysis that follows. These analyses are unusually complete, so as to bring all essential information together in this review.

B. Samples in contact with plastics: a "Kondo-like" anomaly

1. Rationale and overview

New measurements (Yu, Haerle, et al., 1984a; Yu et al., 1985, 1989) of $d\rho/dT$ for K in contact with plastics and with hydrogen-containing oils, including effects of extended room-temperature annealing upon the behavior of $d\rho/dT$ in K samples encased in both polyethylene

and Teflon tubing, were undertaken for two reasons: (1) to follow up the evidence found by Haerle et al. (1983) of low-temperature $d\rho/dT$ and G anomalies in K samples pressed against various forms of polyethylene; (2) to see whether the widely varying values of A_{ee} found by van Kempen et al. and Levy et al. for samples prepared inside polyethylene tubing could be due to the presence of the tubing.

For all samples in polyethylene tubes, both pure K and a dilute KRb alloy, Yu et al. found very similar resistivity and thermoelectric anomalies, whether the samples were prepared and cooled in Ar or in He gas. Figures 44 and 45 illustrate the anomalous behavior of $(1/T)(d\rho/dT)$ for samples prepared in both gases, and Fig. 46 illustrates the associated anomaly seen in G. For comparison, the dashed lines in each figure indicate typical behavior of bare K wires with $d = 0.9$ or 1.6 mm, respectively. Yu et al. discovered that these anomalies had all three of the general characteristics of a "Kondo effect": (1) a logarithmic variation of $\rho(T)$ with tempera-
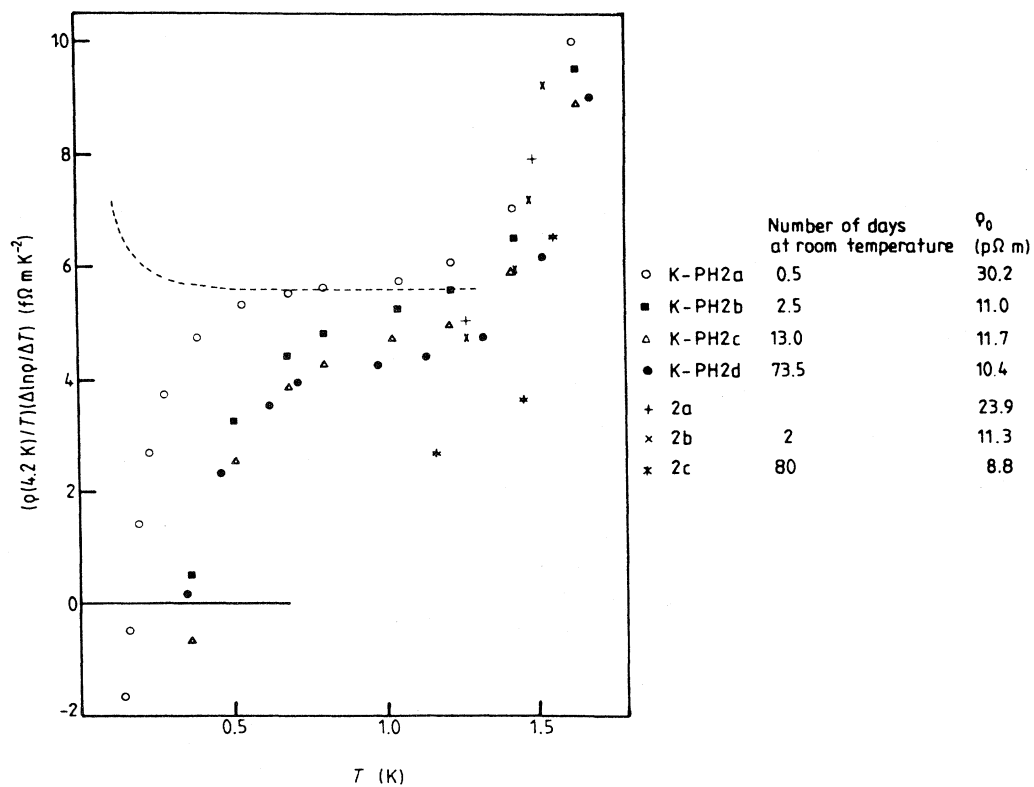

		Number of days at room temperature	ρ_0 (pΩ m)
○	K-PH2a	0.5	30.2
■	K-PH2b	2.5	11.0
△	K-PH2c	13.0	11.7
●	K-PH2d	73.5	10.4
+	2a		23.9
×	2b	2	11.3
×	2c	80	8.8

FIG. 44. $(\rho_{4.2\,K}/\rho T)(d\rho/dT)$ vs T for four runs of sample K-PH2 encased in polyethylene. For comparison, the data of samples 2a, 2b, and 2c of van Kempen et al. (1977) are also plotted. This figure focuses attention on the behavior of data for $T \geq 0.4$ K and on a comparison of the data of sample K-Ph2 with the data of van Kempen et al. The dashed curve indicates typical behavior of bare K samples. From Yu et al., 1985.

ture; (2) an associated thermoelectric anomaly; and (3) strong reductions in the anomalies in both $d\rho/dT$ and G upon application of a small ($B =0.1$ T) magnetic field (Fig. 47). They were not, however, able to isolate the physical source of this effect, which still remains unknown.

We see from Figs. 44–46 that both $d\rho/dT$ and G anomalies are already present in samples cooled and measured within half a day of preparation, and that the anomalies grow in magnitude as the samples are subsequently annealed at room temperature for days to months. While this growth is occurring, the ρ_0's for the samples systematically decrease. The decreases in ρ_0 and in $d\rho/dT$ in the vicinity of 1 K, found upon annealing both, closely resemble the equivalent behaviors seen by van Kempen et al. (1976, 1981) for $d =0.9$ mm K samples in polyethylene measured down to only 1.1 K. These similarities strongly suggest that the behaviors seen by van Kempen et al. are not representative of bare, bulk K,

FIG. 46. G vs T for two K samples encased in polyethylene tubes of different diameters. The symbols are the same as in Fig. 45. The solid curve indicates typical behavior for G for bare K samples. From Yu et al., 1984a.

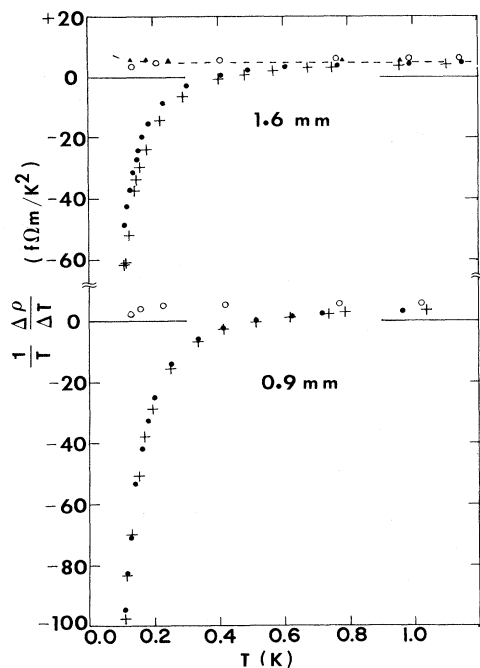| d (mm)	No. of days at room temperature	Symbol on figures	ρ_0 (pΩm)
1.6	~0.5	o	52.0
"	4.5	●	9.7
"	16	+	11.2
0.9	~0.5	o	51.9
"	4.5	●	12.0
"	16	+	11.4

FIG. 45. $(1/T)(d\rho/dT)$ vs T for two K samples encased in polyethylene tubes of different diameters. The dashed curve indicates typical behavior of bare K samples. From Yu et al., 1984a.
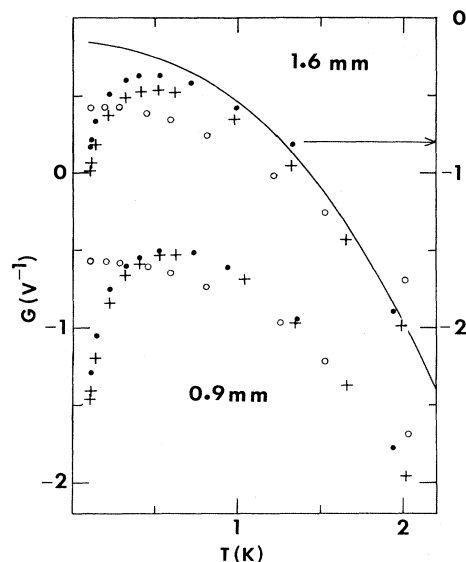
but instead are due primarily to the presence and growth of a "Kondo-like" anomaly with time. We argue that the samples of Levy et al. (1979) were also perturbed by being enclosed in polyethylene tubes.

The $d\rho/dT$ and G anomalies do not result solely from the fact that the K is constrained in tubing, since neither $d\rho/dT$ (Fig. 48) nor G anomalies were seen in a sample encased in a Teflon tube. However, ρ_0 for the sample in Teflon did decrease with room-temperature annealing in a manner similar to the behavior of ρ_0 for samples in polyethylene. These results suggest sample constraint as a possible explanation for the changes in ρ_0 with annealing time seen by Rowlands et al. (1978).

2. Detailed analysis

Yu et al. (1989) measured the following samples in polyethylene tubing: a $d =1.6$ mm K sample and a $d =0.9$ mm K sample prepared together and cooled and measured in Ar; a $d =1.6$ mm K sample prepared and cooled in He and measured against a $d =1.6$ mm bare K sample; a $d =0.9$ mm K sample prepared and cooled in He and measured against a $d =1.5$ mm K sample in a Teflon tube, and a $d =0.9$ mm K (0.077 at. % Rb) sample prepared and cooled in He and measured against a Cu(Ag) reference resistor in a different dilution refrigerator. The polyethylene tubing was initially cleaned by heating for two days at above 373 K in a vacuum of 10^{-6} mm Hg (Yu, 1984). The K was melted in the glove box, and the molten metal drawn up into the cleaned tubing and allowed to cool.

In Ar gas, the anomaly grew quickly for the first five days at room temperature, and then more slowly. In He gas, the slowdown in growth rate occurred somewhat later, as illustrated in Fig. 44. The anomalies were quite similar in $d = 1.6$ mm and $d = 0.9$ mm samples (Fig. 45), although perhaps the anomalies initially grew a little more quickly in the thinner samples. To see whether re-
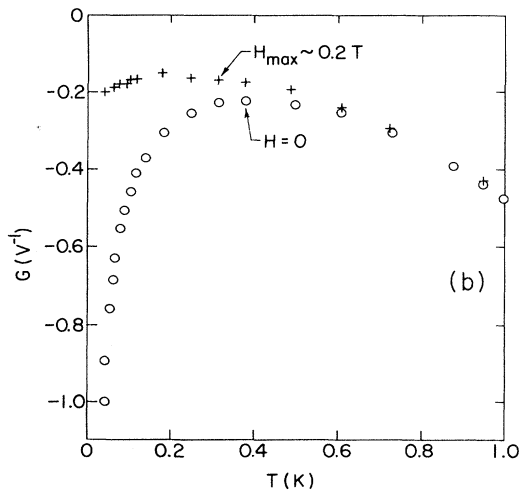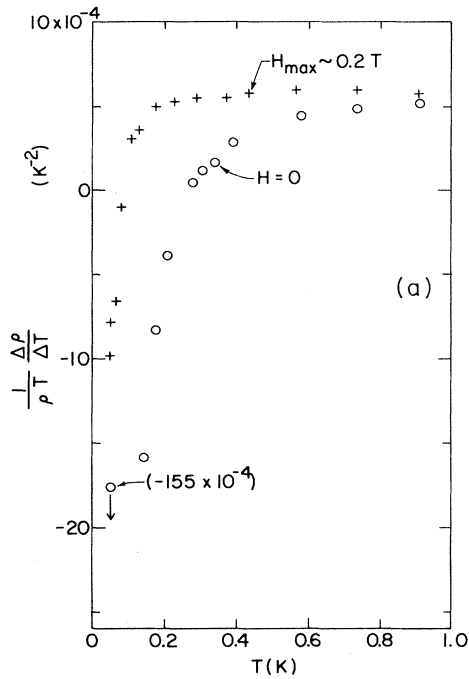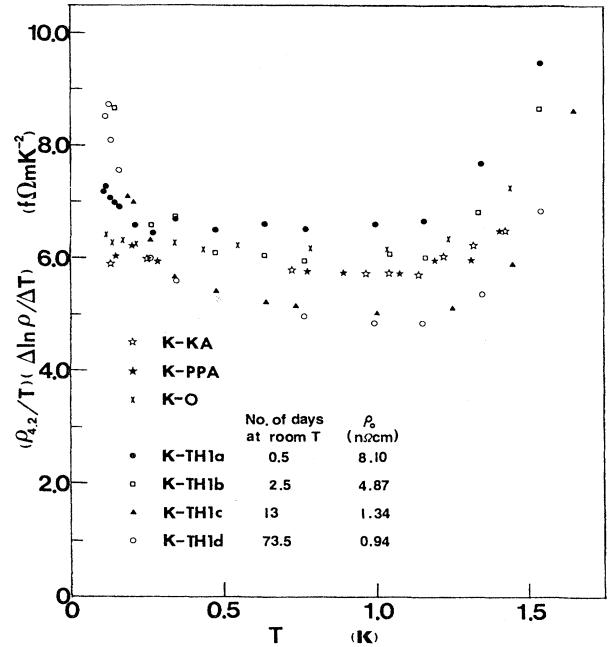
FIG. 48. $(\rho_{4.2\,K}/\rho T)(d\rho/dT)$ vs T for K samples in contact with Teflon (T), or Kel-f (K), covered with oil at room temperature (O), or with potential leads in contact with polyethylene (PPA). From Yu et al., 1989.

FIG. 47. Effect of a magnetic field on $(1/\rho_0 T)(d\rho/dT)$ and G for a K sample in polyethylene. (a) $(1/\rho_0 T)(d\rho/dT)$ vs T and (b) G vs T for longitudinal magnetic fields of $H=0$ (○) and $H=0.2$ T (+). After Bass et al., 1986.

ducing the bulk electron mean free path l would reduce the anomaly, a dilute K (0.077 at. % Rb) sample with a much shorter l (≈ 0.02 mm) was drawn up into a $d = 1.6$ mm polyethylene tubing and held at room temperature for three days before being measured. A large anomaly was seen in $d\rho/dT$ and a small one in G.

In contrast to the anomalies seen with polyethylene, but in agreement with the conclusion reached earlier by Haerle et al. (1983) from measurements on K samples pressed against Teflon, a sample prepared in Teflon tubing showed no evidence of either a $d\rho/dT$ anomaly (Fig. 48) or a G anomaly.

A variety of additional tests were made to try to establish more precisely the conditions under which a Kondo-like anomaly did and did not appear.

The only obvious chemical difference between polyethylene—for which anomalies were always seen—and Teflon and Kel-f—for which anomalies were never seen (Fig. 48)—is that polyethylene contains hydrogen (H), whereas Teflon and Kel-f do not. To test whether some other H-containing material besides polyethylene could produce anomalies, a $d = 1.5$ mm K sample was melted and resolidified slowly under cleaned paraffin oil. A small anomaly appeared in $d\rho/dT$, but none in G. No anomalies were seen when oil was simply dripped onto the surface of a $d = 1.5$ mm K sample (sample K0 in Fig. 48). Yu et al. also tried to put H into K in hopes of producing an anomaly. Bubbling H_2 through molten K, with and without an electrical discharge, and heating K

to a temperature of 450 K in a H_2 atmosphere, failed to produce an anomaly.

During initial studies of the size effect described in Sec. III.H a small dp/dT anomaly appeared when polyethylene touched only the potential leads of a pair of $d = 0.1$ mm K wires. No G anomaly was seen in these samples. This observation stimulated additional measurements to try to establish the importance of physical contact between the K and polyethylene. No anomalies were seen in $d = 0.1$ mm K samples when Teflon touched only the potential leads. No anomalies were seen when polyethylene touched only the potential leads of a much thicker ($d = 1.5$ mm) K wire (sample KPPA in Fig. 48). No anomalies were seen when K was drawn up into a polyethylene tube, left there for three days, reextruded from the tube, and then mounted as a free-hanging sample and measured.

Combining the data of Haerle et al. (1986) and Yu et al. (Yu, Haerle, et al., 1984a; Yu et al., 1985, 1989) leads to the conclusion that anomalies were always seen when a K or a KRb sample was in intimate contact with polyethylene. The anomalies were largest for samples melted in contact with the polyethylene and remaining in contact with it for more than one week. With two exceptions, no anomalies have ever been seen in a sample not touching polyethylene. The exceptions are a small dp/dT anomaly in a $d = 1.5$ mm K sample melted and solidified under paraffin oil, and small dp/dT and G anomalies in two very thin, $d = 0.1$ mm K wires where only the potential leads touched polyethylene.

The temperature dependence of the anomaly is illustrated in Fig. 44. We see that the data for samples in contact with polyethylene overlap the dashed lines representing bare, bulk K samples only in the vicinity of 1 K. As T drops below 1 K, dp/dT steadily decreases below the dashed line, ultimately turning negative (corresponding to a resistivity minimum) in the vicinity of 0.5 K. To see whether this resistivity minimum might be associated with something like a Kondo effect, Yu et al. tested for consistency with the equation

$$p(T) = AT^2 - F \ln T , \qquad (18a)$$

or, equivalently,

$$(1/T)(dp/dT) = 2A - F/T^2 . \qquad (18b)$$

In Eqs. (18a) and (18b), A and F are constants, and the logarithmic term $\ln T$ is characteristic of a Kondo effect in the vicinity of the Kondo temperature T_k (Kondo, 1964; Fischer, 1982). Figure 49 shows that the data are nicely consistent with Eq. (18b). Figure 46 has already shown that the data also display a very-low-temperature thermoelectric anomaly such as is expected for the Kondo effect (Fischer, 1982), and Fig. 47 shows that application of a small longitudinal magnetic field shifts both the dp/dT and the G anomalies to much lower temperatures. This last behavior is compatible with a Kondo system that has an effective magnetic moment ≥ 1 μ_B ($\mu_B = $ Bohr magneton) and a Kondo temperature T_K well below 0.2
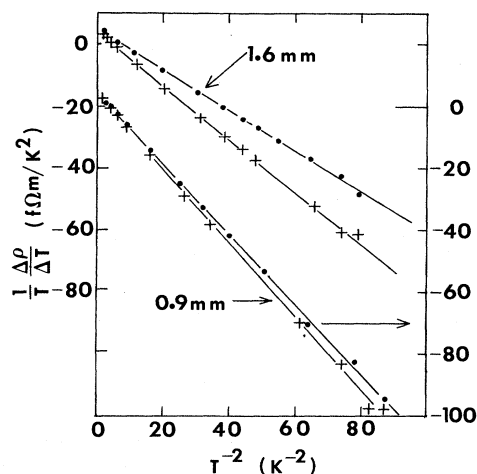

FIG. 49. $(1/T)(dp/dT)$ vs $(1/T^2)$ for K samples in polyethylene tubes of different diameters. Note that the $d = 0.9$ mm data use the right-hand ordinate scale. The symbols are the same as in Fig. 45. From Yu et al., 1984a.

K. These three characteristic behaviors lead one to speak of a "Kondo-like" anomaly, both to describe the effects seen and to distinguish it from other anomalies found when K is perturbed.

This anomaly clearly has implications for the data of van Kempen et al. and Levy et al., which were taken on samples in polyethylene tubes, and for p_0 in the data of Rowlands et al., whose samples were wound on grooved Teflon cylinders.

We consider first the behavior of p_0 in samples constrained in either Teflon or polyethylene tubing. The values of p_0 for K in polyethylene in Fig. 44 and those for K in Teflon in Fig. 48 show qualitatively similar behavior. In both cases p_0 is initially high, but decreases with holding time at room temperature. In polyethylene, the decreases occur mostly in the first few days, just as van Kempen et al. observed for their samples in polyethylene. In Teflon, the decreases occur over a longer time, just as was seen by Rowlands et al. for their samples wound on Teflon cylinders. It seems probable that all of these changes in p_0 result from the fact that both polyethylene and Teflon impose constraints during cooling that most likely cause impurities in the K to be retained in solution. Gugan et al. (1989) recently proposed exactly the same mechanism for decreases in p_0 that they found upon isochronal annealing of initially rapidly cooled K wires constrained in glass tubing.

Levy et al., in contrast, did not find similar reductions in p_0 with annealing time for samples constrained in polyethylene. Perhaps the contamination that Levy et al. introduced into their samples by heating and cold working caused p_0 to increase by more than it decreased due to annealing in the presence of constraints. The interpretation of their data is complicated by their heating of their samples, since Gugan et al. (1989) found p_0 to in-

crease greatly when K wires in glass were allowed to equilibrate for more than 24 h at 320 K and then cooled quickly. Direct comparisons are further complicated by the fact that the annealing times of Levy et al. were much shorter than those of Yu et al., van Kempen et al., or Gugan et al.

For samples in both Teflon and polyethylene tubing, the values of $(1/T)(d\rho/dT)$ found by Yu et al., van Kempen et al., and Levy et al. all also decreased with holding time at room temperature. For the sample of Yu et al. in Teflon, the decreases in $d\rho/dT$ and ρ_0 both occurred over similar time periods, and the decreases in $d\rho/dT$ were consistent with the expected reductions in ρ_{iei}—the contribution from inelastic impurity scattering—due simply to the observed decreases in ρ_0. For Yu et al.'s samples in polyethylene, in contrast, $d\rho/dT$ near 1 K continued to decrease by large amounts after ρ_0 had essentially stopped decreasing. Because Yu et al.'s data extended to well below 1 K, we can see that these reductions in $d\rho/dT$ simply reflected the growth of the negative high-temperature tail of the large Kondo-like anomaly at lower temperatures. Such a mechanism provides a qualitative explanation for the changes in $d\rho/dT$ seen by Levy et al. For the data of van Kempen et al., the explanation is even semiquantitative, as we show next.

Figure 44 shows $(1/T)(d\rho/dT)$ for Yu et al.'s $d = 0.9$ mm sample in a polyethylene tube, which was measured after being held at room temperature for 0.5, 2.5, 13, and 73.5 days, compared with that for van Kempen et al.'s $d = 0.9$ mm sample in a polyethylene tube, which was measured directly after cooling and then again after 2 and 80 days at room temperature. If one restricts attention to the data of Yu et al. (1985) above 1 K—so as to simulate the data of van Kempen et al. (1976)—they reproduce nicely the major features of the anomalous behaviors seen by van Kempen et al.—both ρ_0 and $(1/T)(d\rho/dT)$ decrease with holding time of days to weeks at room temperature. The agreement is thus quantitative for the changes in ρ_0, but only semiquantitative for $(1/T)(d\rho/dT)$, since the van Kempen et al. data fall somewhat lower on the graph of $(1/T)(d\rho/dT)$ than the Yu et al. data, and also decrease by a somewhat larger amount in 70–80 days.

Since the data of Levy et al. were also obtained for samples in polyethylene, we would expect them to have been similarly affected by the polyethylene. In an attempt to reproduce quantitatively the changes in $(1/T)(d\rho/dT)$ seen by Levy et al. (1979) when a sample in polyethylene tubing was deformed by rolling a metal cylinder over it, Yu et al. rolled metal cylinders over two of their samples in polyethylene tubing. In one case, ρ_0 increased and $(1/T)(d\rho/dT)$ decreased between 1 and 1.3 K, as found by Levy et al. However, in the other case ρ_0 decreased slightly, and between 1 and 1.3 K $(1/T)(d\rho/dT)$ remained essentially unchanged. This partially different behavior might be due to the fact that the surface of their sample remained shiny at all times,

while those of Levy et al. became white. We shall see in Sec. IV.C that white surface (and perhaps also bulk) contamination can lead to decreases in $(1/T)(d\rho/dT)$ in wires as thin ($d = 1$ mm) as those used by Levy et al.

We conclude that the studies by Yu, Haerle, et al. (1984a) and Yu et al. (1985, 1989) provide strong evidence that the anomalies in $(1/T)(d\rho/dT)$ seen by van Kempen et al. and by Levy et al. were due largely to extrinsic causes. In the case of van Kempen et al., we think that they were due primarily to the fact that the samples were enclosed in polyethylene. In the case of Levy et al., two additional effects might also have been operative: (1) the effects of short anneals in polyethylene could have been enhanced when Levy et al. raised the annealing temperature to $T \geq 323$ K; and (2) the fact that Levy et al.'s samples had $d = 0.9$ mm means that a "size effect" in the presence of surface contamination, which we consider next in Sec. IV.C, might have contributed to the behavior they found. Yu's data also provide a possible explanation for the decreases in ρ_0 found by Rowlands et al. upon extended room-temperature annealing of their samples.

Very recently, a Kondo-like anomaly was seen by Qian et al. (1988; 1989) under conditions where H does not appear to have been present. They saw a Kondo-like anomaly in thin K films evaporated onto glass microscope slides and single-crystal KF. Only very much smaller anomalies were seen when samples were evaporated onto magnetically clean Si. Since the preparation procedures were the same for all three substrates, their results point to a more general phenomenon of Kondo scattering at magnetically dirty surfaces. Very recently (Qian et al., 1990) they also saw small, unassignable, electron-spin-resonance signals in samples inside polyethylene tubes. What the contaminant might be on these surfaces, and why it or something similar would be present in a variety of different forms of polyethylene, but not in Teflon or Kel-F, are questions that remain to be answered.

C. Thinned K wires: surface contamination and complications

1. Rationale and overview

Zhao et al. (1988) undertook additional measurements on thinned K wires (a) to attempt to better understand the apparently different effects of Ar and He gas on thin K samples described in Sec. III.H above (Figs. 39 and 41); and (b) to test the models for "size effects" described in Sec. III.H. Their procedures were essentially the same as those of Yu, Haerle, et al. (1984b), except that they baked the molecular sieve used to absorb He gas upon cooling (see Appendix B) at 573 K instead of 473 K to try to clean it better. Zhao et al. had initially hoped to produce larger size effects than those seen by Yu, Haerle, et al. (1984b), by making wires much thinner than $d = 0.1$ mm using a combination of smaller-diameter dies and thinning due to surface corrosion. However, when

they prepared new $d \leq 0.1$ mm samples in He, they found anomalies (Figs. 50 and 51) that were generally smaller than those of Yu, Haerle, et al. (1984b) for samples of the same diameter. They decided that they had better clarify the reasons for this different behavior before trying to make still thinner wires.

Zhao et al. (1988) discovered that the discrepancies were due in part to lower-purity starting material and probably also to reduction in surface contamination due to their higher baking temperature for the molecular sieve. They examined the effects of several different variables on the "size effect." In the end they concluded that

(1) all of their thinned wires showed anomalies; (2) anomalies of a given size all had the same temperature dependence, independent of the conditions that produced the anomalies; and (3) surface contamination appeared to enhance the anomalies. However, Zhao et al. were unable to establish the complete set of variables that determined the size of the anomaly in a given sample, and this set remains unknown to today. There is, as yet, no consensus on a theoretical explanation for this size effect anomaly.

2. Detailed analysis

Whereas the bulk RRR for the samples of Yu, Haerle, et al. had been about 7300, those for the samples of Zhao et al. were only either 4800 or 1700. These RRR's are used to label data from the different batches of K in the graphs presented below. A check with the manufacturer revealed that in the several years since purchase of the original batch of K used by Yu, Haerle, et al., MSA has prepared a new batch with a Na content three times that of the old; the K studied by Zhao et al. (1988) was from
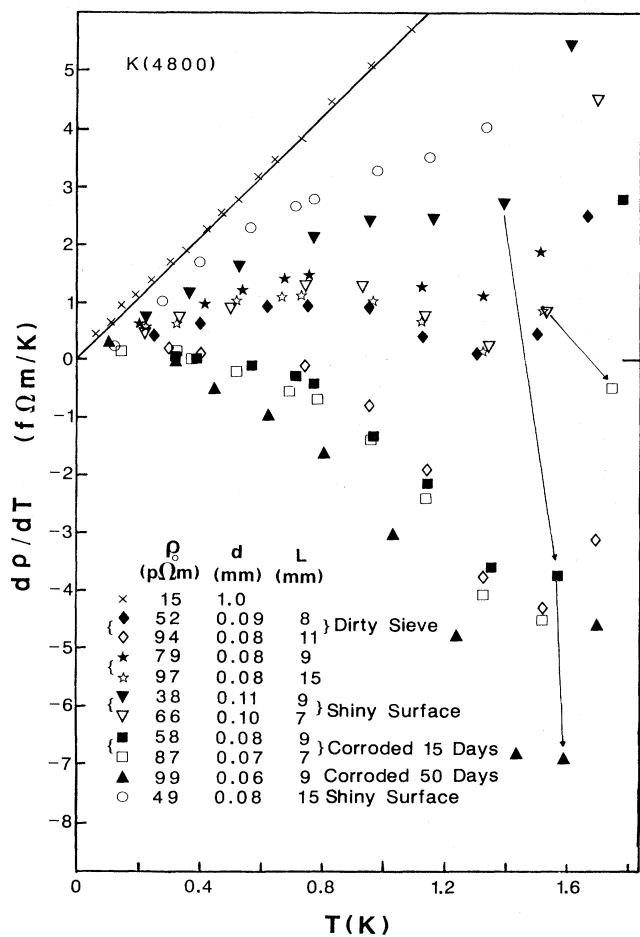

FIG. 50. $d\rho/dT$ vs T for the K(4800) samples. Pairs of samples prepared together are designated by identical symbols, with the open symbol designating the sample prepared first. Note that in each pair the anomaly is always larger for the sample prepared first, and the anomaly is independent of sample length, except for the sample pair denoted by diamonds. This pair was the only one that showed a length dependence approximately proportional to L^2. After their initial cooling, some of the samples were given room-temperature anneals and then cooled and measured again. The progression of behavior after such anneals is indicated by the arrows. From Zhao et al., 1988.
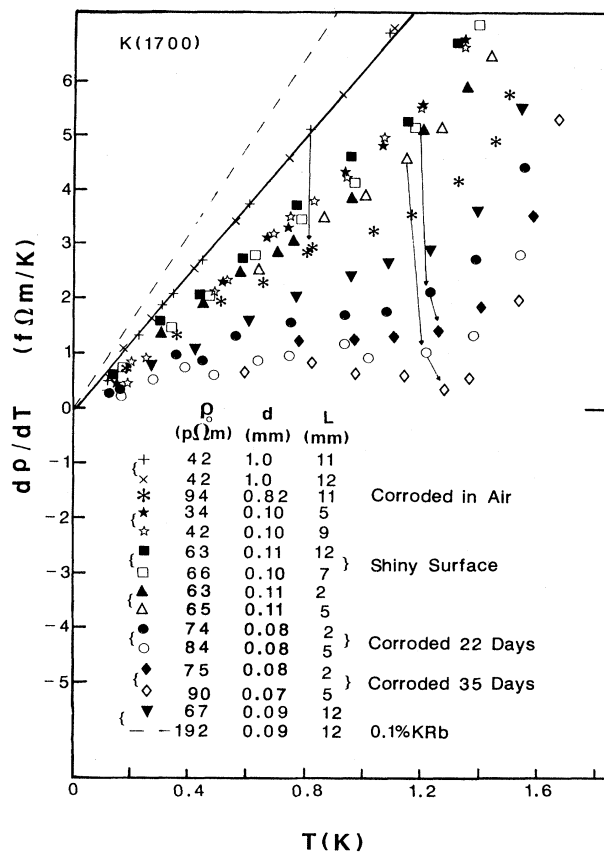

FIG. 51. $d\rho/dT$ vs T for the K(1700) samples. The general remarks in the caption to Fig. 50 apply equally to Fig. 51. From Zhao et al., 1988.

this new batch.

Because inelastic impurity scattering produces different contributions to $d\rho/dT$ for different sample purities, Zhao et al. recognized that it was essential to compare data for a given thin sample with data for a bulk sample of exactly the same starting material. To obtain such data, they measured $d\rho/dT$ for relatively thick ($d = 1$ mm) samples from each of the two batches of K that they studied, and chose appropriate samples as best representatives of bulk behavior. The plus or cross symbols traversed by solid lines in Figs. 39, 50, and 51 indicate the data for the chosen bulk samples. To compare size effects in different sample sets, they defined the quantity Δ to be the difference at $T = 1.0$ K between the value of $d\rho/dT$ for a given thin sample and the bulk value for that same sample set. 1.0 K was chosen to be as high as possible and yet have no contribution to $d\rho/dT$ from electron-phonon scattering. Values of Δ for all of their samples are given in Fig. 52. Clearly Δ depends upon parameters other than just d.

Sample purity was not the only important new variable uncovered by Zhao et al. (1988). They also found that greater amounts of surface contamination usually led to larger values of Δ. For a given thin sample, additional surface contamination always led to an increase in the anomalies, as shown in Figs. 39, 41, 50, and 51. What portion of this increase was due to the contamination itself and what portion to the additional thinning produced by the contamination is not clear. To check whether samples with visually clean surface would still display anomalies, Zhao et al. cleaned the atmosphere in the sample can with a large area of fresh K on a Cu foil
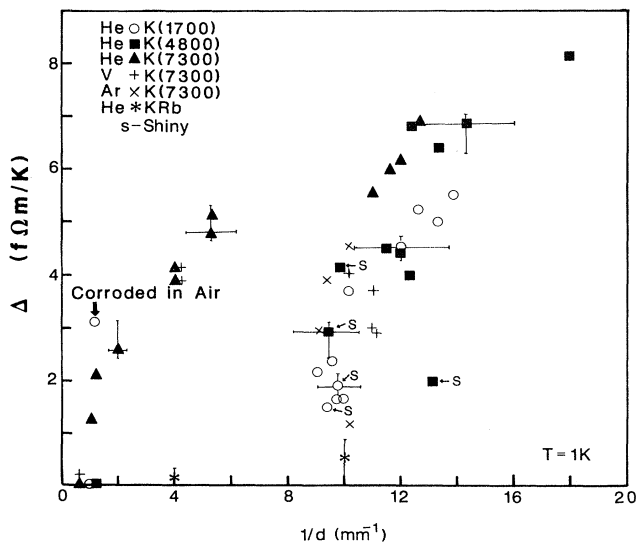
wrapped around the inside surface of the can. This procedure yielded, for the first time, $d \leq 0.1$ mm samples with shiny surfaces when reexamined after being measured. The samples with shiny surfaces all showed anomalies. For the K(1700) samples these anomalies were similar in size to typical anomalies for samples with white surfaces. For the K(4800) samples the anomalies were systematically smaller than those for white-surfaced samples. This means either that surface corrosion is not essential to the anomaly or else that only an extremely thin layer of surface corrosion is sufficient to produce an anomaly in a very thin wire. To see whether surface contamination alone could produce an anomaly, they deliberately produced substantial surface contamination in two $d = 1.5$ mm samples by taking them out into the air. In one sample (see Fig. 52) a significant anomaly was observed. When sliced, this sample was found to consist of three or four thin cylinders of K embedded in a wire of corroded material. In the other sample, no size-effect anomaly was seen. The relation between surface contamination and the "size effect" is apparently not simple.

We now examine the data of both Yu, Haerle, et al. (1984b; Figs. 39 and 41) and Zhao et al. (1988; Figs. 50 and 51) in more detail. Figure 53 shows $\rho_0(d)$ versus $1/d$ for all of the data from both studies. This plot provides a test of whether thinning introduced impurities in the samples. If no impurities were introduced, and if the sample cross sections were reduced uniformly, then $\rho_0(d)$ for thin wires should be directly proportional to $1/d$, with a slope determined by the electronic structure of the host metal (Bass, 1982). Figure 53 shows that this expected behavior is approximately observed for thicker samples. However, as the samples become thinner, the

FIG. 52. $\triangle$ vs $1/d$ for the data of Figs. 39, 41, 50, and 51. $\triangle$ is the deviation at 1.0 K of the anomalous values of $d\rho/dT$ in Figs. 39, 41, 50, and 51 from the bulk behavior shown in each figure. The letter "s" indicates samples with shiny surfaces. From Zhao et al., 1988.
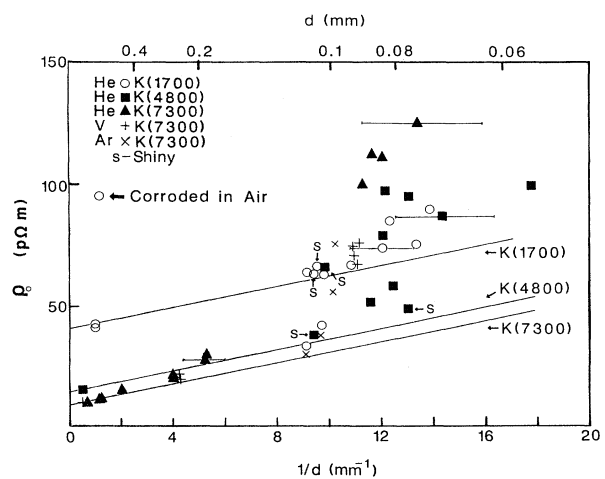
FIG. 53. ρ_0 vs $1/d$ for K wires of different diameters and different bulk purities. The solid lines have the slope expected for a simple "size effect" (see Bass, 1982). The letter "s" indicates samples with shiny surfaces. From Zhao et al., 1988.

data generally rise above the expected lines, breaking away sooner the larger the RRR of the bulk K.

From Figs. 39, 41, 50, and 51, Zhao et al. (1988) derived the values of Δ plotted in Fig. 52 against inverse sample diameter $1/d$. Besides plotting Δ against $1/d$, Zhao et al. (1988) also examined two alternative plots of Δ. One was Δ versus RRR/d—which is proportional to l/d. This plot simply normalized the values of $1/d$ for different bulk mean free paths. The other was Δ against $\rho_0 - \rho_i$. If it is assumed that the wires are not contaminated at all during thinning, but that the estimates of their thicknesses are incorrect, then the rising of the data above the lines in Fig. 53 can be attributed to these incorrect thicknesses. In such a case, the quantity $\rho_0 - \rho_i$ measures the "correct" sample thickness, which is determined by shifting the data points in Fig. 53 to the right until they reach the proper straight line, and then reading off the sample thickness from the abscissa. Since none of these three alternative forms of analysis led to universal behavior of all the data, for simplicity we concentrate on Fig. 52.

Figure 52 shows that for the very thinnest samples (i.e., $1/d \geq 12$) the anomalies for the samples of Zhao et al. (1988) are very similar to those for the K(7300) samples of Yu, Haerle, et al. (1984b), which had the same nominal diameters, independent of sample purity. All of these data were taken on samples in He gas. In contrast, for thicker samples (i.e., $1/d \leq 10$), Zhao et al.'s values of Δ—all of which were obtained with samples in He gas—are closer in size to Yu et al.'s values for most samples in Ar, and much smaller than Yu et al.'s values for samples in He gas.

We already noted in Sec. III.H that Yu, Haerle, et al. (1984b) had found no significant size-effect anomalies in thin wires ($d = 0.1$ mm) of dilute KRb alloys in which the mean free path was much smaller ($l = 0.02$ mm) than the sample thickness. Zhao et al. (1988) reconfirmed this behavior as illustrated in Figs. 51 and 52. As also illustrated in Figs. 50 and 51, Zhao et al. found no significant length dependence of the anomalies.

Finally, as shown in Fig. 54, Zhao et al.'s (1988) size-effect anomalies all have the same temperature dependence for a given anomaly size, independent of wire thickness, bulk resistivity, or the gas in which the wire is prepared and cooled. Below about 1.2 K, where electron-phonon scattering is small, the solid curves in Fig. 54 show that the anomalies can be parametrized as having $\rho(T) \propto T^{7/3}$. Since these curves fall above the data in the vicinity of 1.2 K, this form seems to require an additional negative contribution to $d\rho/dT$ for data in the vicinity of 1.2 K.

Zhao et al.'s (1988) results appear to confirm the presence of a size-effect anomaly in K wires, at least in the presence of some surface contamination. However, the complexity of their results leaves the source or sources of the anomaly still unclear.

Next, we consider the ramifications of Zhao et al.'s new data for the size-effect models (Sec. III.H) developed

to try to explain the 1984 data of Yu, Haerle, et al.

(1) Additional theoretical analysis between 1984 and 1988 has shown that Yu et al.'s tentative attribution of the anomaly to the Gurzhi effect is erroneous.

(2) Neither Yu, Haerle, et al.'s 1984 data nor Zhao et al.'s 1988 data follow the T^5 form predicted by the KW model (1985) for the interaction between surface scattering and normal electron-phonon scattering.

(3) Neither Yu, Haerle, et al.'s 1984 data nor Zhao et al.'s 1988 data follow the simple T^2 form predicted by De Gennaro and Rettori (1984, 1985) for interference between surface scattering and normal electron-electron scattering. Movshovitz and Wiser (1987) initially argued that numerical Monte Carlo studies showed that the De Gennaro and Rettori model was invalid, but Movshovitz and Wiser (1990) have recently reported the discovery of errors in those Monte Carlo calculations.

(4) Zhao et al. attempted to observe the length depen-

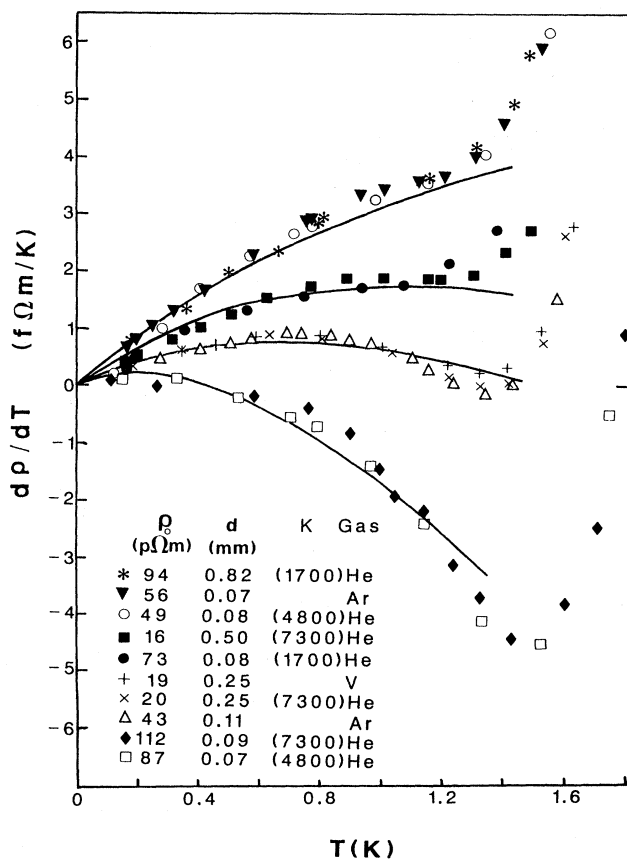FIG. 54. Comparison of data sets with four different size anomalies involving wires having different thicknesses or different RRR's, and/or wires cooled in different gasses. The curves through the low-temperature data are fits up to 1.2 K to an equation of the form $\rho(T) = (A + B\rho_i)T^2 - CT^{7/3}$, where $A + B\rho_i$ is determined by the behavior of thick K wires from the same batch of material. From Zhao et al., 1988.

dence of the $d\rho/dT$ anomaly predicted by the strong-localization model of Farrell et al. (1985). Because of the lower purity of Zhao et al.'s samples, they were only able to test for length effects in samples with $d\rho/dT > 0$; they found none. While one cannot yet rule out a length dependence for samples with $d\rho/dT < 0$, the smooth growth of the anomalous behavior with decreasing d makes it seem unlikely that the correct explanation will involve the combination of two completely different phenomena—(a) an as yet unknown mechanism for $d\rho/dT > 0$ and (b) strong localization for $d\rho/dT < 0$—which fortuitously join nicely together as the anomaly grows larger.

Finally, we mention two very recent theoretical developments. Gurzhi et al. (1989) have examined qualitatively the contributions to $\rho(T)$ of normal electron-phonon and normal electron-electron collisions that occur within a mean free path of the sample surface in a metal with a spherical Fermi surface. They make two main points: (1) that they obtain fundamentally different results from those of De Gennero and Rettori (1984; 1985) and Kaveh and Wiser (1985); and (2) that they can obtain a resistivity minimum if normal electron-phonon scattering predominates over normal electron-electron scattering. However, their effect manifests temperature dependences $(T^3 \rightarrow T^5)$ under different conditions, which are always higher than that observed $(T^{7/3})$.

Movshovitz and Wiser (1990) report obtaining a quantitative fit to both the Rowlands et al. (1978) data and the Yu, Haerle, et al. (1984b) and Zhao et al. (1988) data for relatively thick samples with reasonable choices of unknown parameters with a combination of (a) the KW (1985) model; (b) the de Gennaro and Rettori (1984, 1985) model; and (c) a better treatment of surface scattering, including its dependence on the angle at which an electron strikes the sample surface.

We conclude this discussion of size effects in K by noting that, as briefly indicated at the end of Sec. IV.B, Qian et al. (1989) have recently measured $\rho(T)$ for K films evaporated onto various substrates inside a vacuum chamber in a glove box. The most relevant of these measurements for size effects are those involving evaporation onto Si, where only a very small Kondo effect was seen. Figure 55 shows that, except for a few small resistivity minima at the very lowest temperatures, $d\rho/dT$ increases monotonically with increasing T. No size effect anomaly is observed. If one focuses on the data of Fig. 55 above about 0.3 K, then $d\rho/dT$ is compatible with a linear dependence upon T up to about 1.3 K, with a coefficient that is larger than the one for bulk K and that grows with decreasing film thickness. Above 1.3 K, the data exhibit a large T^n component with $n = 4$, corresponding to a T^5 component in $\rho(T)$. This component also grows substantially with decreasing film thickness.

The Farrell et al. (1985) model involving strong localization would predict no size effect anomaly in a film, because the dimension of the film in its plane is much longer than the bulk electron mean free path l. The
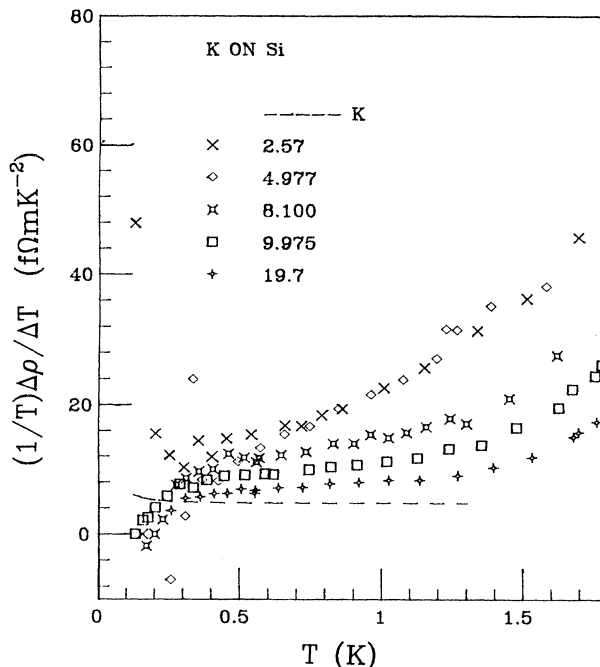

FIG. 55. $(1/T)(d\rho/dT)$ vs T for thin K films on Si. The dashed curve indicates typical behavior for pure bulk K wires. The symbols indicate the behavior of samples having the thicknesses (in microns) indicated.

Movshovitz and Wiser (1990) model just mentioned also appears not to generate a size-effect anomaly in thin films.

D. Deformed samples of K and KRb: vibrating dislocations

1. Rationale and overview

New data on deformed samples were taken in three studies. The first, by van Vucht et al. (1986), extended data by van Vucht et al. (1983) described in Sec. III.G on $d = 3$ mm pure K samples twisted at or below 4 K to one additional sample and to a KRb alloy. The second, by Haerle et al. (1986), extended data described in Sec. III.G on $d = 0.9$ mm samples squashed between Teflon-covered metal plates at 60 K to additional annealing procedures. The third, by Yin et al. (1990; see also Yin, 1987), presented new data for $d = 2$ mm samples twisted at 9.3 K to introduce dislocations and point defects. Yin et al. took new data (1) to use samples thicker than 0.9 mm, so as to avoid the size-effect anomaly that plagued the pure-K data of Haerle et al.; (2) to check whether twisting produced significantly different results from squashing; and (3) to extend higher-precision measurements of the effects of deformation to much lower tem-

peratures ($\simeq 20$ mK) than Haerle *et al.* were able to study ($\simeq 90$ mK), so as to better characterize the low-temperature form of the deformation-induced anomaly. As discussed in Sec. III.B.2, deformation at 4.2 or 9.3 K should produce a combination of point defects and dislocations, whereas deformation at 60 K should leave almost exclusively dislocations, since point defects anneal out below 60 K.

The study of van Vucht *et al.*, which extended only over the temperature range 0.9–4.2 K, generally confirmed the results reported by van Vucht *et al.* (1982; see also van Vucht *et al.*, 1985) for twisted K samples and showed that twisting KRb produced still larger increments in the T^2 term in the resistivity than in pure K, but that these increments followed the same dependence upon ρ_0 (compare Figs. 34 and 56) as for twisted K. They continued to try to attribute the behavior of their data to the KW (1982) model, but noted the difficulties thereof, and pointed out that if the more complex behaviors reported by Haerle *et al.* (1983) were confirmed, their interpretation would probably have to be substantially modified.

The other two studies confirmed the existence of the complex temperature dependence of the $d\rho/dT$ anomaly reported by Haerle *et al.* (1983) for deformed samples. They also revealed nicely systematic changes in $d\rho/dT$ for samples subjected to increasing amounts of deformation and for samples annealed to sequentially higher temperatures after deformation. All of the Haerle *et al.* data turned out to be compatible with predicted behavior for electrons scattered from vibrating dislocations. This model also fits Yin *et al.*'s data when substantial numbers of point defects (vacancies or impurities) are present—i.e., deformed KRb and pure K deformed at 9.3 K and not annealed. However, when dislocations are the dominant defect—i.e., pure K deformed at 60 K, or deformed at 9.3 K and then annealed at 60 K or higher—an additional behavior appears, which can be fit
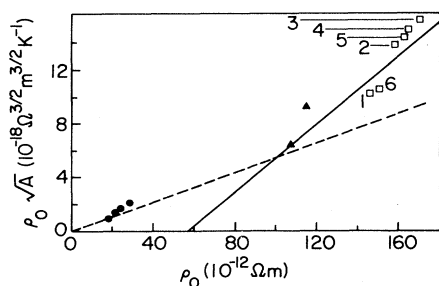

FIG. 56. Equivalent to Fig. 34 extended to show the dilute alloy data of Haerle *et al.*, 1983 (▲) and van Vucht *et al.*, 1986: □, sample K12 of van Vucht *et al.*; ●, sample K8 of van Vucht *et al.*; — — —, the slope obtained for annealed samples; ———, the slope found for the high-purity samples, drawn for comparison. After van Vucht *et al.*, 1986.

with a localized electron-energy-level model. Both studies also confirmed previous evidence from the MSU group for $T \geq 1$ K that dislocations and point defects cause T^5 components of $\rho(T)$ to appear and grow in both pure K and KRb, probably due to partial quenching of phonon drag.

2. Detailed analysis

a. Van Vucht et al.

Information about the two new samples of van Vucht *et al.* (1986) is given in Table VII. The new results confirmed the earlier observations by both van Vucht *et al.* (1982) and Haerle *et al.* (1983) of much larger deformation-induced increases in $\rho(T)$ of K in the vicinity of 1 K than were predicted by the KW (1982) model of anisotropic scattering. In addition, van Vucht *et al.* reported finding similar changes in the T^2 term after deformation of both K and KRb alloys, which was clearly incompatible with the predictions of the KW model. Nonetheless, van Vucht *et al.* structured the rest of their interpretation around the T^2 term predicted by this model [as had van Vucht *et al.* (1982) and van Vucht *et al.* (1985)]. They confirmed their previous observation that annealing out of vacancies caused the nominal T^2 term to increase rather than decrease as would normally have been expected for isotropically scattering point defects in the KW model. They thus had to retain the additional requirement developed in van Vucht *et al.* (1982) that vacancies had to be produced in strings so as to produce anisotropic-scattering-like dislocations. They also confirmed their previous observation that their data on both annealed and deformed samples required only a T^2 term plus an exponential, with no need for a T^5 term. They again noted that this lack of a T^5 term after deformation was contrary to predictions for quenching of phonon drag. They also reported that adding the vibrating dislocation term of Eq. (17) failed to improve the fits to their data, so that they could not confirm the need for such a term. But they carefully noted that their interpretion would probably have to be fundamentally modified if this term was ultimately proved to influence data significantly in deformed K and KRb samples above 1 K.

In the following two sections we show that the Haerle *et al.* (1983) term does significantly influence data in both K and KRb to above 1 K. It is thus important to point out that if one simply discards the KW model, one gains directly an explanation for the lack of difference in behavior between van Vucht *et al.*'s K and KRb data, and one simultaneously eliminates the need for vacancies to form in lines so as to scatter anisotropically.

b. Haerle et al.

Figures 36 and 37, respectively, have already shown Haerle *et al.*'s results for a K(0.077 at. % Rb) alloy that

was first deformed at 60 K and then later annealed at 160 K, and for a pure-K sample deformed by successively greater amounts at 60 K. We see from Fig. 37 that the magnitude of $d\rho/dT$ increases systematically with in-
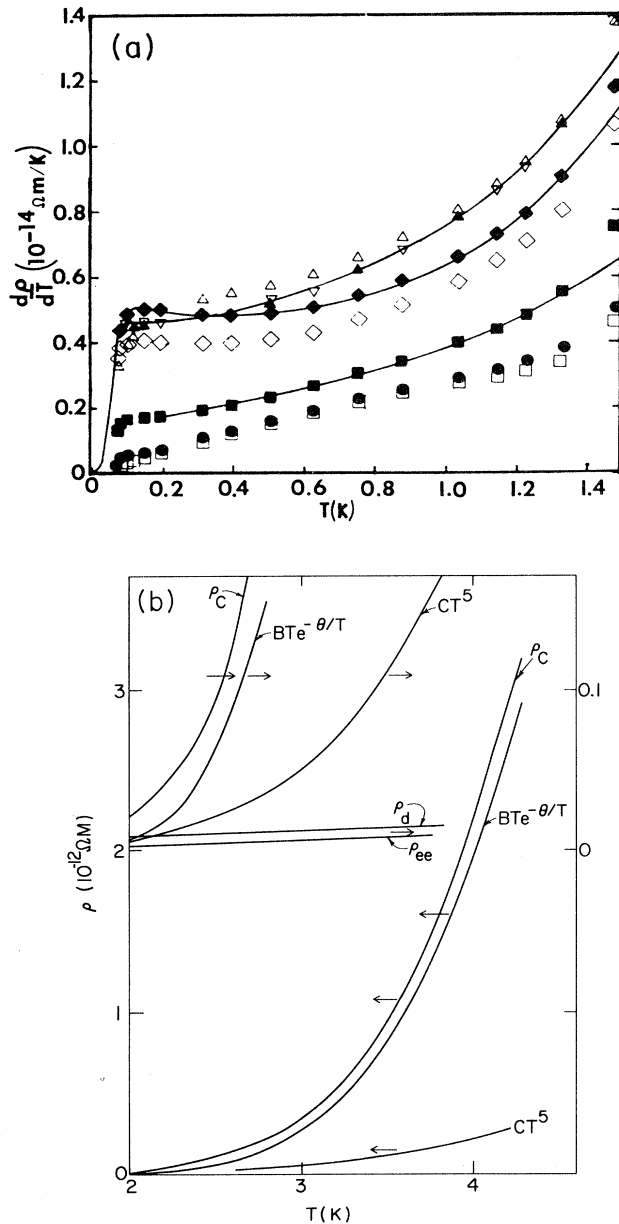

FIG. 57. Behavior of a K sample after deformation and annealing. (a) Effect of annealing on $d\rho/dT$ in deformed K. $d\rho/dT$ vs T for sample K9H: □, no deformation; ▽, deformed at 4.2 K with deformation pressure 32×10^4 PA. Annealed at ▲, 7.5 K; △, 20 K; ◆, 60 K; ◇, 80 K; ■, 120 K; and ●, 165 K. ——, fits to Eq. (17). From Haerle et al., 1986, but with the symbols for 7.5 and 20 K corrected. (b) $\rho(T)$ and its components vs T above 2 K for a deformed K sample. Note that the upper curve uses the right-hand ordinate scale. After Haerle et al., 1986.

creasing deformation and that the form of the additional term added to $d\rho/dT$ by deformation remains practically unchanged.

Figure 57(a) shows Haerle et al.'s results for a K sample deformed at 4.2 K and then annealed to successively higher temperatures. Here, annealing between 7.5 and 60 K produces changes in the form of $d\rho/dT$, and annealing to 160 K returns the sample to its pre-deformation state.

Clearly these data are incompatible simply with a T^2 variation of $\rho(T)$ below about 1 K. Haerle et al. examined three alternative fits to the data of Figs. 36, 37, and 57(a). The first was Eq. (17), in which the third term on the right-hand side is due to scattering of electrons by vibrating dislocations (Gantmakher and Kulesco, 1975). At higher temperatures (i.e., above about 0.5 K), this term contributes a component to $d\rho/dT$ that is independent of T, so that the curves with increasing deformation are just shifted upward by increasing amounts. The second fit involved replacing the term in Eq. (17) for scattering by vibrating dislocations by a term involving scattering from resonant electron states that are presumed to be associated with dislocations (Gantmakher and Kulesco, 1975). The third involved an alternative form of the term for scattering from resonant states, originally derived by Fulde and Peschel (1972) for scattering of electrons by a crystalline electric field. These last two alternatives should contribute terms to $d\rho/dT$ that decrease as $(1/T)^2$ or faster above about 0.5 K.

Haerle et al.'s best fit was found with Eq. (17), scattering from vibrating dislocations. The solid curves in Figs. 37, 38, and 57(a) represent the fits of this four-parameter equation to the data. We see that Eq. (17) is able to describe all of the data for the deformed samples. In the fits to the data of Fig. 38, where the K sample was subjected to successively larger deformations, the coefficient A stayed nearly constant except for a rise after the last deformation, the coefficients D and ϵ increased systematically with increasing deformation, and the coefficient C initially increased but then saturated at a value comparable to the best predictions of the Bloch T^5 term in pure K (see, for example, MacDonald et al., 1981). For the data of Fig. 57(a), in contrast, where a strongly deformed sample was annealed at increasing temperatures, all four coefficients fluctuated in complex fashion. Annealing at 120 K caused both C and D to decrease substantially, which Haerle et al. attributed to annealing out of dislocations.

Haerle et al. also checked whether the parameters obtained from fits of Eq. (17) to $d\rho/dT$ below 1 K were compatible with the behavior of $d\rho/dT$ above 1 K. To fit the data above 1 K, they simply included umklapp electron-phonon scattering by adding to Eq. (17) an exponential term $BT \exp(-\Theta/T)$. If they assumed that B and Θ were both independent of deformation, they found satisfactory agreement with the data. If, instead, both B and Θ were allowed to vary, but the T^5 term was neglected, the fits were not satisfactory. Contrary to what van

Vucht *et al.* had reported for twisted wires, Haerle *et al.* found that a substantial T^5 term was always required for a good fit. As shown in Fig. 57(b), below about 2.6 K, all three terms in Eq. (17) plus the exponential term contributed significantly to $\rho(T)$. Above 2.6 K, however, only the CT^5 and $B \exp(-\Theta/T)$ terms remained important. We note in Fig. 57 that the T^5 term contributes only about 10% of $\rho(T)$ at 4.2 K. Given that the fit of the data by Eq. (17) plus an exponential was only good to about 5% (Haerle *et al.*, 1986), we infer that the data could also have been fit satisfactorily with a smaller T^5 term and a modest increase in the exponential, as expected for phonon drag.

The changes in $d\rho/dT$ that Haerle *et al.* found above 1 K after deformation are much too large to be understood in terms of the initial model of Danino *et al.* (1981b, 1981c) for quenching of phonon drag by phonon-dislocation scattering. The changes are qualitatively compatible with the later predictions of Engquist (1982) and Danino *et al.* (1982, 1983) for quenching of phonon drag when electron-dislocation scattering is highly anisotropic. But, in conflict with the predictions of this model, pure K and KRb alloy samples subjected to similar deformations yield changes in $d\rho/dT$ that are very similar in both magnitude and temperature dependence. But changes in anisotropic scattering cannot be important in the KRb alloy, since the values of ρ_0 in this

FIG. 58. G vs T for sample K8h in the undeformed state and after deformation and subsequent annealings. The symbols are the same as in Fig. 37. Note that the zeros have been shifted for clarity by the numerical amounts (in V) indicated. From Haerle *et al.*, 1986.

alloy remain dominated by isotropic impurity scattering both before and after deformation.

Haerle *et al.* also measured the thermoelectric ratio G for their strained samples, with results illustrated in Fig. 58. The data show two qualitative effects of importance: (1) a systematic reduction with increasing deformation in the phonon-drag minimum just above 3 K; and (2) the appearance of a small maximum in G at about 0.5 K. The first behavior is most easily attributed to quenching of normal phonon drag in $d\rho/dT$ as illustrated in Fig. 57. The source of the small maximum is not yet clear, although it appears to be associated with the presence of dislocations. Presumably its explanation involves details of the energy dependence of the scattering of electrons by dislocations.

c. Yin et al.

Yin *et al.* deformed $d = 2$ mm, $L = 4$ cm K and K(0.087 at. % Rb) wires by twisting at 9.3 or 60 K, and also annealed these wires at successively increasing temperatures. The 2 mm diameter was chosen so that the analysis would not be complicated by the size effects (Sec. IV.C) that affected Haerle *et al.*'s data. The samples were prepared and mounted in an Ar atmosphere. A thin layer of K or Rb smeared on a thin Cu sheet was used to reduce contaminants in the sample can to a level at which the sample surfaces remained "reasonably shiny" for the several weeks needed for a complete measuring run. Yin *et al.* pointed out that surface cleanliness was important, since thick deposits of K compounds on the sample surface were observed to alter significantly the mechanical properties of the sample. As in Haerle *et al.*'s case, measurements were made against reference resistors of a Cu(Ag) alloy designed to have small temperature and current dependences. For their KRb alloy sample, Yin *et al.* used the same $R = 1.6$ $\mu\Omega$ reference resistor used by Haerle *et al.* For their pure K samples, Yin *et al.* used a new resistor with $R = 0.18$ $\mu\Omega$. Yin *et al.* found that twisting changed $R(300 \text{ K})$ in their samples, and thus their geometry, by less than 1%, which was much smaller than the approximately 10% found by Haerle *et al.* with squashing.

For twists of pure K samples at 9.3 K, Yin *et al.* found a linear increase of ρ_0 with increasing twisting angle θ, with a coefficient $d\rho_0/d\Theta \simeq 5.2$ fΩ m/deg, about half as large as that found by van Vucht *et al.* (1984) for twists at 4.2 K (after correcting van Vucht *et al.*'s longer sample length—10 cm versus 4 cm). Yin *et al.* suggested that the difference might be due to the higher yield stress of K at 4.2 K than at 9.3 K.

Figure 59(a) shows $d\rho/dT$ below 1 K as a function of twist angle for the KRb alloy subjected to a series of twists and anneals as listed in Table VIII. Note how between about 0.2 and 0.8 K the curves are closely compatible with straight lines merely shifted with respect to each other. Note also that an anneal at 200 K for two
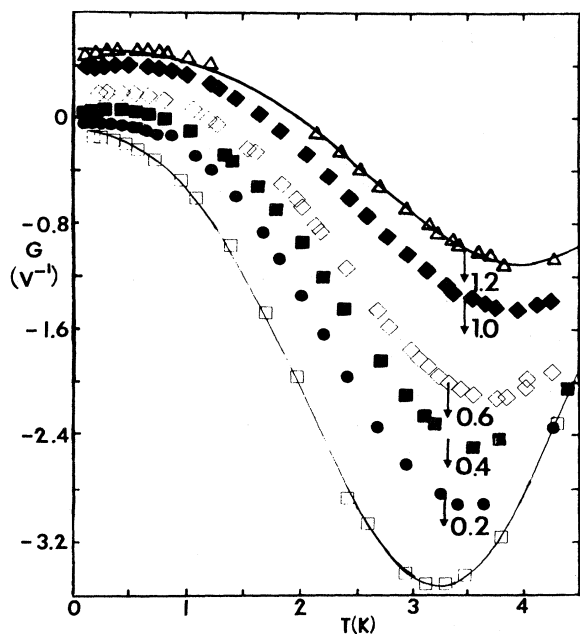
TABLE VIII. Characteristics of deformed KRb sample of Yin (1987).

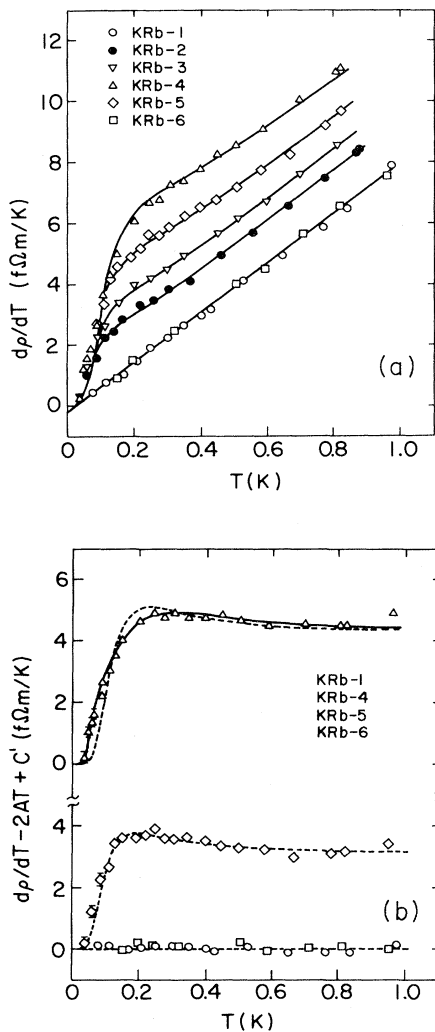| KRb-1	Untwisted
KRb-2	480° twisted at 60 K
KRb-3	4800° twisted (total) at 60 K
KRb-4	Additional 4800° at 9.3 K then annealed at 36 K for 30 min
KRb-5	Annealed at 60 K for 30 min
KRb-6	Annealed at 200 K for 2 h.

FIG. 59. Effects of increasing deformation on a KRb sample. (a) $d\rho/dT$ vs T for a KRb sample deformed by a series of increasing twists. The closely parallel form of the data above about 0.15 K indicates that at these temperatures the dominant contribution to $\rho(T)$ added by the deformation varies linearly with T. Table VIII contains sample information. (b) $d\rho/dT - (2AT - C')$ vs T for four of the samples in Fig. 59(a). This graph focuses attention upon the change in $d\rho/dT$ after twisting. After Yin et al., 1990.

hours comp3tely restored $d\rho/dT$ to its pre-deformation values. The solid curves in Fig. 59(a) correspond to fits to the equation

$$\rho(T) = AT^2 - C'T + (D/4T)\sinh^{-2}(\epsilon/2T) . \qquad (19)$$

Here A and C' are the values of AT^2 (due to electron-electron scattering) and $-CT$ (due to a low-temperature alloy anomaly described in Sec. IV.F below) for the unstrained samples. The additional term, due to scattering from vibrating dislocations, is the same as in Eq. (17). Some of the data sets of Fig. 59(a) are replotted in Fig. 59(b) as $d\rho/dT - 2AT + C'$, so as to focus on the last term on the right-hand side of Eq. (19). One sees in Fig. 59(b) both the steplike nature of the extra term in the vicinity of 0.1 K and its approximate temperature independence above about 0.5 K. The dashed curves in Fig. 59(b) correspond to Eq. (19). They fit very well all of the data after either deformation at 60 K or annealing to 60 K, both of which should involve only dislocations in the sample. The upper data set in Fig. 59(b) (KRb-4) shows deviations from Eq. (19) after deformation at 9.3 K, where the sample should contain a significant concentration of point defects in addition to dislocations. The solid curve in Fig. 59(b) was obtained by expanding Eq. (19) to include two adjustable frequencies.

A pure K sample was also twisted at 9.3 K to a series of increasing values of Θ without annealing. As in the case of the KRb sample twisted at 9.3 K [Fig. 59(b)] a single-frequency model gave too sharp a peak in the fit of Eq. (19) (with the alloy term omitted) to the data. In contrast, a two-frequency model fit the data as nicely as it did for KRb in the upper curve in Fig. 59(b).

When Yin et al. twisted a pure-K sample at 9.3 K and then annealed it at 60 K (sample K-7), or simply twisted it at 60 K (sample K2-2), they found changes in $d\rho/dT$ that were significantly different from those shown in Fig. 59(a). As shown in Fig. 60, these two samples behaved rather similarly in exhibiting too sharp a peak in $d\rho/dT$ for a good fit by the vibrating dislocation model alone. To obtain the good fits to these data shown by the solid curves in Fig. 60, Yin et al. added to the vibrating dislocation term in Eq. (19) a term very similar to that proposed by Gantmakher and Kulesco (1975) for localized electronic levels associated with a dislocation. The reasons for this different behavior are not yet understood.

Haerle et al. had not reported similar "sharp peaks" in their $d = 0.9$ mm pure-K wires squashed at 60 K. Yin et al. argued that this apparent discrepancy probably resulted simply from an inadequate correction for the size-effect contribution (see Sec. IV.B) to the data of Haerle et al.'s undeformed wires. For these wires Haerle et al. had found a T^2 term with $A = 1.5$ fΩ m/K^2, much smaller than the $A = 2.5$ fΩ m/K^2 that Yin et al. found for their $d = 2$ mm samples and that is more typical of free-hanging thick samples (see, for example, Sec. IV.G). When Haerle et al. fit Eq. (17) to their data, the A's before and after deformation appeared to be similar, and
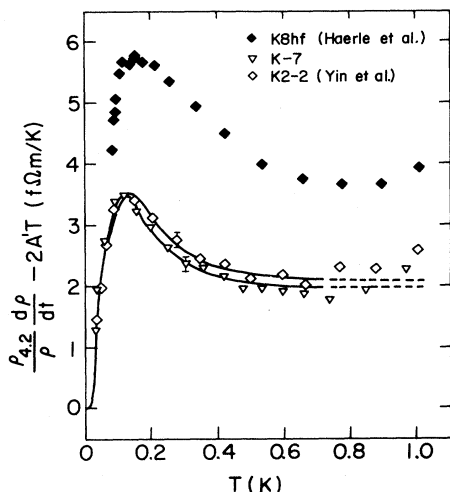
FIG. 60. A demonstration that similar behavior is seen upon annealing at 60 K after twisting at 9.3 K (K-7) and after twisting directly at 60 K (K2-2). Similar behavior is also seen in data from Haerle et al., 1986, when the latter data are properly corrected as described in the text. After Yin et al., 1990.

hence they implicitly assumed that the small value of A in the unstrained samples was not significantly changed by deformation. Yin et al. showed (Fig. 60) that if one assumed that a severe deformation competely eliminated the size effect, thereby raising A to about 2.5 fΩ m/K^2, then Haerle et al.'s maximally deformed pure-K sample K8hf exhibited the same behavior as Yin et al.'s samples. We note that the increase in ρ_0 of Haerle et al.'s sample K8hf above its value in the undeformed state was about three times larger than the almost equal increases for samples K-7 and K2-2 of Yin et al., indicating a considerably larger dislocation density in sample K8hf. This larger density is reflected in the larger values of $d\rho/dT$ for K8hf in Fig. 60.

Finally, Yin et al. also measured G for their samples and found results very similar to those obtained by Haerle et al. as illustrated in Fig. 58.

E. Dilute KRb, KNa, and LiMg alloys: simple consistent behavior

1. Rationale and overview

New measurements on KRb, KNa, and LiMg alloys were undertaken for several reasons. (1) To recheck, with improved measuring techniques, the inelastic impurity scattering coefficient A_I derived by Lee et al. (1980) from measurements on KRb alloys. In particular, an accurate balance inside the glove box permitted better determinations of the impurity contents of the samples. (2) To check whether the T^2 coefficients for KNa and LiMg increase linearly with ρ_0 as the impurity content is increased, as required by the inelastic electron-impurity

scattering model, and thereby to derive the coefficients of inelastic impurity scattering for these alloys. (3) To check the applicability of the KW anisotropic scattering model to Li, by seeing whether data for the T^2 coefficient
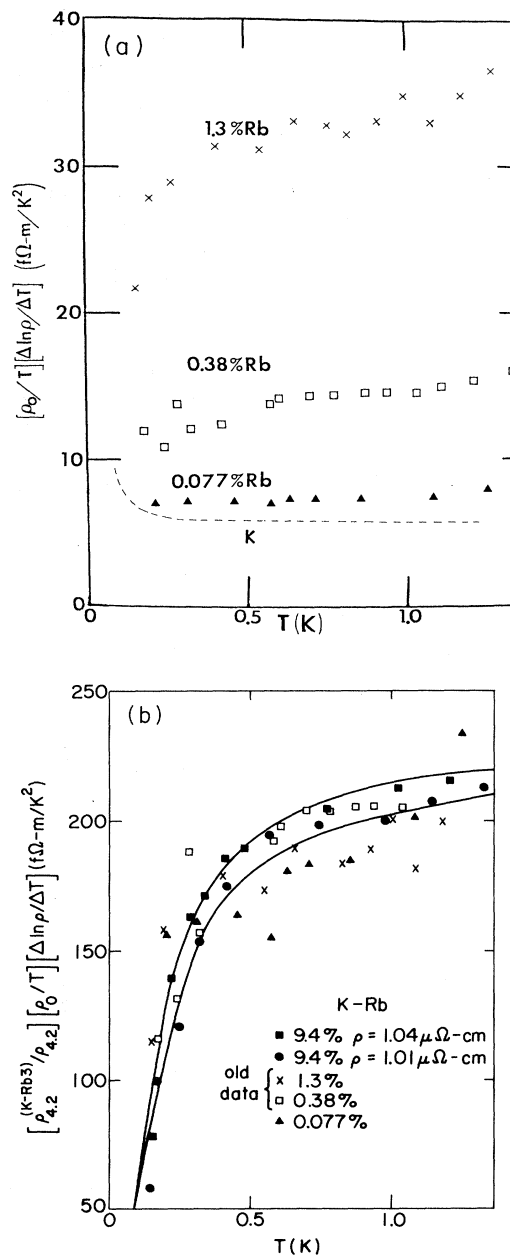
FIG. 61. Original and normalized values of $(1/T)(d\rho/dT)$ for dilute KRb alloys. (a) $(1/T)(d\rho/dT)$ vs T for a series of dilute KRb alloy samples. The dashed curve indicates typical behavior for pure K. After Yu, 1984. (b) Values of $(1/T)(d\rho/dT)$ normalized as described in Sec. IV.F to show the similarity in behavior of the low-temperature anomalies. This figure corrects erroneously plotted data for one 9.4% sample given in Bass et al., 1984.

for dilute LiMg alloys extrapolates for $\rho_0 = 0$ to the value obtained for bulk, free-hanging Li samples.

In the process of making the studies described in this section, Bass *et al.* (1984) discovered a new low-temperature anomaly in $\rho(T)$ as the alloys were made more concentrated. This new anomaly will be described and analyzed in the following section, IV.F.

The new data on $(1/T)(d\rho/dT)$ for dilute KRb, KNa, and LiMg alloys are shown in Figs. 61–63. The T^2 coefficients for all three alloys are plotted together in Fig. 64. Figure 65 shows the detailed behavior of the KRb and LiMg alloys for small values of ρ_0, along with data for pure K and pure Li.

Above about 1 K, the data for the KNa alloys in Fig. 62 show clear evidence of quenching of phonon drag. To eliminate redundancy, we defer discussion of quenching of phonon drag in both KRb and KNa alloys to Sec. IV.E, where we consider the data for dilute and concentrated alloys together.

Below 1 K, Zhao *et al.*'s (1989) new values of A_{iei} for KRb are slightly larger than those of Lee *et al.* (1980), and their values for LiMg are in good agreement with those estimated by Oomi *et al.* (1985) from higher-temperature data. These values are compared in Table III.
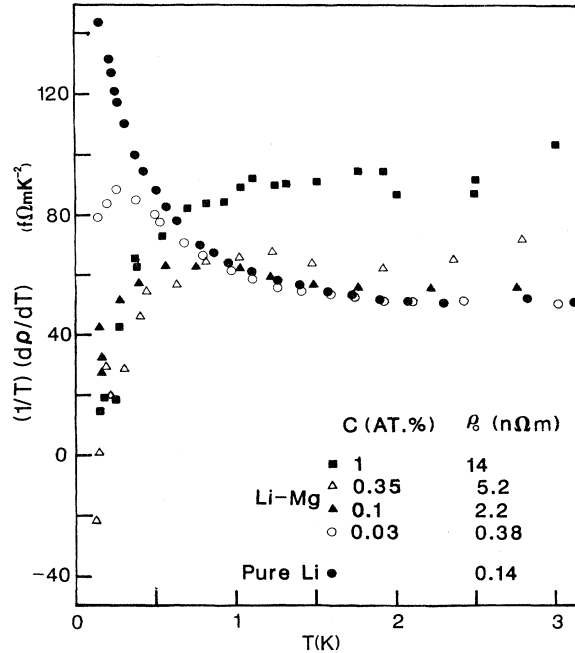
FIG. 63. $(1/T)(d\rho/dT)$ vs T for a series of dilute LiMg alloys, showing development of the low-temperature "alloy anomaly" as ρ_0 increases. From Zhao, 1988.
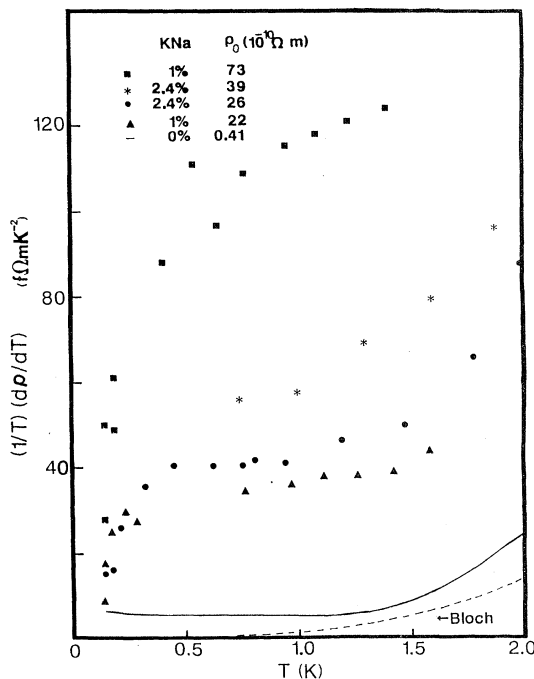
FIG. 62. $(1/T)(d\rho/dT)$ vs T for a series of dilute KNa alloys and a pure-K sample, showing development of the low-temperature "alloy anomaly" as ρ_0 increases. ———, typical behavior for pure bulk K; — — —, approximates the Bloch limit of ρ_{ep} for pure K. From Zhao *et al.*, 1989.

FIG. 64. Collection of the T^2 coefficients of $\rho(T)$—i.e., $(A + B\rho_0)$—vs ρ_0 for KRb, KNa, and LiMg alloys. From Zhao *et al.*, 1989.

FIG. 65. The values of $A + B\rho_0$ from Fig. 64 vs ρ_0 for LiMg alloys ($\triangle$) and pure Li ($\blacktriangle$). The 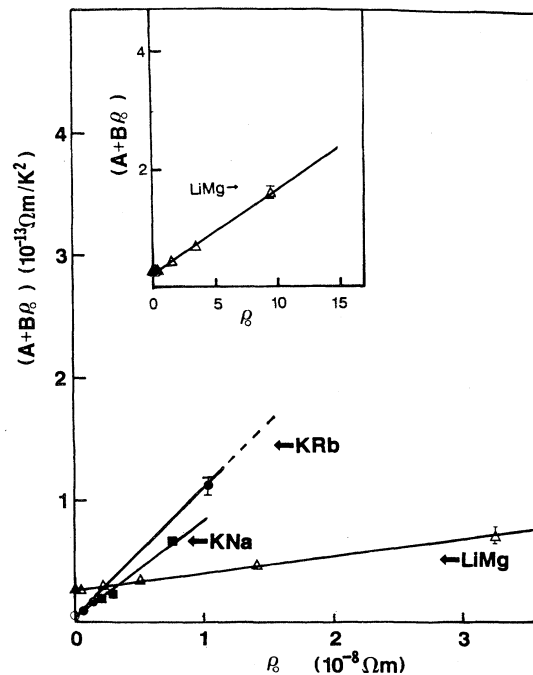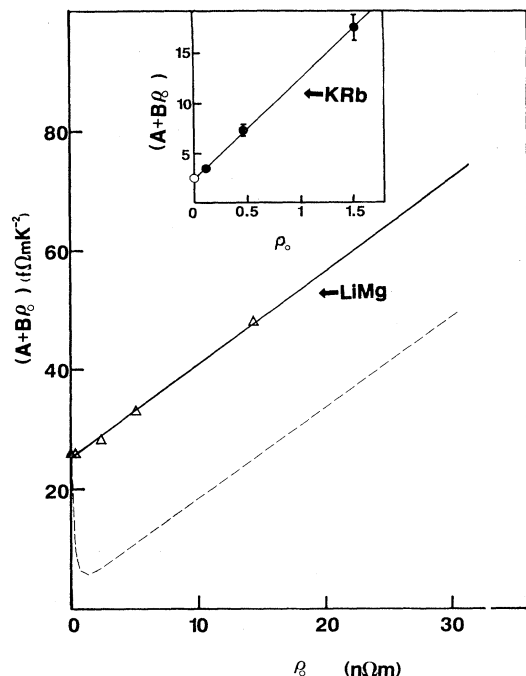dashed curve indicates the expected behavior for LiMg with anisotropic scattering, using the parameters suggested by Sinvani et al. (1981). Data for dilute KRb alloys ($\bullet$) and for pure K ($\circ$) are given in the same units in the inset. Note that both the LiMg and the KRb data extrapolate linearly to their respective pure-metal data points. After Zhao et al., 1986.

The T^2 coefficients for all three alloys extrapolate nicely (Fig. 65) to the values independently measured on pure K and pure Li. The value of A_{ee} for pure K is in excellent agreement with those of Lee et al. (1982) and Yu et al. (1989). The value of A_{ee} for pure Li is slightly lower than that of Yu et al. (1983), but the two sets of data agree to within mutual uncertainties. For both the KRb and LiMg alloys, these extrapolations are sufficiently precise to force the conclusion that they are incompatible with the KW (1980) model of anisotropic scattering.

2. Detailed analysis

With improved sample preparation and measuring techniques, Zhao et al.'s (1989) values of ρ_0 per atomic percent impurity for KRb alloys are in better agreement with literature values than were the old values by Lee et al. (1980). Similar values for LiMg are also in satisfactory agreement with literature values. For KNa, difficulties were encountered in achieving random impurity distributions, since Na is almost insoluble in K, and a substantial amount of precipitation occurs at room tem-

perature. Figure 66 shows the T^2 coefficients for the KNa alloys as a function of ρ_0 with the nominal impurity concentrations listed. For both the 1.0% and 2.4% alloys, the decreases in ρ_0 were obtained simply by letting the samples sit at room temperature for various periods of time, during which impurities precipitated out of solution.

Table III lists the values of the inelastic electron-impurity scattering coefficient A_I determined from (a) Fig. 64, (b) the previous data of Lee et al. (1980), (c) higher-temperature measurements on LiMg alloys (Oomi et al., 1985), and (d) theoretical analyses. We see that Zhao et al.'s new value for KRb is slightly larger than Lee et al.'s older one, and that the experimental values for all three alloys are comparable to the predictions for A_I, with one exception, the value attributed to Hu and Overhauser (1989). As noted in Sec. I.D.3, this value is likely to be less reliable than the others.

We now consider the applicability of the KW model to the data of Fig. 65. If electron-electron scattering has a single value in each host metal A_{ee}, and if the data of Fig. 65 are simply the sum of electron-electron and inelastic electron-impurity scattering, then A should be given by

$$A = A_{ee} + A_I \rho_0 . \tag{20}$$

A plot of A, versus ρ_0 should then yield a straight line with slope A_I and intercept with the ordinate axis A_{ee}. A_I should be representative of a given impurity in a given host metal, but A_{ee} should depend only on the host. Moreover, A_{ee} should be the same as the value measured in high-purity samples of the host.

If, in contrast, the KW model is applicable, then the magnitude of A_{ee} should vary with different amounts of
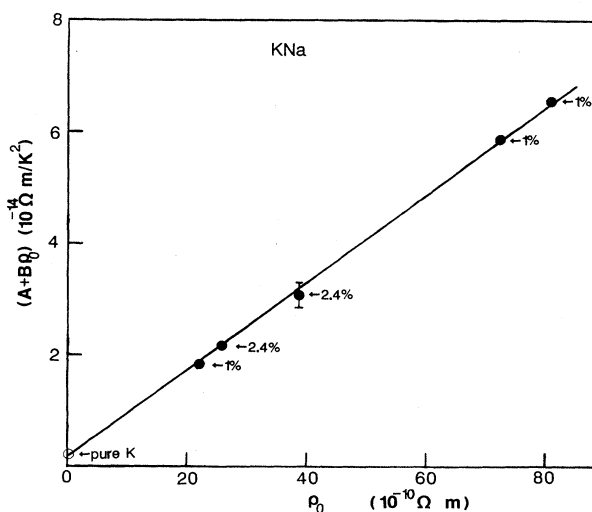

FIG. 66. The values of $A + B\rho_0$ vs ρ_0 from Fig. 64 vs ρ_0 for KNa alloys with the nominal alloy concentrations indicated. From Zhao et al., 1989.

anisotropic scattering. A_{ee} should take on the large value $A_{Nee} + A_{Uee}$ when anisotropic scattering is dominant, and the small value A_{Uee} when isotropic scattering is dominant. Since scattering by impurities is practically isotropic in both K and Li, the alloy data should extrapolate to A_{Uee}. Assume that one starts with a pure metal, with an A that is near the anisotropic limit $A_{Nee} + A_{Uee}$. If, as assumed by Kaveh and Wiser, $A_{Nee} \gg A_{Uee}$, then A should decrease substantially and rapidly when one adds an impurity concentration that is large enough so that impurity scattering dominates ρ_0, but small enough so that $A_I \rho_0$ is still considerably less than $A_{Nee} + A_{Uee}$.

For Li, Zhao *et al.* (1989) used the estimates of impurity anisotropy for Li given by Sinvani *et al.* (1981) to derive the value of ρ_0 at which A would reach its isotropic limit for the KW model. The result is the dashed curve in Fig. 65. We see that the data are completely consistent with Eq. (20) and inconsistent with this dashed curve.

For K, the $A_{ee} \simeq 2.2$ fΩ m/K^2 measured by Lee *et al.* (1980) and by Yu *et al.* (1989) is more than 4 times larger than Kaveh and Wiser's predicted isotropic limit of $A_{Uee} = 0.5$ fΩ m/K^2. We would thus expect similar dashed curves for the KRb and KNa alloys to the one shown in Fig. 65 for LiMg. We see from Fig. 65 that the data for KRb are also completely consistent with Eq. (20) and inconsistent with any such dashed curve. For KNa, we see from Fig. 66 that, while the alloy data are compatible with a linear extrapolation to the pure-K value at $\rho_0 = 0$, the alloys measured were too concentrated to permit an unambiguous extrapolation if the pure-K data point is omitted. That is, to within the sizes of the data points shown, the KNa alloy data are also compatible with an extrapolation to $A = 0$ for the pure-K limit.

We conclude that the data of Fig. 65 strongly support a single value of A_{ee} for each of the two host metals K and Li, as opposed to a value that changes with different relative amounts of isotropic and anisotropic scattering. In K, this A_{ee} is in satisfactory agreement with theory (Table II). In Li it is almost an order of magnitude larger than the value calculated for the bcc structure of Li (Table II). This leads us to conclude that A_{ee}^{exp} is determined by the non-bcc structure into which both Li and LiMg alloys up to well over 20 at. % Mg (Oomi and Woods, 1985) transform upon cooling to 4.2 K.

We end this section with a brief description of a new term that Hu and Overhauser (see Hu, 1987) have argued contributes to the behavior that we and Zhao *et al.* (1989) have attributed to inelastic electron-impurity scattering. This term involves an electron-phonon vertex correction to the electron-impurity scattering potential and becomes visible because of the breakdown of Migdal's theorem at small momentum transfers (Hu and Overhauser, 1988). Elastic scattering then gives rise to a term proportional to $\rho_0 T^2 \ln T$. Hu and Overhauser estimated the magnitude of this term using a Gaussian scattering potential containing a parameter that defined the range of the potential. The value of this parameter

was chosen to give a best fit to the KRb data of the sum of this new term plus their estimate of a reduced inelastic electron-impurity contribution (see Table III). Because of the $\ln T$ variation of the new term, the sum does not yield the simple T^2 form of the experimental data. Given the uncertainty in the magnitude of this new contribution, as well as its deviation from the form of the experimental data, it is not yet clear how important it is in the alloys covered in this review.

F. Concentrated KRb, KNa, and LiMg alloys: a new anomaly and quantum effects

1. Rationale and overview

In the previous section, IV.E, it was argued that when a dilute concentration of impurities is added to K or to Li, the only change in $\rho(T)$ below about 1 K is an increase in its T^2 component due to inelastic electron-impurity scattering. Bass *et al.* (1984), however, reported that when KRb alloys became more concentrated, a new very-low-temperature anomaly became visible and then grew. Their $d\rho/dT$ data for alloys with Rb concentrations extending up to 9.4 at. % are shown in Fig. 61. They found that data which included the low-temperature anomaly could be described by the equation

$$\rho_{alloy}(T) = A_{ee}T^2 + A_I \rho_0 T^2 - C\rho_0 T \ . \qquad (21)$$

Bass *et al.* (1986) and Zhao *et al.* (1989) extended these measurements to higher Rb concentrations, and to both KNa and LiMg alloys, to see what would happen to the form of $d\rho/dT$ when ρ_0 was increased still further, and whether the magnitude of the anomaly would be the same for different solutes and solvents. Of particular interest was whether corrections to the Boltzmann transport equation due to localization of electrons, or to electron-electron interactions in very "dirty" alloys, would become visible when ρ_0 became sufficiently large.

These studies showed that for alloys with $\rho_0 \lesssim 10^{-8}$ Ω m, $\rho(T)$ is nicely consistent with Eq. (21), with a coefficient C that is practically the same in KRb, KNa, and LiMg alloys. The physical source of this anomaly does not yet appear to be satisfactorily understood. For $\rho_0 \gtrsim 10^{-7}$ Ω m, the anomaly in $\rho(T)$ increases more rapidly than linearly with ρ_0 and is better fit by a $T^{1/2}$ temperature dependence. It will be argued that this latter behavior is compatible with the correction to the Boltzmann transport equation due to electron-electron interactions in a high-ρ_0 material.

Changes in $\rho(T)$ above 1 K in KRb and KNa alloys will also be examined, to investigate effects of phonon drag.

2. Detailed analysis

The values of $(1/T)(d\rho/dT)$ for KRb, KNa, and LiMg alloys are shown in Figs. 62, 63, 67, and 68. If there were
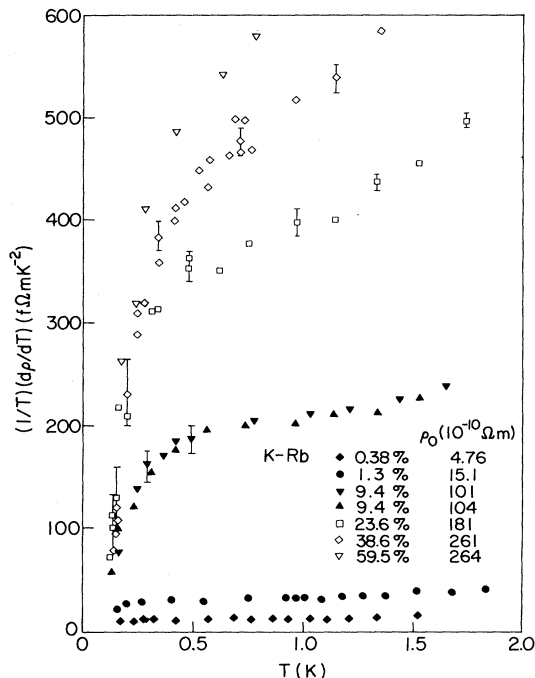
FIG. 67. $(1/T)(d\rho/dT)$ vs T for dilute and concentrated KRb alloys, showing how the low-temperature "alloy anomaly" grows with increasing Rb content. After Zhao *et al.*, 1989.

no low-temperature anomalies, the data in all of these figures would simply be flat below about 1.5 K.

We note first that the very-low-temperature anomalies grow systematically larger in all three alloys as the impurity concentration increases. The LiMg data in Fig. 63 are especially interesting, in that they show a smooth transition from the very-low-temperature anomaly in pure Li, in which $(1/T)(d\rho/dT)$ increases with decreasing T, to the alloy anomaly, in which $(1/T)(d\rho/dT)$ decreases with decreasing T. Note in Fig. 68 that the anomaly in LiMg ultimately becomes so large as to completely swamp the $A_{ee}T^2$ component.

In addition to these low-temperature anomalies, the KRb and KNa alloys also show high-temperature upturns which are probably due mainly to quenching of phonon drag. As we noted in Sec. III.F, the Debye temperature for Li is so high that no evidence of electron-phonon scattering appears below 10 K.

For the concentrated KRb alloys, coefficients for Eq. (21) were obtained both by fitting horizontal straight lines to the data of Fig. 67, where feasible, and from the intersections with the ordinate axes of the straight line fits to the data of Fig. 71 discussed later. To within mutual uncertainties, both procedures yielded the same coefficients. These coefficients, already shown in Fig. 64, are compatible—to within the substantial uncertainties for the more concentrated alloys—with the dilute alloy results reported in the previous section.

To examine both the low-temperature downturns and

the high-temperature upturns in Figs. 62, 63, 67, and 68 in more detail, Bass *et al.* (1986) and Zhao *et al.* (1989) took for guidance the model of Bass *et al.* (1984), which assumed that the low-temperature anomalies increased linearly with ρ_0. To test for such a variation, the data are assumed to be described by the equation

$$\rho(T) = f(\rho_0, T) + AT^2 + B\rho_0 T^2 + g(\rho_0, T) \ . \qquad (22)$$

Here AT^2 and $B\rho_0 T^2$ are the contributions from electron-electron and inelastic electron-impurity scattering, respectively, $f(\rho_0, T)$ represents the low-temperature anomaly, and $g(\rho_0, T)$ represents the high-temperature anomaly—assumed to become significant only for $T > 1.2$ K. To examine whether f and g vary linearly with ρ_0, the data are normalized to the form

$$X = \left[\frac{1}{\rho_0 T}\right]\left[\frac{d\rho}{dT}\right] - \frac{2A}{\rho_0} = \left[\frac{f'}{\rho_0 T}\right] + 2B + \frac{g'}{\rho_0 T} \ , \qquad (23)$$

where f' and g' are the temperature derivatives of f and g. If both f and g are proportional to ρ_0, then X should be independent of the impurity concentrations in the alloys.

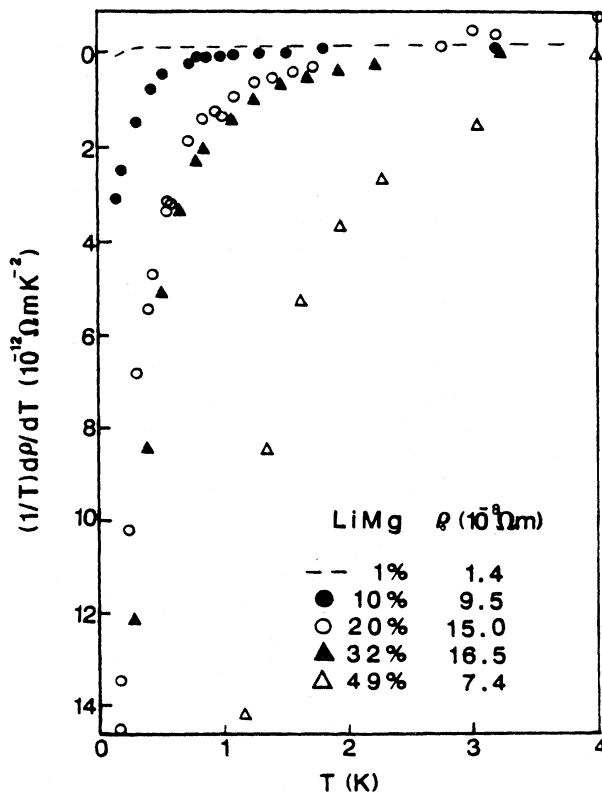Figure 69 shows that such plots provide a generally sa-

FIG. 68. $(1/T)(d\rho/dT)$ vs T for concentrated LiMg alloys, showing how the low-temperature "alloy anomaly" grows with increasing Mg content. From Zhao *et al.*, 1987.
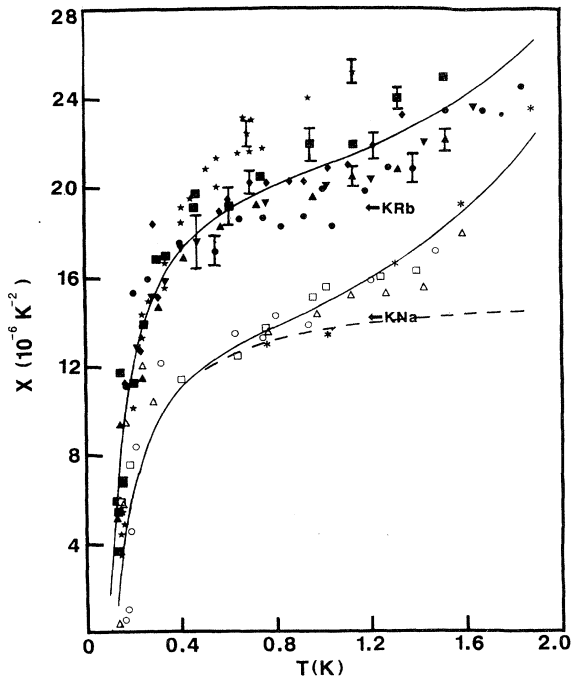
FIG. 69. Normalized data X vs T for KNa and the KRb data up to 38.6 at. % Rb, showing that the anomaly in $\rho(T)$ is approximately proportional to $\rho_0 T$. X is defined in Eq. (20). ———, fits with $X = -C/T + 2B + HT^3$; — — —, the same fit to the KNa data with the HT^3 term removed. For the KNa and KRb samples, the symbols are the same as in Fig. 62 or 67, respectively. From Zhao et al., 1989.

clear, since no mechanism involving point defects has yet been shown to produce substantial quenching of phonon drag. Taylor (1989) has suggested that the strain fields due to size differences between impurity and host ions might scatter phonons and thereby quench phonon drag, but no calculation has yet been made of the magnitudes of any such effects in K. For more concentrated alloys, the increases in $\rho_{ep}(T)$ were much larger than the Bloch limit for pure K. For the KRb alloys, Wiser (1988) showed that a combination of phonon drag with a decrease in Θ_D as the Rb concentration increased could account for the experimental data. Unfortunately, this model does not seem appropriate for KNa, since Θ_D for Na is higher than that of K. An analysis of inelastic impurity scattering by Kagan and Zhernov (1966) yields a contribution to $\rho(T)$ that varies as T^4 and as ρ_0. Unfortunately, it predicts a sign change between KRb and KNa alloys. We thus have no satisfactory explanation for the behavior of the KNa data at high temperatures.

Turning now to the low-temperature anomaly, Bass et al. (1986) and Zhao et al. (1989) examined three

tisfactory description of the data for both KNa and KRb, considering that the normalization varies by a factor of about 60 for the KRb alloys and 4 for the KNa alloys. The anomaly in K-based alloys thus increases approximately as ρ_0. The large anomaly in pure Li makes such a plot impossible for the LiMg alloys. An alternative analysis is presented for these alloys below.

We consider first the high-temperature anomaly. For pure K, phonon drag causes $\rho_{ep}(T)$ to be negligible below 1 K. From Fig. 69, however, addition of Rb or Na seems to cause $\rho_{ep}(T)$ to reappear. From the calculations of Leavens (1977) and Jumper and Lawrence (1977), discussed in Sec. III.D.3, we conclude that DMR, due to changes in Φ_k cannot produce such large increases in $\rho_{ep}(T)$ at temperatures in the vicinity of 1 K. Their explanation must thus be sought elsewhere. One obvious possibility is quenching of phonon drag. Zhao et al. (1989) showed that the high-temperature increase could be fit either with a term of the form $g \propto \rho_0 T^n$, with $n \simeq 5 \pm 1$, or with a combination of a T^5 term plus an exponential. For the dilute KRb and KNa alloys, the data could be described in terms of quenching of phonon drag, bringing back the Bloch T^5 term for pure K. The details of how such quenching occurs, however, are not yet
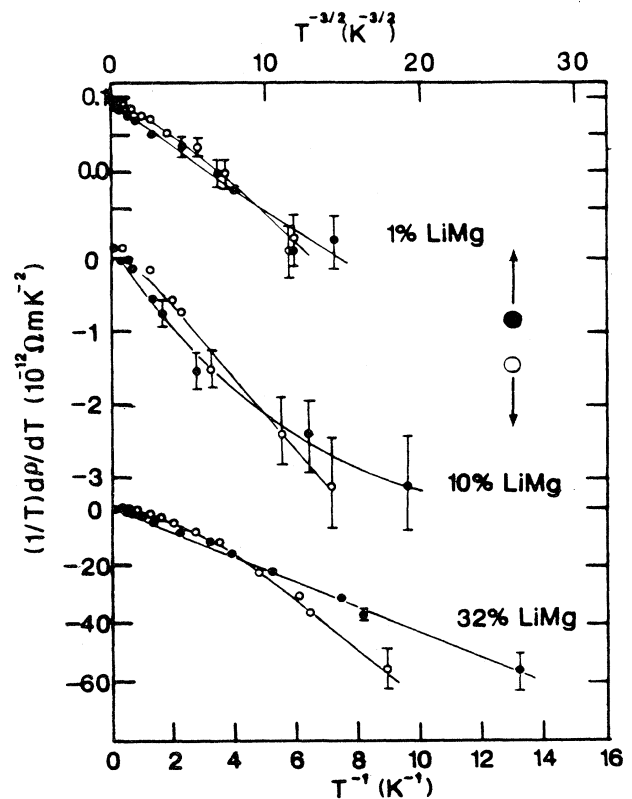

FIG. 70. $(1/T)(d\rho/dT)$ vs T^{-1} (open symbols and lower scale) and $T^{-3/2}$ (solid symbols and upper scale) for three LiMg alloys. Straight-line behavior vs T^{-1} ($T^{-3/2}$) indicates an anomaly in $\rho(T)$ that varies as $T(T^{1/2})$. The curves are hand drawn to guide the eye. From Zhao et al., 1987.

different temperature dependences, each initially suggested by a different physical source:

$$f \propto -T, \quad \text{localization},$$ (24a)

$$f \propto -T^{1/2}, \quad \text{electron-electron interactions},$$ (24b)

$$f \propto -\ln T, \quad \text{Kondo effect}.$$ (24c)

For these three alternatives, $(1/T)(d\rho/dT)$ would be proportional to T^{-1}, $T^{-3/2}$, and T^{-2}, respectively. When Zhao et al. (1989) plotted $(1/T)(d\rho/dT)$ as a function of each of these three powers of T for various samples, they found that the T^{-1} abscissa gave slightly the best fits for all of the KRb and KNa alloys and for the dilute LiMg alloys. The concentrated LiMg alloys were fit best with a $T^{-3/2}$ abscissa (Fig. 70).

Assuming a temperature dependence of $f(T) \propto T$, Zhao et al. (1989) extracted coefficients for all of the KRb, KNa, and dilute LiMg alloy data by replotting the data in the form $d\rho/dT$ versus T. The results are shown in Figs. 71 and 72. The coefficients C in $f(T) = -C\rho_0 T$ derived from Figs. 71 and 72 are plotted versus ρ_0 on logarithmic scales in Fig. 73. We see that the data for all
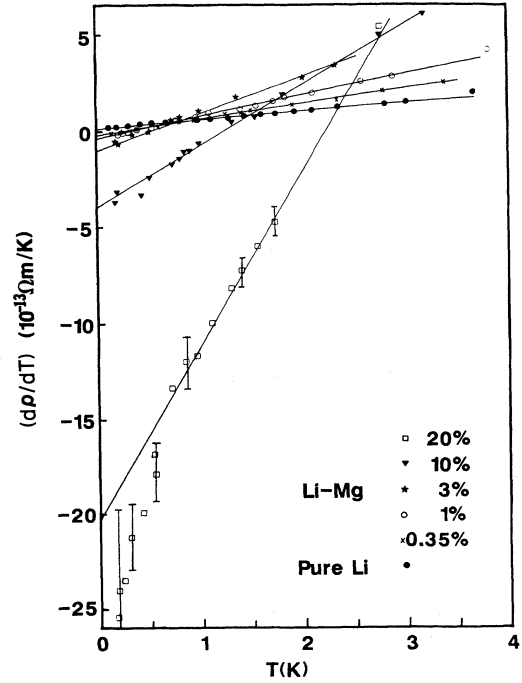
FIG. 72. $(d\rho/dT)$ vs T for LiMg alloys, showing that the data are consistent, up to 10 at. % Mg, with the linear behavior expected from Eq. (21). From Zhao et al., 1989.
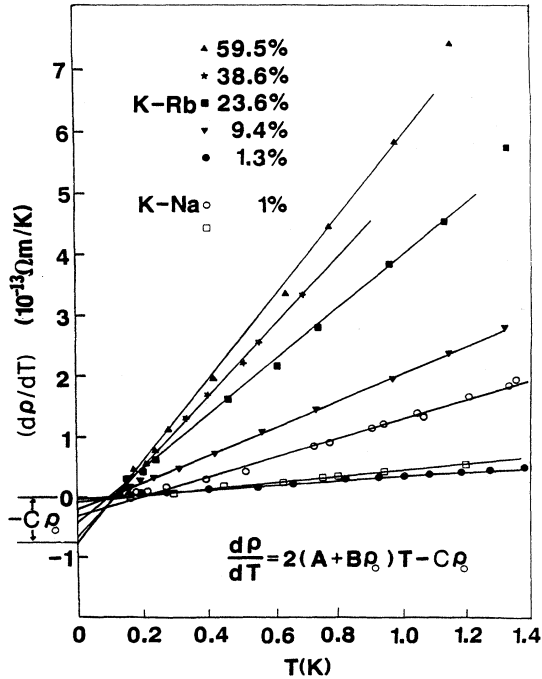
FIG. 71. $d\rho/dT$ vs T for KRb and KNa alloys, showing that the data are consistent with the linear behavior expected from Eq. (21) (which is repeated in the figure in its derivative form). The slope of the line defines the contribution due to electron-electron scattering plus inelastic impurity scattering. The intercept $C\rho_0$ with the ordinate axis defines the magnitude of the "alloy anomaly." From Zhao et al., 1989.
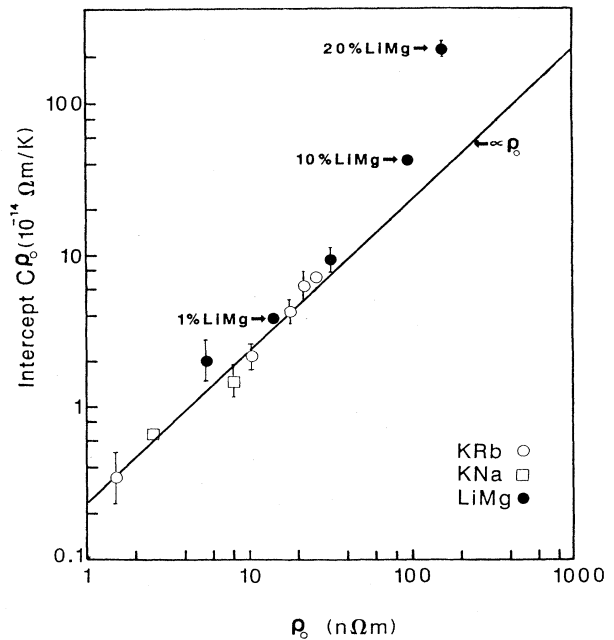
FIG. 73. Log-log plot of the intercepts $C\rho_0$ from Figs. 71 and 72 vs ρ_0 for KRb, KNa, and dilute LiMg alloys. The solid line indicates a linear dependence on ρ_0. Note that the dilute-alloy data are compatible with this dependence up to $\rho_0 \simeq 30$ nΩ m. From Zhao et al., 1989.

three alloy systems fall closely on a single line in Fig. 73. The slope of this line is approximately unity, as required for a variation linear in ρ_0.

The small value of the increase in ρ_0 per at. % Rb in KRb alloys, and the very limited Na solubility in KNa alloys, made it impossible to investigate the behavior of this anomaly for values of ρ_0 greater than 0.26×10^{-7} Ω m. For LiMg, however, it was possible to extend measurements up to $\rho_0 = 1.6 \times 10^{-7}$ Ω m. Above about $\rho_0 = 10^{-7}$ Ω m, both the temperature dependence and the ρ_0 dependence of the anomaly in LiMg changed. $\rho(T)$ was now better fit by a $T^{3/2}$ variation, as illustrated in Fig. 70. If all of the data for KRb, KNa, and LiMg are forced to fit this same form, so as to permit a consistent comparison of data with different values of ρ_0, then the coefficient varies as shown in Fig. 74. The dilute alloy data are again compatible with a linear dependence on ρ_0, as indicated by the dashed line on the graph, but the more concentrated LiMg alloy data clearly rise above this line. The solid line in Fig. 74 is an estimate of the expected contribution of corrections to the Boltzmann transport equation—with electron-electron interactions
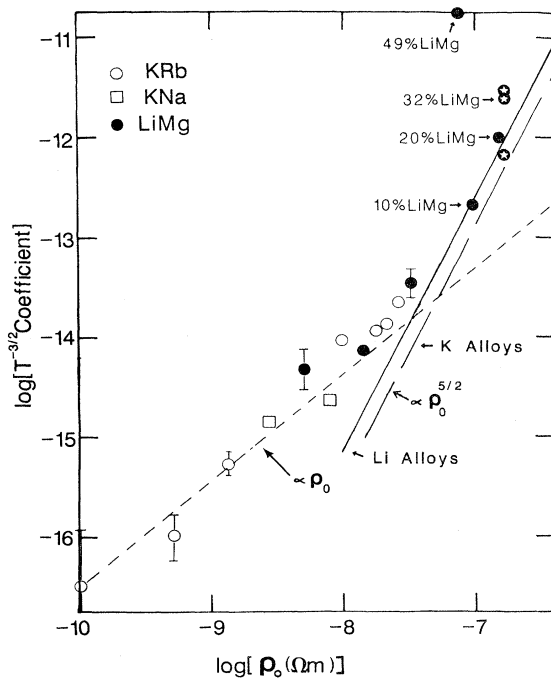
dominating over localization effects under the conditions investigated. This line was derived using the equation for electron-electron interactions given by Lee and Ramakrishnan (1985) and assuming that $\rho(T)$ in the absence of these corrections was dominated by ρ_{iei} due to inelastic electron-impurity scattering. The data appear to approach this line for values of $\rho_0 \geq 10^{-7}$ Ω m, although the very-high-concentration data manifest large variations. Perhaps these variations are the result of a subtle metallurgical effect involving different microscopic impurity distributions within the samples, due to different mixtures of bcc and 9R crystal structures. The data of Oomi and Woods (1985) indicate that these concentrated alloys are in the vicinity of the Li concentration at which the phase transition to the 9R low-temperature phase no longer occurs. If so, these different structures seem to have little effect on the residual resistivity, since the ρ_0's of the various 32 at. % Mg samples are all very close to each other. Lastly, we note that if the concentrated alloy data are attributed to corrections to the Boltzmann transport equation, then such effects decrease much too rapidly with decreasing ρ_0 to be able to explain what is occurring below $\rho_0 = 10^{-7}$ Ω m.

Finally, to see whether the anomaly had a magnetic origin, Bass et al. (1986) tested whether a longitudinal magnetic field of 0.2 T affected $(1/\rho T)(d\rho/dT)$ in K(9.7 at. % Rb) and Li(1 at. % Mg) samples. As shown in Fig. 75, such a field produced no effect to within experimental

FIG. 74. Log-log plot of the $T^{-3/2}$ coefficients in $(1/T)(d\rho/dT)$ vs ρ_0 for KRb, KNa, and both dilute and concentrated LiMg alloys. The coefficients were determined by fitting the best straight lines to data plotted as the filled symbols in Fig. 70. The solid lines labeled Li alloys and K alloys are the predicted behaviors for electron-electron interactions in Li- and K-based alloys, respectively. The dashed line is a fit to the low-concentration data of a variation proportional to ρ_0. From Zhao et al., 1989.
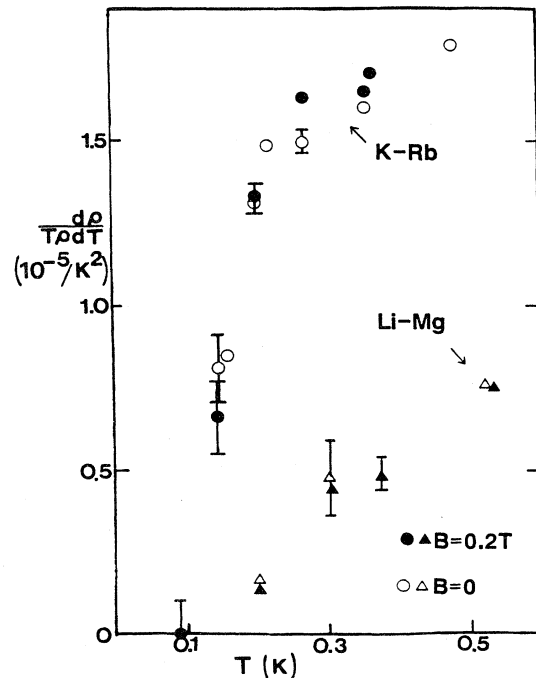

FIG. 75. $(1/\rho T)(d\rho/dT)$ vs T for a K(9.7 at. % Rb) alloy (circles), and a Li(1 at. % Mg) alloy (triangles) for magnetic fields of 0 T (open symbols) and 0.2 T (solid symbols). After Bass et al., 1986.

uncertainty.

Two models have been proposed to explain the anomalous behavior of the data below $\rho_0 = 10^{-7}$ Ω m. (1) Kaveh and Wiser (1987) have argued that the source of the anomaly is the ineffectiveness of long-wavelength phonons in scattering electrons. Adopting the criterion originally introduced by Pippard (1955) to explain the anomalous skin effect, they were able to fit the experimental data approximately for dilute KRb samples using one adjustable parameter, as shown by the dashed curves in Fig. 76. However, application of this same model using the same parameter to data for dilute KNa and LiMg alloys yielded (Zhao et al., 1989) less satisfactory agreement with experiment, as illustrated for LiMg in Fig. 77. These agreements could be improved by varying the adjustable parameter separately for each alloy. (2) Hu and Overhauser (1985; see also Hu, 1987) have recently argued that this anomaly results from the fact that a CDW ground state in K leads to vertex corrections due to the electron-phason interaction. They took the Fermi surface of K in the presence of a CDW to be approximated mostly by a sphere, but also with a small cylindrical portion. Assuming a random distribution of CDW domain orientations, they were able to fit the KRb data semi-
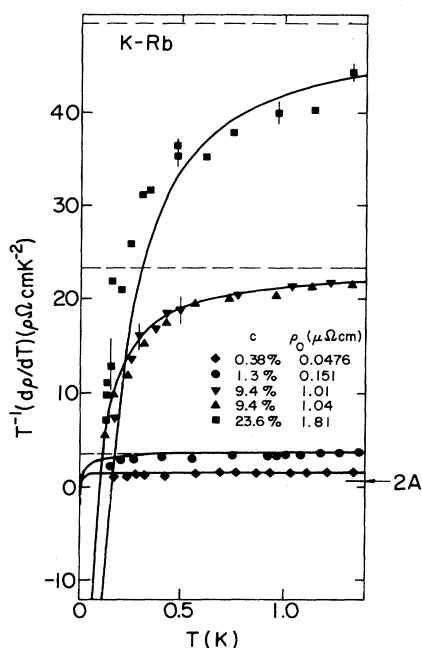

FIG. 77. $(1/T)(d\rho/dT)$ vs T for three LiMg alloys. The solid curves are fits with the Pippard ineffectiveness-condition analysis of Kaveh and Wiser (1987) as discussed in the text. The arrows indicate the data to which each curve is fit. The dashed curves show the addition to these fits of the electron-electron interaction term, Eq. (24b). After Zhao et al., 1989.

quantitatively with a one-parameter fit. However, the fit drops off a bit too rapidly with decreasing temperatures at high temperatures, and appears to saturate in value at low temperatures, whereas the anomaly seems to diverge. Both of these models warrant further theoretical analysis. Explanations based upon a Kondo effect, or upon two-level systems (see, for example, Cochrane and Strom-Olsen, 1984; Harris and Strom-Olsen, 1983), do not appear promising (Zhao et al., 1989).

G. Pure, bulk potassium: simple consistent behavior

1. Rationale and overview

We have seen in Secs. IV.B–IV.D that anomalies in $d\rho/dT$ appear at temperatures below about 1 K in high-purity K samples when they are (1) thinned in the presence of surface contamination; (2) touched by polyethylene; and (3) deformed. Thus, if we wish to determine the behavior of pure bulk K samples, we must examine only samples that are free from such anomalies or in which the anomalies are small enough to be neglected. Once we establish which samples can be safely examined, we want to use these samples to determine the range of variation of the magnitude of the AT^2 term in $\rho(T)$.

In this section, we first examine all available data on undeformed, high-purity, bulk, free-hanging samples of K. These come from studies by the MSU group and by van Vucht et al. (1982). We shall find that the AT^2 components for these samples fall in the range $1.9 \le A \le 3.1$ fΩ m/K^2, with a largest value only about 60% greater than the smallest value. This percentage variation is an

FIG. 76. $(1/T)(d\rho/dT)$ vs T for KRb alloys with four different Rb concentrations from Bass et al., 1986. The solid curves give the theoretical values for each alloy based upon the Pippard ineffectiveness-condition analysis of Kaveh and Wiser (1987). The dashed lines indicate the behavior expected in the absence of any "alloy anomaly." The contribution due to electron-electron scattering is indicated by the arrow labeled $2A$. After Kaveh and Wiser, 1987.
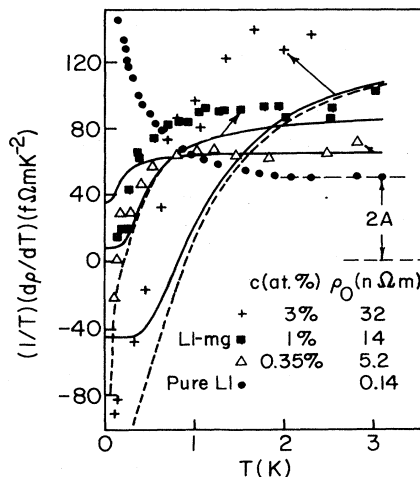
order of magnitude smaller than the 700% change over the range $0.5 \leq A \leq 4$ fΩ m/K^2 associated by Kaveh and Wiser and Bishop and Overhauser with variations in A_{ee} for pure K. And this 60% variation is an overestimate, since the highest values of A are those of van Vucht et al., which were derived by extrapolation from higher-temperature data and are thus uncertain to several tenths of a fΩ m/K^2. We shall show that values of A_{ee} for data from van Kempen et al. Rowlands et al., and Levy et al. that are chosen to match criteria necessary to keep the anomalies small also fall mostly in this smaller range. We shall conclude that we can isolate reliable values of A_{ee} for K. The best value, $A_{ee} = 2.1 \pm 0.3$ fΩ m/K^2 (see Table II), will be obtained using only the MSU data, since these have much the smallest uncertainties. Here, the difference between the largest and smallest values is only $\simeq 30\%$.

2. Detailed analysis

We first analyze all data on undeformed, high-purity, bulk, free-hanging K samples. This includes all of the data from the MSU group on free-hanging, high-purity K samples with $d > 1$ mm that were never deformed, and similar samples before deformation and after room-temperature annealing. It also includes all of the data of van Vucht et al. (1982) on free-hanging samples with $d = 3$ mm before deformation and after room-temperature annealing.

Because we know that impurities increase the T^2 coefficient A due to inelastic impurity scattering, we need to distinguish between values of A measured on samples
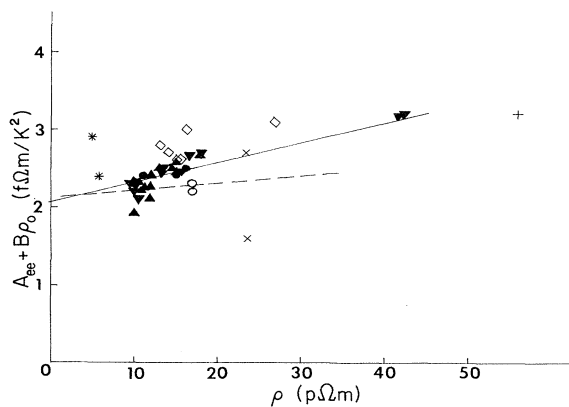

FIG. 78. The inferred T^2 coefficients A_{ee} from a variety of sources vs ρ_0. The filled symbols ($\blacktriangledown$, Zhao et al., 1988; $\blacktriangle$, Yu et al., 1989; $\bullet$, Lee et al., 1982) and open diamonds (van Vucht et al., 1982) are for data on bare, free-hanging samples with diameters ≥ 1.0 mm. The open circles (Lee et al., 1982) are for bare free-hanging samples in Ar gas with $d = 0.9$ mm. The stick symbols ($*$, Levy et al., 1979; $+$, Rowlands et al., 1978; $\times$, van Kempen et al., 1976) are for other samples with diameters ≤ 1.0 mm, either bare or encased in polyethylene.

with different values of ρ_0 (i.e., different RRR's). We do this by plotting the values of A against ρ_0 and seeing whether they increase linearly with increasing ρ_0 in a manner generally consistent with known values of A_{iei} for different impurities (see Sec. IV.E). Figure 78 shows as filled symbols all of the data for free-hanging samples with $d \geq 1$ mm. We see that these data fall along a single line, with some scatter. Taking the region of the highest-purity samples ($\rho_0 \simeq 10$ pΩ m), we see that the values of A all fall between $1.9 \leq A \leq 3.1$ fΩ m/K^2. Although the spread of these values for A is not negligible, it is very much smaller than the range $0.5 \leq A_{ee} \leq 4$ fΩ m/K^2 assumed by Kaveh and Wiser for developing their anisotropic scattering model. Before deriving a "best value" for A_{ee}, we consider additional data that might be close to that for pure K.

Because of the three anomalies listed at the start of this section, it seems clear that most of the data from other laboratories (i.e., van Kempen et al., Rowlands et al., and Levy et al.) are not representative of the behavior of pure bulk K. It might be, however, that some of these data are not far from that for pure bulk K.

The data of van Kempen et al., Rowlands et al., and Levy et al., were all taken on samples with 0.8 mm $< d < 1.0$ mm. If we are to include any of these data, then to be consistent we must also include all data from the MSU group with $d = 0.9$ mm that are not known to manifest a size effect—i.e., data taken in Ar (Lee et al., 1982). We shall plot data for $d \leq 1$ mm as open or line symbols, so that they can be clearly distinguished from the thick-sample data.

For samples encased in plastic tubing, the studies of Yu et al. (1989) indicate that it takes time for the tubing to produce a large Kondo-like effect. We thus plot data of van Kempen et al. and Levy et al. only for samples as initially prepared.

For thin samples, the data of Yu (1984) and Zhao et al. (1989) indicate that adding impurities reduces the size-effect anomaly. From the data of Rowlands et al. we thus plot only the initially prepared sample with a RRR of only 1500.

These are the only samples of van Kempen et al., Levy et al., and Rowlands et al. that have a reasonable chance of being only weakly affected by perturbations.

We see from Fig. 78 that the open and stick symbols scatter around the filled symbols. Although we shall not use the open and stick data in our final analysis, their general agreement with the most reliable results strengthens our confidence that we can correctly specify and isolate the conditions necessary to produce behavior representative of pure bulk K.

We see also that the data of Fig. 78 are compatible with a linear increase with ρ_0, although the magnitude of this increase is highly uncertain. The slope of the dashed line indicates the average of the approximate increases found for Rb and Na impurities (Sec. IV.E).

To determine a best estimate for A_{ee} in K, we limit ourselves to data from the MSU group, since the uncer-

tainties in the T^2 coefficients of all of the other data are much larger due to the limited temperature ranges over which that component could be observed. A simple extrapolation of the thick-sample MSU data in Fig. 78 to $\rho_0=0$ (solid line) yields $A_{ee}(\rho_0=0)=2.1\pm0.3$ fΩ m/K^2, where the uncertainty corresponds to the maximum range of values compatible with any plausible straight-line fit. This range is only about 30% of the chosen "best estimate" for $A_{ee}(\rho_0=0)$. We note that this variation is not much larger than the 10% variation seen in A_{ee} for Al (Ribot et al., 1979, 1981), which manifests none of the recently discovered exotic anomalies that complicate the behavior of K.

If we examine the data of Yu et al. and Lee et al. for pure K collected together in Fig. 27, we see that there is a possible correlation between the magnitude of the horizontal line through each set of data and the size of the anomaly below about 0.3 K; the largest values of A_{ee} are associated with the largest anomalies, and the smallest values of A_{ee} with the smallest anomalies. We therefore checked to see whether correction for the anomaly would reduce the range of values of A_{ee} in the experimental data. Of the two fits proposed by Lee et al. (1982) for the anomalous term—i.e., $\rho_{anom}(T)=B \ln T$ or $BT^{-0.3}$— we found that the $\ln T$ form fit the data of Yu et al. much better and that it produced no significant change from the coefficients A derived simply from the horizontal portions of the data in Fig. 27. This fitting procedure thus led to no significant change in the best estimate of A_{ee} given just above. We note that some of the variation in Fig. 27 is due simply to differences in the ρ_{iei} contribution to $\rho(T)$ for samples with different values of ρ_0.

From Fig. 78 and this subsequent analysis, we conclude that the behavior of A for high-purity, unperturbed, bulk K is not very different for all published studies, when care is taken to eliminate the various anomalies that are now known to be present and to correct for the small amounts of inelastic impurity scattering due to residual impurities.

When the extrapolated values for A_{ee} found from the MSU data in Fig. 78 are combined with the narrow range of values found for extrapolation to $\rho_0=0$ of the dilute KRb alloy data described in Sec. IV.E just above, they demonstrate a heartening internal consistency. This consistency argues strongly against the need for either the KW model, with its sensitivity to the presence of anisotropic scatterers, or the CDW model, with its sensitivity to details of the orientations of CDW domains, to explain the behavior of A in pure bulk unconstrained K.

V. COMPARISONS BETWEEN VARIOUS MODELS AND EXPERIMENTAL DATA

With the experimental data now all in hand, we are ready to examine how well the proposed Kaveh-Wiser (KW) and Bishop-Lawrence (BL) models for the behavior of $\rho(T)$ in K below 1.3 K are able to describe the new data, and to explain how we interpret the older data.

A. The Kaveh-Wiser model versus the new data

The KW model involving anisotropic scattering due to residual extended defects such as dislocations was developed to explain the changes by up to a factor of 5 in the values of $\rho(T)$ in K in the vicinity of 1 K reported by van Kempen et al. (Sec. III.D.1), Rowlands et al. (Sec. III.D.2), and Levy et al. (Sec. III.D.5). The model assumes that the behavior reported is due to changes in the T^2 electron-electron scattering coefficient A_{ee} and that the behavior is characteristic of pure bulk K subject to no perturbations except those involving defect concentrations that are unavoidable in sample preparation. The essential parameter in the model is the ratio (ρ_{0i}/ρ_{0d}) of the impurity residual resistivity ρ_{0i} to the dislocation residual resistivity ρ_{0d}. The model predicts that adding impurities to a sample that is not already in the KW "isotropic limit" $(\rho_{0i}\gg\rho_{0d})$ will decrease A_{ee}, and adding dislocations to a sample not in the KW "anisotropic limit" $(\rho_{0d}\gg\rho_{0i})$ will increase A_{ee}.

The new data have shown the following.

(1) (Sec. IV.B) Encapsulation of K in the polyethylene tubing that both van Kempen et al. and Levy et al. used to protect their samples produces a complex anomaly in $\rho(T)$, one characteristic of which is exactly the kind of increasingly large reductions in $\rho(T)$ in the vicinity of 1 K seen by van Kempen et al. and Levy et al. as their samples spent increasing time at room temperature.

(2) (Secs. III.H and IV.C) High-purity K wires exposed to surface contamination show complex "size effects" when their diameters become as small as those studied by Rowlands et al., and the Rowlands et al. data have the same form as these size effects and display the same decreases in $d\rho/dT$ with increasing sample purity.

(3) (Sec. IV.G) High-purity K samples free from these two anomalies display T^2 coefficients A_{ee} that vary not by a factor of 5, but only by $\simeq30\%$.

(4) (Sec. IV.E) Adding dilute concentrations of impurities to K or Li samples that are near the KW "anisotropic limit" causes an increase in the T^2 coefficients, rather than the decrease predicted by the KW model, and the alloy data extrapolate directly back to the measured pure-metal coefficients, rather than to the very different "isotropic limit" values predicted by Kaveh and Wiser.

(5) (Secs. III.G and IV.D) While deformation of K wires does cause $\rho(T)$ in the vicinity of 1 K to increase, these increases are much larger than predicted by the KW model and have a much more complex form than simply T^2. Moreover, in contradiction to the KW model, when T^2 coefficients are included in the fit to these data, they exhibit little or no change as the dislocation density increases.

(6) (Sec. III.G) Also in contradiction to the KW model, deformation of K and KRb alloys produces very similar changes in $\rho(T)$, even though the ratio ρ_{0i}/ρ_{0d} changes by a large amount in the K samples but only by a small amount in the KRb alloys.

Items (4), (5), and (6) are incompatible with the KW model. Items (1) and (2) provide an alternative explanation for the effects seen by Kaveh and Wiser, Rowlands *et al.*, and Levy *et al.* in terms of extrinsic phenomena that are now known to be present in K samples subjected to the two perturbations described. Item (3) indicates that there is no need for the KW model in K. However, the small residual variations in A_{ee} for K mean that the KW model cannot be absolutely ruled out at the uncertainty level for A_{ee} of $\pm 15\%$.

B. The CDW-based model versus the new data

The CDW-based model begun by Bishop and Overhauser (Sec. III.D.4) and extended by Bishop and Lawrence (Sec. III.J) was developed to explain the facts that (a) the data of Rowlands *et al.* (Sec. III.D.2) were fit better by a $T^{3/2}$ form than by T^2; (b) the data of van Kempen *et al.* (Sec. III.D.1) and Levy *et al.* (Sec. III.D.5) appeared to vary as T^2; and (c) the coefficients of all three sets of data varied substantially, by up to a factor of 5. This model assumed that these behaviors were characteristic of pure K with a CDW ground state. The form of the Rowlands *et al.* data was attributed to domination of $\rho(T)$ by electron-phason scattering. The large variations in the coefficients of all three sets of data were ascribed to the fact that both the electron-phason and electron-electron scattering contributions to $\rho(T)$ were strong functions of the orientation of CDW domains. All of the samples were assumed to contain many CDW domains, the orientations of which were changed by handling or simply by annealing at room temperature.

The new data have shown the following.

(1) (Secs. III.H and IV.C) High-purity K wires exposed to surface contamination show complex size effects when their diameters become as small as those studied by Rowlands *et al.*, and the Rowlands *et al.* data have the same form as these size effects and display the same decreases in $d\rho/dT$ with increasing sample purity. The form of $\rho(T)$ for these size effects is not the one predicted by the Bishop and Overhauser model.

(2) (Sec. IV.B) Encapsulation of K in the polyethylene tubing that both van Kempen *et al.* and Levy *et al.* used to protect their samples produces a complex anomaly in $\rho(T)$, one characteristic of which is exactly the kind of increasingly large reductions in $\rho(T)$ in the vicinity of 1 K seen by van Kempen *et al.* and Levy *et al.* as their samples spent increasing time at room temperature.

(3) (Sec. IV.G) High-purity K samples free from these two anomalies display T^2 coefficients A_{ee} that vary not by a factor of 5, but only by $\simeq 30\%$.

(4) (Sec. IV.E) Adding dilute concentrations c of impurities to either K or Li simply causes $\rho(T)$ to increase linearly with c, at a rate compatible with simple inelastic electron-impurity scattering, ρ_{iei} (Sec. I.D.3.a).

Items (3) and (4) are incompatible with a CDW-based explanation in which the magnitude of $\rho(T)$ in the vicinity of 1 K is highly sensitive to a CDW domain structure

that changes substantially as samples are handled or held at room temperature. Items (1) and (2) provide alternative explanations for the behavior observed by van Kempen *et al.*, Rowlands *et al.*, and Levy *et al.* in terms of extrinsic effects that are now known to be present in K samples subjected to the respective perturbations described. Item (3) indicates that there is no need in pure K for the sensitivity to CDW domain structure of the CDW-based model. But if one wishes to include a less sensitive CDW-based behavior in pure K, the small residual variations in A_{ee} for K mean that such a model cannot be ruled out at the uncertainty level for A_{ee} of $\pm 15\%$.

C. How we interpret other people's data

A summary of our picture of how all of the published data can be understood will be given in Sec. VI. This picture was developed to take account of complex behaviors due to size effects (Sec. IV.C); prolonged contact with polyethylene (Sec. IV.B); deformation (Sec. IV.D); concentrated alloy anomalies (Sec. IV.F); and phonon drag and quenching of phonon drag. In this section we examine in detail how this picture can explain the data in every paper published by a group other than our own. Since none of the data in those papers extended to below 0.5 K, and none pertained to alloys, we need invoke only the following phenomena: (a) phonon drag in $\rho_{ep}(T)$; (b) the constant values of A_{ee} for K, Li, and Na; (c) the size-effect anomaly in K; (d) the Kondo-like anomaly due to contact of K with polyethylene; and (e) the anomaly in deformed K. Our explanations for each data set follows.

(1) Gugan (1971) and Ekin and Maxfield (1971). The data of Gugan (1971) and Ekin and Maxfield (1971; see Sec. III.B.2) are so similar that we consider them together. Only $\rho_{ep}(T)$ is involved, since their values of $\rho(T)$ extend down to only about 2 K. For high-purity samples of K, $\rho(T)$ is dominated by $\rho_{Uep}(T)$, which may be reduced somewhat from the Bloch limit at the lowest of their temperatures by phonon drag. Neither the amount of phonon drag present above 2 K nor how it varies with temperature is clear. For less pure samples, the fractional DMR, $\delta(T)$—defined in Sec. III.B.2—is small and has a form similar to that of $\rho_{ep}(T)$. Above about 4 K, this $\delta(T)$ is compatible simply with the DMR expected from anisotropy and energy dependence of Φ_k. However, it might also involve a small amount of quenching of phonon drag in $\rho_{Uep}(T)$. Rapidly cooled high-purity samples probably contain mostly impurities in solution, and their DMR are compatible with those for impure samples. Samples subject to deformation initially contain roughly equal contributions to ρ_0 from point defects and dislocations. An explanation of the $\delta(T)$ for these samples requires either partial quenching of phonon drag in both $\rho_{Uep}(T)$ and $\rho_{Nep}(T)$ or some other mechanism for DMR. Below about 2.5 K, scattering of electrons from vibrating dislocations may also play a role—see the data of Haerle *et al.* in Sec. IV.C.

(2) Krill (1971). In the data of Krill (1971) on pure Li above 2 K (Sec. III.B.2); the high Θ_D for Li means that we can neglect $\rho_{ep}(T)$. From 10 K down to 4 K, the data vary as T^2. We attribute this behavior to simple electron-electron scattering. The fact that the observed value of $A_{ee} \simeq 33$ fΩ m/K^2 is almost ten times larger than the best prediction for bcc Li makes it necessary to assume either that the calculation is incorrect or that this value is representative of the complex $9R$ structure to which Li transforms upon cooling below about 75 K. Both of these alternatives are compatible with the fact that the coefficients of the T^2 terms in LiMg alloys extrapolate nicely to the T^2 coefficient for pure Li. We prefer the latter alternative, both because of the good agreement of the calculated A_{ee} for K with the experiment data, as discussed in Sec. IV.F, and because we think it unlikely that the calculation is an order of magnitude off for bcc Li.

(3) Van Kempen et al. (1976, 1981). Van Kempen et al. studied K samples with $d = 0.9$ mm encased in polyethylene tubes at temperatures between 4.2 and 1.1 K (Sec. III.D.1). We attribute the relatively high values of ρ_0 seen in initially prepared samples, and the subsequent slow decrease of these ρ_0's over months, to the retention and slow annealing out of defects in the K because of the constraint imposed by the polyethylene sheath. The nature of these defects is not known, but they probably involve a combination of grain boundaries, impurities in solution, and perhaps some dissolved gases.

Van Kempen et al.'s values of $\rho_{ep}(T)$ for slowly cooled samples of both pure and impure K are in excellent agreement with the data of Gugan and of Ekin and Maxfield, and are interpreted in the same way. We attribute a much higher $\rho_{ep}(T)$ found in one rapidly quenched sample to quenching of phonon drag by a combination of point defects (mostly impurities retained in solution) and dislocations produced by the rapid cooling. Van Kempen et al. reported that if they assumed that the $\rho(T)$ for their samples contained a component that varied exactly as T^2, then they found no evidence of any T^5 component in $\rho_{ep}(T)$ for any of their samples. We attribute their failure to see at least a small T^5 component in the rapidly cooled sample to the failure of this assumption of T^2 behavior, as we discuss next.

Below about 1.5 K, van Kempen et al found strong deviations from the exponential behavior of $\rho_{ep}(T)$. Their data do not extend to low enough temperatures to define accurately the form of these deviations. We assume that, since the samples of van Kempen et al. were solidifed in polyethylene tubing, they must manifest the Kondo-like anomaly described above. We infer that their low-temperature deviations in $\rho(T)$ from exponential form do not vary exactly as T^2. We attribute the first values of A_{ee} measured by van Kempen et al. on a given sample to simple electron-electron scattering in K, which is dominant before the Kondo-like anomaly becomes significant. The decreases in $d\rho/dT$ that then occur with increasing holding time at room temperature are attributed primari-

ly to increasing development of the Kondo-like anomaly, with some contribution from a decrease in inelastic impurity scattering as ρ_0 decreases. We note, however, that we have not been able to reproduce experimentally the full magnitude of the decreases seen by van Kempen et al. A small size-effect anomaly could also be present if surface contamination is not essential for the appearance of this anomaly.

(4) Rowlands et al. (1978). Rowlands et al.'s measurements of K extended from 4.2 to 0.5 K (Sec. III.D.2). Their samples were $d = 0.8$ mm wires, wound around grooved Teflon holders and cooled in He gas. We attribute the high values of ρ_0 seen in samples when first cooled to 4 K to defects (mostly impurities in solution) retained in the sample during cooling, perhaps due to a constraint imposed upon the sample by the Teflon holder; although, since Teflon contracts more than K upon cooling, the nature of any such constraint is not clear. We attribute the decrease in ρ_0 with holding time at room temperature to slow annealing away of these defects.

Rowland et al's data for $\rho_{ep}(T)$ are compatible with everyone else's for pure K and are interpreted similarly.

We attribute the approximately $T^{3/2}$ form of $\rho(T)$ for their data below 1.5 K primarily to the size-effect anomaly in the presence of surface contamination; Rowlands et al. reported evidence of some surface contamination in their samples. This attribution accounts directly for both the form and the magnitude of the data. Since the size-effect anomaly decreases with decreasing bulk electron mean free path, it also accounts for most of the decrease in magnitude of $\rho(T)$ as ρ_0 decreases. The rest of the decrease in $\rho(T)$ is ascribed to reduction in inelastic impurity scattering as ρ_0 decreases.

(5) Levy et al. (1979). Levy et al. studied samples of $d = 0.9$ mm K and Na encased in polyethylene tubing, at temperatures from 4.2 to 1.1 K (Sec. III.D.5). They observed behaviors of $\rho_{ep}(T)$ and A_{ee} in Na compatible with the same simple models of electron-phonon and electron-electron scattering that we have proposed for K. Their reported value of A_{ee} for Na is probably only an upper bound, the value of which is compatible with the best available theory.

Levy et al.'s data for $\rho_{ep}(T)$ in K are similar to everyone else's and are interpreted in the same way.

Levy et al.'s data for K below 1.5 K did not extend to low enough temperatures to define their temperature dependence accurately. We assume that most of the data of Levy et al. did not vary exactly as T^2, due to the combined presence of Kondo-like and possible size-effect anomalies. Samples as initially prepared had values of A_{ee} compatible with simple electron-electron scattering in high-purity K. We assume that neither anomaly was yet fully developed. Given the high RRR's of these samples as initially prepared, there is some weakness in this assumption concerning the size effect, since the high RRR's combined with any surface contamination would normally have been expected to lead to fairly sizable

size-effect anomalies. The samples were then heated to produce white contamination on their surfaces. In some cases, this contamination was rolled into the body of the sample. We would expect heating of the sample to increase the rapidity of development of the Kondo-like anomaly, and production of white contamination on the surface of a $d = 1$ mm sample to both thin the sample and then help produce a significant size-effect anomaly in this thinner sample. We presume that the combination of these two effects, each of which acts to reduce the magnitude of $\rho(T)$, was responsible for the large decreases in $\rho(T)$ seen by Levy et al. in the vicinity of 1 K as they contaminated their samples. Given the very low initial ρ_0's of their samples, we would expect these two effects to dominate the small increases in A_{ee} due to increases in inelastic impurity scattering as ρ_0 increased. The main weakness we see in this interpretation is that it does not naturally produce the approximately linear variation of the nominal A_{ee} component with $(\rho_0)^{-2}$ found by Levy et al. It is, of course, compatible with such a variation.

(6) Sinvani et al. (1981). Sinvani et al. studied Li from 4.2 to 1.1 K (Sec. III.D.8). Their data are explained in the same way as the Krill data. Their value of $A_{ee} = 30$ fΩ m/K^2 is consistent with Krill's value to within mutual uncertainties.

(7) Van Vucht et al. (1982, 1986)). Van Vucht et al. studied twisted K and KRb at temperatures from 4.2 to 0.9 K (Secs. III.G.1 and IV.D.1). Above 1.5 K, they found deformation-induced increases in $\rho(T)$ generally compatible in magnitude with those found by Gugan for strained samples. We explain these increases in the same way as we explained Gugan's. There are two not completely resolved questions: (1) why van Vucht et al. found values of $\rho(T)$ in the vicinity of 4 K for unstrained samples that were smaller than everyone else's; and (2) why they seemed to find no T^5 component in the vicinity of 1–2 K. We have no answer to the first question. We presume that the answer to the second is that their choice of a simple T^2 fit for the contribution to $\rho(T)$ below 1 K is incorrect. We argued in Sec. IV.C that the data of Haerle et al. and of Yin on strained K taken to lower temperatures show that the actual form of $\rho(T)$ in the vicinity of 1 K is more complex than T^2. We must note, however, that van Vucht et al. reported that incorporating a vibrating dislocation term did not improve the fit to their data.

Below 1.5 K, van Vucht et al. reported finding T^2 components of $\rho(T)$ with coefficients that were large and increased with increasing deformation. We attribute the observed behavior not to T^2 components, but rather to the more complex behavior associated with the scattering of electrons from vibrating dislocations. Our picture naturally explains two observations by van Vucht et al.— and also by Haerle et al. and Yin et al.—that are puzzles for the KW model that van Vucht et al. adopted, namely, (a) that $\rho(T)$ increases by about the same amount for similar concentration of defects introduced into K

and KRb by deformation; and (b) that annealing out of point defects causes $\rho(T)$ in the vicinity of 1 K to decrease. For the KW model, changes in anisotropy of scattering as the relative concentrations of point and line defects changes require that the changes in $\rho(T)$ should be much smaller in the KRb than in the K and that $\rho(T)$ should increase as point defects anneal away and leave a larger percentage of the total elastic scattering to be due to dislocations. For our picture, the defects are the same in K and KRb and should produce very similar effects: The annealing away of vacancies removes scatterers, thereby reducing $\rho_{iei}(T)$ and thus $\rho(T)$, and also reduces $\rho(T)$ near 1 K via the change in type of scattering, as discussed in Sec. IV.D.2.c.

VI. SUMMARY, CONCLUSIONS, AND SUGGESTIONS FOR ADDITIONAL STUDIES

In this section, we summarize the contributions to $\rho(T)$ that have been observed in both pure and perturbed alkali metals and their alloys, describe what we know about these contributions, and indicate the additional experimental and theoretical work that is still needed to clarify items that remain obscure. We first briefly summarize the components and then consider each one in more detail. In the more detailed analyses, we list for each specific item the section(s) where that item is discussed.

It is useful to separate samples into three different categories: (a) pure, bulk samples (Secs. I.D.1 and I.D.2); (b) alloys (Sec. I.D.3); and (c) samples subjected to perturbations (Sec. I.D.4). For the pure bulk samples, $\rho(T)$ is dominated at high temperatures by $\rho_{ep}(T)$, at intermediate temperatures by $\rho_{ee}(T)$, and at the lowest temperatures by a "very-low-temperature anomaly," which might not be intrinsic to the pure samples. We discuss each item separately. For the alloys we distinguish between dilute alloys for which we examine $\rho_{iei}(T)$, more concentrated alloys for which we examine a not-yet-understood anomaly, and very concentrated alloys for which the data appear to approach the expectation for electron-electron interactions in the presence of substantial disorder. The perturbations of interest apply primarily to K. They involve (1) thin K wires and films; (2) contact of K and KRb with polyethylene; and (3) deformation of K and KRb.

A. Pure, bulk samples

1. Electron-phonon scattering $\rho_{ep}(T)$

(a) $T \geq 20$ K (Sec. III.B.1). Calculations of $\rho_{ep}(T)$ for K and Na based upon free-electron Fermi surfaces, and with no adjustable parameters, agree with the experimental data to within a few percent over the entire temperature range. We thus conclude that $\rho_{ep}(T)$ in these metals is well understood down to at least 20 K, with no need to

invoke the presence of CDW's. The situation in Li and Rb is less clear at high temperatures, since the disagreement between theory and experiment is as large as 50%, but it is presumed to be due primarily to Debye-Waller and multiphonon effects that were not included in the calculations and that nearly canceled in K and Na.

(b) $20 \text{ K} \geq T \geq 4$ K. Between 20 and $\simeq 4$ K, the most detailed calculations are for K (Sec. III.B.3), and the two published calculations are contradictory. One fits the K data to within about 10% with no adjustable parameters and no phonon drag. The other gives an equally good fit with one adjustable parameter and phonon drag that is very large at 4 K and does not disappear until above 20 K. The issue of how much phonon drag is present in K at temperatures between 20 and 4 K can only be resolved by a more realistic self-consistent treatment of electron-phonon and phonon-phonon scattering acting simultaneously. For Rb, the fit in this range is fair for a calculation that does not take into account distortions of the Fermi surface from a sphere, possible phonon drag, etc. For Na the agreement is also reasonable given its phase transition and neglected factors in the calculation. For Li, the combination of a phase transition with strong effects of electron-electron scattering up to about 10 K makes a detailed comparison with theory for electron-phonon scattering difficult.

(c) $T \leq 4$ K. For K (Secs. III.B.3, III.D.3, III.G.2, IV.D, and IV.E), the experimental data on pure K, deformed K, and dilute K-based alloys all clearly require the presence of substantial phonon drag up to at least 2.5 K. The main problem at these temperatures is to explain how impurities and dislocations can quench phonon drag strongly enough to produce the increases in $\rho_{ep}(T)$ found when these defects are added to K.

For Na (Sec. III.F), comparison between theory and experiment from 4 to 1 K suggests the possibility of significant phonon drag, but a more realistic calculation is needed before a definitive conclusion can be reached. For Rb (Sec. III.F), the data at the lowest temperatures are much larger than predicted, suggesting that calculational improvements are needed here too—especially taking into account distortions of the Fermi surface from spherical.

2. Electron-electron scattering $\rho_{ee}(T)$

(a) Li (Secs. III.B.2, III.D.8, III.D.9, and IV.E). Because of the unusually high Debye temperature of Li, $\rho_{ee}(T)$ dominates $\rho(T)$ to above 10 K. A_{ee} in Li is nearly constant from sample to sample, and data on LiMg alloys extrapolate nicely to the pure-metal value given in Table II. These two facts indicate that there is only a single value of A_{ee} in the Li samples studied to date. The best available calculation of $\rho_{ee}(T)$ for Li is an order of magnitude smaller than this value. This disagreement is attributed to the fact that the calculation was made for the bcc phase of Li, rather than for the $9R$ phase, which is already dominant by 10 K. A calculation of $\rho_{ee}(T)$ for the

$9R$ phase of Li is needed to validate this attribution.

(b) K (Secs. III.D.1,2,4,5,6,9, III.E, and IV.G). In K, $\rho_{ee}(T)$ becomes dominant below about 1 K, where phonon drag has eliminated $\rho_{ep}(T)$. When care is taken to remove the effects of the recently discovered perturbations described in this review, A_{ee} in pure K is found to have the nearly constant value given in Table II; data on dilute alloys extrapolate nicely to this same value, and the value agrees with the best calculation to within 30%, well within the factor of 2 uncertainty in the calculation. There is no need for either the KW model of effects of anisotropic scattering on $\rho_{ee}(T)$ or a CDW-based model to explain A_{ee} in pure bulk K.

(c) Na and Rb (Sec. III.F). For both of these metals, we can derive only upper bounds on A_{ee}. For Na, the difficulty results from a crystallographic phase transition upon cooling, coupled with a large very-low-temperature anomaly. For Rb, the difficult results from a very low Debye temperature combined with a large very-low-temperature anomaly. For both metals, the upper bounds on A_{ee} are consistent with the best available calculations (see Table II).

3. Very-low-temperature anomaly

High-purity samples of K, Li, Na, and Rb all show anomalous behaviors in $\rho(T)$ at the very lowest temperatures (Secs. III.E and III.F). The magnitudes of these anomalies vary from sample to sample. Their forms are compatible with what is seen (Sec. IV.D) in deformed samples containing extended defects. It thus seems plausible that they result from residual extended defects in the samples. More data are needed below 1 K on K samples handled with special care, as well as with still lower values of ρ_0, to see whether the anomaly below 0.3 K becomes smaller as the sample becomes purer and more defect free. In particular, data on single crystals would eliminate any effects due to grain boundaries. For Li and Na, data on samples with controlled amounts of the bcc and $9R$ phases would be very desirable.

B. Alloys

1. Dilute K- and Li-based alloys

As dilute concentrations of impurities are added to either K or Li, $\rho(T)$ increases as $A_I \rho_0 T^2$ (Secs. III.E and IV.E), with coefficients A_I in good agreement with calculations of $\rho_{iei}(T)$ due to inelastic electron-impurity scattering (Sec. I.D.3 and Table III). The behavior of $\rho_{iei}(T)$ in dilute alkali metal alloys thus appears to be well understood. A proposed contribution due to many-body effects (Secs. I.D.3 and IV.E) requires further analysis.

The addition of impurities to K also causes the magnitude of $\rho(T)$ to increase by an additional amount above 1 K (Sec. IV.E). This additional increase is most easily attributed to quenching of phonon drag, but no calcula-

tions yet show how point defects could produce such large quenching. Taylor's (1989) suggestion that the strain fields of impurities having different sizes than the host atoms could scatter phonons and thereby partially quench phonon drag should be studied quantitatively.

2. More concentrated alloys

As K- and Li-based alloys become more concentrated, two phenomena appear that are not yet adequately understood (Sec. IV.F).

First, in K-based alloys above 1 K, increasing impurity content causes $\rho(T)$ to grow too large for the increase to be due solely to quenching of phonon drag. In KRb alloys this growth can be attributed to decreases in the Debye temperature upon alloying; such an explanation appears to fail for KNa, where the effects appear to be very similar to those in KRb, but the Debye temperature should increase.

Second, as ρ_0 increases, a very-low-temperature anomaly appears, which varies approximately as $-C\rho_0 T$ and has very similar magnitudes in KRb, KNa, and LiMg alloys. Qualitative (and for KRb even semiquantitative) descriptions of this behavior have been obtained with adjustable parameters by two models: one involving the Pippard ineffectiveness condition for electron-phonon scattering and the other a CDW ground state. Both models require theoretical validation and further study. Alternative explanations may still be needed.

For both phenomena, measurements on additional alloy systems would be helpful, but the most pressing need is for further theoretical analysis.

3. Highly concentrated alloys

For values of $\rho_0 \geq 10^{-7} \Omega$ m, the data appear to approach the behavior expected for the correction to the Boltzmann transport equation associated with electron-electron interactions in the presence of substantial disorder. Additional experimental data would be useful here.

C. Samples subjected to perturbations

1. Thin K wires and films

When K wires are thinned in the presence of surface contamination, there appears a size-effect anomaly, the detailed form and nature of which still remain unclear (Secs. III.H and IV.C). Roughly speaking, in a wire of diameter d the anomaly in $(1/T)(d\rho/dT)$ increases in magnitude as $d^{-1} T^{1/3}$. Several models of this phenomenon have been proposed, but only a few still appear viable. A model of strong localization in thin K wires, with or without a CDW ground state, should be tested via experiments in which larger anomalies are produced on thinner samples with varying lengths. Further

theoretical work is still needed on this model, on new models proposed by Gurzhi et al. (1989), and by Movshovitz and Wiser (1990). Experimental data are needed on very thin K wires with ultra-high-vacuum clean surfaces to see whether the anomaly persists and grows still larger with decreasing wire thickness. Taylor (1989) has suggested that this anomaly might involve inelastic scattering of electrons from oxygen atoms on the sample surface, noting that oxygen is highly polarizable. Controlled studies of surface contamination would be useful.

Measurements of $\rho(T)$ for thin K films so far show no evidence of the thin-wire anomaly. Such a difference is expected for the strong-localization model, since from the point of view of this model, the film is a two-dimensional system, while the wire is one-dimensional. The model by Movshovitz and Wiser also appears to yield no such anomaly in thin films. Much more complete studies of thin films of high-purity K with controlled surface interactions are thus also important. The use of very-high-precision resistivity measurements on thin K films to make controlled studies of scattering of electrons by magnetic impurities or polarizable molecules placed on the film surface could be an exciting extension of such studies.

2. Contact of K and KRb with polyethylene: the Kondo-like anomaly

Placing K or KRb in contact with polyethylene (Secs. III.G.2 and IV.B) leads to a Kondo-like anomaly, consisting of a resistivity minimum, a thermoelectric anomaly, and a strong sensitivity to magnetic fields as small as 0.1 T. The physical source of this anomaly is not yet known. The anomaly does not appear for contact with Teflon or Kel-f. A substantial resistivity minimum has also been seen in thin K films in contact with glass and KF and a much smaller one for contact with Si. It is not yet known whether these latter minima have the same origin as that due to contact with polyethylene. Is the Kondo-like effect a volume or a surface phenomenon? Does it involve magnetic or nonmagnetic interactions? Is it due simply to the presence of a specific impurity or is it a more complex phenomenon? Do the Kondo-like anomalies in ρ in thin K films have associated G anomalies, and are these anomalies affected by a magnetic field as are those for samples in contact with polyethylene? More experiments are needed to answer these questions and give guidance to the theorists.

3. Deformed K and KRb

Above about 1 K in both K and KRb (Secs. III.G and IV.D), deformation causes $\rho(T)$ to increase in a way that seems to require substantial quenching of phonon drag by dislocations. There is not yet unanimity among investigators as to whether a T^5 term appears after deformation, although the preponderance of the evidence is that

it does. There is as yet no adequate understanding of how given concentrations of dislocations can produce the large amounts of apparent quenching of phonon drag that are needed to explain the data. Taylor (1989) has suggested that the simple Klemens (1969) formula used to estimate the strength of phonon-dislocation scattering might underestimate such scattering by one or two orders of magnitude. There is a need for more realistic calculations of both simple phonon-dislocation scattering and of phonon-dislocation scattering in the presence of anisotropic electron-dislocation scattering. In the absence of such calculations, the possibility that some non-standard source of DMR could be present cannot be completely ruled out.

Both above and below 1 K, deformation also produces (Secs. III.G.2 and IV.D) additional complex changes in $\rho(T)$ in K and dilute KRb alloys, most of which can be qualitatively described (Sec. IV.D) in terms of scattering of electrons from vibrating dislocations, or in some cases also from localized electron states on dislocations. But why data in which a substantial number of point defects are present should be described well by the vibrating dislocation model alone, whereas data in which dislocations are dominant require the addition of the localized-states model, is not yet understood. More data are needed on $\rho(T)$ in deformed K under a wider variety of conditions, and to still lower temperatures, to completely characterize the experimental phenomena. More detailed theoretical analyses of both of these scattering mechanisms are also needed, as is an explanation for the very-low-temperature G anomaly that seems to appear in strained K samples. Investigations of whether similar ρ and G anomalies appear in strained Li, Na, and Rb are also needed. We reiterate that K is a unique system for studying the scattering of electrons by dislocations in a bcc metal at temperatures so low that $\rho_{ep}(T)$ is not important.

D. Concluding remarks

We have argued in this review that the behavior of $\rho(T)$ in high-purity, bulk, unperturbed samples of K—and to a large extent also Li, Na, and Rb—is simple and well understood from the melting point down to below 1 K. For K, there is quantitative agreement between theory and experiment with no adjustable parameters down to about 10 K and also from 1 K down to at least 0.3 K. At low temperatures, the behavior of $\rho(T)$ in dilute K- and Li-based alloys also seems to be well understood. The primary questions that remain concerning unperturbed samples of these metals involve (1) the amount of phonon drag that is present at temperatures of several K in K, Rb, and Na; (2) the nature of anomalies at the very lowest temperatures in all four metals; and (3) effects of phase changes on Li and Na and of Fermi-surface distortion in Rb and Li.

In contrast to this simplicity, we have provided clear evidence of the presence of several unexpected anomalies

in K subjected to perturbations due to deformation, adding substantial amounts of impurities, thinning wires in the presence of surface contamination, and placing samples in contact with certain materials—especially polyethylene. Li shows a similar anomaly due to addition of impurities. Our understanding of the physics underlying all of these anomalies is rudimentary at best. A substantial amount of both experimental and theoretical work remains to be done on these anomalies in the resistivities of the alkali metals at very low temperatures, before we can say that these "simplest" metals are completely understood.

ACKNOWLEDGMENTS

APPENDIX A: THEORY BACKGROUND

This appendix is intended to give the reader the essential information needed to understand what is involved in a practical calculation of $\rho(T)$ at low temperatures under various circumstances, so as to be able to evaluate the theoretical contributions described in this review. Further details beyond those given in this appendix can be found in Ziman (1972)—from which much of this appendix is abstracted—and in the specific articles referred to in the text. In this appendix, as in the text, vectors will be written in boldface—i.e., **k**.

All of the calculations we shall describe in this review start from the semiclassical linearized Boltzmann transport equation (LBTE). This equation describes how the out-of-balance electronic distribution function Φ_k—defined in Eq. (A2) below—changes with time under the combined influences of an applied electric field **E** and several different entities that scatter electrons. The scatterers include (a) point and extended defects (primarily impurities and dislocations); (b) phonons (quantized lattice vibrations); and (c) other electrons. In principle,

calculations of $\rho(T)$ involve two fundamental parts: (1) solving the LBTE for Φ_k; and then (2) performing the appropriate multidimensional integral in k-space using this function. In practice, in a metal with a closely spherical Fermi surface, a simple Φ_k [Eq. (A7)] often appears to be adequate for both low and high temperatures.

If the phonon system is not in thermal equilibrium, it is necessary simultaneously to solve a LBTE for the phonon distribution function ψ_q—defined in Eq. (A9) below—and to use this function in the determination of $\rho(T)$.

The single most important point to understand is that no calculations of $\rho(T)$ are truly rigorous and exact. All the calculations we describe involve approximations. The quality of the calculation depends on the quality of these approximations.

1. The Boltzmann transport equation, the linearized Boltzmann transport equation, and Φ_k for electrons

The BTE for electrons describes the time rate of change of the electronic distribution function f_k for an electron in state k under the influence of both external "forces"—such as electric fields and temperature gradients—and scattering processes—designated initially as $-df_k/dt\big|_{\text{scatt}}$. When the only "force" applied is an electric field E, the electronic BTE is

$$\left[\frac{e}{\hbar}\right]E v_k \frac{\partial f_k}{\partial \epsilon_k} = -\frac{\partial f_k}{\partial t}\bigg|_{\text{scatt}} . \tag{A1}$$

In Eq. (A1), e is the electronic charge, $\hbar$ is Planck's constant divided by 2π, $v_k = \nabla_k \epsilon$ is the velocity of the electron in state k, and ϵ_k is the energy of the electron. At thermal equilibrium, $f_k = f_k^0 = 1/(1+\exp\eta)$ is the Fermi-Dirac function with $\eta = (\epsilon - \epsilon_f)/(k_B T)$, T is the absolute temperature, k_B is Boltzmann's constant, and ϵ_f is the Fermi energy of the electrons. f_k^0 changes from its value of 1 below ϵ_f to its value of 0 above ϵ_f over an energy range $\simeq 2 k_B T$. Since the typical ϵ_F for a metal corresponds to a temperature $T_f = \epsilon_f/k_B \simeq 10\,000$ K, only a tiny fraction of the electrons have values of $f_k^0 \neq 1$ or 0.

The combined action of E plus scattering causes f_k to differ from f_k^0. Since the energy that E can give to an electron between scattering events is small compared to ϵ_f, the difference between f_k and f_k^0 is small except very near ϵ_f. It is thus useful to write the deviation of f_k from f_k^0 in the form

$$f_k = f_k^0 - \Phi_k \left[\frac{\partial f_k^0}{\partial \epsilon_k}\right] \tag{A2}$$

and thereby to define the quantity Φ_k as an alternative measure of this deviation. Since $\partial f_k^0/\partial \epsilon_k$ is strongly peaked at ϵ_f, Φ_k is generally a smoother function than f_k in the vicinity of ϵ_f.

If we write the scattering terms explicitly in terms of Φ_k, and drop all terms on both sides of the resulting equation that are of higher order than linear in Φ_k, we obtain an inhomogeneous, integro-differential equation for Φ_k called the linearized Boltzmann transport equation (LBTE),

$$e v_k \cdot E \Phi_k = \frac{1}{k_B T} \int (\Phi_k - \Phi_{k'}) p_k^{k'} d k' ,$$

$$+ \frac{1}{k_B T} \int \int (\Phi_k + \Phi_q - \Phi_{k'}) p_{k,q}^{k'} d k' d q + \frac{1}{kT} \int \int (\Phi_k - \Phi_q - \Phi_{k'}) p_k^{q k'} d k' d q ,$$

$$+ \frac{1}{k_B T} \int \int \int (\Phi_k + \Phi_{k''} - \Phi_{k'} - \Phi_{k'''}) P_{k,k''}^{k',k'''} d k' d k'' d k''' \tag{A3}$$

Here $P_k^{k'}$ is the probability of elastic scattering of an electron from state k to k', $P_{k,q}^{k'}$ and $P_k^{k',q}$ are the scattering probabilities with absorption or emission of a phonon of wave vector q, and $P_{k,k''}^{k',k'''}$ is the probability of electrons in states k and k'' scattering to states k' and k'''.

Linearization of the BTE ensures the validity of Ohm's law—i.e., ρ_t independent of E. On the right-hand side of Eq. (A3), the first term is due to scattering of the electrons by defects, the second and third to scattering in which a phonon is created or destroyed, respectively, and the fourth to scattering by other electrons. The quantities $P_k^{k'}$, etc., are the probabilities for scattering of one (or more) electron(s) in state k (k'') to state k' (k'''), assuming thermal equilibrium electronic distribution functions. As an example, Eq. (A4) gives the detailed form of $P_{k,k''}^{k',k'''}$ for electron-electron scattering,

$$P_{k,k''}^{k',k'''} = \frac{2\pi}{h} |\langle k,k''|H|k',k'''\rangle|^2 f_k^0 f_{k''}^0 (1-f_{k'}^0)(1-f_{k'''}^0)(\delta_{G,k+k''-k'-k'''})\Theta(E_{k'}+E_{k'''}-E_k-E_{k''}) , \tag{A4}$$

In Eq. (A4), H is the appropriate Hamiltonian, Θ is effectively a δ function in energy, G is a reciprocal lattice vector, and $\langle \cdots \rangle$ is the matrix element connecting the initial and final states.

Conservation of total energy and momentum take

different forms concerning the electrons alone in the four terms on the right-hand side of Eq. (A3). The scattering processes in the first and last terms are called "elastic," since the energy of the electron scattered by an impurity is conserved, and the total energy of the two incoming

electrons which scatter off each other is also conserved. The processes in the two terms involving phonons are called inelastic, since the incoming electron either gains or loses energy in absorbing or emitting a phonon. Scattering events in which $\mathbf{G}=0$ are called "normal" (N) processes. Scattering events in which $\mathbf{G}\neq0$ are called "umklapp" (U) processes.

To determine the P's in Eq. (A3), one must know both the electronic wave functions and the interaction of a given electron with an impurity, a phonon, or anther electron. Since the ground state of a metal is a complex many-body state, both the wave functions and the interactions are fundamentally many body in nature. The standard procedure is to use one-electron wave functions and to correct—as well as possible—for many-body effects in the interactions.

In principle the one-electron wave functions should contain an infinite series of plane-wave components and should be orthogonalized to the core electron states. In practice, core orthogonalization is rarely taken into account, and often only a one-plane-wave state is assumed. Only for an alkali metal could a one-plane-wave state have any chance of being a decent approximation over the entire Fermi surface.

The interactions are described by means of pseudopotentials with approximate corrections for many-body screening. Pseudopotentials themselves are always approximate and never unique. Nonetheless, in some cases rather good screened pseudopotentials can be constructed. In general, the required screening of the pseudopotential is "nonlocal"—i.e., velocity dependent. Nonlocality has often been ignored, but can be treated approximately. Some of the calculations we describe use a pseudopotential with an adjustable parameter that is determined by fitting the calculated result to the experimental data at one temperature.

2. The relaxation-time approximation

A general approximation—the relaxation-time approximation—is sometimes used for part or all of the calculation. We now describe this approximation, which has two parts: (1) the treatment of the entire scattering function on the right-hand side (RHS) of Eq. (A3); and (2) the treatment of $\Phi_\mathbf{k}$ alone. Most important for our present purposes is the treatment of $\Phi_\mathbf{k}$. Examples of its use are given in Sec. A5 of this appendix.

Notice that the RHS of Eq. (A3) is linear in $\Phi_\mathbf{k}$. This means that it is also linear in $f_\mathbf{k}-f^0_\mathbf{k}$. The simplest possible form for the RHS of Eq. (A3) that might have any chance of applying to reality is thus

$$e\mathbf{v_kE}\left[\frac{\partial f^0_\mathbf{k}}{\partial\epsilon_\mathbf{k}}\right]=\frac{f_\mathbf{k}-f^0_\mathbf{k}}{\tau_\mathbf{k}} , \tag{A5a}$$

where the proportionality factor $\tau_\mathbf{k}$—called the relaxation time—has the units of time. This approximation has converted the integro-differential equation (A3) into a

simple differential equation (A5). Note that $\mathbf{k}$ in Eq. (A5) runs over all of $\mathbf{k}$ space—i.e., $\tau_\mathbf{k}$ is not limited simply to the Fermi surface. If we go one more step and assume that $\tau_\mathbf{k}$ is independent of energy and constant over the Fermi surface, we get the extreme relaxation-time approximation

$$e\mathbf{v_kE}\left[\frac{\partial f^0_\mathbf{k}}{\partial\epsilon_\mathbf{k}}\right]=\frac{f_\mathbf{k}-f^0_\mathbf{k}}{\tau} . \tag{A5b}$$

When one speaks of including a term in the LBTE using the relaxation-time approximation, it is usually the much more restrictive Eq. (A5b) that is meant.

Rewriting Eq. (A5a) in terms of $\Phi_\mathbf{k}$ yields

$$e\mathbf{v_kE}=\frac{\Phi_\mathbf{k}}{\tau_\mathbf{k}} , \tag{A6a}$$

and multiplying through by $\tau_\mathbf{k}$ then gives for $\Phi_\mathbf{k}$

$$\Phi_\mathbf{k}=e\tau_\mathbf{k}\mathbf{v_kE} . \tag{A6b}$$

If $\tau_\mathbf{k}$ depends only on the magnitude of the momentum transfer $|\mathbf{k}-\mathbf{k'}|$, then Eq. (A6b) turns out to be exact on a completely spherical Fermi surface (i.e., $\mathbf{v_k}$ everywhere parallel to $\mathbf{k}$). In such a case we can rewrite Eq. (A6b) in the simplified form

$$\Phi_\mathbf{k}=e\tau(\epsilon,\theta_{\mathbf{kk'}})\mathbf{v_kE} , \tag{A6c}$$

where we show explicitly that τ is now a function only of electron energy and the scattering angle $\theta_{\mathbf{kk'}}$ between $\mathbf{k}$ and $\mathbf{k'}$.

For a metal with a spherical Fermi surface we can rewrite Eqs. (A6a) and (A6c), respectively, as

$$\Phi_\mathbf{k}=\left[\frac{e\hbar}{m}\right]\tau_\mathbf{k}\mathbf{kE} \tag{A7a}$$

and

$$\Phi_\mathbf{k}=\left[\frac{e\hbar}{m}\right]\tau(\epsilon,\theta_{\mathbf{kk'}})\mathbf{kE} , \tag{A7b}$$

where m is the electron mass.

For scattering in which $\tau_\mathbf{k}$ depends only upon $|\mathbf{k}-\mathbf{k'}|$, the resistivity obtained using Eq. (A6c) or (A7b) has the well-known form

$$\rho_t=\frac{m}{ne^2\langle\tau\rangle} , \tag{A8}$$

where $\langle\tau\rangle$ is obtained by averaging $\tau_\mathbf{k}$ over θ with the weighting factor $(1-\cos\theta_{\mathbf{kk'}})$ and then evaluating the result at $\epsilon=\epsilon_f$. The factor $(1-\cos\theta_{\mathbf{kk'}})$ accounts for the fact that large-angle scattering is more effective than small-angle scattering in transferring crystal momentum out of the direction of flow of the electrical current and thereby producing electrical resistance.

We note that if one is simply interested in defining the $\Phi_\mathbf{k}$'s in Eq. (A3)—for reasons which will be discussed in detail in Sec. A3—then Eqs. (A6b) and (A7a) both

represent general formal expressions for Φ_k, since they involve no restrictions on τ_k. It is only when one restricts τ_k by reducing Eq. (A6b) to (A6c) or (A7a) to (A7b) that one makes a single relaxation-time approximation for Φ_k itself.

Because Eqs. (A7a) and (A7b) are simpler to handle mathematically than Eqs. (A6b) and (A6c) when the Fermi surface is not perfectly spherical, Eq. (A7b) is the form for Φ_k usually used as the basis for the trial function in variational calculations of $\rho(T)$ at both low and high temperatures in the alkali metals.

For an alkali metal, Eq. (A7b) with a constant τ is expected to be an excellent expression for Φ_k for handling electron-impurity scattering at any temperature, since such scattering is elastic (i.e., needs to be known only at ϵ_f) and should also be nearly isotropic. Since electron-electron and electron-phonon scattering are inherently inelastic processes, the energy dependence of τ must be taken into account in any serious calculation of either contribution to $\rho(T)$. Energy dependence alone should be sufficient for electron-electron scattering at all temperatures and for electron-phonon scattering for $T \geq \Theta_D$, since large-angle scattering predominates in these circumstances and such scattering is unlikely to have a strong angular dependence (P.L. Taylor, 1963). For electron-phonon scattering at low temperatures, in contrast, both the anisotropic phonon spectra of the alkali metals and the importance of small-angle scattering require serious attention to be given to the possible angular dependence of τ_k—i.e., to k-space anisotropy. At low temperatures, one must also take into account phonon drag.

3. The linearized Boltzmann transport equation and ψ_q for phonons

For phonons, one has an analogous LBTE to Eq. (A3) that contains terms due to scattering of the phonons by impurities, electrons, and other phonons. As with f_k and Φ_k for the electrons, it is useful to rewrite the phonon number n_q in terms of a ψ_q as

$$n_{q,p} = n^0_{q,p} - \psi_{q,p} \left[\frac{\partial n^0_{q,p}}{\partial(h\nu_q)} \right] , \qquad (A9)$$

and thereby to define an out-of-balance function $\psi_{q,p}$. In Eq. (A9), q is the phonon wave vector, p is a polarization index, and $h\nu_q$ is the phonon energy. For brevity, we shall hereafter suppress the polarization index. In calculations of $\rho(T)$ at high temperatures, it can be assumed that phonon-phonon umklapp processes keep the phonon system in thermal equilibrium, in which case $\psi_q = 0$. At low temperatures, however, it is possible to have $\psi_q \neq 0$ when phonon-phonon and phonon-defect collisions are too weak to keep the electron-phonon interaction from causing the phonons to drift along with the moving electrons. When $\psi_q \neq 0$, the system is said to be subject to phonon drag. Depending upon the relative strengths of

the various interactions, phonon drag may be complete—i.e., the phonons are completely dragged along with the electrons—or only partial.

Phonon drag is expected to be important only in the alkali metals, since in all other metals the Fermi surface contacts Brillouin-zone boundaries. Electronic states near the Brillouin-zone boundaries must be described by multiple plane waves, which causes them to interact very differently with phonons than do electronic states not near the boundaries. If electrons having some values of k interact much more strongly with phonons than electrons with other values of k, a coherent mutual exchange of momentum cannot be obtained between the electron and phonon systems, and thus they do not flow along together.

When phonon drag is present, the coupled LBTE equations for electrons and phonons must be solved simultaneously for Φ_k and ψ_q. In general, this must be done including both electron-defect and phonon-phonon scattering. Solving these two equations exactly when several scatterers are present is beyond present capabilities, even with large computers. Approximations must thus always be made on physical grounds. At low enough temperatures that phonon-phonon and phonon-defect scattering may be neglected, the phonon LBTE can be used to determine ψ_q in terms of Φ_k as noted in Sec. III.B.3 of this review. Then only Φ_k must be independently determined.

With phonons, as for electrons, one can write down a relaxation-time approximation similar to Eq. (A7b) (omitting the constant e and taking v_q to be parallel to q),

$$\psi_q \propto qE . \qquad (A10)$$

This function conveniently makes the contribution of phonon-phonon N processes vanish from the transport coefficients. Unlike Eq. (A7b), Eq. (A10) is never exact and can give substantially erroneous results, as we describe in Sec. III.B.3.

4. Calculation of ρ_t: general principles

To explain how one calculates ρ_t at any given temperature T, it is convenient to rewrite Eq. (A3) in simplified operator form. We assume that the different terms in Eq. (A3) are simply additive to each other, and define $P_i(\Phi)$ ($i=1,2,3$) by the following relations: $P_1(\Phi)=$ the first term on the RHS of Eq. (A3); $P_2(\Phi)=$ the second term; etc. (for simplicity we have also suppressed the wave-vector index of Φ). We expect interference effects between the different scatterers not to be of major importance at low temperatures in the alkali metals.

Each P_i defined in this way is a complex integral operator. In operator form, Eq. (A3) for Φ for the electrons becomes

$$X(\Phi) = P_1(\Phi) + P_2(\Phi) + P_3(\Phi) . \qquad (A11)$$

In Eq. (A11) we have combined the two electron-phonon

terms, since it turns out that they contribute terms having exactly the same form to ρ_t (Ziman, 1972, p. 358). There is a similar equation to Eq. (A11) for the phonon function ψ_q.

If one knew the exact solutions Φ_k and ψ_q for the coupled electron and phonon LBTE, one could calculate ρ_t by simply integrating the right-hand side of the following equation (Ziman, 1972, pp. 275, 283, 285):

$$\rho_t = \frac{\{\Phi, P_1\Phi + \Phi, P_2\Phi + \Phi, P_3\Phi + \Phi, P_4\Phi\}}{\{\Phi, X\}^2} \ . \quad \text{(A12)}$$

Here $\{\Phi, P_i\Phi\}$ is an integral of the form (e.g., for elastic scattering)

$$\{\Phi, P\Phi\} = \frac{1}{2k_B T} \int \int \{\Phi_k - \Phi_{k'}\}^2 P_k^{k'} dk \, dk' \ , \quad \text{(A13)}$$

and $\{\Phi, X\}$ is

$$\{\Phi, X\} = \int e\mathbf{v}_k \Phi_k \frac{\partial f_k^0}{d\epsilon_k} d\mathbf{k} \ . \quad \text{(A14)}$$

Equation (A13) is a complex multidimensional integral that is very difficult to carry out over complex Fermi surfaces, since the conservation of both energy and crystal momentum must be satisfied at each step. Because of these restrictions, the integrals are formidable even on spherical or nearly spherical Fermi surfaces. Even if one could perform the integrals exactly by numerical methods, using a large computer, an exact determination of ρ_t would be fundamentally limited by the fact that exact solutions Φ_k and ψ_q are never known for real metals.

Fortunately, there is an avenue for progress when Φ_k and ψ_q are not exactly known. Equation (A12) is not only an exact expression for ρ_t when Φ_k and ψ_q are known. It is also a variational equation for ρ_t when Φ_k and ψ_q are not known (Ziman, p. 283). That is, if the P_i are taken as known, then using Eq. (A12) to calculate ρ_t for any arbitrary choice of Φ_k will yield an upper bound on ρ_t. Since the RHS of Eq. (A12) is strictly ≥ 0, the lower bound cannot be negative. Importantly, a first-order error in Φ_k will cause only a second-order error in ρ_t (Ziman, p. 286).

All of the calculations we describe in this review are variational calculations in which Φ_k is assumed to be a linear combination of known functions with variable coefficients, and Eq. (A12) is minimized to determine these coefficients. Assuming that the P's are correct, the better the guess concerning the form of these functions, and the larger the number of functions, the better estimate one expects for ρ_t. Once the functions are chosen, the solution for ρ simply involves calculation of integrals followed by a matrix inversion (Ziman, pp. 279, 280, and 285). As Ziman says, the art is to choose functions that "may look akin to the true solution and yet allow the (necessary) integrals to be evaluated easily." In practice, at low temperatures for a metal with a nearly spherical Fermi surface one makes a fairly simple guess for Φ_k and uses only a few parameters. Notice that one cannot sim-

ply choose a single function with a single multiplying constant to represent Φ_k, since a constant will cancel out of Eq. (A12).

At very low temperatures, one must actually calculate $\rho_t = \rho_0 - \rho(T)$. However, since ρ_0 is temperature independent, the first term on the RHS of Eq. (A12) is often dropped from consideration when calculating $\rho(T)$.

Before turning to specific applications of Eq. (A12), we consider a general application to the topic of deviations from Matthiessen's rule (DMR) (Bass, 1972). Matthiessen's rule says that a reasonable approximation to the resistivity of an alloy can be obtained by simply adding the temperature-independent resistivity due to elastic scattering from the impurities to the temperature-dependent resistivity of the pure host metal. In terms of Eq. (A12), Matthiessen's rule says to approximate

$$\frac{\{\Phi, P_1\Phi + \Phi, P_2\Phi\}}{\{\Phi, X\}^2} = \frac{\{\Phi_1, P_1\Phi_1\}}{\{\Phi_1, X\}^2} + \frac{\{\Phi_2, P_2\Phi_2\}}{\{\Phi_2, X\}^2} \ . \quad \text{(A15)}$$

We can divide the LHS of Eq. (A15) into two parts, so that this equation becomes

$$\frac{\{\Phi, P_1\Phi\}}{\{\Phi, X\}^2} + \frac{\{\Phi, P_2\Phi\}}{\{\Phi, X\}^2} = \frac{\{\Phi_1, P_1\Phi_1\}}{\{\Phi_1, X\}^2} + \frac{\{\Phi_2, P_2\Phi_2\}}{\{\Phi_2, X\}^2} \ , \quad \text{(A16)}$$

where each term on the LHS now looks similar to one of the terms on the RHS. Equation (A16) would be exact if all three of the Φ's were the same. But to evaluate ρ_t on the LHS we are constrained to use a common Φ. For the RHS, in contrast, Φ_1 will generally be different from Φ_2. Using either one of these different Φ's on the LHS, or any linear combination of the two of them, will yield a ρ_t that is strictly $\geq$ the RHS calculated with each of the proper Φ's. Thus for any particular set of P's, the LHS must be $\geq$ the RHS, since its two components cannot be simultaneously minimized. If one of the two terms on the RHS of Eq. (A16) is much larger than the other, then its Φ should dominate the LHS, and thus represent a fairly good approximation for this side. The most difficult situation is when the two contributions to ρ_t are of comparable magnitude.

5. Examples of the use of Eq. (A12) in calculations of $\rho(T)$

Equation (A12) may be used to calculate $\rho(T)$ under a variety of conditions, including high, very low, and intermediate temperatures.

(a) High temperatures ($T \geq \Theta_D$) in a pure alkali metal: $\rho_{ep}(T)$. In this case, only the electron-phonon terms in Eqs. (A3) and (A12) are important. As we noted in Sec. A2, Φ_k should be well approximated by Eq. (A7b), provided that this equation is multiplied by an arbitrary function of energy, the value of which is determined from the variational calculation. When the pseudopotential is

carefully chosen to permit low-order perturbation theory to be used, when a good screening function for the electron-electron interaction is chosen, when nonlocality in the electron-electron interaction is properly taken into account, and when the calculation is carried out carefully, then predictions that agree with experiment to within $\simeq 2$-3% from the melting point down to about $\Theta_D/2$ have been achieved for both K and Na with only single-plane-wave matrix elements and no adjustable parameters (Shukla and Taylor, 1976; R. Taylor, 1982). In K the agreement remained at $\simeq 5\%$ down to 20 K ($\simeq \Theta_D/5$); in Na it deteriorated to 25% at 20 K.

(b) *Low temperatures in pure metals and alloys.* In a real metal, the scattering at very low temperatures is dominated by the electron-impurity term in Eqs. (A3) and (A12). We thus speak of $\rho(T)$ as being in the "dirty"—i.e., impurity-dominated—limit. Since electron-impurity scattering is elastic and nearly isotropic, Eq. (A7b) should represent a very good first approximation for Φ_k. In an ideally pure metal, completely free from impurities and other defects (including the sample surface), either electron-phonon or electron-electron scattering would have to dominate ρ_t. We are then in the "clean" limit, and we must be more careful about Φ_k.

In a non-alkali metal, where the Fermi surface contacts Brillouin-zinc boundaries, Eq. (7b) is inappropriate for both cases. If energy dependence is taken into account, it is probably not terrible for electron-electron scattering, which is inherently large-angle scattering and thus might be approximated as "quasi-isotropic." It is completely inappropriate for electron-phonon umklapp scattering, which is highly anisotropic at very low temperatures when the Fermi surface contacts Brillouin-zone boundaries. In such a case, the "clean" limit of $\rho(T)$ should differ substantially from the "dirty" limit calculated using Eqs. (A7b). This simple physical argument is the essential content of the primary source of DMR in non-alkali metals.

In an alkali metal, umklapp electron-phonon scattering is also anisotropic, but its exponential temperature dependence causes it to disappear at very low temperatures. Normal electron-phonon scattering is also eliminated at the very lowest temperatures by phonon drag. Thus at these temperatures only electron-electron scattering should remain. We consider first electron-electron scattering in the clean limit at the very lowest temperatures, and then electron-phonon scattering at slightly higher (but still "low") temperatures.

(c) *Lowest temperatures: electron-electron scattering* A_{ee}. For a metal with a practically spherical Fermi surface that does not contact Brillioun boundaries, we would expect that calculations of $\rho_{ee}(T)$ using Eq. (A7b) would be practically the same in both the "clean" and "dirty" limits—i.e., that there would be little or no DMR in the electron-electron term $A_{ee}T^2$. It was this expectation that gave rise to the Kaveh and Wiser (1984) model of anisotropic scattering of electrons due to dislocations in order to explain the apparently large changes in A_{ee} re-

ported in the first studies of $\rho(T)$ in K down to 1 K.

Using the simple equation (A7b) for Φ_k in calculating A_{ee} in the alkali metals at low temperatures, and taking into account energy dependence, Lawrence and Wilkins (1973) found essentially no difference between the clean and dirty limits for K and the other alkali metals, and only 20% effects in metals with complex Fermi surfaces. Even with Eq. (A7b), however, the calculation of A_{ee} is still quite difficult, because it involves both Coulomb and phonon-assisted electron-electron scattering, as well as a calculation of Δ, the "fractional umklapp scattering" term, which is very small for the alkali metals. Because large changes in A_{ee} result from small changes in calculational procedures, we estimate that even the most sophisticated calculation of A_{ee} currently available is probably uncertain by a factor of two.

(d) *Slightly higher temperatures: electron-phonon scattering* $\rho_{ep}(T)$. At temperatures high enough that $\rho_{ep}(T)$ is still visible, but low enough that phonon-defect and phonon-phonon scattering are unimportant, one can rewrite the phonon LBTE to give ψ_q in terms of Φ_k, and then use Eq. (A7b) for Φ_k without either energy or angular dependence, since the electrons are still scattered primarily by impurities. In this limit, one finds strong phonon drag, and $\rho_{ep}(T)$ is dominated by its umklapp component $\rho_{Uep}(T)$. Given a good pseudopotential, etc., a decent calculation can also be performed for $\rho_{ep}(T)$ in this regime. When the concentrations of either point or extended defects become large enough so that phonon-defect scattering becomes important, some quenching of phonon drag is expected. Only approximate calculations of this effect have been performed to date, and they involved the extreme-relaxation-time approximation of Eq. (A5b) for phonon-defect scattering. The results were not large enough to explain the observed increases in $\rho(T)$ due to addition of such defects. Whether this is due to limitations on the calculations or to the presence of a different physical mechanism is not known.

(e) *Intermediate temperatures in a pure metal or an alloy.* As the temperature is raised above the very low temperatures of situation (d), two different phenomena occur. (1) $\rho_{ep}(T)$ becomes comparable to ρ_0, and (2) phonon-phonon scattering begins to become important. In each case, both energy and k (i.e., angular) dependences must be added to the Φ_k of Eq. (A7).

When phonon-phonon scattering can still be neglected, the calculation becomes like case (a), except that now both energy and k dependences must be included in Φ_k. Explicit calculations were made in different ways by Leavens and Laubitz (1976) and Leavens (1977) on the one hand, and by Jumper and Lawrence (1977) on the other. Both calculations yielded essentially the same results. For K, k and energy dependences together produced a maximum decrease in the calculated $\rho_{ep}(T)$ of about 30% at $\simeq 6$ K, with decreasing effects both above and below 6 K. Of this decrease, energy dependence caused about twice as large an effect as k dependence. Both effects were very similar in the Bloch and phonon-

drag limits. These results indicate that one does not expect large effects in the alkali metals from the standard mechanism of DMR due to changes in $\Phi_{\mathbf{k}}$.

When phonon-phonon scattering cannot be neglected, one must solve both the electron and phonon LBTE's simultaneously. No one has yet performed an adequate calculation for this situation. The best that has been done is a highly approximate calculation by Kaveh and Wiser (1977) for K, involving the extreme-relaxation-time approximation [Eq. (A5b)] for the phonon-phonon interaction combined with an assumption concerning the magnitude of the phonon-phonon interaction that was not rigorously justified.

APPENDIX B: EXPERIMENTAL PROBLEMS AND SOLUTIONS IN LOW-TEMPERATURE RESISTANCE MEASUREMENTS

Low-temperature transport measurements are usually technology limited. To show the difficulties involved, we describe the requirements for making high-precision measurements and how the capabilities to meet these requirements have evolved in the past decade. The experimental task is to isolate the small component $\rho(T)$ (which below 1 K is typically a part in 10^4 or less of ρ_0) and to determine its magnitude and temperature variation.

The quantities actually measured are either R, the total resistance of the sample, or dR/dT, its temperature derivative. R is usually made as large as possible, to minimize errors due to limited voltage sensitivity. For a wire sample of length L and diameter d, ρ_t is related to R by

$$R = \rho_t L / (\pi d^2 / 4) . \qquad (B1)$$

For a given ρ_t, R can be increased by increasing L or by decreasing d. There are several different issues to be considered in the determination of R, the most fundamental of which are measuring precision, measuring sensitivity, and measuring accuracy.

Measuring accuracy is the least onerous problem, since it is not possible to calculate the absolute magnitude of $\rho(T)$ to better than a few percent under even the best circumstances. Provided that one can achieve high enough precision and sensitivity, the absolute magnitude of $d\rho/dT$—the quantity of primary interest in this review—can usually be determined with adequate accuracy, as we discuss below.

We discuss in more detail the following experimental problems: (1) measuring precision; (2) measuring sensitivity; (3) limits on measuring currents due to Joule heating and self-magnetoresistance; (4) sample contacts, and keeping the resistance of the measuring circuit low; (5) carefully preparing reference resistors; and (6) reaching low temperatures, temperature determination, and temperature control. We conclude with a description (7) of the present state of the art in sample preparation and measuring facilities.

1. Achieving adequate measuring precision

As T becomes smaller, $\rho(T)$ also becomes progressively smaller compared to ρ_0, and a progressively higher measuring precision is required to isolate $\rho(T)$. Take, for example, high-purity K (RRR=7000). At 4.2 K, $\rho(T) \simeq 3 \times 10^{-2} \rho_0$ and is decreasing exponentially with temperature. By 1 K, $\rho(T) \simeq 10^{-4} \rho_0$ and is decreasing as T^2. By 0.1 K, $\rho(T) \simeq 10^{-6} \rho_0$. Achieving a precision of 1% in $\rho(T)$ thus requires measuring precisions of 10^{-4} at 4.2 K, 10^{-6} at 1 K, and $\simeq 10^{-8}$ at 0.1 K.

Until the mid 1970s, resistances were determined by measuring the voltage across the sample of interest for a given input current. The measuring precision was limited both by the stability of the current source (which could reach parts-per-million) and, more importantly— as we describe in item 2 just below—by the sensitivity of the voltage measuring device. By the mid 1970s, it was recognized that a bridge device, called a current comparator (Kusters and MacMartin, 1970), permitted the ratio of two currents to be measured with a precision of < 1 part in 10^8. With this device, the ratio of two resistances in a potentiometer circuit could be measured, in principle, with the same precision, provided that the null detector was sensitive enough. However, the achievement of such high precision in measurements of the very small resistances of high-purity metals at low temperatures required the satisfying of other conditions, which we consider next. For this reason, improvements in precision occurred in steps, 10^{-4}, 10^{-6}, 10^{-7}, and, finally, the present limit, 2×10^{-8}.

2. Achieving adequate voltage sensitivity

For high-purity metals at low temperatures, achieving the full measuring precision permitted by either a very stable current source or a current comparator requires very high voltage sensitivity, both because the samples have very low resistances R and because the measuring current must be kept low to minimize effects of Joule heating and self-magnetoresistance.

R is determined at low temperatures by ρ_0, d, and L [Eq. (B1)]. For a high-purity K sample (RRR=7000), ρ_0 is 10^{-11} Ω m. To avoid size effects, the sample diameter d must be greater than the electron mean free path l ($l \simeq 0.2$ mm in K with a RRR of 7000); to be safe, most investigators have chosen $d \geq 1$ mm. Physical constraints usually limit the length of a straight sample to about 0.1 m. To obtain the large voltages they needed, most investigators have wound their sample wires into cylinders to obtain $L = 1$ m, a procedure which involves some constraint on the sample. With $\rho_0 = 10^{-11} \Omega$ m, $d = 1$ mm, and $L = 1$ m, we have $R = 10^{-5}$ Ω. A measuring current of $I_m = 1$ A gives a potential difference of 10^{-5} V, so that a measuring sensitivity of 10^{-4} [sufficient for 1% measurements of $\rho(T)$ down to about 2 K, as shown just above] requires a voltage sensitivity of 10^{-9} V. Section III.B.2 shows that the achievement of sensitivities of

10^{-8} to 10^{-9} V with room-temperature dc detectors first enabled precision studies of $\rho(T)$ to be extended down to $\simeq 2$ K. Today, 10^{-9} V still remains the limit for room-temperature dc detectors.

The extension of measurements to below 1 K on straight, unconstrained samples requires not only a means for reaching such temperatures, but also much higher voltage sensitivities. For example, at 0.1 K, a high-purity sample with $L = 5$ cm, $d = 1$ mm, and $I_m = 50$ mA (to keep self-magnetoresistance low—see item 3 below) requires a voltage sensitivity of $\simeq 10^{-15}$ V to achieve a precision of 10^{-7}. Such sensitivities can now be achieved using superconducting detectors, especially superconducting quantum interference devices or SQUID's (Lounasmaa, 1974) held at low temperatures. Edmunds et al. (1980) have shown how to solve the problems associated with coupling a highly sensitive rf SQUID to a current comparator that inherently emits electronic noise in its control process.

3. Measuring current: Joule heating and self-magnetoresistance

If the measuring current I_m is too large, it can cause too much Joule heating and self-magnetoresistance in the sample. The higher the precision needed to isolate $\rho(T)$, the more important both effects become. At 4.2 K, $I_m \geq 1$ A may be used for a high-purity $d = 1$ mm sample submerged in liquid He, because heat conduction from the sample is good and precision of better than 10^{-4} is not required. In contrast, for the same sample in vacuum well below 1 K, currents as small as 20–50 mA are required to reduce unwanted effects adequately. Even 10 mA can produce self-magnetoresistances that change ρ_0 by several parts in 10^5 (Rowlands et al., 1978). However, the changes due to such currents in $d\rho/dT$, the quantity of primary interest, can be less than a part in 10^8 (Edmunds et al., 1980).

4. Keeping circuit and contact resistances low

It was important, even with older potentiometric measuring systems, to keep contact resistances to the sample low to minimize Joule heating at the contacts and to ensure a uniform current distribution in the sample. The recent use of superconducting detectors to achieve higher voltage sensitivity has made a low total circuit resistance even more important, since these detectors are inherently current-sensitive devices (Lounasmaa, 1974).

Various techniques for making reliable low-resistance contacts to the alkali metals have been described (Ekin and Maxfield, 1971; van Kempen et al., 1981; Edmunds et al., 1980). With free-hanging samples in controlled atmospheres, the best contacts can usually be made using the same material as the samples (Pratt, 1982). By using superconducting wires for connections and taking great care with contacts, one can keep the total resistance of

the connecting wires and contacts below 10^{-7} Ω (Edmunds et al., 1980) and thus smaller than the sample resistance.

To eliminate temperature-dependent geometric effects, it is important to have as uniform as possible a current distribution within the samples. Thus it is important to keep the current attachments several sample widths away from the potential leads. The sample length between the potential leads should also be at least five to ten times the width of the sample, and the potential leads themselves should be several times longer than their widths (Pratt, 1982).

5. Reference resistances

With the change from determining resistances directly by measuring a voltage and a current, to measuring the ratio of two resistances with a potentiometric circuit involving a current comparator and an appropriate null detector (see Fig. 79), the characteristics and stability of the reference resistor became important. The current comparator gives optimal precision when the reference resistance is equal to the resistance of interest. To minimize Johnson noise in the circuit, the reference resistance should also be at least as cold as the sample. Initially,
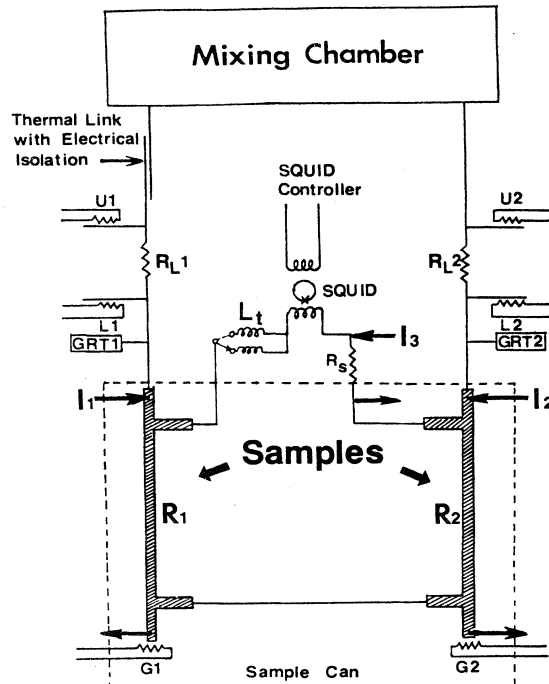

FIG. 79. The Michigan State University (MSU) low-temperature measuring circuit. The components inside the dashed lines are located inside the sample can. From Zhao, 1988.

great care was taken to make special reference resistors with low resistances that were insensitive to both temperature and measuring current (van Kempen et al., 1979; Rowlands and Woods, 1976). For measurements below about 4 K, however, it was later recognized (Edmunds et al., 1980) that—when possible—it is better simply to make two nearly identical samples and use each as the reference for the other. If the self-normalized temperature derivative of ρ_t—i.e., $(1/\rho)(d\rho/dT)$—is measured, then the reference resistance drops out of the determination of $\rho(T)$, as we now show.

When the sample resistance $R(T)$ and the reference resistance $R_r(T)$ are at the same temperature T, and the potentiometric circuit is balanced, the current comparator measures the ratio $C(T)=R(T)/R_r(T)$. If R is raised to the temperature $T+\Delta T$, but R_r is maintained at T, the current comparator then reads $C(T+\Delta T)=R(T+\Delta T)/R_r(T)$. Taking the difference, $C(T+\Delta T)-C(T)$, and dividing by $C(T)\Delta T$ gives

$$[C(T+\Delta T)-C(T)]/C(T)\Delta T$$

$$=\{[R(T+\Delta T)-R(T)]/R_r(T)\Delta T\}/\{R(T)/R_r(T)\}$$

$$=[R(T+\Delta T)-R(T)]/R(T)\Delta T \ . \tag{B2a}$$

For small ΔT, the right-hand side just becomes

$$(dR/dT)/R(T) \ . \tag{B2b}$$

At very low temperatures, the quantity $[R(T)-R(0 \text{ K})]/R(0 \text{ K})$ is very small—e.g., $\leq 10^{-4}$ for K at 1 K. Moreover, $R(T)$ and R_0 are related to $\rho(T)$ and ρ_0, respectively, by the same geometric factors. Equation (B2b) then becomes

$$(dC/dT)/C=(d\rho/dT)/\rho_0 \ . \tag{B2c}$$

Multiplying both sides of Eq. (B2c) by ρ_0 gives

$$\rho_0(dC/dT)/C=d\rho/dT \ . \tag{B2d}$$

ρ_0 can be determined as follows. As already indicated, below 1 K, ρ_t is closely equal to ρ_0. In addition, the geometric factor of the sample changes by only 1–2 % from room temperature to 0 K. ρ_0 can thus be found with an accuracy of 1–2 % simply by measuring the resistances R of the sample at a well-defined room temperature—i.e., $R(295 \text{ K})$—and also well below 1 K—i.e., $R(0 \text{ K})$—and then using the equation

$$\rho_0=[R(0 \text{ K})/R(296 \text{ K})]\times\rho(295 \text{ K}) \ . \tag{B3}$$

In Eq. (B3), $\rho(295 \text{ K})$ is the resistivity of the pure metal at 295 K (Bass, 1982).

6. Reaching low temperatures; temperature calibration and control

To fully utilize the capabilities just described, it is necessary to reach and maintain mK temperatures. Temperatures down to a few mK can now be routinely

reached with commercially available (Oxford-Instruments, Oxford, England) continuous-flow ^{3}He–^{4}He dilution refrigerators (Lounasmaa, 1974). Temperatures below 1 mK can be reached by adding an adiabatic demagnetization stage (Lounasmaa, 1974) to a dilution refrigerator, but such temperatures are not relevant to this review, because the $\rho(T)$'s of interest become too small a fraction of ρ_0 to be detected with available measuring precisions.

With high measuring precision and high voltage sensitivity, uncertainties in the temperature scale can limit how well one can determine the form of the temperature variation of $\rho(T)$. To measure $d\rho/dT$, one must know the temperature scale well enough to produce reliable values of small temperature differences. Techniques for careful temperature calibration and determination have been described in some detail (Edmunds et al., 1980; van Kempen et al., 1981). As noted in Sec. II.C of this review, it is also often useful to examine low-temperature deviations from T^2 behavior by plotting the quantity $(1/T)(d\rho/dT)$. If the samples are coupled to the bath by means of known resistances, then, as described in the following section, the Wiedemann-Franz law can be used to determine the product $T \ dT$ directly, and thereby independently check the quality of the temperature calibration.

Because of their convenience, stability, and reproducibility, germanium resistance thermometers are often used for temperature measurements down to mK temperatures. These must be calibrated at a few temperatures against primary standards, such as superconducting fixed-point devices, and then more completely against secondary standards such as cerium magnesium nitrate (CMN) and commercially calibrated germanium resistance thermometers. Care must be taken to fit a smooth temperature scale to these calibration points (Edmunds et al., 1980).

Similar germanium resistance thermometers can also be used as sensing elements with standard temperature control systems to achieve temperature regulation to fractions of a mK.

7. State-of-the-art sample preparation and measuring system

We conclude this discussion of experimental problems and solutions by describing the present state of the art in alkali metal sample preparation and in measuring systems for low-temperature transport. The system we describe is one we have developed at MSU. In addition to providing the capabilities for measuring $d\rho/dT$ indicated above, it has the advantage of permitting routine measurements of the thermoelectric ratio G (Blatt et al., 1976) on the same samples for which $\rho(T)$ is measured. At very low temperatures, the Wiedemann-Franz ratio in a metal is essentially equal to the Sommerfeld value of the Lorenz number, $L_0=2.44\times10^{-8}$ W Ω/K^2 (Ashcroft

and Mermin, 1976). When this is true, ρ_i and G together completely characterize the electronic-transport properties of a cubic metal (Ashcroft and Mermin, 1976).

(a) Sample preparation and mounting. It is essential to have a sample handling system in which alkali metals can be manipulated in a controlled atmosphere and then mounted so that the sample length between the potential leads is not in contact with any other material. These requirements necessitate a high-quality glove box for sample handling and a sealable sample container that permits the sample to be removed from the glove box and mounted on the cryostat without opening the sample container. Glove boxes with atmospheric purifiers that keep residual gas (especially O_2 and H_2O) concentrations to a few parts per million (ppm) or less are commercially available (Vacuum Atmospheres Corp., USA). A good glove box is able to keep the freshly cut surface of K shiny for several hours. A copper foil coated with K and placed inside the sample can ensures a shiny sample surface for several days. A vacuum bell jar inside the glove box permits outgassing the sample, evaporating K samples, treating K with various surface contaminants, etc.

The sample material, typically 99.95% pure or better, is melted into a stainless steel press inside the glove box and then extruded through stainless steel dies or capillaries into wire of the desired diameter. The wires are mounted free-standing in a Cu sample can, which is sealed with an indium o-ring. Provision for evacuating the can after the samples are mounted can be made by connecting a small pumping line, consisting of a thin brass tube, partially filled with indium, plus a vacuum valve. After the can is evacuated, the brass is crimped off and the valve removed (Haerle et al., 1986). The sample can should be completely surrounded by a radiation shield to intercept thermal radiation from the surrounding walls at 4.2 K (Pratt, 1982).

In initial studies by the MSU group, the glove box and the sample can were filled with one atmosphere of Ar, both because Ar can be conveniently obtained in somewhat higher purity than He and because Ar freezes into a solid before reaching 4.2 K. It thus provides an exchange gas during cooling to below liquid N_2 temperature, but the samples are in a good vacuum at the measuring temperatures. Later measurements were also made with one atmosphere of He from a He-filled glove box, or, occasionally, with a vacuum of 10 μ Hg obtained by pumping away the He gas and sealing off the sample can as described above. When one atmosphere of He was used, the bottom of the sample can was filled with molecular sieve to absorb the helium upon cooling, thus maintaining a good vacuum in the can. The sieve was held in place by a thin stainless steel screen. Prior to being placed in the glove box, the sieve was heated and outgassed in a vacuum of 10^{-6} Torr for 2 days. In initial studies, the sieve was outgassed at 473 K; in later studies, 573 K was used.

The sample holder supports two samples mounted symmetrically. The structural elements of the holder are made entirely from an insulating plastic such as nylon to ensure that the heat flow through these elements is very small. Nylon has a thermal expansion coefficient similar to those of the alkali metals, so that the samples will not be strained during cooling. Cu blocks, having very small resistances, are used to connect the superconducting wires coming from the external circuit to the current and potential leads of the sample. These wires are brought into the sample can through epoxy seals. The Cu blocks are smeared with a thin layer of K to ensure good contact to the two ends of the sample serving as current leads and to the separately attached potential leads. The potential leads are normally of the same material as the sample. When clean, the alkali metals—especially K—are soft and sticky, and the potential leads usually stick to the sample upon touching, making a solid, low-resistance contact.

The Cu block attached to one end of each sample makes thermal contact with the refrigerator and contains a thermometer and a heater used to change the temperature of its sample. The Cu block at the other end of each sample contains a heater used for G measurements. Great care is taken to ensure that the thermometers are in good thermal contact with the samples.

Each of the two samples is connected (Fig. 79) to the mixing chamber of the dilution refrigerator through a weak thermal link consisting of Ag (0.1 at. % Au) wires having electrical resistances (50 $\mu\Omega$) that are essentially temperature independent below 4 K and can easily be measured with an accuracy of better than 1%. The cold ends of these Ag(Au) wires are thermally anchored to the mixing chamber by thick, annealed pure-silver wires. The hot ends are thermally anchored in similar fashion to the samples inside the sample can via epoxy seals. One sample is also electrically isolated from the mixing chamber. heaters on both sides of the Ag(Au) wires provide independent control of the temperatures of the two samples relative to the temperature of the mixing chamber. Typically, equal powers Q are put into the heaters labeled U_1 and U_2 in Fig. 79 to raise the temperatures of both samples to a fixed "low temperature" T_L, slightly larger than that of the mixing chamber. Then one sample (call it sample 1) is held fixed at T_L, while the other (call it sample 2) is raised to a higher temperature T_H by turning off U_2 and turning on L_2, so that the power Q now flows through its Ag(Au) resistance. The temperatures T_H and T_L are measured using the appropriate germanium resistance thermometer, GRT 2, and both the average temperature $T = (T_H + T_L)/2$ and the temperature difference $\Delta T = T_H - T_L$ are calculated.

The value of ΔT can then be independently checked using the Lorenz number as follows. The Lorenz number for each Ag(Au) resistance has been separately verified to be L_0 to within 1% below 4.2 K (Pratt, 1982). From the measurements already described, a "Lorenz number" temperature difference across the Ag(Au) can be calculated as $\Delta T_L = RQ/(L_0 T)$, where R is the resistance of the Ag(Au) wire. ΔT_L can then be compared with the ΔT

determined using GRT 2. Alternatively, the quantity $T\Delta T/Q$ can be calculated to verify that it is equal to the known value of R/L_0. This latter procedure gives a direct check of the product $T\,dT$, which Sec. II.C of this review shows to be of interest in very-low-temperature resistivity measurements.

The sample can is clamped to the mixing chamber of the dilution refrigerator for mechanical support. To minimize heat transfer to the refrigerator by physical vibrations of the laboratory, the refrigerator is mounted on a vibration isolation table and all pumping connections to the refrigerator are made via flexible bellows. The refrigerator is located inside a double-walled screened room. The outer wall is soft steel to eliminate low-frequency magnetic fields, and the inner wall is Cu to eliminate high-frequency radiation. To ensure that electrical noise does not enter the room through electrical lines or metallic pumping lines, all electrical connections pass through filters in the room walls, and pumping lines have epoxy tubing connections through the walls which are surrounded by metal tubes that greatly attenuate any incoming electromagnetic noise.

(b) The measuring circuit. The measuring circuit, illustrated schematically in Fig. 79, consists of the twin samples, the SQUID null detector, an inductor, a standard resistor R_s that has a known resistance at 4.2 K but becomes superconducting below about 3.8 K, and the current comparator (not shown).

A standard resistor such as the one just mentioned has the great advantage of producing no Johnson noise below 3.8 K. We have found a Sn(0.1%In) alloy with $R_s = 1.21$ $\mu\Omega$ to be very satisfactory. This resistor is thermally attached to the 1 K pot of our refrigerator. It is used to measure $R(4.2\text{ K})$ directly on our samples at the beginning of the run when the sample and the 1 K pot are both at 4.2 K, and also to measure $R(0\text{ K})$ as follows. When the measuring run is completed, the refrigerator circulation is stopped, and a heater is used to raise the temperature of R_s to 4.2 K. Because of the good thermal isolation of the sample can from the 1 K pot, it and the sample remain below 1 K. R_s is then used to measure $R(T<1\text{ K})$, which is closely equal to $R(0\text{ K})$, as already noted. ρ_0 is then found from Eq. (B3).

The inductors are used to adjust the time constant of the circuit for samples with different resistances. For thick, high-purity samples $(R \simeq 10^{-7}\ \Omega)$, the response time is already many seconds with only the basic circuit inductance, so no additional inductor is added. However, for higher-resistance samples, an inductance large enough to keep the time constant from falling below about 1 s reduces the sensitivity of the SQUID circuit to high-frequency noise and thus improves its stability.

With these sample preparation and measuring techniques, including a current comparator, a SQUID null detector, and a ^{3}He-^{4}He dilution refrigerator to reach mK temperatures, reliable measurements of $d\rho/dT$ can now be made with precisions in R approaching 10^{-8} and voltage sensitivities (e.g., 10^{-15} V) limited only by

Johnson noise in the sample and its twin reference resistance, down to about 10 mK.

APPENDIX C: NEARLY-FREE-ELECTRON OR CHARGE-DENSITY-WAVE GROUND STATE?

The fundamental question of whether the ground state of the alkali metals is a nearly-free-electron (NFE) state or a charge-density-wave (CDW) state has remained unresolved for over 20 years, ever since Overhauser (1962, 1968) first suggested the possibility of a CDW ground state in these metals. The experimental evidence for and against the CDW hypothesis has been reviewed by Cracknell (1969), Overhauser (1978, 1985a) and van Vucht et al. (1985). The general theoretical issues have been examined by Overhauser (1978; 1985a). To examine in detail all of the experimental data and theoretical analyses involved in this controversy would take a review article of its own. In this appendix, we first briefly describe the current model of a CDW ground state in the alkali meals and then attempt to give the reader with little previous knowledge of the debate a feeling for the difficulties involved in resolving the fundamental question of whether or not this ground state is present in these metals. We focus primarily upon experimental data and analyses published since 1985; for information about most older data the reader is referred to the literature just cited.

1. The present CDW model in K

The ground state of the noninteracting electron gas in the Jellium model consists of a negatively charged, uniform electron sea on top of a uniform background of positive charge. For an interacting electron gas in a metal where the ions can be easily modulated, exchange and correlation effects lead to the possibility of broken symmetries such as charge-density-wave (CDW) or spin-density-wave (SDW) ground state. In the CDW ground state, the electronic charge and the positions of the ions are both modulated, with modulations such that the resulting electrical fields approximately cancel. The static sinusoidal modulation of the electronic charge density $g(\mathbf{r})$ is given as a function of position $\mathbf{r}$ by

$$g(\mathbf{r}) = g_0[1 + p\cos(\mathbf{Q}\cdot\mathbf{r} + \phi)]\ , \qquad (\text{C1})$$

where g_0 is the average charge density, $\mathbf{Q}$ is the CDW wave vector, p is the fractional modulation, and ϕ is the phase of the CDW. In K, $\mathbf{Q}$ is incommensurate with the reciprocal-lattice vectors $\mathbf{G}$ and is assumed to lie nearly parallel to the [110] axes—i.e., the angle between $\mathbf{Q}$ and the [110] reciprocal-lattice vector $\mathbf{G}$ is only a few degrees. This CDW potential gives rise to a primary energy gap, which is taken from analysis of experimental data to be 0.6 eV, slightly larger than the approximately 0.4 eV of the Brillouin-zone band gap. Solution of the Schrödinger equation with the ionic and CDW potentials leads to three main families of higher-order energy gaps:
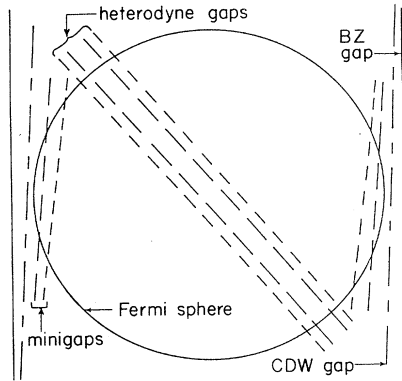
FIG. 80. Schematic drawing of present model of the different kinds of CDW-induced gaps on the free-electron Fermi surface of K. The solid vertical lines indicate two of the twelve Brillouin-zone gaps, which are separated by a reciprocal-lattice vector **G**. The two CDW gaps are separated by **Q**. The periodicities of the other gaps are given in the text. After Overhauser, 1985.

(a) minigaps at $K = (n+1)\mathbf{Q} - n\mathbf{G}$; (b) heterodyne gaps at $\mathbf{K} = n(\mathbf{G} - \mathbf{Q})$; and (c) second-zone minigaps at $\mathbf{K} = (n+1)\mathbf{G} - n\mathbf{Q}$. For each type of gap, $n = 1, 2, 3, \ldots$. The first minigap is taken to be about 0.1 eV and the first heterodyne gap to be about 0.02 eV. Only the minigaps and heterodyne gaps truncate the Fermi surface, as illustrated schematically in Fig. 80. The presence of all of these gaps leads to quite a complex Fermi-surface structure.

In a high-purity metal, the energy of the system is independent of the value of the phase ϕ. This energy invariance leads to low-frequency collective excitations—called phasons—whose frequency spectrum goes to zero at the point **Q** in **k** space. The phase $\phi(\mathbf{r}, t)$ is slowly modulated in both space and time. To provide appropriate screening, the phase of the lattice must also be modulated as

$$\psi(\mathbf{L}, t) = \sum_q \phi_q \sin(\mathbf{q} \cdot \mathbf{L} - \omega_q t) , \qquad (C2)$$

where **L** describes the location in the lattice, **q** and ω_q are the wave vector and frequency of a particular phason, and ϕ_q is its amplitude. A phason is a normal mode of the lattice with a frequency that is zero at **Q** and increases linearly with q. Its spectrum is expected to be highly anisotropic. Formally, a phason is a coherent linear combination of two appropriate phonons of the undistorted lattice. As do the phonons, phasons can scatter electrons. Bishop and Overhauser (1979, 1981) have shown that at low temperatures in K such scattering should produce a highly anisotropic, Bloch-Gruneisen-like resistivity contribution, but with a characteristic temperature of only about 6 K, much lower than K's Debye temperature of about 100 K.

2. The basic problems

For the theorist, the basic problem in resolving the NFE versus CDW question is an inability to calculate correlation effects rigorously in metals—especially in metals with electron densities as small as those of the alkali metals. Thus a rigorous proof that the ground state is either a NFE or a CDW state does not yet exist.

The experimentalist also has problems. The fundamental problem is that it is practically impossible to prove any model wrong if its supporters persist in attributing discrepancies between data and the model to a combination of (a) experimental errors; (b) defects in, or uncontrolled characteristics of, samples; and (c) lack of adequate understanding of what the model requires in a given case. We describe below examples of uses of these arguments by both sides. It is important to recognize that while new, apparently discrepant, data have occasionally seemed temporarily to stump one side or the other, each side has eventually been able to rationalize away such data to its own satisfaction.

Many measurements on the alkali metals yield results nicely consistent with a NFE Fermi surface. Quite a few, however, yield anomalous results that differ from NFE predictions—sometimes modestly and sometimes dramatically. Experimental data are not always reproducible. Advocates of a NFE state focus on the agreements of data with NFE predictions and attribute the discrepancies to the three arguments listed in the preceding paragraph. Advocates of a CDW ground state focus upon the anomalies and attribute the irreproducibilities to the presence of a complex CDW domain structure that changes in an as yet uncontrollable way with different sample treatments; they, too, attribute discrepancies to the arguments listed above.

3. Role of low-temperature transport in zero magnetic field

Because the analysis of low-temperature transport measurements in zero magnetic field involves complex integrations over the Fermi surface, such measurements are unlikely to provide sufficiently definitive results to resolve the NFE versus CDW debate by themselves. But we believe that such measurements can play two different roles in the CDW versus NFE debate.

First, the alkali metals are highly susceptible to contamination, which is often invoked by CDW opponents to explain unexpected behaviors. Low-temperature resistivity measurements are unusually sensitive to the presence of such contamination. Such measurements can thus be useful in (1) uncovering unexpected defects and contamination; and (2) assisting in determining the extent to which such entities can account for observed anomalies within a NFE framework. We describe in this review the discovery of several completely unexpected effects of defects and contamination which are so new that their significance for the debate is not yet clear.

Second, the theory of $\rho(T)$ in the presence of a CDW indicates that its form should remain invariant under changes in domain structure (Bishop and Overhauser, 1979, 1981). Thus, if the alkali metals have a CDW ground state, only the magnitudes of any CDW contributions should depend upon the CDW domain structure. It is therefore important to see whether the predicted form appears in experimental data. We argue in this review that there is no compelling evidence that such a form is present.

4. Examination of anomalies, especially in recent data

The anomalies we examine are as follows:

(a) One of the oldest anomalies attributed to a CDW ground state is the universally observed linear magnetoresistance (LMR) in K—a linear increase in the electrical resistance with increasing applied magnetic field. It is also universally agreed that the magnitude of the LMR varies substantially from sample to sample and even in individual samples subjected to a wide variety of treatments. The NFE picture of magnetoresistance predicts unambiguously (see, for example, Abrikosov, 1972) that a homogeneous bulk sample of a metal that has a Fermi surface lying completely within the first Brillouin zone and not contacting Brillouin-zone boundaries must display a magnetoresistance that saturates in magnitude at high magnetic fields ($w_c \tau \gg 1$, where w_c is the cyclotron frequency and τ is the electronic relaxation time). In contrast, if the ground state is a CDW state, the Fermi surface must contact the Brillouin-zone boundaries, and the resulting complex deviations of the Fermi surface from sphericity (see, for example, Hwang and Overhauser, 1989) can give rise to both longitudinal (Huberman, 1987) and transverse LMR (see, for example, Overhauser, 1973). Advocates of a NFE ground state attribute the observed LMR to a combination of phenomena such as magnetic-field-induced symmetry breaking between outscattering and backscattering of electrons by phonons (Mahan, 1983); LMR due to bulk defects (Beers et al., 1978; Yoshida, 1981) and surface defects (Bruls et al., 1981, 1985) in the samples; and LMR due to nonuniform magnetic fields along the sample (Gostishchev et al., 1978). Predicted (Jain and Verma, 1973) size-dependent LMR have also recently been seen in K (Griden et al., 1989). Microscopic extended defects such as dislocations were considered to be a potential source of LMR, but a recent careful examination (Fletcher, 1985) revealed no appreciable changes in LMR when deliberately introduced dislocations were annealed out. Although the NFE advocates are generally not able to explain in detail the observed LMR for a given sample, they seem to have enough alternatives available for the LMR not to represent a fundamental problem.

(b) The nonspherical Fermi surface due to a CDW ground state should give rise to open orbits in **k** space (see, for example, Overhauser, 1982) and thus to large an-

gular variations of magnetoresistance measured on single-crystal samples. Huge, complex angular variations that look qualitatively like the behavior expected for open orbits have been reported in induced torque measurements on K (Coulter and Datars, 1985) and Na (Coulter and Datars, 1986) in high magnetic fields. The CDW-based model has been shown (Huberman and Overhauser, 1982; Overhauser, 1982) to be able to describe the torque data qualitatively, although not yet to predict the precise positions of the open orbit peaks. In apparent contradiction to these results, recent contactless measurements of helicon resonances (De Podesta and Springerford, 1986, 1987) and of induced eddy currents (Elliott and Harris, 1989) in K have found no evidence of open orbits at levels well below those required to reproduce the data of Coulter and Datars. In addition, it has recently been argued (Elliott et al., 1988) that the reported complex induced torque structure is not intrinsic to K or Na, but rather results from frictional effects in the sample holder. Such frictional effects must be ruled out in order for torque measurements again to be the major problem for NFE advocates that they had previously seemed to be.

(c) Very recently, observations were published (Soethout et al., 1987) of large variations in the transverse resistance of single-crystal samples of K as the samples were rotated in the presence of a large transverse magnetic field. Especially surprising were negative resistances seen at certain field orientations in some samples measured at 4.2 K and 7.5 T. An explanation for such a negative resistance based on a CDW ground state has been proposed (Overhauser, 1987b). The NFE advocates have not yet provided an alternative explanation.

(d) There also exist reports in the literature (e.g., Penz, 1968; Penz and Bowers, 1968; O'Shea and Springford, 1981) of deviations of the Hall coefficient of K from the NFE value of simply $1/ne$, where n is the electron density corresponding to one electron per atom and e is the electronic charge. However, the most recent searches for such deviations failed to find any (Fletcher, 1982; De Podesta and Springford, 1986, 1987), and field-dependent deviations reported in previous helicon measurements have now been plausibly attributed to sample movement (De Podesta, 1987). The Hall data thus currently appear to pose no significant problem for NFE advocates.

(e) The nonspherical Fermi surface associated with a CDW ground state should also be visible in de Haas–van Alphen measurements, and should give rise to CDW-based satellites in neutron and x-ray scattering. Early attempts to see CDW satellites in neutron and x-ray scattering were unsuccessful, leading the CDW advocates to argue that the satellites were greatly reduced in size due to phason smearing. Recently, new studies have been made with greatly improved sensitivity.

Published measurements of the de Haas–van Alphen effect (Cracknell, 1969; O'Shea and Springford, 1981) support Fermi surfaces of the alkali metals in their body-centered-cubic (bcc) phases that are nearly spheri-

cal and completely contained within the first Brillouin zone. The most recent de Haas–van Alphen measurements (O'Shea and Springford, 1981) showed a spherical Fermi surface for K samples which simultaneously showed LMR in contactless helicon measurements. While the CDW advocates have speculated that the near isotropy of the de Haas–van Alphen effect for K might result from an averaging over a random distribution of many very small CDW domains, an adequate explanation for these data remains a problem for the CDW model.

Evidence for CDW satellites from neutron scattering was recently reported (Giebultowicz et al., 1986; Werner et al., 1987), but the measurements are difficult, the evidence not much above noise, and one not-yet-understood characteristic of the data is their relative insensitivity to sample temperature. The report was quickly challenged (Pintschovius et al., 1987) as being an experimental artifact, and the challenge as quickly rebutted (Werner et al., 1989). The situation is not yet resolved, but plans are underway for joint measurement by the two groups that currently disagree, and the results of this cooperative effort should be of major importance.

No evidence for CDW satellites was seen in x-ray measurements at 10 K (You et al., 1987). The CDW advocates argue that the measurements did not extend to low enough temperatures.

(f) A predicted CDW-induced intrinsic broadening of the nuclear-magnetic-resonance signal in K was sought, but not found (Follstaedt and Slichter, 1976). The CDW advocates have proposed that the expected broadening might be motionally narrowed by phase fluctuations (Wang and Overhauser, 1985) or by long-range indirect exchange (Giuliani and Overhauser, 1982) and have requested measurements to still lower temperatures.

(g) The presence of perpendicular-field cyclotron-resonance transmission signals in Na and K (Grimes, 1969—referenced in Lacueva and Overhauser, 1986; Dunifer et al., 1989) has been attributed to the presence of a CDW ground state (Lacueva and Overhauser, 1986, 1989). Proposed NFE-based models [see Baraff (1974) and references therein] can rationalize some, but not yet all, of the different behaviors observed.

(h) Angle-resolved photoemission studies recently revealed an apparent deformation of the electron bands in Na near the Fermi surface (Jensen and Plummer, 1985), and both angle-resolved photoemission (Jensen and Plummer, 1985; Lyo and Plummer, 1988) and K-edge absorption measurements (Citrin et al., 1988) indicate significant band narrowing relative to NFE-based predictions based upon simple local-density-approximation calculations. The band narrowing appears to be adequately described by the NFE picture when an appropriate dielectric response function is used to make the necessary self-energy correction (Lyo and Plummer, 1988). The band deformation has been attributed to a CDW ground state (Overhauser, 1985b), but is has also been argued that the apparent deformation can be understood in terms of a NFE Fermi surface (Shung and Mahan, 1986).

This latter proposal has been disputed (Overhauser, 1987a) and defended (Shung and Mahan, 1987). This topic requires further theoretical work.

(i) It has been shown (Taylor and MacDonald, 1986) that the high-temperature thermopower of K can be calculated quantitatively with a NFE Fermi surface using no adjustable parameters. It was argued that the data are incompatible with a CDW-based explanation, since the calculations are extremely sensitive to the behavior of the pseudopotential at $2k_f$ (k_f is the Fermi momentum), and the form of the potential at $2k_f$ must be very different for a CDW ground state than for a NFE state. No CDW-based calculation has yet been put forward.

(j) The CDW model predicts that the residual resistance of a CDW domain should be anisotropic. Two attempts have recently been made (van de Walle, 1982; Bohm et al., 1989) to freeze in a preferential orientation of CDW domains by cooling single-crystal K samples to 4.2 K in the presence of a large magnetic field. No resistance anisotropies were observed to within experimental uncertainties.

5. Conclusions

We conclude that neither side in this debate has yet explained all of the observed behavior in the alkali metals, but also that neither side has yet conceded its inability to do so. The debate is thus not yet decided. For the near future, it will be interesting to see the results of the collaborative neutron scattering studies noted in item (e) [Giebultowicz et al., (1986); Werner et al. (1987); Pintschovius et al., (1987)] and how these results are interpreted by both sides.

REFERENCES

Abrikosov, A. A., 1972, *Introduction to the Theory of Normal Metals,* Solid State Physics Suppl. 12, edited by F. Seitz and D. Turnbull (Academic, New York).

Aleksandrov, B. N., O. L. Lomonos, O. S. Ignatev, O. G. Gromov, and E. P. Lokshin, 1968, Z. Eksp. Teor. Fiz. **55**, 2065 [Sov. Phys. JETP **28**, 1092 (1969)].

Ashcroft, N. W., and N. D. Mermin, 1976, *Solid State Physics* (Holt, Rinehart, and Winston, New York).

Awasthi, O. N., 1981, Physica B **107**, 135.

Awasthi, O. N., and S. Sathish, 1981, Phys. Lett. A **83**, 283.

Baber, W. G., 1937, Proc. R. Soc. London, Ser. A **158**, 383.

Bailyn, M., 1958, Phys. Rev. **112**, 1587.

Bailyn, M., 1960, Phys. Rev. **120**, 381.

Baraff, G. A., 1974, Phys. Rev. B **9**, 4008.

Basinski, Z. S., J. S. Dugdale, and A. Howie, 1963, Philos. Mag. **8**, 1989.

Bass, J., 1972, Adv. Phys. **21**, 431.

Bass, J., 1982, Landolt-Bornstein Tables, New Series, **III-15a,b** (Springer, Berlin/Heidelberg/New York).

Bass, J., M. L. Haerle, W. P. Pratt, Jr., P. A. Schroeder, and Z.-Z. Yu, 1984, in *LT-17: Proceedings of the 17th International Conference on Low Temperature Physics,* edited by U. Eckern, A. Schmid, W. Weber, and H. Wühl (North-Holland, Amster-

dam), Part II, p. 1107.

Bass, J., M. L. Haerle, W. P. Pratt, Jr., Y. J. Qian, P. A. Schroeder, S. Yin, Z.-Z. Yu, and J. Zhao, 1986, Phys. Rev. Lett. **56**, 957.

Beers, C. J., J. C. M. van Dongen, H. van Kempen, and P. Wyder, 1978, Phys. Rev. Lett. **40**, 1194.

Berliner, R., H. G. Smith, J. Copley, and J. Trivisonno, 1989, Bull. Am. Phys. Soc. **34**, 769.

Bishop, M. F., and W. E. Lawrence, 1985, Phys. Rev. B **32**, 7009.

Bishop, M. F., and A. W. Overhauser, 1979, Phys. Rev. Lett. **42**, 1776.

Bishop, M. F., and A. W. Overhauser, 1981, Phys. Rev. B **23**, 3638.

Black, J. E., 1980, Phys. Rev. B **21**, 3279.

Blaschko, O., M. de Podesta, and L. Pintschovius, 1988, Phys. Rev. B **37**, 4258.

Blatt, F. J., P. A. Schroeder, C. L. Foiles, and D. Greig, 1976, *Thermoelectric Power of Metals* (Plenum, New York).

Bloch, F., 1930, Z. Phys. **59**, 208.

Bohm, H. V., R. E. Brauer, G. L. Dunifer, P. H. Keesom, and A. W. Overhauser, 1989, Phys. Rev. B **40**, 12 499.

Brown, R. A., 1977, J. Phys. F **7**, 1283.

Bruls, G. J. C. L., J. Bass, A. P. van Gelder, H. van Kempen, and P. Wyder, 1981, Phys. Rev. Lett. **46**, 553.

Bruls, G. J. C. L., J. Bass, A. P. van Gelder, H. van Kempen, and P. Wyder, 1985, Phys. Rev. B **32**, 1927.

Chi, T. C. 1979, J. Phys. Chem. Ref. Data **8**, 439.

Cimberle, M. R., G. Bobel, and C. Rizzuto, 1974, Adv. Phys. **23**, 639.

Citrin, P. H., G. K. Wertheim, T. Hashizume, F. Sette, A. A. MacDowell, and F. Comin, 1988, Phys. Rev. Lett. **61**, 1021.

Cochrane, R. W., and J. O. Strom-Olsen, 1984, Phys. Rev. B **29**, 1088.

Collins, J. G., and J. M. Ziman, 1961, Proc. R. Soc. London, Ser. A **264**, 60.

Cook, J. G., 1979a, Can. J. Phys. **57**, 871.

Cook, J. G., 1979b, Can. J. Phys. **57**, 1216.

Cook, J. G., 1981, Can J. Phys. **59**, 25.

Cook, J. G., 1982, Can. J. Phys. **60**, 1759.

Cook, J. G., M. P. Van der Meer, and M. J. Laubitz, 1972, Can. J. Phys. **50**, 1386.

Coulter P. G., and W. R. Datars, 1985, Can. J. Phys. **63**, 159.

Coulter, P. G., and W. R. Datars, 1986, Phys. Rev. B **34**, 2963.

Cowley, R. A., A. D. B. Woods, and G. Dolling, 1966, Phys. Rev. **150**, 487.

Cracknell, A. P., 1969, Adv. Phys. **18**, 681.

Danino, M., M. Kaveh, and N. Wiser, 1981a, J. Phys. F **11**, L107.

Danino, M., M. Kaveh, and N. Wiser, 1981b, Physica B **108**, 907.

Danino, M., M. Kaveh, and N. Wiser, 1981c, J. Phys. F **11**, 2563.

Danino, M., M. Kaveh, and N. Wiser, 1982, J. Phys. F **12**, L259.

Danino, M., M. Kaveh, and N. Wiser, 1983, J. Phys. F **13**, 1665.

De Gennaro, S., and A. Rettori, 1984, J. Phys. F **14**, L237.

De Gennaro, S., and A. Rettori, 1985, J. Phys. F **15**, 2177.

De Podesta, M., 1987, J. Phys. F **17**, 629.

De Podesta, M., and M. Springford, 1986, J. Phys. F **16**, L131.

De Podesta, M., and M. Springford, 1987, J. Phys. F **17**, 639.

Dugdale, J. S., and D. Gugan, 1960, Proc. R. Soc. London, Ser. A **254**, 184.

Dugdale, J. S., and D. Gugan, 1962, Proc. R. Soc. London, Ser.

A **270**, 186.

Dugdale, J. S., and D. Gugan, 1963, J. Sci. Instrum. **40**, 28.

Dugdale, J. S., and D. Phillips, 1965, Proc. R. Soc. London, Ser. A **287**, 381.

Dunifer, G. L., J. R. Sambles, and D. A. H. Mace, 1989, J. Phys: Condens. Matter **1**, 875.

Edmunds, D. L., W. P. Pratt, Jr., and J. A. Rowlands, 1980, Rev. Sci. Instrum. **51**, 1516.

Ekin, J. W., 1971, Phys. Rev. Lett. **26**, 1550.

Ekin, J. W., 1972, Phys. Rev. B **6**, 371.

Ekin, J. W., and B. W. Maxfield, 1971, Phys. Rev. B **4**, 4215.

Elliott, M., and M. G. M. Harris, 1989, unpublished.

Elliott, M., M. G. M. Harris, and M. de Podesta, 1988, J. Phys. F **18**, L207.

Engquist, H. L., 1982, Phys. Rev. B **25**, 2175.

Farrell, M. E., M. F. Bishop, N. Kumar, and W. E. Lawrence, 1985, Phys. Rev. Lett. **55**, 626.

Fischer, K. H., 1982 *Landolt-Bornstein Tables,* New Series III-15a (Springer, Berlin/Heidelberg/New York).

Fletcher, R., 1982, Can. J. Phys. **60**, 679.

Fletcher, R., 1985, Solid State Commun. **54**, 787.

Follstaedt, D., and C. P. Slichter, 1976, Phys. Rev. B **13**, 1017.

Frobose, K., 1977, Z. Phys. B **26**, 19.

Fulde, P., and I. Peschel, 1972, Adv. Phys. **21**, 1.

Gantmakher, V. F., and G. I. Kulesko, 1975, Sov. Phys. JETP **40**, 1158.

Garcia-Molinar, F., 1958, Proc. Phys. Soc. London **72**, 996.

Garland, J. C., and R. Bowers, 1968, Phys. Rev. Lett. **21**, 1007.

Giebultowicz, T. M., A. W. Overhauser, and S. A. Werner, 1986, Phys. Rev. Lett. **56**, 1485.

Giuliani, G. F., and A. W. Overhauser, 1982, Phys. Rev. B **26**, 1671.

Gostishchev, V. I., A. A. Drozd, and S. E. Dem'yanov, 1978, Fiz. Nizk. Temp. **4**, 1131 [Sov. J. Low Temp. Phys. **4**, 532 (1978)].

Griden, V. V., W. R. Datars, and Y. B. Ning, 1989, J. Phys. Condens. Matter **1**, 713.

Gruneisen, E., 1933, Ann. Phys. **16**, 530.

Guenault, A. M., and D. K. C. MacDonald, 1961, Proc. R. Soc. London, Ser. A **264**, 41.

Gugan, D., 1971, Proc. R. Soc. London, Ser. A **325**, 223.

Gugan, D., 1982, J. Phys. F **12**, L173.

Gugan, D., R. T. L. Lim, and G. M. Meaden, 1989, J. Phys: Condens. Matter **1**, 299.

Gurney, W. S. C., and D. Gugan, 1971, Philos. Mag. **24**, 857.

Gurzhi, R. N., 1963, Zh. Eksp. Teor. Fiz. **44**, 771 [Sov. Phys. JETP **17**, 521 (1963)].

Gurzhi, R. N., 1964, Zh. Eksp. Teor. Fiz **47**, 1415 [Sov. Phys. JETP **20**, 953 (1965)].

Gurzhi, R. N., A. N. Kalinenko, and A. I. Kopeliovich, 1989, Solid State Commun. **72**, 777; Sov. Phys. JETP **69**, 863 (1989).

Haerle, M. L., W. P. Pratt, Jr., and P. A. Schroeder, 1983, J. Phys. F **13**, L243.

Haerle, M. L., W. P. Pratt, Jr., and P. A. Schroeder, 1986, J. Low Temp. Phys. **62**, 397.

Harris, R., and J. O. Strom-Olsen, 1983, in *Glassy Metals II,* edited by H. Beck and H. Guntherodt (Springer, New York), p. 325.

Hayman, B., and J. P. Carbotte, 1973, Can. J. Phys. **51**, 1109.

Heeger, A., 1969, in *Solid State Physics 23,* edited by F. Seitz and D. Turnbull (Academic, New York), p. 283.

Hu, S., 1987, Ph.D. thesis (Purdue University).

Hu, S., and A. W. Overhauser, 1985, Bull. Am. Phys. Soc. **30**, 261.

Hu, S., and A. W. Overhauser, 1988, Phys. Rev. B **37**, 8618.

Huberman, M. L., 1987, Phys. Rev. B **35**, 8969.

Huberman, M. L., and A. W. Overhauser, 1982, Phys. Rev. B **25**, 2211.

Hwang, Y. G., and A. W. Overhauser, 1989, Phys. Rev. B **39**, 3037.

Jain, G. C., and B. S. Verma, 1973, Thin Solid Films **15**, 115.

Jensen, E., and E. W. Plummer, 1985, Phys. Rev. Lett. **55**, 1912.

Jensen, H. H., H. Smith, and J. W. Wilkins, 1969, Phys. Rev. **185**, 323.

Jumper, W. D., and W. E. Lawrence, 1977, Phys. Rev. B **16**, 3314.

Kagan, Yu., and A. P. Zhernov, 1966, Zh. Eksp. Teor. Fiz. **50**, 1107 [Sov. Phys. JETP **23**, 737 (1966)].

Kaveh, M., C. R. Leavens, and N. Wiser, 1979, J. Phys. F **9**, 71.

Kaveh, M., and N. Wiser, 1971, Phys. Rev. Lett. **26**, 635.

Kaveh, M., and N. Wiser, 1972, Phys. Rev. Lett. **29**, 1374.

Kaveh, M., and N. Wiser, 1974a, Phys. Lett. A **49**, 47.

Kaveh, M., and N. Wiser, 1974b, Phys. Rev. B **9**, 4042.

Kaveh, M., and N. Wiser, 1974c, Phys. Rev. B **9**, 4053 (1974).

Kaveh M., and N. Wiser, 1975a, Phys. Lett. A **51**, 89.

Kaveh, M., and N. Wiser, 1975b, Phys. Lett. A **53**, 407.

Kaveh, M., and N. Wiser, 1977, Solid State Commun. **23**, 927.

Kaveh, M., and N. Wiser, 1979, Solid State Commun. **29**, 531.

Kaveh, M., and N. Wiser, 1980, J. Phys. **10**, L37.

Kaveh, M., and N. Wiser, 1981, J. Phys. F **11**, 419.

Kaveh, M., and N. Wiser, 1982, J. Phys. F **12**, 935.

Kaveh, M., and N. Wiser, 1984, Adv. Phys. **33**, 257.

Kaveh, M., and N. Wiser, 1985, J. Phys. F **15**, L195.

Kaveh, M., and N. Wiser, 1987, Phys. Rev. B **36**, 6339.

Khoshnevisan, M., W. P. Pratt, Jr., P. A. Schroeder, and S. D. Steenwyk, 1979, Phys. Rev. B **19**, 3873.

Kittel, C., 1976, *Introduction to Solid State Physics* (5th Ed.) (Wiley, New York).

Klemens, P. G., 1969, in *Thermal Conductivity,* edited by R. P. Tye (Academic, New York), p. 1.

Kondo, J., 1964, Prog. Theor. Phys. **32**, 37.

Kondo, J., 1969, in *Solid State Physics,* Vol. 23, edited by F. Seitz and D. Turnbull (Academic, New York), p. 183.

Koshino, S., 1960a, Prog. Theor. Phys. **24**, 484.

Koshino, S., 1960b, Prog. Theor. Phys. **24**, 1049.

Koshino, S., 1963, Prog. Theor. Phys. **30**, 415.

Krill, G., 1971, Solid State Commun. **9**, 1065.

Kus, F. W., and D. W. Taylor, 1980, J. Phys. F **10**, 1495.

Kusters, N. L., and M. P. MacMartin, 1970, IEEE Trans. Instrum. Meas. **IM-19**, 291.

Lacueva, G., and A. W. Overhauser, 1986, Phys. Rev. **33**, 3765.

Lacueva, G., and A. W. Overhauser, 1989, Bull. Am. Phys. Soc. **34**, 1033.

Landau, L. D., and I. Pomeranchuk, 1936, Phys. Z. Sowjet **10**, 649.

Landau, L. D., and I. Pomeranchuk, 1937, Zh. Eksp. Teor. Fiz. **7**, 379.

Laubitz, M. J., 1970, Phys. Rev. B **2**, 2252.

Lawrence, W. E., 1978, in *Thermal Conductivity,* edited by V. V. Mirkovich, (Plenum, New York), Vol. 15, p. 197.

Lawrence, W. E., and J. W. Wilkins, 1973, Phys. Rev. B **7**, 2317.

Leavens, C. R., 1977, J. Phys. F **7**, 1297.

Leavens, C. R., and M. J. Laubitz, 1974, Solid State Commun. **15**, 1909.

Leavens, C. R., and M. J. Laubitz, 1975, J. Phys. F **5**, 1519.

Leavens, C. R., and M. J. Laubitz, 1976, J. Phys. F **6**, 1851.

Leavens, C. R., and R. Taylor, 1978, J. Phys. F **8**, 1969.

Lee, C. W., M. L. Haerle, V. Heinen, J. Bass, W. P. Pratt, Jr., J.

A. Rowlands, and P. A. Schroeder, 1982, Phys. Rev. B **25**, 1411.

Lee, C. W., W. P. Pratt, Jr., J. A. Rowlands, and P. A. Schroeder, 1980, Phys. Rev. Lett. **45**, 1708.

Lee, P. A., and T. V. Ramakrishnan, 1985, Rev. Mod. Phys. **57**, 287.

Levy, B., M. Sinvani, and A. J. Greenfield, 1979, Phys. Rev. Lett. **43**, 1822.

Lounasmaa, O., V., 1974, *Experimental Principles and Methods Below 1K* (Academic, New York).

Lyo, I.-W., and E. W. Plummer, 1988, Phys. Rev. Lett. **60**, 1558.

MacDonald, A. H., 1980, Phys. Rev. Lett. **44**, 489.

MacDonald, A. H., and D. J. W. Geldart, 1980, J. Phys. F **10**, 677.

MacDonald, A. H., and M. J. Laubitz, 1980, Phys. Rev. B **21**, 2638.

MacDonald, A. H., R. Taylor, and D. J. W. Geldart, 1981, Phys. Rev. B **23**, 2718.

MacDonald, D. K. C., G. K. White, and S. B. Woods, 1956, Proc. R. Soc. London, Ser. A **235**, 358.

Mahan, G. D., 1983, J. Phys. F **13**, L257.

Mahan, G. D., and Z. Wang, 1989, Phys. Rev. B **39**, 4926.

Matthiessen, A., and C. Vogt, 1964, Ann. Phys. (Leipzig) **129**, 19.

Meaden, G. T., 1965, *Electrical Resistance of Metals* (Plenum, New York).

Melville, H., 1851, *The Whale;* the title *Moby Dick* was adopted for the later American edition. For a modern edition, see *Norton Critical Edition of Moby Dick,* edited by H. Hagford and H. Parker (Norton, New York, 1967).

Movshovitz, D., and N. Wiser, 1987, J. Phys. F **17**, 985.

Movshovitz, D., and N. Wiser, 1990, in *LT-19: Proceedings of the 19th International Conference on Low Temperature Physics* (North-Holland, Amsterdam), in press.

Natale, G. G., and I. Rudnick, 1968, Phys. Rev. **167**, 687.

Olsen, J. L., 1958, Helv. Phys. Acta. **31**, 713.

Oomi, G. M. A. K. Mohamed, and S. B. Woods, 1985, J. Phys. F **15**, 1331.

Oomi, G., and S. B. Woods, 1985, Solid State Commun. **53**, 223.

Opsal, J. L., B. J. Thaler, and J. Bass, 1976, Phys. Rev. Lett. **36**, 1211.

Orlov, V. G., 1975, Sov. Phys. Solid State **16**, 2175.

O'Shea, M. J., and M. Springford, 1981, Phys. Rev. Lett. **46**, 1303.

Overhauser, A. W., 1962, Phys. Rev. **128**, 1437.

Overhauser, A. W., 1968, Phys. Rev. **167**, 691.

Overhauser, A. W., 1971, Phys. Rev. B **3**, 3173.

Overhauser, A. W., 1978, Adv. Phys. **27**, 343.

Overhauser, A. W., 1982, Can. J. Phys. **60**, 687.

Overhauser, A. W., 1984, Phys. Rev. Lett. **53**, 64.

Overhauser, A. W., 1985a, in *Highlights of Condensed-Matter Theory, Proceedings of the International School of Physics "Enrico Fermi"* Course LXXXIX, edited by F. Bassani, F. Fumi, and M. P. Tosi (North-Holland, Amsterdam), p. 194.

Overhauser, A. W., 1985b, Phys. Rev. Lett. **55**, 1916.

Overhauser, A. W., 1987a, Phys. Rev. Lett. **58**, 959.

Overhauser, A. W., 1987b, Phys. Rev. Lett. **59**, 1966.

Peierls, R., 1930, Ann. Phys. (Leipzig) **4**, 121.

Penz, P. A., 1968, Phys. Rev. Lett. **20**, 725.

Penz, P. A., and R. Bowers, 1968, Phys. Rev. **172**, 991.

Pintschovius, L., O. Blaschko, G. Krexner, M. de Podesta, and R. Currat, 1987, Phys. Rev. B **35**, 9330.

Pippard, A. B., 1955, Philos. Mag. **46**, 1104.

Pratt, W. P., Jr., 1982, Can. J. Phys. **60**, 703.

Pratt, W. P., Jr., C. W. Lee, M. L. Haerle, V. Heinen, J. Bass, J. A. Rowlands, and P. A. Schroeder, 1981, Physica B **108**, 863.

Qian, Y. J., W. P. Pratt, Jr., J. Zhao, and P. A. Schroeder, 1988, Bull. Am. Phys. Soc. **33**, 569.

Qian, Y. J., W. P. Pratt, Jr., and P. A. Schroeder, 1989, Bull. Am. Phys. Soc. **34**, 1033.

Qian, Y. J., W. P. Pratt, Jr., and P. A. Schroeder, 1990, unpublished.

Ribot, J. H. J. M., J. Bass, H. van Kempen, and P. Wyder, 1979, J. Phys. F **9**, L17.

Ribot, J. H. J. M., J. Bass, H. van Kempen, R. J. M. van Vucht, and P. Wyder, 1981, Phys. Rev. B **23**, 532.

Rowlands, J. A., and S. B. Woods, 1976, Rev. Sci. Instrum. **47**, 795.

Rowlands, J. A., C. Duvvury, and S. B. Woods, 1978, Phys. Rev. Lett. **40**, 1201.

Sambles, J. R., and T. W. Preist, 1982, J. Phys. F **12**, 1971.

Sampsell, J. B., and J. C. Garland, 1976, Phys. Rev. B **13**, 583.

Schroeder, P. A., 1982, Physica B **109/110**, 1901.

Seitz, F., 1940, *The Modern Theory of Solids* (McGraw-Hill, New York), Chap. XV.

Senoussi, S., and I. A. Campbell, 1973, J. Phys. F **3**, L19.

Shukla, R. C., 1980, Phys. Rev. B **22**, 5810.

Shukla, R. C., and R. Taylor, 1976, J. Phys. F **6**, 531.

Shukla, R. C., and M. VanderSchans, 1980, Phys. Rev. B **22**, 5818.

Shung, K. W.-K., and G. D. Mahan, 1986, Phys. Rev. Lett. **57**, 1076.

Shung, K. W.-K., and G. D. Mahan, 1987, Phys. Rev. Lett. **58**, 960.

Sinvani, M., A. J. Greenfield, M. Danino, M. Kaveh, and N. Wiser, 1981, J. Phys. F **11**, L73.

Smith, H. G., 1987, Phys. Rev. Lett. **58**, 1228.

Smith, H., and J. W. Wilkins, 1969, Phys. Rev. **183**, 624.

Soethout, L. L., H. van Kempen, J. T. P. W. van Maarseveen, P. A. Schroeder, and P. Wyder, 1987, J. Phys. F **17**, L129.

Sprengel, J., G. Thummes, and J. Appel, 1989, J. Phys.: Condens. Matter **1**, 3621.

Stinson, M. R., R. Fletcher, and C. R. Leavens, 1979, J. Phys. F **9**, L107.

Stump, D. R., 1986, unpublished.

Taylor, P. L., 1962, Proc. Phys. Soc. London **80**, 755.

Taylor, P. L., 1963, Proc. R. Soc. London, Ser. A **275**, 209.

Taylor, P. L., 1964, Phys. Rev. A **135**, 1333.

Taylor, R., 1978, Solid State Commun. **28**, 167.

Taylor, R., 1982, Can. J. Phys. **60**, 725.

Taylor, R., 1989, private communication.

Taylor, R., and A. H. MacDonald, 1980a, J. Phys. F **10**, L181.

Taylor, R., and A. H. MacDonald, 1980b, J. Phys. F **10**, 2387.

Taylor, R., and A. H. MacDonald, 1986, Phys. Rev. Lett. **57**, 1639.

Taylor, R., C. R. Leavens, M. S. Duesbery, and M. J. Laubitz, 1978, J. Phys. (Paris) Colloq. **C6**, 1058.

Taylor, R., C. R. Leavens, and R. C. Shukla, 1976, Solid State Commun. **19**, 809.

Templeton, I. M., 1982, J. Phys. F **12**, L121.

Thaler, B. J., R. Fletcher, and J. Bass, 1978, J. Phys. F **8**, 131.

Tsoi, V. S., and V. F. Gantmakher, 1969, Zk. Eksp. Teor. Fiz. **56**, 1232 [Sov. Phys. JETP **29**, 663 (1969)].

van de Walle, G. F. A., 1982, Ph.D. Thesis, University of Nijmegen, Holland.

van der Maas, J., and R. Huguenin, 1987, Jpn. J. Appl. Phys. **26**, (Proc. LT-18), Suppl. 26.3, 653.

van Kempen, H., J. S. Lass, J. H. J. M. Ribot, and P. Wyder, 1975, in *LT-14: Proceedings of the 14th International Conference on Low Temperature Physics,* edited by M. Krusius and M. Vuoris (North-Holland, Amsterdam), Vol. 3, p. 94.

van Kempen, H., J. S. Lass, J. H. J. M. Ribot, and P. Wyder, 1976, Phys. Rev. Lett. **37**, 1574.

van Kempen, H., H. W. Neyenhuisen, and J. H. J. M. Ribot, 1979, Rev. Sci. Instrum. **50**, 161.

van Kempen, H., J. H. J. M. Ribot, and P. Wyder, 1981, J. Phys. F **11**, 597.

van Vucht, R. J. M., G. G. A. van de Walle, H. van Kempen, and P. Wyder, 1982, J. Phys. F **12**, L217.

van Vucht, R. J. M., H. van Kempen, and P. Wyder, 1985, Rep. Prog. Phys. **48**, 853.

van Vucht, R. J. M., G. F. A. van de Walle, H. van Kempen, and P. Wyder, 1986, J. Phys. F **16**, 1525.

Wang, Y. R., and A. W. Overhauser, 1985, Phys. Rev. B **32**, 7103.

Werner, S. A., T. M. Giebultowicz, and A. W. Overhauser, 1987, Phys. Scr. **T19**, 266.

Werner, S. A., A. W. Overhauser, and T. M. Giebultowicz, 1989, Bull. Am. Phys. Soc. **34**, 607.

Werner, S. A., A. W. Overhauser, and T. M. Giebultowicz, 1990, unpublished.

White, G. K., and S. B. Woods, 1958, Can. J. Phys. **36**, 875.

Wilson, J. A., and M. de Podesta, 1986, J. Phys. F **16**, L121.

Wiser, N., 1982, Can. J. Phys. **60**, 693.

Wiser, N., 1984, Contemp. Phys. **25**, 211.

Wiser, N., 1988, J. Phys. F **18**, 457.

Woods, S. B., 1956, Can. J. Phys. **34**, 223.

Yin, S., 1987, Ph.D thesis (Michigan State University).

Yin, S., Y. J. Qian, W. P. Pratt, Jr., and P. A. Schroeder, 1990, unpublished.

Yoshida, K., 1981, J. Phys. F **11**, L245.

You, H., J. D. Axe, D. Hohlwein, and J. B. Hastings, 1987, Phys. Rev. B **35**, 9333.

Yu, Z.-Z. 1984, Ph.D. thesis (Michigan State University).

Yu. Z.-Z., J. Bass, and W. P. Pratt, Jr., 1984, in *LT-17: Proceedings of the 17th International Conference on Low Temperature Physics,* edited by V. Eckern, A. Schmid, W. Weber, and H. Wühl (North-Holland, Amsterdam), Part II, p. 1109.

Yu, Z.-Z., J. Bass, and W. P. Pratt, Jr., Phys. Lett. **108A**, 164 (1985).

Yu, Z.-Z., J. Bass, W. P. Pratt, Jr., and P. A. Schroeder, 1985, J. Phys. F **15**, L147.

Yu, Z.-Z., M. L. Haerle, J. Bass, W. P. Pratt, Jr., and P. A. Schroeder, 1984a, in *LT-17: Proceedings of the 17th International Conference on Low Temperature Physics,* edited by V. Eckern, A. Schmid, W. Weber, and H. Wühl (North-Holland, Amsterdam), Part II, p. 1105.

Yu, Z.-Z., M. Haerle, J. W. Zwart, J. Bass, W. P. Pratt, Jr., and P. A., Schroeder, 1983, Phys. Lett. A **97**, 61.

Yu, Z.-Z., M. Haerle, J. W. Zwart, J. Bass, W. P. Pratt, Jr., and P. A. Schroeder, 1984b, Phys. Rev. Lett. **52**, 368.

Yu, Z.-Z., S. Yin, M. L. Haerle, Y. J. Qian, H. Bidadi, W. P. Pratt, Jr., P. A. Schroeder, and J. Bass, 1989, Phys. Rev. B **40**, 7601.

Zhao, J., 1988, Ph.D. thesis (Michigan State University).

Zhao, J., J. Bass, W. P. Pratt, Jr., and P. A. Schoeder, 1986, J. Phys. F **16**, L271.

Zhao, J., J. Bass, W. P. Pratt, Jr., H. Sato, and P. A. Schroeder, 1987, in Proc. LT-18, Jpn. J. Appl. Phys. **26**, Suppl. 26-3, 711.

Zhao, J., W. P. Pratt, Jr., H. Sato, P. A. Schroeder, and J. Bass, 1988, Phys. Rev. B **37**, 8738 (Part I); **37**, 8749 (Part II, with ad-

ditional co-author Z. Z. Yu).

Zhao, J., Y. J. Qian, Z.-Z., Yu, M. L. Haerle, S. Yin, H. Sato, W. P. Pratt, Jr., P. A. Schroeder, and J. Bass, 1989, Phys. Rev. B **40**, 10 309.

Ziman, J. M., 1954, Proc. R. Soc. London, Ser. A **226**, 436.

Ziman, J. M., 1969, in *The Physics of Metals; Vol. 1. Electrons*, edited by J. M. Ziman (Cambridge University, Cambridge, England), p. 272.

Ziman, J. M. 1972, *Electrons and Phonons* (Clarendon, Oxford, England).